THE UNIVERSITY
of EDINBURGH

An Investigation into the Role of HER2 Receptor Signalling in Hypoxia-Inducible Factor Regulation in Breast Cancer

THE UNIVERSITY *of* EDINBURGH

Edward Joseph Jarman

Doctor of Philosophy
2017

Declaration

I declare that this thesis has been composed entirely by me, the work presented within was also performed by me alone unless otherwise stated. Where applicable, credit to additional contributors is clearly given. No part of this work has been submitted for any other degree or professional qualification except as specified.

Edward Jarman

September 2017

Scientific Abstract

Areas of hypoxia caused by poor perfusion are a common occurrence in breast cancer. Hypoxia-inducible factors-1 and 2 (HIF1/2) drive the cellular response to hypoxia in such areas, resulting in the upregulation of genes which facilitate the survival of cancer cells and promote growth, invasion, metastasis and angiogenesis, generally leading to more aggressive tumour characteristics. Previous research has demonstrated that growth factor signalling, such as the ligand-mediated activation of HER receptors, can promote the action of HIFs in normoxia, and correlation between HER2 expression and HIFα proteins has been demonstrated in clinical samples of breast cancer. Despite this, little research has been conducted on how the growth factor-driven regulation of HIFα subunits might modify the cellular response to hypoxia. In this thesis, the role of HER2 overexpression in HIFα modulation was assessed in breast cancer cell lines and publically available clinical datasets for breast cancer with the aim of further understanding the implications of hypoxia and HIFα expression in the context of HER2-positive breast cancer.

The upregulation of HIF1α and HIF2α by hypoxia was observed across breast cancer cell lines, and the role of HER2 in this process was assessed using an isogenic MCF7 cell line model overexpressing HER2. This demonstrated an increased hypoxic upregulation of HIF2α but not HIF1α when HER2 was overexpressed. The increased upregulation was shown to be facilitated by an increase in normoxic HIF2α, which is driven by a higher transcriptional rate of the *EPAS1* (HIF2α) gene as a direct result of HER2 overexpression. HER2 overexpression also resulted in the increased hypoxic upregulation of known hypoxia response genes in 2D and 3D culture models. This demonstrates a novel mechanism for growth-factor mediated HIFα regulation in the context of HER2 overexpression, with an important role for HIF2α.

Microarray analysis of MCF7 and MCF7-HER2 cells was used to compare the global transcriptional response to acute (24 hrs) and chronic (>10 weeks) hypoxia (0.5% O_2) and demonstrated a broadly increased upregulation of hypoxic response genes in the HER2 overexpressing cell line when compared to wild-type MCF7. This included an increase in previously described HIF1 and HIF2 target genes. MCF7-HER2 also illustrated an increased expression of hypoxia response genes in normoxia, and an analysis of the genes involved

showed the promotion of a number of pathological processes including proliferation, invasion, angiogenesis and epithelial to mesenchymal transition.

Large-scale, publically available expression datasets for breast cancer cell lines and clinical patient data were used to investigate the expression of HIF2α and hypoxia response genes in relation to HER2 expression. A set of pathologically important genes which were primed for hypoxia in MCF7-HER2 were also demonstrated to correlate with HER2 across breast cancer cell lines, suggesting that HER2 may more broadly promote a readiness to respond to hypoxia in breast cancer cells. Assessment of HIF2α in clinical samples has shown its increased expression in the HER2-positive subtype, and HIF2α was shown to be associated with worse disease-specific survival in the context of HER2-positive samples only. To investigate whether HIF2α is a potential target in HER2 overexpressing breast cancer, the effect of HIF2α inhibition through siRNA or HIF2-specific chemical inhibitors was assessed in cell lines with high or low HER2 expression, and this demonstrated an increased sensitivity of HER2 overexpressing cell lines to HIF2α inhibition.

This work highlighted HER2 as an important modulator of the cellular response to hypoxia in breast cancer, demonstrating a previously overlooked role for HIF2α in this process. HIF2α expression can be directly driven by HER2 and this differs mechanistically from that previously reported for HIF1α. Finally, further work into the potential for HIF2α as a target for anti-cancer therapy is suggested, as an increased sensitivity of HER2-positive cell lines to anti-HIF2α agents was shown, as well as a HER2-specific relationship between HIF2α expression and worse prognosis. More generally, this work has shown an important interplay between growth factor receptor expression and the cellular response to hypoxia, suggesting that HER2 may promote a stronger response to hypoxia in breast cancer, which may contribute to the increased aggressiveness of HER2-positive tumours.

Lay Abstract

Uncontrolled cellular growth and abnormal blood vessel formation in breast cancer often leads to areas where oxygen levels are reduced (hypoxia). The hypoxia-inducible factors HIF1 and HIF2 are the main cellular machinery for dealing with hypoxia; their levels are directly regulated by oxygen, and when oxygen levels are limiting they activate the production of a number of other proteins which facilitate cell survival under these conditions. In cancer this not only provides the cells with a coping mechanism but also encourages other processes associated with worse prognosis, such as metastasis, the ability for cancer cells to migrate through the blood vessels and for tumours to develop in new locations. In addition to responding to hypoxia, HIF1 levels have been shown to be increased by growth factor signalling; this occurs even in normal oxygen conditions through the stabilisation of its alpha-subunit. This provides a mechanism which allows the harmful actions of HIF activity to occur regardless of oxygen levels, especially when growth factor signalling is high, such as in HER2-positive breast cancers, which represent approximately 20% of breast cancers and are characterised by their high expression of the HER2 growth factor receptor. Despite this, we still have relatively little understanding of the full implications of HER2-HIF interactions. Further research into such interactions will provide a fuller understanding of how HIFs contribute to tumour pathology and help to identify circumstances where direct targeting of hypoxia or growth factor signalling may be more effective.

In this thesis I investigated the relationship between HER2 overexpression and HIF activity by asking how HER2 might affect the normal cellular response to hypoxia. This has been investigated in terms of HIF proteins and known downstream effectors of HIF biology in both 2D and 3D cell line models of breast cancer. In addition, a large scale gene expression experiment was used to investigate how thousands of genes are regulated in response to hypoxia in both short and long term experiments, and this was compared with and without HER2 overexpression, providing a comprehensive overview of the gene expression changes in response to hypoxia in these two contexts. In doing this, I was able to demonstrate that the cellular response to hypoxia was exacerbated in the HER2-positive breast cancer cell line and that HER2 overexpression places cells in a primed state ready for hypoxia.

This increased hypoxic response included an increase in the level of the HIF2α protein. I was able to show that HIF2α is expressed at higher levels when HER2 is overexpressed, and this leads to a stronger upregulation of HIF2α in response to hypoxia. For the first time this demonstrates an important role for HIF2α as part of the growth factor-modulated response to hypoxia. I have shown that the increase in HIF2α caused by HER2 occurs through a different mechanism to that previously described for HIF1α, suggesting that both HIF factors may be regulated by growth factors in different signalling contexts.

Experiments were then conducted to assess whether inhibiting HIF2 activity could reduce cell growth in breast cancer cell lines. Generally, cell lines expressing higher levels of the HER2 receptor had an increased sensitivity to HIF2 inhibition. Large scale datasets of publically available clinical data were then used to investigate the relationship between HER2 and HIF2α expression in breast cancer patients and revealed that HIF2α expression was commonly higher in cases of high HER2 expression. Finally, survival rates for patients with HER2-positive breast cancer were shown to be reduced in cases of high HIF2α expression. This effect was not detectable in HER2-negative cases or when HER2-positive and negative cases were combined. This demonstrates that HIF2α may be an important determinant of patient survival, but only in the context of HER2-overexpression.

This work has highlighted an important role for HER2-HIF2 interaction in terms of the cellular response to hypoxia. It has provided initial evidence that this interaction may promote poorer patient outcome, whilst demonstrating a potential sensitivity of HER2-positive cells to HIF2α inhibition.

Acknowledgements

First of all, I would like to thank my supervisors Dr Simon Langdon and Dr Carol Ward whose door was always open. Not once have I felt like I was being bothersome, and not once have I left their office without feeling reassured by their advice and direction. Their calm and friendly demeanours have allowed what should have been a difficult and stressful time to be wholly enjoyable. I would also like to thank Dr Andy Sims and Prof Val Brunton, who, along with Simon and Carol, formed my thesis committee. Their careful measure of praise and criticism allowed me to recognise the issues along with the merit of my work, and their offers of assistance with models and analysis is duly appreciated.

In terms of collaborative work, I would like to express my thanks to Dr Arran Turnbull, Dr Carlos Martinez-Perez, Dr Chrysi Xintaropoulou and Dr James Meehan, who worked together with me on the microarray experiment. Particular thanks goes to Arran, who provided his expertise and guidance in performing the microarray and the resulting data analysis. I learned a lot from Arran and without his patience this thesis would not have been half as interesting. Additionally, my thanks goes to Helen Caldwell and Elaine McLay, who performed the processing and sectioning of tissue for my IHC work as well as overseeing the general running of the lab. Without them the lab would certainly have fallen apart.

I would like to thank the MRC for providing studentships which allow so many young scientists such as myself to pursue a PhD. Thanks to the IGMM, who run the PhD programmes and have provided me with an invaluable infrastructure, and the University of Edinburgh which has somehow kept me inspired and motivated to learn since 2009.

On a personal level, I would like to thank everyone at the Division of Pathology Laboratories, who have made me feel extremely welcome and provided such a fun working environment for the past few years. Thanks to all of you (a personalised list would simply be too long) for your friendship and collective dysfunction.

I thank my loving family, who have always been a source of grounding and perspective. My Dad, who provides much needed pragmatism in times of despair, and my mum, who has always provided unconditional support from afar despite my infrequent calls.

My final and biggest thanks has to be to Natasha, who has stuck by my side and supported me for the entirety of this PhD, never once appearing disinterested by either my incessant complaints or enthusiastic ramblings about cells. You mean more to me than any cell or any thesis, even if it doesn't always appear to be the case.

Table of Contents

List of Figures

List of Tables

List of Appendices

Chapter 1: Introduction

1.1 Cancer and breast cancer epidemiology

The term 'cancer' represents a large, heterogeneous group of diseases characterised by the uncontrolled replication of cells which go on to invade healthy tissue and metastasise to other organs. Different cancers can vary enormously depending on the tissue and cell-type of origin as well as the specific genetic defects and molecular abnormalities driving the initiation and progression of the disease. Thus, cancer is a multifaceted disease which is difficult to define both concisely and accurately. However, in 2000, Hanahan and Weinberg first described the six 'hallmarks of cancer' in their seminal paper, providing a framework for describing and understanding the disease. These hallmarks were proposed as the fundamental capabilities acquired by cells in the multi-step process of human tumorigenesis and include the abilities to sustain proliferative signalling, resist cell death, evade growth suppressors, enable replicative immortality, activate invasion and metastasis, and induce angiogenesis. These ideas were more recently updated in 2011 to include two new 'hallmarks' reflecting our latest understanding of the interplay involved in cancer emergence and progression: deregulating cellular energetics and avoiding immune destruction, as well as two 'enabling characteristics' of cancer: genome instability/mutation, and tumour-promoting inflammation [1, 2]. These hallmarks are shown in Figure 1.1.

Recent global statistics from the GLOBOCAN project estimated over 14 million new cases of cancer and 8.2 million cancer-related deaths worldwide in 2012 [3]. Breast cancer was named as the most common cancer in women, with an estimated 1,676,000 new patients and 521,900 deaths worldwide that year [3]. In 2014 the UK saw an estimated 356,860 cancer cases with 163,444 cancer-related deaths, and 55,222 new breast cancer patients alongside 11,433 breast cancer-related deaths [4]. As such, breast cancer is the third most common cause of cancer deaths in the UK and the second most common in women, accounting for 7% of all cancer deaths. Despite this, the last decade has seen a 17% reduction in breast cancer mortality in the UK and likelihood of 10-year survival between 2010 and 2011 in England and Wales was at 78% [4].

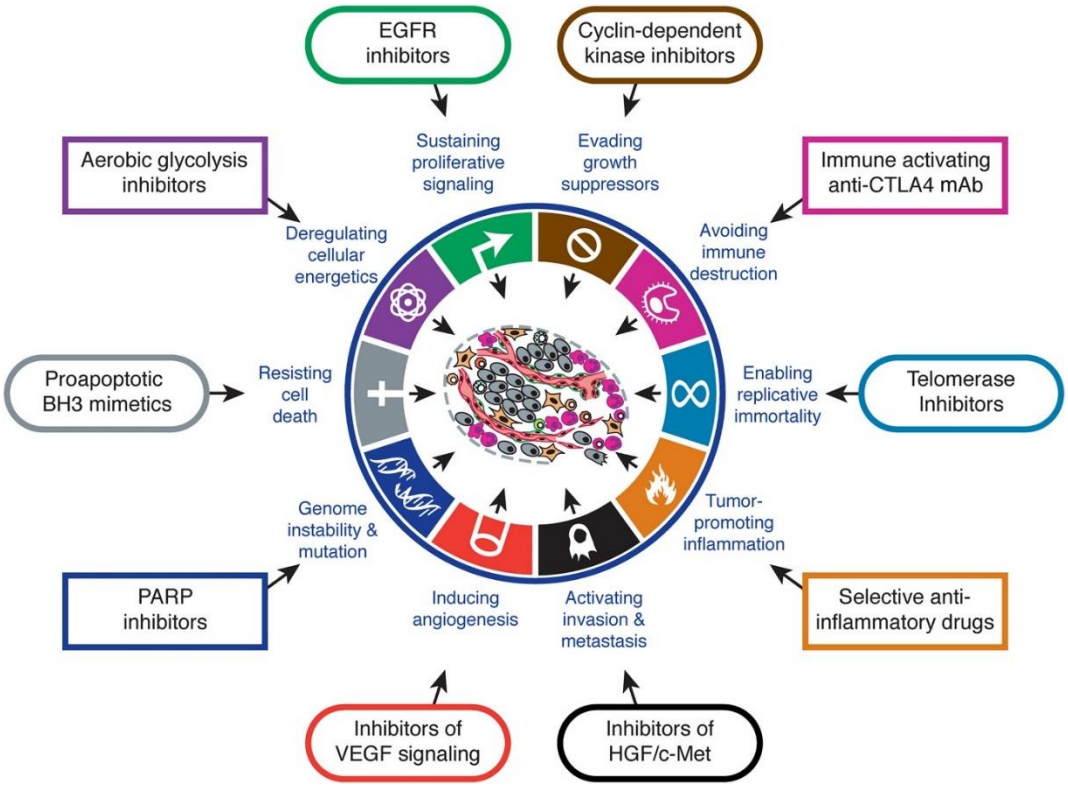

Figure 1.1: The Hallmarks of cancer

The hallmarks of cancer as defined by Hanahan and Weinberg in 2011. The 10 hallmarks are shown as sectors of the circle each contributing to cancer formation. These include 8 hallmarks: evading growth suppressors, avoiding immune destruction, enabling replicative immortality, activating invasion and metastasis, inducing angiogenesis, resisting cell death, deregulating cellular energetic and sustaining proliferative signalling, as well as 2 enabling characteristics: genome instability and mutation and tumour promoting inflammation. The methods which can be used to target each of these hallmarks are shown on the outside of the circle. (Figure taken from Hanahan and Weinberg 2011 [1]).

1.2 Breast cancer

1.2.1 Anatomy of the breast

The breast is composed of the mammary gland surrounded by adipose tissue and supported by a framework of connective tissue. The mammary gland is a network of ducts, consisting of a layer of epithelial cells surrounded by a layer of contractile myoepithelial cells and with approximately 15 to 20 lobes leading towards the nipple [5, 6]. It is highly proliferative and undergoes repeated tissue restructuring under hormonal control; during the menstrual cycle it goes through repetitive cycles of rapid growth and involution and during pregnancy high levels of prolactin, oestrogen and progesterone stimulate the branching and growth of ductal tissues [7]. As gestation progresses, high progesterone levels lead to further branching and the formation of milk producing alveoli through the differentiation of epithelial cells at the end of each duct [8, 9]. These structures develop to perform the breast's primary function of milk production for the nourishment of the new born infant and, after weaning, regress through controlled apoptosis, returning to a pre-pregnancy state [10]. A diagram describing normal breast and alveolar physiology can be seen in Figure 1.2.

1.2.2 Histological classification of breast cancers

Breast cancers are commonly categorised and characterised in a number of ways to facilitate prognosis and the development of a treatment strategy. This includes histological classification, which places invasive cancers and pre-invasive cancers into groups based on the histological origin of the disease; grading and staging, which scores cancers broadly based on tissue differentiation and extent of disease, and molecular subtyping, which separates cancers based on the expression of key molecular determinants, helping to indicate which targeted therapeutics may be effective.

The histological classification of breast cancers initially divides neoplasms into invasive carcinomas and carcinomas *in situ* (or pre-invasive cancers) based on the integrity of the basement membrane which is traversed by invasive disease. The carcinomas *in situ* can be further divided into ductal carcinoma *in situ* (DCIS) and lobular carcinoma *in situ* (LCIS), of which DCIS is by far the most common, accounting for 90% of all breast pre-cancers [11, 12].

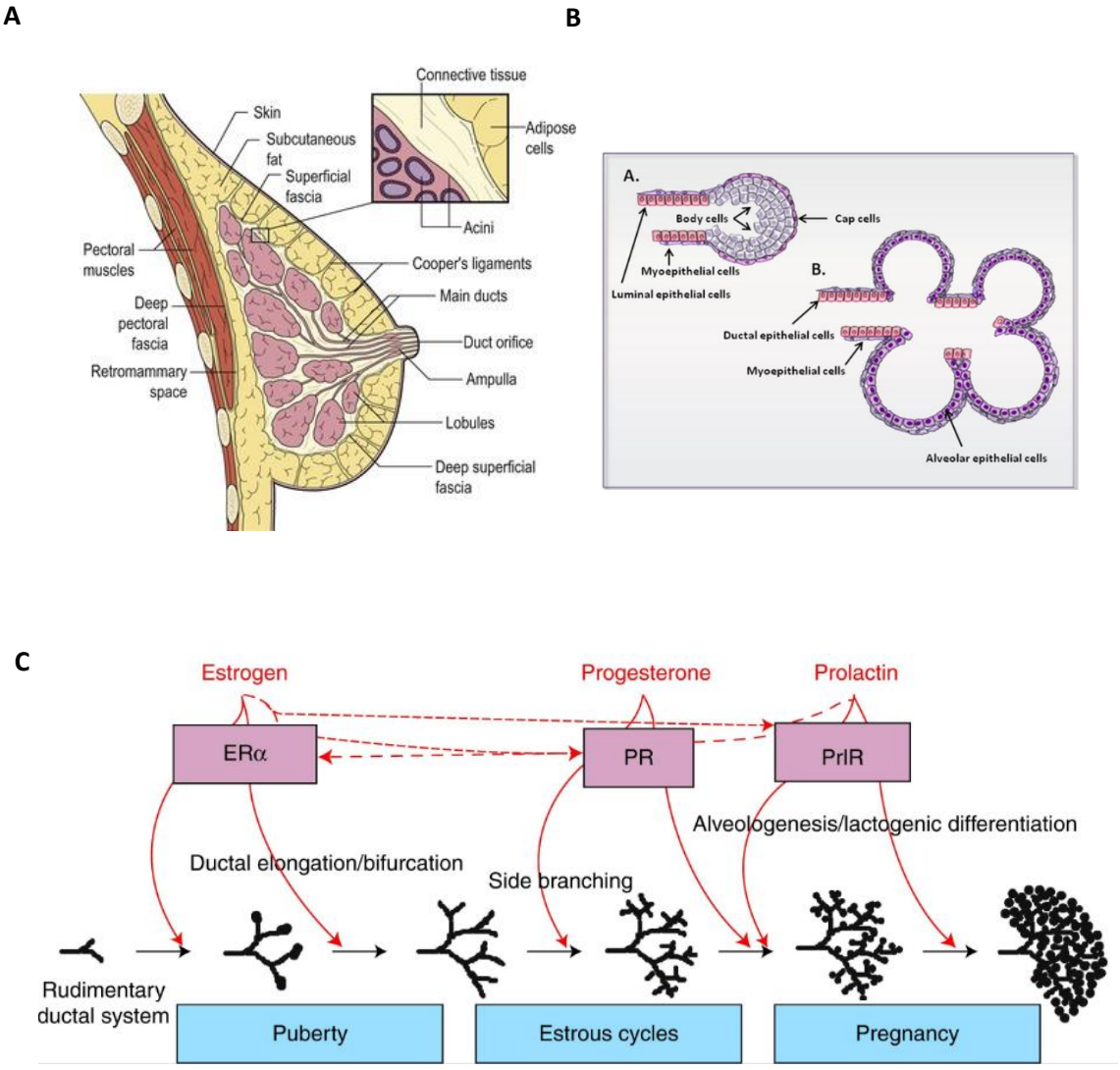

Figure 1.2: Normal anatomy and physiology of the breast

A) The anatomy of a healthy breast; the mammary gland is made up of approximately 15-25 glandular units, each made up of a terminal ductal lobular units (TDLU) with collecting ducts all leading towards the nipple opening. The gland is surrounded by stromal and adipose tissue and supported by cooper's ligaments. (Image adapted from radiologykey.com) B) A schematic representation of mammary gland differentiation during pregnancy, showing the highly proliferative terminal end bud (TEB) of the mammary duct in its pre-pregnancy state (i), and the ductal branching that occurs during pregnancy (ii). (Image adapted from Gajewska et al. 2013 [9]*). C) A schematic of how hormonal signalling contribute to side branching of mammary ducts during development, puberty and pregnancy. This includes the formation of alveolar structures during pregnancy which are the site of milk production (Adapted from Brisken et al. 2010* [7]*).*

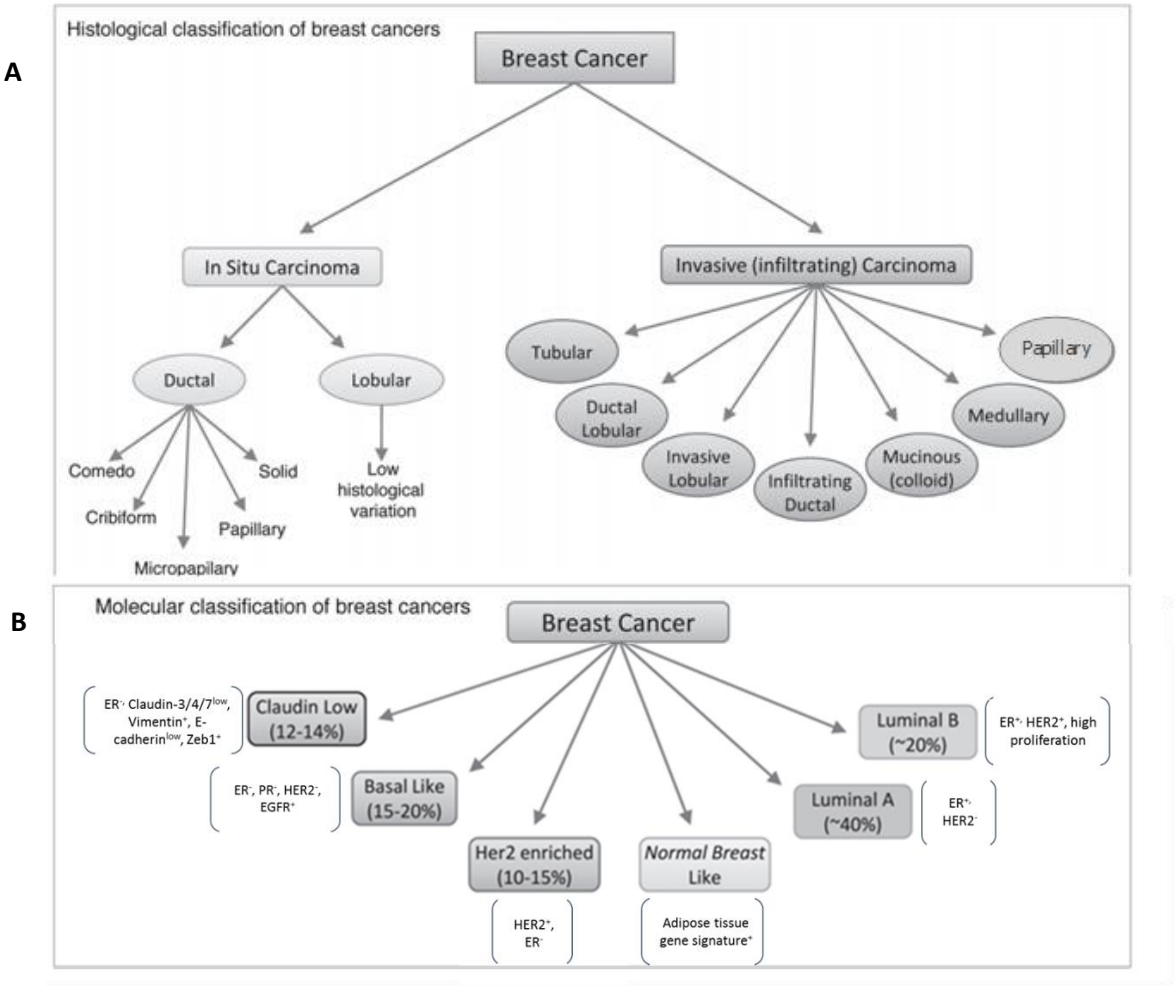

Figure 1.3: Histological and molecular classifications of breast cancer

A) Histological classification of breast lesions into invasive and non-invasive breast cancer subcategories. The majority of breast cancers are invasive ductal carcinomas. B) The stratification of invasive breast cancer based on intrinsic molecular markers. The percentage of cancers in each group are shown in brackets and defining gene expression characteristics are shown next to each group. Figure adapted from Malhotra 2010 [13].

Whilst LCIS shows generally low histological variation, DCIS is comparably heterogeneous and is therefore further categorised into five well-recognised subtypes based on architectural features of the neoplasm (Comedo, Cribiform, Micropapillary, Papillary and Solid) [13].

Invasive tumours can also be further stratified into the following groups: infiltrating ductal carcinoma (IDC), invasive lobular carcinoma (ILC), ductal/lobular, tubular, mucinous (colloid), medullary and papillary, with IDC accounting for 70 – 80% of these invasive breast tumours [14]. Rarer breast cancers include inflammatory breast cancer and Paget's disease. A summary of these histological subtypes can be seen in Figure 1.3.

1.2.3 Breast cancer grading and staging

Even within histological categories, the growth rate and other characteristics of breast cancers can vary enormously. Therefore, universally recognised grading and staging procedures for invasive breast cancer have been developed to allow clinicians to consistently describe the progression and malignancy of the disease, and thereby reliably assign individual tumours to discrete categories based on general severity [15-17].

The TNM system is used for staging a variety of cancer types. It was developed in 1947 by the Union International Cancer Centre (UICC) and was adapted for use in breast cancer in 1960 [18-21]. Staging is designed to give an indication of how far a tumour has progressed by taking a number of features into account. Tumours are grouped into five stages (with pre-invasive cancers denoted as stage 0 and invasive cancers given a stage of I–IV). This is achieved by first scoring tumours based on tumour size (T), whether tumour cells have accessed the lymph nodes (N) and the presence or absence of distant metastases (M). The stage is then designated based on a combination of these factors [22, 23]. How T, N and M values are determined and how this corresponds to the assigned stage is shown in tables 1.1 and 1.2.

Histological grading of breast cancers is used to score tumours based on expected malignancy. Grades are assigned 1-3, with higher grades being associated with more aggressive disease and therefore a worse prognosis. Grading is achieved by a combined scoring of three individual attributes of the tumour. Firstly, tumours are scored 1-3 for tubule formation. A high number of regularly formed tubules are indicative of well differentiated healthy tissue (scoring 1), whilst poorly differentiated tissue is associated with a loss of

Table 1.1 Staging of breast cancers using the TNM system			
Tumour size (T)	TX		Tumour size cannot be assessed
	T0		No primary tumour
	Tis		Ductal carcinoma *in situ* (DCIS)
	T1	Mi	Less than 0.1 cm across
		A	0.1 – 0.5 cm across
		B	0.5 – 1 cm across
		C	1 – 2 cm across
	T2		2 – 5 cm across
	T3		Greater than 5 cm across
	T4	A	Tumour has spread into the chest wall
		B	Tumour has spread into the skin
		C	Tumour has spread into the skin and chest wall
		D	Inflammatory breast cancer
Node status (N)	NX		Lymph nodes cannot be assessed
	N0		No lymph node involvement
	N1	N1	Cancer cells in the lymph nodes in the armpit, but lymph nodes are not stuck in surrounding tissue
		pN1mi	One or more lymph node contains micrometastases (less than 0.2 mm)
		pN1a	Cancer has spread to 1 – 3 lymph nodes with at least one larger than 2 mm
		pN1b	Cancer cells have spread into internal mammary nodes but are not palpable
		pN1c	Cancer has spread to 1 -3 lymph nodes in the armpit and to internal mammary nodes, but are not palpable
	N2	N2a	Cancer cells in the lymph nodes of the armpit, with nodes sticking to each other and other structures
		N2b	Cancer cells in internal mammary nodes (not the armpit), which are palpable or visible on a scan
	N3	N3a	Cancer cells in the lymph nodes below the collar bone
		N3b	Cancer cells in the internal mammary nodes and the armpit
		N3c	Cancer cells in lymph nodes above the collar bone
Metastasis (M)	M0		No sign of metastasis
	cMo(i+)		No sign of metastasis in physical examinations, but cancer cells are present in blood, bone marrow or distant lymph nodes according to laboratory tests.
	M1		Cancer has metastasised to a distant site

Table 1.1: Staging of breast cancers according to the TNM system

Tumours are graded based on size (T), node status (N) and whether there is any sign of metastasis (M). The various assignments for T, N and M are shown with details of what observations are expected for tumours to be assigned to that category [23].

Table 1.2: Staging of breast cancers					
Stage		Description	Associated TNM scores	Classification	
Stage 0		No spread of abnormal cells into surrounding tissue		*In situ*	
Stage I	A	Tumour is 2 cm or smaller and not spread outside the breast	T1N0N0	Invasive breast cancer	Early stage breast cancer
	B	Small areas of cancer cells found in lymph nodes close to the breast and primary site is less than 2 cm	T0N1miM0 T1N1miM0		
Stage II	A	Primary tumour less than 2 cm with cancer cells in 1-3 lymph nodes in the armpit or near the breast bone.	T0N1M0 T1N1M0 T2N0M0		
	A	Tumour 2-5 cm in size with no lymph node involvement			
	B	Tumour 2-5 cm in size and some small areas of cancer cells in the lymph nodes	T2N1M0 T3N0M0		
	B	Tumour 2-5 cm in size and the cancer has spread to 1-3 lymph nodes in the armpit or near the breast bone			
	B	Tumour is larger than 5 cm but not lymph node involvement			
Stage III	A	Tumour of any size and cancer found in 4-9 lymph nodes under the arm or near the breast bone.	T0N2M0 T1N2M0 T2N2M0 T3N1M0 T3N2M0		Locally advanced breast cancer
	A	Tumour larger than 5 cm in size and small clusters of breast cancer cells in the lymph nodes			
	A	Tumour is larger than 5 cm in size and has spread to 1-3 lymph nodes in the armpit or near the breast bone			
	B	The tumour has spread into the skin or breast wall and may have spread into up to 9 lymph nodes near the armpit or breast bone	T4N0M0 T4N1M0 T4N2M0		
	C	Tumour of any size which has spread into the skin or breast wall along with any of the following: reached 10 or more lymph nodes in the armpit, reached lymph nodes above or below the collar bone, reached lymph nodes both in the armpit and by the breast bone.	T(0-4)N3M0		
Stage IV		Tumour of any size with or without lymph node involvement, but cancer has metastasised to other parts of the body.	T(0-4)N(0-3)M1		Metastatic breast cancer

Table 1.2: Staging of breast cancers

A table showing how stages I, II or III are assigned based on characteristics of the tumour and TNM score [23].

regular tubules (scoring 2-3). Secondly, tissue is scored 1-3 for nuclear pleomorphism, a high number of aberrant vesicular nuclei scoring highly. Finally, the tissue is scored 1-3 for mitotic index. These three scores are added to give an overall score which is indicative of the tumour grade: less than 3 = non-tumour; 3-5 = grade 1; 6-7 = grade 2; 8-9 = grade 3 [15-17].

Tumour grading and staging provide a valuable tool for taking tumour heterogeneity into account when considering prognosis and appropriate treatment strategies. Whilst the broad groupings provide relatively little information about the precise nature of the individual tumour, the power of this classification comes from its widespread and reproducible clinical implementation. This means that consistency in clinical practice can be obtained, a requirement if such classification is to be used as a tool for retrospective research to understand factors determining differences in tumour aggressiveness and the benefits of treatment regimens in different clinical contexts.

1.3 Current treatment strategies

The molecular and histological classification of breast cancer provides clinicians with information on the specific tumour, which can be used to determine prognosis and to develop a treatment strategy. A number of approaches are available for treating the disease and in most instances more than one of these are used in combination whilst clinicians constantly keep measure of therapeutic responses and reassess the ongoing stratagem. Below I will briefly describe how various therapeutic approaches are applied to breast cancer and indicate some of the challenges that remain in tackling the disease.

1.3.1 Surgery

In the majority of cases, surgery is still the best option for the treatment of breast cancer. Depending on the size, severity and location of the tumour, breast resection will be performed to various degrees. In the event of small, localised tumours, a lumpectomy can be undertaken, removing just the cancerous tissue and a small area around it [24]. Additionally, in some cases a partial section of the breast is removed (quadrantectomy) leaving a large proportion still intact. These are referred to as breast-conserving surgeries and are typically considered appropriate for women with stage I or II breast cancer [24-27]. In more advanced

cases, a mastectomy (removal of the entire breast) or radical mastectomy (removal of the breast, axillary lymph nodes and some underlying chest muscle) may be performed in the case of highly disseminated tumours to reduce the risk of recurrence, or to remove a large or highly disseminated tumour. In some cases, people at high risk of developing breast cancers in their lifetimes (such as those with identified BRCA 1/2 mutations) can receive a prophylactic mastectomy [28-30].

Whilst surgery is the most effective intervention for breast cancer, in most instances it is used in combination with radiotherapy, chemotherapy, endocrine therapy, HER2 therapy or novel therapies. This allows for the application of breast-conserving surgery instead of radical or non-radical mastectomies when used to shrink the tumour before surgery (neoadjuvant setting), or can be used to reduce the risk of recurrence and increase overall survival when used post-surgery (adjuvant setting).

1.3.2 Radiotherapy

Radiotherapy is widely used for the management of breast cancer typically in the adjuvant setting after lumpectomy or mastectomy [31, 32]. This may be used alone, with chemotherapy [33-35] or with endocrine therapy [36]. The most common method for the delivery of radiotherapy is through external beam radiation. This uses a linear accelerator to direct irradiation at the breast and is typically performed 5 days a week for 5–7 weeks post-surgery, with a higher level radiation boost often given for the last week [37, 38]. Beyond external beam radiation, radiotherapy can also be given either internally or intraoperatively. Internal radiotherapy, often called brachytherapy, involves small pieces of radioactive material or ‘seeds’ being placed inside the breast next to the site of the removed tumour. Radiation sources can be inserted/removed through small tubes and are typically given either in 10-minute doses twice a day for 5 days, or as a single treatment left in for 3 days (depending on whether high-dose or low-dose radiation sources are being used). Intraoperative radiotherapy uses a single high dose of irradiation to treat the underlying breast tissue during surgery. This is usually achieved using a linear accelerator to deliver a short-range electron beam to the affected tissue before finishing surgery. Internal and intraoperative radiotherapy are beneficial in that they can target the area of the tumour more directly, therefore allowing higher doses of radiation with reduced risk to the surrounding tissue. This comes with the added benefit of reduced treatment times, meaning

therapy can be completed over the course of a single week, or even in a single dose during surgery, compared to the 5-7 weeks required for external beam radiotherapy. Despite this, external beam radiotherapy is currently standard procedure as the benefits in relation to recurrence and mortality are better established [39].

Radiotherapy used in the adjuvant setting after either lumpectomy or mastectomy of early stage breast cancer has been shown to reduce the risk of recurrence and mortality in a number of trials [40, 41]. The use of radiotherapy after lumpectomy or other breast-conserving surgery has been shown to reduce the risk of recurrence to equate with that of radical mastectomy, meaning the use of adjuvant radiotherapy permits the use of less disfiguring surgical techniques with little or no added risk [41-45].

1.3.3 Chemotherapy

Chemotherapy involves the treatment of cancer by the systemic administration of one or more cytotoxic agents. Chemotherapy agents generally work by inhibiting the process of DNA synthesis or cell division, meaning highly proliferative cancer cells are particularly sensitive. Unfortunately, the lack of specificity for cancer cells mean these agents can also affect other highly proliferative cells in the body. This includes those of the blood, intestinal tract and hair follicles, often resulting in the side-effects commonly associated with chemotherapy, such as fatigue, nausea, myelosuppression and alopecia [46, 47]. The majority of chemotherapeutic agents target cell division in this way, but can do this through a number of mechanisms; anthracylines such as epirubicin and doxorubicin inhibit DNA synthesis by intercalating between DNA bases and impeding the progress of the DNA replication machinery [48, 49], alkylating agents such as cyclophosphamide, carboplatin and cisplatin cause irreversible DNA crosslinking (once again preventing effective DNA replication) [50, 51], antimetabolites such as fluorouracil block the production of metabolites such as thymidine which are required for DNA synthesis [52], and a number of agents, such as the taxanes docetaxel and paclitaxel, prevent the separation of chromosomes during metaphase by perturbing microtubule assembly dynamics [53].

Chemotherapy is usually used in the adjuvant setting to reduce the risk of recurrence after surgery, often in combination with endocrine or radiotherapy. In early breast cancer this has been shown to improve overall survival by 10% [54], whilst a meta-analysis of 194

trials, reported in 2005, demonstrated that a multiple agent chemotherapy approach such as FAC or FEC (combination treatments of either fluorouracil, doxorubicin and cyclophosphamide (FAC) or fluorouracil, epirubicin and cyclophosphamide (FEC)) resulted in a significant reduction in recurrence and mortality, independent of a number of tumour variables [55, 56]. Additionally, chemotherapy can be used in the neoadjuvant setting in the case of locally advanced, primarily inoperable and inflammatory breast cancer to reduce tumour size before surgery [57].

Whilst there are clear benefits of chemotherapy and radiotherapy for breast cancer in the neoadjuvant and adjuvant settings, the extent to which both of these treatment modalities can be employed is limited by harmful side-effects elicited by their impact on normal, healthy tissue. The benefits of radiotherapy must be weighed against the risk of overexposure to irradiation and cardiac toxicity [58-63], whilst chemotherapy doses must be constantly reassessed and often moderated to avoid the short and long-term detrimental side-effects ranging from cardiac disease to cognitive dysfunction or leukaemia [46, 64, 65]. It is these inherent limitations which have driven research into therapies better designed to target just cancer cells and leave healthy tissue relatively untouched, this being the goal of endocrine and targeted therapies.

1.3.4 Endocrine therapy

Endocrine therapy refers to the treatment of hormone-dependent breast cancers through the disruption of specific hormonal signalling pathways. In breast cancer this is most often through the inhibition of oestrogenic signalling. The effective disruption of oestrogenic signalling can be achieved through direct inhibition of the oestrogen receptor with selective oestrogen receptor modifiers (SERMs) or selective oestrogen receptor down-regulators (SERDs) [66], by the inhibition of oestrogen biosynthesis using aromatase inhibitors [67, 68], or by inhibiting oestrogen production in the ovaries. The above can be done either pharmaceutically using GnRH agonists [69, 70] or surgically through oophorectomy [71, 72]. SERMs such as tamoxifen inhibit the cellular activity of the oestrogen receptor by binding in place of oestrogen, reducing its ability to drive the transcription of oestrogen-regulated genes, whilst SERDs such as fulvestrant similarly bind the oestrogen receptor but result in its degradation [73]. Tamoxifen has been the gold-standard for the treatment of endocrine-responsive breast cancer [66, 74] and can be used in both pre and postmenopausal women.

An overview of randomised trials published in 2005 demonstrated that tamoxifen, used in the adjuvant setting for 5 years, reduced recurrence risk by 41% and mortality by 33% [55], and the results of longer term studies have shown that the benefits of 5-year tamoxifen in terms of recurrence and survival are still present up to 15 years after diagnosis [75, 76].

Aromatase inhibitors (AIs) work by inhibiting the final step of oestrogen biosynthesis; the conversion of androgen precursors into oestrone or oestradiol, which is catalysed by the enzyme aromatase [67, 68, 77]. The use of AIs such as letrozole, anastrazole and exemestane in the treatment of breast cancer is mostly limited to postmenopausal women, as their use in premenopausal women results in a feedback mechanism through the hypothalamus and pituitary gland, leading to an increased stimulation of oestrogen production in the ovaries [74, 78]. Their use in postmenopausal women has proven very effective; individual clinical trials for letrozole, anastrazole and exemestane have all shown clinical benefits when used as a second-line treatment in tamoxifen-resistant disease [79-82], and results from clinical trials of AIs as a front-line therapy for advanced or metastatic breast cancer have demonstrated a better response when compared to tamoxifen in terms of clinical response rates and time to progression [83-86].

In premenopausal women, the majority of circulating oestrogen is produced in the ovaries, and inhibiting ovarian oestrogen production has proven an effective means of inhibiting breast cancer growth. This can be achieved through ablation of the ovaries through surgery or irradiation, or through treatment with GnRH agonists [69-71, 74]. Ovarian ablation has been shown to reduce recurrence and mortality rates by 25% in a combination of 12 randomised trials with women under 50 years of age [87], whilst in 2000 an overview by the Early Breast Cancer Trialists' collaborative group (EBCTCG) confirmed a clinical benefit for ovarian ablation through GnRH agonists [40, 74].

In general, targeting oestrogen signalling has proven an effective tactic in the treatment of oestrogen or progesterone receptor positive breast cancers, predominantly in the adjuvant setting [88]. The current challenges are to determine how these therapies may be best combined with each other and with chemotherapy to provide the optimum clinical response, and to understand how resistance to endocrine therapies arises and how it may be overcome [89-91].

1.3.5 HER2-directed and other targeted therapies

Targeted therapies, like endocrine therapy, function by inhibiting known pathways or molecules which may drive breast cancer progression. The use and choice of targeted therapy depends on the specific characteristics of the tumour. The use of inhibitors targeting the human epidermal growth factor receptor 2 (HER2) is an exemplar for the potential of targeted therapies in breast cancer. The HER2 receptor is overexpressed in around 20% of breast cancers [92, 93], so HER2 inhibition has become a therapeutic option for a large proportion of breast cancers. Many HER2-positive tumours are hormone receptor-negative, while HER2 may also be up-regulated in endocrine-resistant disease, hence this molecule is an attractive target for therapy. Current HER2 targeted therapies include monoclonal antibodies such as trastuzumab (Herceptin) and pertuzumab (Perjeta) as well as small molecular inhibitors such as lapatinib (Tykerb), and antibody-chemotherapy conjugates such as trastuzumab-emtansine (Kadcyla).

Trastuzumab is a humanised monoclonal antibody which binds to the extracellular domain of the HER2 receptor. This antibody predominantly works by inhibiting receptor dimerization and stopping the activation of the receptor which normally occurs through transphosphorylation of the intracellular domain [94]. However, other mechanisms are also believed to contribute to its cytotoxic effect; binding of the antibody reduces HER2 activation by driving receptor endocytosis, inhibits receptor cleavage leading to the active ligand-independent p95 isoform and also drives cell-mediated cytotoxicity through the recruitment of immune effector cells [95-97]. These mechanisms all contribute to the efficacy of trastuzumab seen clinically. Following a number of successful clinical trials [96, 98-102] trastuzumab has been approved for use alongside chemotherapy in the adjuvant setting. The efficacy of trastuzumab in this setting was summarised by a meta-analysis in 2012 of 8 such studies looking into the efficacy of trastuzumab plus chemotherapy versus chemotherapy alone [103]. This analysis favoured trastuzumab containing regimens, with significant improvements in overall and disease-free survival [103]. Additionally, trastuzumab has been shown to be beneficial in the neoadjuvant setting for HER2-positive breast cancer, doubling the likelihood of patients achieving pathological complete response when used alongside chemotherapy [104].

Ado-trastuzumab emtansine (T-DM1 or Kadcyla) consists of the trastuzumab monoclonal antibody conjugated to emtansine, a chemotherapy agent that inhibits microtubule assembly [105, 106]. T-DM1 allows the targeted delivery of chemotherapy to the site of HER2-positive cancers and has become a standard second-line therapy for HER2-positive disease [96]. In the phase III EMELIA trial [107], the effectiveness of T-DM1 was compared to lapatinib with capecitabine in women with advanced HER2-positive breast cancer who were previously treated with trastuzumab and taxane chemotherapy. The results of this trial demonstrated that T-DM1 treatment led to an increase in overall and progression-free survival. T-DM1 has also been shown to provide benefits in patients with progressive disease (TH3RESA trial) [108]. Here improvements to progression-free survival were seen in the T-DM1 arm, when compared to the "physician's choice" arm, including when the physician's choice included trastuzumab treatment. Despite this, comparisons of T-DM1 with trastuzumab as a first-line treatment in HER2-positive advanced disease have shown mixed results, demonstrating a reduced risk of disease progression when compared to trastuzumab and docetaxel in a phase II trial [109], whilst a more recent phase III trial (MARIANNE) demonstrated no significant difference in progression-free survival between T-DM1-treated patients and those on trastuzumab and taxanes as a combination therapy (also this trial showed no increased efficacy of T-DM1 with the addition of pertuzumab) [110, 111].

Pertuzumab (Perjeta) is another humanised monoclonal antibody that targets the HER2 receptor [112]. It differs from trastuzumab in that it targets the dimerization domain of the receptor (extracellular domain II, compared to trastuzumab which targets extracellular domain IV) and is an inhibitor of receptor heterodimerisation, allowing more effective inhibition of HER2/HER3 heterodimerisation in the presence of a ligand [112-114]. For this reason it is considered complimentary to the effects of trastuzumab [96]. The use of pertuzumab in certain contexts has been shown to provide clinical benefit, predominantly when given with trastuzumab and chemotherapy. This combination has been demonstrated to improve invasive disease-free survival as a first line adjuvant treatment for aggressive, early, HER2-positive breast cancer in the phase III APHINITY trial [115, 116]. In the neoadjuvant setting, pertuzumab has similarly been shown to provide added benefit in terms of pathological complete response rate in two separate clinical trials comparing trastuzumab and chemotherapy with and without the addition of pertuzumab [117, 118]. Together this has led to pertuzumab being FDA-approved for use with trastuzumab and docetaxel as a first-

line adjuvant therapy in HER2-positive metastatic breast cancer and in the neoadjuvant setting for HER2-positive, locally-advanced, inflammatory or early stage breast cancer [119].

Lapatinib is a small molecular inhibitor of both HER1 (EGFR) and HER2 activity. By occupying the ATP-binding site in the intracellular domain of either receptor, lapatinib is able to prevent ATP-dependent tyrosine kinase activity of the receptors and thereby prevents their activation despite ligand binding and dimerization [96, 120-122]. In the adjuvant setting lapatinib has shown poor efficacy in clinical trials when used alone (TEACH) [123] or in combination with trastuzumab (ALTTO) [124]. In the neoadjuvant setting lapatinib treatment has been shown to be less effective than trastuzumab, but can offer some benefit when combined with trastuzumab and chemotherapy [125-127]. Lapatinib can also provide some benefit in the treatment of locally advanced or metastatic HER2-positive breast cancer, where it can be used in combination with trastuzumab and provides improved overall and progression-free survival [128].

Whilst HER2 targeted therapies have made a large contribution to improved prognosis in individuals with HER2-positive breast cancers, they are inherently limited by their applicability to only 20% of tumours. As such, a number of targeted therapies have been developed or are under development which may be beneficial in the treatment of breast cancers with otherwise limited options. Those which have been made available clinically include, CDK4/6 inhibitors such as palbociclib (Ibrance) and ribociclib (Kisqali), as well as the mTOR inhibitor everolimus (Afinitor) [129].

Palbociclib and ribociclib are inhibitors of cyclin dependent kinases 4 and 6 (CDK4/6). These have been shown to be particularly effective in aggressive ER-positive breast cancers. Both palbociclib [130-132] and ribociclib [133, 134] have recently been approved for clinical use in combination with letrozole for advanced and metastatic hormone receptor-positive breast cancers.

Everolimus is an inhibitor of the mammalian target of rapamycin (mTOR) a regulator of cellular growth, metabolism and proliferation. As with CDK4/6 inhibition, inhibition of the pathways regulating cellular proliferation are particularly effective in ER-positive breast cancers, and as such Everolimus has been approved for use in cases of advanced hormone receptor-positive, HER2-negative breast cancers in conjunction with exemestane. It has been also been shown in the BOLERO-2 trial to improve overall survival [135].

Besides these approved targeted therapies a large number of compounds are currently in early development as possible treatments for selected breast cancers. These inhibitors target a number of pathways in cancer and include but are not limited to; growth signalling pathways including PI3K/AKT/mTOR and MEK inhibitors, alternative growth factor receptors such as IGFR, MET, FGFR and EGFR/HER3, epigenetic regulators such as histone deacetylases (HDAC) inhibitors and DNA methyltransferases (DNMT), cancer stem cell signalling pathways such as notch and β-catenin, and regulators of the hypoxic tumour microenvironment such as HIF1 [136]. The wide range of targetable pathways common to cancer provides future possibilities for fighting this disease.

Whilst this approach seems to be a good counter for the problem of breast cancer heterogeneity and the poor response rates of broad-range treatments, more work is still needed to be done in order to understand when particular targeted therapies are the best option. The tumours in which these inhibitors work best require identification and their potential impact on normal cells and associated toxicities need to be understood. Targeted therapies have the potential to provide improved treatment modalities for all types of breast cancer, but this requires further work both in the laboratory where we can gain an understanding of the targetable pathways that define and drive breast cancer, and clinically, where trials can provide a better understanding of the efficacy of targeted treatments alone or in combination.

1.4 Gene expression profiling and the molecular subtypes of breast cancer

The advent of gene expression and microarray technologies has increased interest in the molecular basis of the heterogeneity seen in breast cancer. Seminal studies by Perou [137] and Sorlie [138] in 2000, were the first to show that gene expression patterns derived from microarray experiments could be used to stratify breast cancers into at least 5 subclasses, with significant differences in clinical outcome. These were termed the ‘intrinsic subtypes’ of breast cancer and consisted of Luminal A (ER+ subtype with low HER2), Luminal B (an ER+ subtype often with increased HER2 expression), HER2-positive (generally ER- with high HER2 expression), Basal (generally triple negative (ER-/PR-/HER2-) with expression of basal cytokeratins and EGFR) and Normal-like (with a similar genetic signature to adipose

tissue of the breast) groups. These classifications were later extended by the addition of claudin-low as a subset of the basal group (characterised by low expression of claudins 3, 4 and 7 as well as by an epithelial to mesenchymal transition (EMT) phenotype) [139, 140]. In 2012 research published by The Cancer Genome Atlas Network [141] defined these subtypes more comprehensively using an integrated analysis of genetic, epigenetic, transcriptome and protein array data. With this approach they were able to demonstrate that breast cancers can be separated into the four phenotypically distinct classes: Luminal A, Luminal B, HER2-enriched and Basal-like. This study showed that these molecular subtypes exhibit different frequencies of specific driver mutations and differences in dominant signalling pathways [141].

The intrinsic subtypes consolidated the idea that breast cancer is best defined as, not one disease, but a group of diseases, and has formed the basis of the molecular taxonomy of breast cancer. However, the clinical application of subtype stratification has been slow, as assigning intrinsic subtype to samples is only possible retrospectively using large patient cohorts, and so is not particularly amenable to single patient stratification [142-144]. As such, recent years have focussed on the identification of single sample predictors, gene sets which can provide prognostic or predictive information about a patient through the gene expression profile of that patient alone [145]. These were designed to stratify patients into risk categories to aid treatment decisions independently of subtype (however some do provide indication of intrinsic subtype (PAM50)) [146]. A number of such multigene predictors have been established and are used frequently in the clinic; brief descriptions of gene signatures used clinically can be seen in Table 1.3 [147-150]. Despite the utility of such gene expression signatures in helping to predict response to therapy, they have only proven useful predictors in ER+ breast cancers, and have not been able to replace clinical pathological features such as tumour size, grade, node status and expression of ER/PR/HER2 as prognostic indicators and generally must be used alongside such observations in cases of intermediate risk, to decide if additional chemotherapy is necessary [147]. Additionally, simple immunohistochemical tests such as IHC4+C , a 4 protein IHC test which takes clinical features into account, and measures ER, PgR, HER2 and Ki67, may be equally effective in predicting response to therapy whilst being much cheaper and easier to apply universally in the clinic [151, 152].

Thus, the stratification of breast cancer using multigene signatures has been shown to be useful in aiding treatment decisions in the clinic, but is currently limited in its uses. At present, these are only informative in ER-positive breast cancers, often placing the vast majority of ER-negative tumours in the high risk category and so providing no stratification in these cases [153]. Current efforts are focussed on devising better prognostic and predictive tests for other types of breast cancer, as well as developing tests capable of predicting outcome from specific chemotherapy drugs or regimens [143, 146, 154]. Finally, whilst the use of molecular stratification into intrinsic subtypes has itself changed little in the clinic, using such categorisation has provided researchers with a way to divide breast cancers into distinct categories allowing a more targeted approach to understanding the molecular biology of the disease [142].

Table 1.3: Prognostic and predictive gene signatures for breast cancer				
Test Name (Manufacturer)	**Assay (Platform)**	**Application**	**Results**	**Predictive value**
Mammaprint (Agendia) [155]	70 gene signature (Microarray)	ER-positive, node negative, stage I/II in women <61 years of age	Placing tumours into good or poor prognosis categories	Predicts response to chemotherapy in the poor prognosis group
Oncotype DX (Genomic Health) [156]	21 gene signature (qRT-PCR)	ER-positive, node negative, tamoxifen treated	Provides a recurrence score (0-100)	Predicts response to chemotherapy in those with a high recurrence score
PAM50 (Prosigna/Nanostring) [157]	50 gene signature (Nanostring platform)	Stage I-III post-menopausal women treated with endocrine therapy	Provides a risk of recurrence score, categorising patients into high, intermediate or low risk.	Predicts pathological complete response in patients treated with neoadjuvant chemotherapy
Endopredict (Sividon diagnostics) [150]	12 gene signature (qRT-PCR)	ER-positive patients treated with endocrine therapy	Provides a risk of recurrence score (0-15) with which patients are classified as high or low risk. This can be combined with tumour size and node status to provide the EPclin score.	Used to predict whether chemotherapy is necessary
Breast cancer index (BioTheranostics) [158]	7 gene signature (qRT-PCR)	ER-positive, node negative breast cancer	Provides a binary risk score of high or low for late distant recurrence	Predicts benefit of extended endocrine therapy (beyond 5 years)

Table 1.3: Prognostic and predictive gene signatures for breast cancer

A table showing various gene signatures which can be used as prognostic or predictive indicators for breast cancer, along with a description the various characteristics of each

1.5 Tumour microenvironment

Atmospheric oxygen concentration (approximately 21%, 160 mmHg), frequently referred to as 'normoxia', is not representative of the oxygen concentrations to which cells are routinely exposed when in their natural setting. True physiological oxygen concentrations ('physoxia') are known to be highly variable and tissue specific ranging from approximately 14.5% (110 mmHg) in the alveolar tissue of the lung, to around 4% in certain peripheral tissues [159]. Oxygen levels are further reduced in most solid tumours, falling below 2% in most cases [159]. The situation in breast tissue is no different; the median oxygen concentrations in healthy breast tissue has been shown to be approximately 6.8% (52 mmHg) [160-162], compared to a median of 1.3% (10 mmHg) in breast cancers, which exhibit oxygen concentrations below 0.33% (2.5 mmHg) in more than 60% of cases [160].

Hypoxia in tumours develops as the growing mass outstrips its blood supply. As the tumour outgrows its vasculature, cells distant from oxygen rich blood vessels become limited in their oxygen supply. This is often countered by an increase in angiogenic signalling in breast cancers [163], which promotes the formation of new blood vessels. However, new tumour vasculature tends to be poorly formed [164, 165]. Blood vessels in tumours are highly disorganised and contain a large number of morphological abnormalities including loss of vascular hierarchy, aberrant branching, and the formation of blind endings. In addition, vascular permeability increasingly results in 'leaky' vessels. In general, blood flow is poorly regulated through these vessels resulting in weak and unreliable blood perfusion. This means that low oxygen levels persist within the tumour [164, 165].

There is a well-established link between areas of hypoxia and poor outcome in breast cancer [162, 164, 166-169]. A contributing factor is the negative impact that hypoxia has on response to both radiotherapy and chemotherapy. Tumour hypoxia reduces the effectiveness of radiotherapy, as molecular oxygen and the generation of reactive oxygen species (ROS) are required for radiotherapy-induced DNA damage [170, 171], thus radiotherapy leads to fewer DNA double-strand breaks in hypoxic regions [171]. The lowered proliferative rate of cells in hypoxia also makes them less sensitive to accumulated DNA damage from both radiotherapy and DNA damage-inducing chemotherapeutic agents [171]. Furthermore, poor tumour perfusion as a result of malformed vasculature prevents the action of systemic chemotherapy agents which are unable to be delivered properly to the tumour area as a result of ineffective blood supply and high interstitial pressure [165]. In

addition to resistance to therapy, poor outcome has also been attributed to an increase in angiogenic and migratory phenotypes in hypoxia, resulting in increased invasion and metastasis [162]. Hypoxia is also thought to contribute to an increase in stem cell characteristics resulting in a larger stem cell population [172]. Many of these characteristics are thought to be driven predominantly through hypoxia-inducible factor (HIF) transcription factors [172, 173] and the role of HIFs in hypoxic breast cancers will be discussed below.

1.6 Hypoxia-inducible factors (HIFs)

1.6.1 HIF family and structure

The cellular response to hypoxia is predominantly mediated by a family of transcription factors called hypoxia-inducible factors (HIFs). Active HIF transcription factors are heterodimers which consist of a HIFα subunit bound to a HIFβ subunit [174]. There are three different HIFα proteins (HIF1α, HIF2α and HIF3α), all of which are quickly degraded in the presence of oxygen and only allowed to accumulate when oxygen is limited [175-179]. This oxygen-dependent degradation of HIFα forms the mechanistic basis for how the transcriptional response to hypoxia is regulated [180].

HIF proteins show a high level of homology and are characterised by the presence of a number of important functional protein domains (a comparison of HIF family protein domain structures is shown in Figure 1.4). Starting at their N-terminal ends all HIF proteins contain a basic helix-loop-helix domain (bHLH) followed by two PAS domains (PAS-A and PAS-B). These domains are required for HIF dimerization and are thus highly conserved between factors [176, 181]. HIFα subunits also contain an oxygen-dependent degradation domain (ODDD), required for the oxygen-mediated regulation of these factors, and transactivation domains important in regulating gene transcription. In HIF1α and HIF2α there are two transactivation domains, an N-terminal transactivation domain (N-TAD) nestled within the ODDD, and a C-terminal transactivation domain (C-TAD) near the C-terminus of the protein [180-182]. HIF3α is a truncated HIFα protein and thus only the N-TAD is present, with the C-TAD being replaced by a leucine zipper (LZ) domain [183].

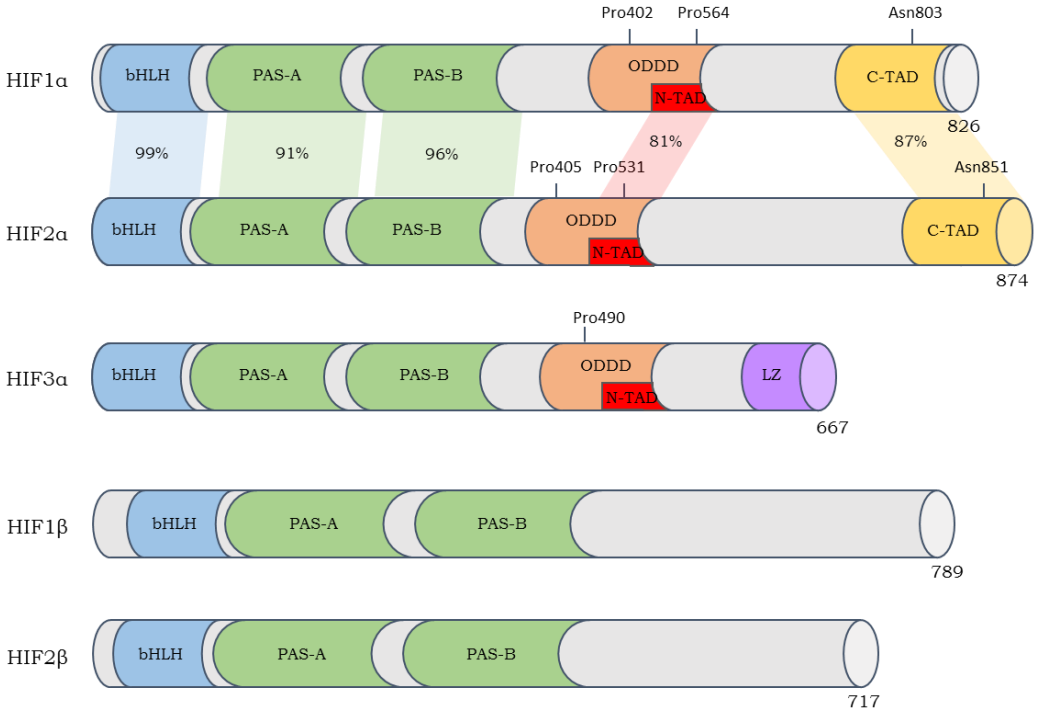

Figure 1.4: Hypoxia-inducible factor family domain structures

Basic structure of HIFα and HIF1β proteins showing the layout of functional domains. Important phosphorylation sites for oxygen dependent regulation are shown. Percentages show amino acid similarity between HIF1α and HIF2α for each domain. Amino acid length of each protein is shown on the right hand side. Each member of the family contains two Per-Arnt-Sim (PAS) domains, which allow the formation of alpha-beta dimers, and a basic helix-loop-helix domain which facilitates DNA binding. The HIFα proteins all contain an oxygen-dependent degradation domain (ODDD). HIF1α and HIF2α contain an N-terminal and C-terminal transactivation domain (N-TAD/C-TAD), whilst HIF3α has a truncated C-terminus containing a Leucine zipper (LZ) domain but lacking a C-TAD. .

The general functions of HIF proteins are reflected in their structures, HIF1α and HIF2α, which share the largest degree of homology, are together considered the predominant mediators of the cellular response to hypoxia, and drive a largely overlapping transcriptional programme [184]. HIF3α, which is truncated at its C-terminal end and therefore differs from HIF1α and HIF2α, has been understood to be a dominant-negative inhibitor of the other two HIFα proteins, acting as a form of negative feedback [183, 185-187]. This role of HIF3α has recently been challenged by the demonstration that HIF3α is also able to drive the transcription of a largely unique set of genes in response to hypoxia, and so

its contribution to the cellular response to hypoxia may be more complex than originally thought [185, 188]. The HIFβ subunits, otherwise known as aryl hydrocarbon nuclear translocator (ARNT) include two HIFα-binding proteins: HIF1β (ARNT/ARNT1) and HIF2β (ARNT2) [189]. HIFβ subunits are not regulated by oxygen concentration as they lack an ODDD, and instead are constitutively expressed even in normoxic conditions. In healthy adults, HIF1β is expressed in the vast majority of cell types, whilst HIF2β expression is strictly limited to renal and neural tissues. In breast cancer, HIF1β is therefore the typical binding partner for HIFα subunits [190, 191].

1.6.2 Canonical oxygen-dependent HIFα regulation

As mentioned above, the oxygen-dependent regulation of HIFα subunits is critical for their role as responders to hypoxia. Thus the molecular mechanisms involved in this regulation have been thoroughly investigated and are generally well understood. A schematic for this process is shown in Figure 1.5. In the presence of molecular oxygen, HIFα subunits are constantly degraded, denying them the chance to accumulate [192]. The degradation is mediated by the PHD (prolyl hydroxylase domain) family of prolyl hydroxylases, which use molecular oxygen and 2-oxoglutarate as co-substrates and ascorbate and iron as co-factors to attach a hydroxyl group to proline residues (P402 and P564 in HIF1α, P405 and P531 in HIF2α or P490 in HIF3α) in the ODDD [193-196]. Hydroxylation at these sites allows recognition by the VHL E3 ubiquitin ligase complex, which targets the HIFα proteins for proteasomal degradation by the attachment of multiple ubiquitin molecules [197-199]. In hypoxia oxygen is limited as a substrate and generally unavailable for the hydroxylation of HIFα by PHDs. The resulting failure of HIFα to be targeted for degradation leads to an accumulation of the protein, which at sufficient levels is able to dimerise with the constitutively present HIFβ subunit and relocate to the nucleus. In the nucleus, HIF dimers recognise a consensus sequence called a hypoxia-response element (HRE) and with the help of co-activator p300 are able to recruit the basal transcriptional machinery and drive gene transcription [200].

In addition to the PHD-mediated hydroxylation of proline residues in the ODDD, HIFα activity is also regulated by asparagine hydroxylation (N803 in HIF1α and N851 in HIF2α) in the C-TAD [201]. This process is catalysed by the factor-inhibiting HIF protein (FIH). Hydroxylation of asparagine at these residues can occur at lower oxygen concentrations than

PHD-mediated proline hydroxylation and so hydroxylation can still occur when oxygen levels are moderate. Asparagine hydroxylation in the C-TAD without proline hydroxylation does not result in protein degradation, but instead limits the transcriptional activity of the C-TAD, modifying HIF target gene transcription [181, 195]. The general role of PHD and FIH hydroxylation in HIFα regulation is summarised in Figure 1.6.

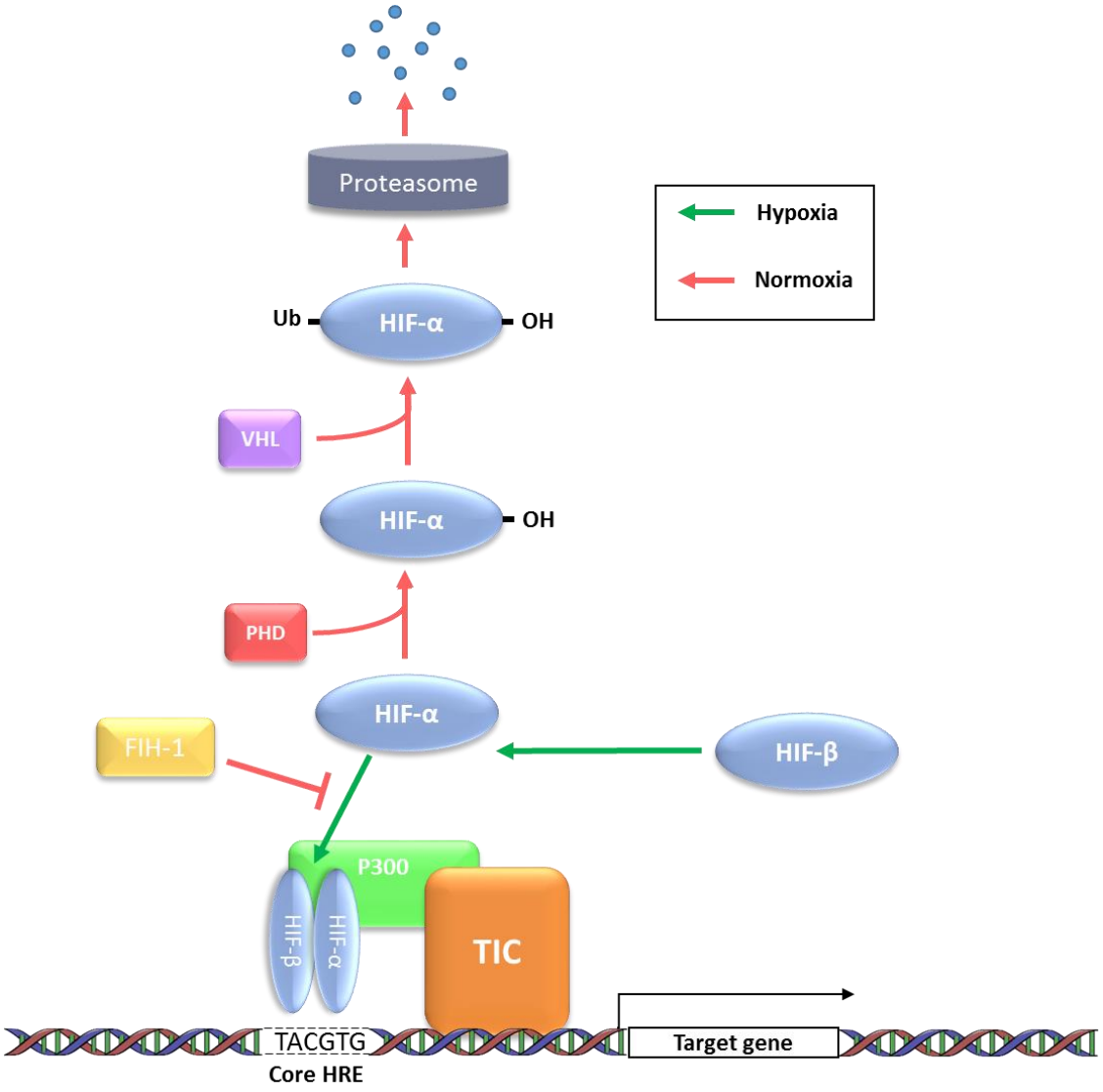

Figure 1.5: Canonical/oxygen-dependent regulation of HIFα proteins

A schematic of how HIFα proteins are regulated by oxygen concentration. Under high oxygen concentrations (red arrows), HIFα is hydroxylated both by FIH-1, which disrupts binding of co-activators CBP/P300 and inhibits transcriptional activity, and by PHD enzymes which promote binding and ubiquitination by the VHL E3-ligase complex, leading to the proteasomal degradation of HIFα. When oxygen is limited (green arrows), hydroxylation by FIH and PHDs is inhibited and HIFα is permitted to accumulate and bind co-activators, leading to the recruitment of the transcription initiation complex (TIC) and the initiation of the transcription of HIF target genes containing the HRE core HIF recognition sequence.

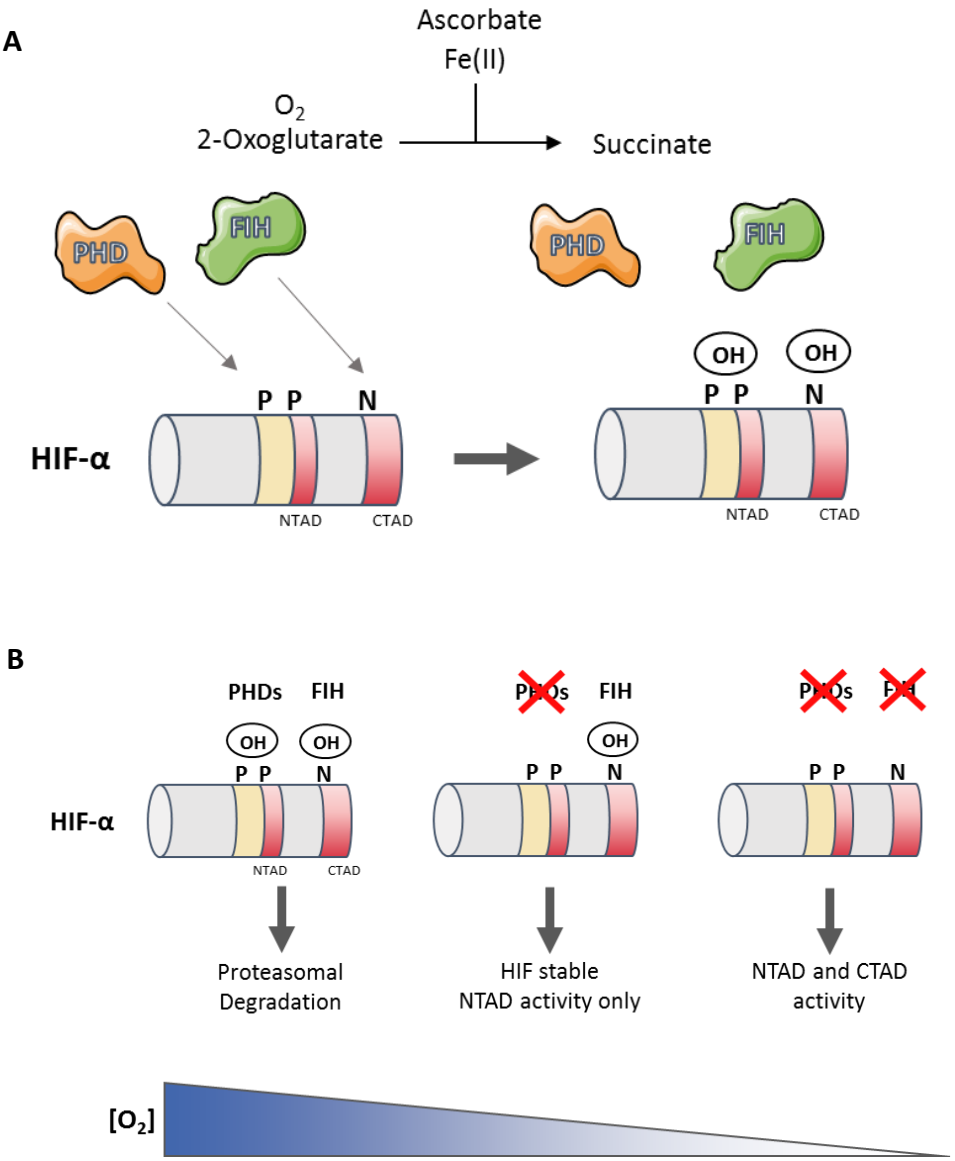

Figure 1.6: FIH and PHD-mediated regulation of HIFα proteins

A) PHD and FIH1 enzymes hydroxylate proline and asparagine residues on HIFα respectively. This reaction requires molecular oxygen and 2-oxoglutarate as co-substrates. 2-oxoglutarate is converted to succinate in this process. Ascorbate and Fe (II) are required as cofactors for the reaction. B) Differential oxygen requirements for prolyl and asparagyl hydroxylation by PHDs and FIH1 respectively allows regulation of HIFα over a gradient of oxygen concentration. Whilst complete hydroxylation at low oxygen inhibits HIFα, moderate oxygen allows only FIH-mediated hydroxylation only, inhibiting the C-TAD without tagging HIFα for degradation.

1.6.3 Non-canonical regulation of HIFα

Whilst the canonical oxygen-dependent regulation of HIFα proteins is considered the main HIF regulatory system, there are a number of non-canonical mechanisms which can also modulate HIFα levels in the cell. These include pathways affecting the stability and degradation of HIF1α protein, as well as pathways which modulate the translational and transcriptional rate.

Modulation of VHL-regulated HIFα protein stability

The rate of VHL-dependent degradation of HIFα subunits is influenced by a number of factors, some of which have been shown to contribute to HIFα dysregulation in cancers. Proteins osteosarcoma-9 (OS-9), spermidine/spermine-N-acetyltransferase 2 (SSAT2) and the pVHL-interacting de-ubiquitylating enzyme (VDU2) can all modify the rate of HIF1α ubiquitination and subsequent proteasomal degradation through various mechanisms. OS-9 has been shown to bind directly to HIF1α and PHD enzymes 2 or 3 to increase stability of the complex. This increases the rate of HIF1α proline hydroxylation thereby increasing the rate of recognition and binding by VHL [202]. Similarly to OS-9, SSAT2 is able to increase the rate of HIF1α degradation by stabilising HIF1α binding to the degradation machinery. In this case SSAT2 mediates the interaction between HIF1α, VHL and elongin C, promoting the ubiquitination of HIF1α through VHL [203]. VDU2 is currently the only known protein to de-ubiquitinate HIF1α [204]; in doing so it is able to rescue HIF1α from proteasomal degradation by removal of ubiquitin [205]. These studies demonstrate the complexity of regulation involved in the VHL-dependent degradation of HIFα subunits. Unfortunately, due to a lack of research into HIF2α at the time, none of these studies investigated whether these interactions were specific to different HIFα proteins or more generally applicable. Whilst these studies were effective in discerning some of the cellular mechanisms involved in HIFα regulation, they were performed in cell lines most amenable to HIF research, predominantly renal cancer cell lines, and so it is still unclear what role these mechanisms may play in breast cancer.

One VHL-modulating pathway which has been shown to be applicable to a number of cancers including breast cancer is the ubiquitin carrier protein (UCP). UCP has been shown to increase the levels of HIF1α by ubiquitinating VHL, leading to its proteasomal degradation [206]. UCP was therefore found to correlate inversely with pVHL in cancer cell lines, and was detected coincidentally with HIF1α in primary liver, colon and breast tumours [206]. Whilst

HIF2α was once again not included in this investigation, VHL downregulation would be presumed to cause an upregulation of all HIFα proteins, and so the importance of this regulatory mechanism in breast cancer may involve roles for both HIF1α and HIF2α.

VHL-independent regulation of HIFα protein stability

In addition to VHL-mediated degradation, studies have also shown that VHL-independent mechanisms exist to control the degradation rate of HIFα. One of these pathways involves the proteins 90 kDa heat shock protein (HSP90) and receptor of activated protein kinase C (RACK1), which are in competition with one another to bind HIF1α. RACK1 is also able to recruit components of the E3 ligase complex to HIF1α and promote its ubiquitination and proteasomal degradation without the requirement for PHD hydroxylation or VHL [207]. The competitive binding of RACK1 and HSP90 is the basis for HSP90 inhibitors as a therapeutic tool to inhibit HIF1. By inhibiting HSP90, RACK1-mediated degradation is allowed to proceed unhindered and HIF1α levels are reduced [207]. RACK1 activity can be inhibited through phosphorylation mediated by the calcium-dependent protein calcineurin A, thus providing a mechanism by which cellular calcium signalling can modulate HIF1α levels [208].

In addition to RACK1, the proteins glycogen synthase kinase 3β (GSK3β) and forkhead box-O-4 (FOXO4) have been shown to drive the degradation of HIF1α through VHL and oxygen-independent ubiquitination [209, 210]. Both of these factors are negatively regulated by AKT signalling, suggesting that growth factor signalling which has been shown to mediate HIF activity [211, 212] may act by inhibiting non-canonical degradation pathways. This may occur in concert with the effects that these signalling pathways have on HIF1α translation (discussed below).

Regulation of HIFα at the translational level

In addition to post-translational regulation of HIFα levels, it has been demonstrated that cells can control the level of HIFα by altering the rate of its translation. In general, cells appear to reduce protein synthesis in response to both acute and chronic hypoxia [213, 214]. Despite this, it has been noted that HIF1α translation can be increased under hypoxic conditions. Whilst the mechanisms controlling this are still subject to debate [204], work by Braunstein et al 2007 [215] demonstrated that the overexpression of 4E-BP1 and eIF4G in breast cancer can help mediate the increase in HIF1α and VEGF translation seen in hypoxia,

leading to increased expression of these proteins in breast cancer cell lines and increased angiogenesis in a mouse xenograft model of breast cancer.

In addition to increased translation in hypoxia, it has been demonstrated that HIF1α translation can also be induced by growth factor signalling. A large number of cytokines and hormones have been shown to regulate HIF1α in various ways [216]. These include insulin and interleukin-1β in a hepatoma cell line [212], insulin-like growth factor 1 in colon cancer cell lines [217], EGF in prostate cancer cell lines [218], and PTEN inactivation in glioblastoma cell lines [211], all of which have been shown to increase HIF1α levels through increased translation via MAPK or PI3K/AKT signalling pathways [219]. In breast cancer, it has been shown that treatment with HER3 growth factor ligand neuregulin-1β can also increase the translation of HIF1α in MCF7 cells in a PI3K, AKT and mTOR-dependent manner [220].

Regulation of HIFα at the transcriptional level

Despite the large amount of research into post-transcriptional regulation of HIFα proteins, surprisingly little is known about how they are transcriptionally regulated. *HIF1A* gene transcription has been shown to increase in response to hypoxia in a number of contexts, however this is considered to play a minor role in HIF1α regulation when compared to the canonical post-translational mechanisms described above [221]. In normoxia a number of factors have also been shown to drive *HIF1A* gene transcription; mechanical stress, reactive oxygen species (ROS), and vascular agonists such as angiotensin-II, thrombin and VEGF are all able to induce HIF1α in endothelial or smooth muscle cells [222-224]. In the context of cancer certain cytokines have been shown to regulate *HIF1A* expression, this includes IL-8 in melanoma and hepatocyte growth factor (HGF) in both liver and certain breast cancer cell lines [225]. Additionally, the ability of NF-κB signalling to drive *HIF1A* gene expression has been well established [225-227].

Research into the non-canonical regulation of HIFα has focussed almost exclusively on HIF1α, and it is still unclear in most instances whether the same or equivalent mechanisms regulate HIF2α levels. Additionally, whilst our knowledge of HIF1α regulation has vastly improved, our understanding of how these factors interact to modulate HIF1α in breast cancer is still not clear. One recurring theme, seen at the transcriptional, translational and post-translational levels of regulation, is the involvement of cytokine and growth factor signalling, predominantly through PI3K/AKT or MAPK signalling pathways, which indicates

that perturbations to these pathways which are often seen in cancer, can have an effect on the non-canonical regulation of HIFα subunits.

1.6.4 Differential roles of HIF1 and HIF2

Due to lack of research, our understanding of HIF2α regulation is limited in comparison to HIF1α. However, now that the differences between HIF proteins are being increasingly recognised, more research is being published on how these factors differ in terms of their roles and their regulation.

Differences between HIF1α and HIF2α have been noted in a number of functional knock-out studies which assessed the effects of reducing the expression of individual HIFs on development and tumorigenesis. Such studies were able to demonstrate specific roles in embryogenesis [228], haematopoiesis [229], vascular remodelling [230], stem cell maintenance [231], and roles in tumour growth [232-235] for different HIFα proteins. To understand these functional differences, especially in terms of tumorigenesis, a number of studies have assessed the differences in cellular roles of HIF1 and HIF2 transcription factors and have successfully demonstrated that HIF1 and HIF2 drive the transcription of unique targets with differing roles in cancer pathogenesis. HIF1 has been shown to uniquely regulate cellular metabolism in response to hypoxia through the upregulation of a number of glycolysis genes (e.g. *PGK1*, *LDHA* and *PKM*). Whilst HIF2 does not drive the upregulation of these genes, it has been shown to uniquely upregulate genes such as *CCND1*, *TGFA*, *EPO* and *OCT4* [231, 235-238]. In breast cancer, the targets of HIF1 and HIF2 transcriptional activity have been investigated in studies by Mole et al. 2009 [239] and Schödel et al 2011 [240], who were able to use genome-wide chromatin immunoprecipitation of HIF1α and HIF2α in MCF7 cells to identify HIFα binding sites. This research was able to demonstrate a non-redundant role for these factors in this cell line, showing an increased role for HIF1 in driving genes involved in glycolysis and carbohydrate metabolism and a specific role for HIF2 in driving Oct4-regulated pluripotency genes in concordance with previous findings in other cell types [239, 240]. Despite differences in target selection by HIF1 and HIF2, high-resolution genome-wide mapping of HIF binding sites by Schödel et al. [240] was also able to demonstrate that both HIF1 and HIF2 bind to the core HRE RCGTG motif, with no discernible consensus sequences specific to either factor. This suggests that differential target selection by these factors is not mediated by differences in direct DNA binding sites. Instead target specificity is

thought to be controlled, at least in part, by differences in the N-TAD (but not the C-TAD) [241, 242] and differential co-factor association with HIF1α and HIF2α [242, 243].

In addition to differences in target gene transcription, HIF1α and HIF2α have been shown to have different, even opposing, interactions with important mediators of cancer pathogenesis such as Myc, P53 and mTOR signalling. Myc controls cellular proliferation by regulating G1/S phase transition and is commonly overexpressed or otherwise upregulated in various cancers. HIF1α is able to facilitate cell cycle arrest by inhibiting MYC transcriptional activity under hypoxic conditions [244]. This inhibitory role is seen in both acute hypoxia, where HIF1α can rapidly disrupt the association of MYC with its transcription factor binding partner MAX [245], and in chronic hypoxia, where HIF1α drives the expression of MAX interactor 1 (MXI1) to displace MAX from MYC and also directly promotes the degradation of MYC itself [246, 247]. In contrast HIF2α has been shown to increase MYC promoter occupancy and transcriptional activity, promoting cell cycle progression in hypoxic cells. This is believed to be mediated by direct interactions between HIF2α and MAX which stabilises MYC-MAX binding [248, 249].

P53 is a tumour suppressor gene commonly mutated in cancers and an important driver of genes involved in DNA repair and the maintenance of genome integrity under cellular stress [250, 251]. HIF1α and HIF2α have also been demonstrated to have opposite effects on its stabilisation and activity in response to hypoxia. HIF1α has been shown to stabilise p53 in response to hypoxic stress by binding to the p53-targeting ubiquitin ligase MDM2. This inhibits p53 ubiquitination and thereby protects it from the proteasome degradation pathway [252, 253]. In contrast HIF2α has been shown to both reduce p53 stability and transactivation and to increase the expression of MDM2 through HIF2 target genes TGFα and PDGF (demonstrated in RCC cells [254, 255]).

Finally, mTOR signalling, which regulates protein synthesis in response to nutrient and growth factor availability, can be differentially regulated by different HIFα proteins. HIF1α has been shown to drive the expression of DDIT4 and BNIP3, which inhibit mTORC1 activity through different mechanisms [256, 257], but HIF2α promotes mTORC1 activity through the HIF2 target gene RB1CC1, which inhibits the TSC1-TSC2 mTORC inhibitory complex [258]. Whilst research into these roles of HIFs in regulating such pathways has focussed on their roles in RCC, the general applicability of defects in Myc, p53 and mTOR

signalling to numerous if not all cancer types suggests that these interactions are important when considering the roles of HIF1α and HIF2α in the context of breast cancer.

1.6.5 Differential regulation of HIF1α and HIF2α

The emerging differences in the roles of HIF1α and HIF2α, especially in cancer, has led to an increase in research aiming to understanding how these two proteins may be differentially regulated. Whilst our understanding is far from complete, a number of regulatory mechanisms have been identified which can equip cells with the tools to individually regulate different HIFα proteins activity.

Temporal control of HIF1α and HIF2α by HAF

Whilst the canonical, oxygen-dependent regulation of HIF1α and HIF2α has generally been shown to work through the same pathway [259, 260], it has been observed that HIF2α is stabilised in more moderate oxygen concentrations (2-5%) when compared to HIF1α (0-2%), and in a number of different cell types HIF2α upregulation is maintained over a longer time period than HIF1α [249, 261]. These differences are believed to reflect the varying roles which these two factors play, with HIF1α mediating an immediate hypoxic response and HIF2α helping cells to survive in long term hypoxia. Differences in the oxygen tensions required for the activation of HIF1α and HIF2α are thought, at least in certain contexts, to be mediated by a slight preference of FIH towards HIF1α asparagine hydroxylation [262]; the less stringent hydroxylation of HIF2α allows it to become transcriptionally active at higher oxygen tensions. These differences are also mediated by regulators of degradation; HIF-associated factor (HAF) is a protein with E3-ubiquitin ligase activity which has been shown to mediate ubiquitination and subsequent proteasomal degradation of HIF1α independent of HIF1α prolyl hydroxylation [263]. The ubiquitin ligase activity of HAF has been shown to be specific to HIF1α, as it is unable to ubiquitinate HIF2α. However, HAF has been shown to bind to the carboxy-terminal end of HIF2α and promote its transcriptional activity [264]. HAF expression has been shown to decrease in acute hypoxia but increase with prolonged exposure, suggesting that HAF may act to switch cells from a HIF1α-governed acute hypoxic response into a HIF2α-governed response to chronic hypoxia [265]. Similarly, the Int6 gene is an E3 ubiquitin ligase found to have specific activity for HIF2α, driving VHL and oxygen-independent degradation in a similar way to HAF. Int6 was originally discovered as an insertion site for the mouse mammary tumour virus, suggesting that Int6 loss-of-function may drive breast cancer tumorigenesis, potentially through HIF2α stabilisation [266-269].

The precise role of Int6 in HIFα regulation is unknown and more research is required. However, it seems likely that the HIF2α specific activity will allow Int6 to act in opposition to HAF, and it may function to inhibit early upregulation of HIF2α in response to acute hypoxia.

Differential regulation by PHD enzymes

As mentioned above, the PHD enzymes are the oxygen-dependent hydroxylases responsible for canonical HIFα regulation. The PHD family of prolyl hydroxylases includes 3 members: PHD1, PHD2 and PHD3 (also known as EGLN2, EGLN1 and EGLN3 respectively). It has been shown that PHD family members can differ in their activity towards HIF1α or HIF2α, providing an important level of regulation that can be applied individually to different HIFα proteins.

It has been previously described that PHD2 plays the central role in the normoxic regulation of HIF1α [270], and by using siRNA specific to PHD1, 2 or 3 to assess the subsequent upregulation of HIF1α and HIF2α in MCF7 cells, Appelhoff et al. [196] demonstrated that HIF1α is most strongly induced by the reduction of PHD2 compared to PHD1 or PHD3, confirming this result. In addition, they were able to show that PHD2 inhibition had a smaller effect on HIF2α, whereas PHD1 or PHD3 knockdown was more effective in the upregulation of HIF2α over HIF1α. Under hypoxic conditions (48 hrs, 1.5% O_2), they demonstrated a lone capability of PHD3 knockdown to further upregulate HIFα subunits. This effect was predominantly on HIF2α, suggesting a specific role for PHD3 in keeping HIF2α regulated even under hypoxia.

As well as being important regulators of HIFα level, it is now known that PHD proteins can themselves be induced by hypoxia, allowing a form of negative feedback. In general PHD1 is considered non-hypoxia inducible [196, 271], whereas PHD2 and PHD3 are both upregulated. Interestingly, the level by which PHD2 and PHD3 are induced by hypoxia appears cell line dependent, and even between breast cancer cell lines there appears to be a distinction between lines which strongly upregulate PHD2 and those which more highly upregulate PHD3 in response to hypoxia [196]. Aprelikova et al. [271] examined the HIF-mediated regulation of these 2 PHD enzymes in hypoxia and demonstrated differential roles for HIF1 and HIF2. Upregulation of PHD3 was inhibited by the knockdown of either HIF1α or HIF2α by siRNA. On the other hand, PHD2 upregulation was affected only by HIF1α knockdown, not HIF2α, and was only reduced at longer hypoxic time points. This suggested the hypoxia-induced increase in PHD2 noted at the earlier time point may be both HIF1α and

HIF2α independent but that HIF1α may play a role in the longer term induction of PHD2. It has also been shown that the overexpression of stable forms of HIF1α and HIF2α (mutated at proline 564 and 531 respectively) in HEP3B cells was enough to upregulate PHD3 transcription, with HIF2α having a more prominent effect than HIF1α. In addition to this, it was shown in the 786-0 renal cell line, which does not express HIF1α, that PHD3 was downregulated by the expression of active VHL (but not an inactive form) and could also be upregulated in hypoxia, suggesting that in this cell line at least, PHD3 upregulation by both mechanisms is mediated by HIF2α. Whilst not performed in breast cancer cell lines, these experiments demonstrate that the regulation of HIFα subunits and PHD proteins is bidirectional and the hypoxic regulation of PHDs probably works to ensure a quick turnover of HIFα subunits upon reoxygenation. Interestingly an affiliation seems to exist between specific HIF and PHD proteins in both directions, and such specific regulation probably works to balance the relative activities of HIF1 and HIF2 in response to hypoxia in different cellular contexts.

Investigation into different PHD proteins *in vivo* has shown that expression can have implications for prognosis. PHDs 1, 2 and 3 have all been shown to be overexpressed in breast cancer [272-274]. However, the specific functional and pathological roles of individual PHDs is still not particularly well understood, and whilst PHD2 expression and nuclear localisation have both been associated with tumour aggressiveness and poor clinical parameters [275, 276], little has been reported on the pathological consequences of PHD1 or 3 expression [272].

Research suggests that the relative expression of PHDs can vary in breast cancer and is highly dependent on cellular context. Analysis of Affymetrix microarray data alongside immunohistochemical analysis of 129 breast cancer samples shows an interesting relationship between ER and HER2 levels with PHD expression. PHD1 is more highly expressed in ER-positive samples (agreeing with previous findings that PHD1 is oestrogen-inducible [277]), PHD2 is more highly expressed in ER-negative/ HER2-negative samples and PHD3 is higher in the ER-negative, HER2-positive samples [278, 279]. This shows that intrinsic subtypes may correlate to specific PHD expression but it still remains to be seen whether this has direct implications for the activity of HIF1 and HIF2 in breast cancer subtypes.

PHD enzymes and HIF activity act to regulate one another and form a feedback loop which ensures a suitable response to hypoxia. However, non-redundancy between PHD

proteins and their preferential regulation of HIF1α or HIF2α means that the expression of these enzymes may determine not only the basal level of either HIF1α or HIF2α in normoxia but also their specific regulation under hypoxia. Such differential expression has been shown to exist in breast cancer, and correlation with important drivers such as ER and HER2 suggests that molecular subtype may play an important role in this.

Differential regulation of translation

Another important difference between the regulatory mechanisms of HIFα proteins comes in the form of differential translational control. It has been shown that HIF2α mRNA, but not HIF1α, contains an iron response element (IRE) in the 5' untranslated region of the transcript, and that IRE binding protein 1 (IREBP1) is able to bind the IRE and inhibit the translation of HIF2α mRNA. IREBP1 is unable to bind HIF1α mRNA and thus confers a specific mechanism of regulation onto HIF2α. IREBP binds IREs in mRNA transcripts when iron levels are low, and it is suggested that this mechanism may underpin the specific role of HIF2α in the regulation of erythropoiesis and cellular iron metabolism [249, 280-282]. The role of IREBP1 in HIF2α-specific inhibition is the basis for the action of HIF2α targeting compound C76 discussed below (in Section 1.7.3) [283].

1.6.6 Expression of HIF1α and HIF2α and their roles in breast cancer

HIF1α

With the role of hypoxia in driving breast cancer being well-recognised (Section 1.5), a number of studies have aimed to assess the levels of HIFα expression in breast cancer, as well as its association with survival, metastasis and the expression of other known drivers of the disease. As with the majority of HIF research in breast cancer, this has been focussed on HIF1α. The levels of HIF1α expression seen in breast cancer vary from study to study, as a result of differences in methodology and sample selection. In a large retrospective analysis of 745 patients performed by Dales et al. in 2005 [284] HIF1α expression was observed in all samples, but was found to be highly variable between tumours, with a larger degree of spatial heterogeneity within tumour samples; a median value HIF1α expression was seen in 16.32% of cells [284]. In line with the role of hypoxia, HIF1α expression has been shown to correlate with poor survival in a number of studies. This includes association with overall survival [284-286], recurrence/disease-free survival [285-290] and distant-metastasis-free survival [287,

290]. HIF1α has also been associated with tumour size, grade [289, 291], treatment resistance [288] and the expression of Ki67 [285, 289, 291], cyclin D1 [289] and known hypoxic cancer drivers including VEGF [285, 291], GLUT1 [292] and CAIX [290, 292]. Interestingly, HIF1α has also been shown to correlate with HER2 expression in a number of breast cancer studies [285, 289, 291, 293]. The relationship of HIFs and HER2 will be discussed in more detail in Section 1.9.

Mechanistically, HIF1α has been shown to play multiple roles in breast cancer pathogenesis, acting to drive angiogenesis [294], metastasis [295], stem cell characteristics [296] and resistance to both endocrine and chemotherapy [297, 298].

Hypoxia is understood to be a key regulator of angiogenesis. This is thought to be mediated predominantly through HIF1α-driven VEGF expression [294] and as such HIF1α expression has been correlated with both VEGF expression and increased microvessel density in breast cancer [299].

In terms of metastasis, a number of mechanisms have been discovered which allow HIF1α to drive this process in breast cancer. This would clearly have an impact on breast cancer pathogenesis as over 90% of breast cancer deaths are attributable to metastasis [295]. Epithelial-to-mesenchymal transition (EMT) can be regarded as an initial step of metastasis [300, 301]. During EMT, cells lose cell-cell contacts by reducing their expression of E-cadherin and claudins, resulting in changes to cell morphology and increased motility as well as a propensity to detach from the tumour mass [295]. HIF1 activity has been shown to drive EMT through the upregulation of EMT transcription factors SNAIL, ZEB1, TWIST and TCF3 [302, 303]. With regards to breast cancer it has been shown that exposure to hypoxia can cause an EMT phenotype in MDA-MB-468 cells through ZEB1 expression [304], but this was not directly attributed to HIF1 activity. The process of metastasis also involves cells acquiring the capability to invade locally, move into blood vessels (intravasation), exit blood vessels at a new site (extravasation) and settle successfully in the metastatic location. Interestingly, HIF1 driven gene expression has been shown to promote each of these processes in breast cancer. HIF1 has been shown to drive extra cellular matrix (ECM) remodelling through the expression of matrix metallo-proteinases MMP-2 and MMP-9 [302, 305] and collagen biosynthesis enzymes P4HA1 and P4HA2. MMPs degrade components of the ECM, facilitating local cancer invasion, and have been correlated with increased rates of metastasis in breast cancer [306-308], whilst pro-collagen prolyl hydroxylases P4HA1 and P4HA2 are required for collagen

deposition and metastasis in breast cancer [309]. Extravasation in breast cancer has also been shown to be enhanced by HIF1 [310], and is mediated through the increased expression of angiopoietin-like 4 (ANGPLT4), a secreted factor known to increase vascular permeability, and its expression has been associated with increased lung metastasis in breast cancer [311]. Finally, HIF1 supports metastasis in breast cancer by driving the expression of lysyl oxidases LOX, LOXL2 and LOXL4. LOX enzymes have been shown to remodel the ECM, not only at the primary tumour site, but additionally at distant sites. These secreted factors contribute to the formation of a breast cancer premetastatic niche and have been associated with hypoxic regions and metastasis in breast cancer [312-315].

In addition to the direct role of hypoxia in resistance to cancer therapies discussed above, HIF1 has been shown to mediate resistance to treatment in breast cancer. Using a mouse mammary tumour model, Moeller et al. [316] were able to demonstrate that HIF1 is upregulated by reactive oxygen species during tumour reoxygenation after radiotherapy. In this context, HIF1 drives the expression of VEGF which contributes to cell radioresistance. HIF1 has also been shown to mediate hypoxia-induced resistance to chemotherapeutic agents in MDA-MB-231 triple-negative breast cancer cells by protecting cells against drug-induced senescence [317]. In addition, Samanta et al. [297] were able to show that treatment of triple-negative breast cancer cells with paclitaxel or gemcitabine lead to an increase in HIF expression and activity, promoting stem cell characteristics which contribute to therapy resistance.

Finally, HIF1 activity promotes breast cancer pathogenesis by promoting a stem cell phenotype. Breast cancer stem cells possess the capacity for continuous self-renewal and ability to form secondary tumours [296]. Hypoxia has been shown to induce a breast cancer stem cell (BCSC) phenotype in breast cancer cells, mediated by HIF1, and which drives the expression and activity of TAZ, a transcriptional co-activator which promotes the BCSC phenotype. HIF1 drives TAZ both directly through increased transcriptional activity and indirectly through the expression of SIAH1, which promotes the degradation of TAZ inactivating kinase LATS2 [318].

HIF2α

In contrast to HIF1α, the roles of HIF2α in breast cancer pathogenesis have not been extensively studied. Whilst subject to far fewer studies, HIF2α, like HIF1α, has been shown to correlate with pathological variables in IHC analysis of patient breast cancer samples. An early

study which compared HIF1α and HIF2α expression in a series of cancer types, including breast cancer, was able to demonstrate important differences between the two proteins [319]. HIF1α and HIF2α were both found to be highly expressed in breast cancer, with higher staining seen at peri-necrotic regions where oxygen levels are likely to be low. However, HIF1α and HIF2α were not expressed in matching regions, with HIF2α less restricted to peri-necrotic zones. In addition, this study demonstrated the increased expression of HIF2α but not HIF1α in tumour associated macrophages (TAMs), which was later shown to be associated with tumour vascularisation and grade [319, 320]. This led to subsequent studies which focussed on the role of HIF2α expression in breast cancer survival. In 2006, a study by Giatromanolaki et al. [321] found strong expression of HIF2α protein in 35.9% of samples (n=62) and demonstrated that HIF2α expression was associated with increased vascular density and nodal status, suggesting that HIF2α expression is a driver of angiogenesis and metastasis in breast cancer. This pathological role for HIF2α was supported by a study by Helczynska et al. in 2008 [261], which used a tissue microarray containing 512 patient samples to correlate HIF1α, HIF2α and VEGF expression to clinical parameters. They demonstrated that whilst overlap between HIF1α and HIF2α was not significant, both were individually associated with increased VEGF expression. Despite this, only HIF2α demonstrated an association with survival, being an independent prognostic factor for recurrence-free and breast cancer-specific survival.

Mechanistically, less is understood about how HIF2α drives breast cancer pathogenesis. However, a number of genes known to be drivers of breast cancer progression have been shown to be HIF2α targets in other cell types. Like HIF1, HIF2 is also known to drive VEGF expression, which, in line with the clinical studies discussed above, provides a mechanism by which angiogenesis can be driven by either factor [322]. HIF2 has also been shown to increase the expression of key drivers of metastasis including TWIST1, LOX and CXCR4 [312, 322-324], and work by Aprelikova in 2006 [243] was able to demonstrate a HIF2α specific role in amplifying the expression of a number of important genes in MCF7 cells. This includes *IGFBP3*, *EFNA1*, *LOXL2* and *HEY1*, which have been shown to increase premenopausal cancer risk, tumour growth, invasion, and EMT in breast cancer respectively [325-328]. The HIF2α driven expression of these genes was shown to depend on ETS-1 as a co-activator, implicating a role for ETS family transcription factors in HIF target selection in breast cancer [243, 329]. Finally, HIF2α is understood to have an important role in promoting stem cell characteristics, such as the increased expression of pluripotency regulator Oct4

[231, 330]. Hypoxia has been shown to promote a dedifferentiated state and stem cell characteristics, and roles for both HIF1 and HIF2 in this process have been demonstrated in breast cancer [331, 332]. In a 3D cell line model of glioblastoma a switch from HIF1 to HIF2 signalling mediated by HAF has been associated with the enrichment of the stem cell population, suggesting that this phenotype may be favoured by HIF2 [264].

1.7 Targeting hypoxia-inducible factors for cancer therapy

Given the role of both HIFs and the hypoxic microenvironment in driving both breast cancer pathogenesis and resistance to therapy, targeting these mechanisms offers a promising approach for cancer therapy. Generally, this has been approached in two ways; targeting cells in hypoxia using hypoxia-activated prodrugs, and targeting hypoxia-inducible factor activity [333].

1.7.1 Hypoxia-activated prodrugs

Hypoxia-activated prodrugs are inactive (or relatively low toxicity) compounds which are converted to cytotoxic agents only in hypoxic tissues [334]. This can be achieved, for example, as prodrugs are constantly reduced by cellular reductases to produce a molecular intermediate, which in the presence of molecular oxygen is oxidized back into its prodrug form. When oxygen is limited, the intermediate is not oxidized and instead is converted into its active cytotoxic form, producing a build-up of this compound selectively in hypoxic tissues [333-335]. A number of hypoxia-activated prodrugs have been assessed in clinical trials for a several cancer types [333]. Whilst trials with some compounds have produced disappointing results [336, 337], these have resulted in the development of second generation molecules with improved activity [338], or in the case of apaziquone treatment (EO9) in bladder cancer, adjustment of treatment delivery to promote improved activity [333]. Another hypoxia-activated prodrug, evofosfamide (TH-302), has shown more success in clinical trials, demonstrating efficacy when used in combination with gemcitabine in pancreatic cancer or with doxorubicin in soft tissue sarcoma in phase II clinical trials [339, 340]. In both cases phase III trials have been completed and are awaiting the publication of results (NCT01440088 and NCT01746979). TH-302 has been tested in preclinical models of breast

cancer, where it was shown *in vivo* to reduce mammary tumour growth in combination with paclitaxel [341].

1.7.2 HIF inhibitory compounds

Whilst targeting hypoxia with prodrugs is an attractive strategy, many research studies have assessed the potential of inhibiting HIF signalling directly. As discussed above, HIF is a key regulator of hypoxic cell survival and cancer pathogenesis, and so direct inhibition of HIF activity offers a means to target cancer cell survival in the hypoxic microenvironment and also reduce invasion and angiogenesis driven by HIFs in hypoxia. Early experiments into the effects of HIF1 inhibition using dominant negative constructs were able to demonstrate that reduction in HIF1 activity could reduce tumour growth in pancreatic, colon and breast cancer xenograft models [342-344]. This led to screens for HIF1 targeting compounds and the further development of a large number of molecules shown to perturb HIF1 activity [344, 345], and resulted in clinical and preclinical investigations into a diverse set of HIF1 inhibiting compounds, most of which have an indirect effect on HIF1, and some of whose mechanism of action is still unknown.

HSP90 inhibitors

As discussed in Section1.6.3, inhibition of HSP90 can lead to degradation of HIF1α through RACK1-mediated ubiquitination [207]. As such, compounds which inhibit HSP90 can also be used to target HIF1α for cancer therapy. The first generation HSP90 inhibitors were developed from the natural compounds Geldamycin (GD) (isolated from *Streptomyces hygroscopicus*), or Radicicol (RD) (isolated from *Monocillium nordinii and Monosporium bonorden*) [346]. GD and its derivatives 17-AAG and 17-DMAG have demonstrated promising anticancer activity in phase I, II and III trials [346]. Most notably for breast cancer, 17-AAG was shown to have good tolerability and antitumour activity in combination with trastuzumab in HER2-positive breast cancer refractory to trastuzumab alone [347]. Despite this, these compounds have not been developed further [346]. RD derivatives KF55823 and KF25706 were also well-tolerated and demonstrated anti-tumour efficacy in xenograft models of human breast and colon cancer [348], but have not yet reached clinical trials. The development of second generation HSP90 inhibitors now aims to develop similar compounds without the solubility and toxicity issues associated with compounds of this class [346]. One

particularly promising second generation HSP90 inhibitor for the inhibition of HIF1α is EC154. Initial *in vitro* experiments demonstrated the ability of EC154 to inhibit HIF1 and HIF2 activity at concentrations 10-fold lower than 17-AAG [349]. Whilst the further development of such inhibitors seems a promising option for cancer therapy, the mechanisms of action are still not entirely clear. As a chaperone protein, HSP90 has a number of client proteins, many of which will be affected by this class of inhibitor. Thus understanding in more detail the cellular effects of HSP90 inhibition may help elucidate which patients could benefit from their use.

Histone deacetylase (HDAC) inhibitors

A number of histone deacetylase inhibitors exist and have already been FDA approved for the treatment of various cancers where they have been shown to generally lead to inhibition of tumour growth and apoptosis [350]. In breast cancer a number of HDAC inhibitors such as SAHA (vorinostat, Zolinza), trichostatin A and etinostat have been shown to be effective in preclinical models of breast cancer, and are able to reduce proliferation, induce apoptosis and inhibit EMT in breast cancer models [350]. Whilst in a phase II study in metastatic breast cancer, SAHA showed only modest effects [351], etinostat has shown significantly improved recurrence-free survival in metastatic ER-positive breast cancer resistant to aromatase inhibition when used in combination with exemestane [352]. HDAC inhibitors have been shown to inhibit HIF1α translation and promote degradation [353], but it is still unclear whether their HIF inhibitory actions are responsible for their efficacy in breast cancer.

Topoisomerase I inhibitors

FDA-approved topoisomerase I inhibitors irinotecan and topotecan have been shown to possess HIF inhibitory activity. Topotecan is an inhibitor of HIF1α translation [354-356], and has been shown clinically to reduce HIF1α expression as well as VEGF and GLUT-1 levels in a small pilot study of matched tumour samples [357]. PEG-SN38, a solubilised metabolite of irinotecan, has been shown to effectively reduce the expression of both HIF1α and HIF2α in a neuroblastoma model [358] and demonstrated low toxicity in a phase I trial in neuroblastoma [359]. Whilst limited work on the efficacy of topoisomerase I inhibitors has been conducted in breast cancer, their efficacy in other tumour models and their ability to inhibit HIF1α and HIF2α suggests that they could be a useful tool in targeting HIF-driven breast cancer progression.

Cardiac glycosides

Cardiac glycosides are a family of drugs including the well characterised compounds digoxin and digitoxin, commonly used for the treatment of cardiac congestion and arrhythmias [360]. A role for cardiac glycosides has been demonstrated in breast cancer where digitalis has been shown to improve patient survival and reduce malignant characteristics in studies undertaken as far back as the 1970s [361-363]. In 2008 Zhang et al. [364] were able to demonstrate that a number of cardiac glycosides, including digoxin, ouabain and proscillaridin were able to inhibit HIF1 gene transcription in Hep3B cells. In addition, they demonstrated that ouabain and proscillaridin were able to reduce both HIF1α and HIF2α protein levels, while digoxin inhibited tumour growth *in vivo*, an effect which was inhibited by the enforced expression of HIF1α. Whilst the mechanisms by which cardiac glycosides inhibit HIF proteins is still unknown, their effect on HIFs offers a novel mechanism for their anticancer activity. A phase II trial to investigate the effects of digoxin treatment on HIF1α expression in breast cancer prior to surgery is currently underway (NCT01763931) [333].

2ME2 and analogues

Potentially one of the more promising sets of HIF inhibitors are 2-methoxyestradiol (2ME2, Panzem) and its analogues. 2ME2 is an oestrogen metabolite which both targets microtubules, promoting mitotic arrest, and inhibits the translation of HIF1α [333, 365]. This inhibition of HIF1α resulted in the downregulation of VEGF in prostate and breast cancer cells and a reduction in tumour growth and angiogenesis in an orthotopic breast cancer model [365]. 2ME2 has also been shown to reduce HIF2α levels in hepatocellular carcinoma, while overcoming resistance to the TKI inhibitor sorafenib [366]. ENMD-1198 is a more recently developed 2ME2 analogue which has been selected as the most promising 2ME2 analogue in development [367]. ENMD-1198 was found to be well-tolerated in a phase I dose-escalation study [368], whilst the tolerability and effectiveness of 2ME2 has been demonstrated in phase I and II studies [333].

Chemotin

Chemotin is a naturally occurring fungal metabolite found to inhibit HIF by preventing transcriptional activity of the HIF C-TAD through the inhibition of HIF-p300 interactions [369]. This was shown to inhibit p300 binding to both HIF1 and HIF2, reducing both VEGF expression

and proliferation in colorectal carcinoma cell lines [370]. Whilst the high toxicity of chemotin precludes its clinical utility [333], similar natural compounds gliotoxin and chartocin have been shown to have antiproliferative effects in prostate cancer xenograft models, and appear to work through the downregulation of a number of HIF1 genes [371].

YC-1 and its analogues

YC-1 also appears to be a promising compound for HIF targeted cancer therapy despite its mechanism of action being unclear. YC-1 is an activator of soluble guanylate cyclase, but has been shown to inhibit HIF activity via a mechanism independent of this action. The effects of YC-1 on HIF seem to be mediated at multiple levels as YC-1 is able to decrease EPO and VEGF through reduced levels of HIF1α protein and by reducing DNA binding [372], whilst also inhibiting HIF1 activity by preventing interactions with p300 [373]. Although these investigations have focussed on HIF1, the downregulation of EPO suggests that HIF2 may also be affected [374]. YC-1 has been shown to inhibit cell motility in preclinical models of various cancers [375] and has HIF1 inhibitory effects as well as anti-angiogenic and anti-tumour effects in xenograft models of liver, stomach, kidney, cervical and brain cancers [376]. YC-1 has not been tested in any clinical trials, but second generation analogues for the inhibition of HIF1 activity have been synthesised and are currently under preclinical evaluation [377].

More specific inhibition of HIF1α

Whilst the majority of the inhibitors discussed so far have indirect mechanisms, some attempts have been made to design HIF1-specific targeted therapies. A number of approaches have been taken to achieve this. Polyamides are small molecules which can be designed to bind pre-determined DNA sequences of up to 16 base pairs with high affinity. This allows polyamides to be targeted to specific transcription factor binding sites and to inhibit activity at that site [378]. Polyamides designed to target the HRE have been shown to be able to block VEGF expression in HeLa cells [379] as well as in prostate and glioma cell lines in a second study [380]. Issues have been raised concerning polyamide uptake in xenograft models [381], but if this can be overcome then these programmable molecules may represent an interesting novel approach to HIF targeted therapy.

Another approach to HIF1 specific inhibition is the use of synthetic antisense oligonucleotides (ASO), which can bind HIF1 mRNA leading to its degradation [382]. Two such

ASOs have proven effective in preclinical cancer models, RX-0047 and EZN-2968. RX-0047 has been shown to be cytotoxic in a number of cancer cell lines including breast cancer [383], and was able to inhibit tumour formation and metastasis in prostate and lung xenograft models respectively. EZN-2968 is a 16-mer nucleotide 100% complementary to the HIF1α coding sequence [333], which is able to inhibit HIF1α mRNA in a dose-dependent manner with much weaker effects on HIF2α [384]. EZN-2968 has been evaluated in multiple phase I clinical trials where it has been shown to reduce HIF1α mRNA and protein [385], and is also enrolled in a phase I trial as a proof-of-mechanism trial in hepatocellular carcinoma [386].

A novel method of specific targeted therapies is the use of nanobodies; these provide a smaller alternative to monoclonal antibodies and have been shown to be highly robust in terms of stability and binding [382, 387]. Initial *in vitro* studies of a nanobody able to bind the ODD of HIF1α have shown it can prevent the activation of known HIF1 target genes [388], and more recently developed nanobody AHPC is able to recognise the HIF1α PAS-B domain and prevent dimerization, reducing tumour proliferation and metastasis in pancreatic cancer models [382]. However, nanobodies are still in their infancy and the transfection-mediated expression of nanobodies required for them to target intracellular proteins is currently a limiting factor in their clinical development [382].

1.7.3 Specific inhibition of HIF2

Specific HIF2 inhibition

Whilst a large number of inhibitors are available to target HIF1α, and a number of these have demonstrated activity on HIF2α also, relatively little research has been done on the development of HIF2α specific inhibitors. However, recent work has led to several molecules with specific activity towards HIF2α, and whilst most research has been performed in the context of renal cell carcinoma (RCC), where VHL mutations often lead to an upregulation of HIF2α, these provide useful tools for the inhibition of specific HIFα proteins in other cancer types.

HIF2α translation inhibitor (Compound 76, C76)

In 2007 Sanchez et al. [280], having discovered an iron response element (IRE) in the 5’ UTR of HIF2α mRNA, demonstrated that this element confers post-transcriptional

regulation of mRNA through a novel iron-dependent mechanism. This mechanism involves the binding of iron regulatory proteins IRP1 and IRP2 to the IRE in HIF2α mRNA when iron levels are low. This binding was shown to reduce translation of the mRNA and therefore reduce the accumulation of HIF2α independently of hypoxia. HIF1α mRNA lacks an IRE, and thus this is a HIF2α specific level of regulation probably linked to the role of HIF2α in erythropoiesis. By limiting HIF2α accumulation, the production of red blood cells in response to low oxygen is prevented when the iron required for this process is likely to be unavailable. In 2009 Zimmer et al. [283] performed a screen for compounds able to specifically inhibit HIF2α translation through modulation of IRP binding. They were able to identify a number of compounds which inhibited HIF2α translation in renal 786-O cells by promoting the binding of IRP1 to the IRE in the HIF2α 5' UTR. The lead compound from this study was compound 76 (C76). Whilst C76 has not been involved in clinical studies for HIF2α inhibition in cancer, it offers a unique mechanism of specific HIF2α inhibition and as such will be one of the compounds investigated in this thesis. The structure of C76 is shown below.

HIF2a translation inhibitor (C76)

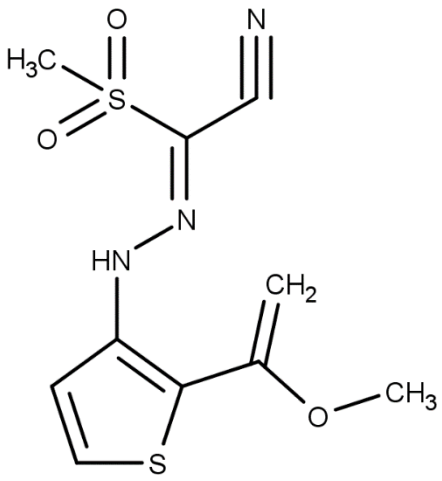

Inhibitors of HIF2α dimerization (Compound 2, PT2385 and PT2399)

Most success to date with inhibitors of HIF2 activity have come from small molecules designed to bind a small cavity in the PAS-B domain of HIF2α. PAS domains are found in a large variety of proteins and often mediate protein-protein interactions which can be modulated by the binding of small molecule cofactors [389]. The PAS-B domain of HIF2α,

which facilitates heterodimerisation with HIFβ subunits, contains a binding cavity in the absence of any known cofactors. The design of small molecules to bind this cavity resulted in the development of a number of compounds which could inhibit the dimerization of HIF2 through allosteric changes to the PAS-B domain [389, 390]. A study by Scheuermann et al. in 2013 [391] was able to functionally characterise a number of these molecules and demonstrated that lead compound, compound 2 (C2), inhibited VEGF expression without changes to HIF2α mRNA or protein levels in 786-O cells, a cell line where HIF activity is fully attributable to HIF2 [392]. The specificity of C2 was confirmed in Hep3B cells where it was demonstrated that it can reduce the hypoxic upregulation of mRNA for the HIF2 target gene EPO with no discernible effect on HIF1 target gene PGK1, indicating the specific inhibition of HIF2 activity. Additionally chromatin immunoprecipitation experiments demonstrated that C2 prevented the hypoxia induced DNA binding of HIF2α, with no effect on HIF1α [391]. C2 is one of the HIF2 inhibitors that will be used in this thesis, the structure of C2 is shown below.

HIF2 Inhibitor 2 (Compound 2)

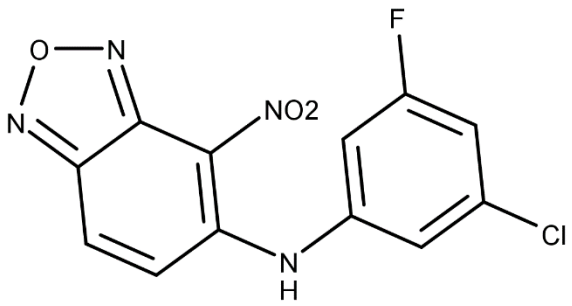

The modest cellular potency and poor physical properties of these inhibitors led to the design of second generation HIF2 dimerisation inhibitors [393]. PT2385 and PT2399 are novel HIF2 dimerisation inhibitors which function through selective binding to the HIF2α PAS-B domain. These compounds have been developed by Peloton therapeutics mainly for research into HIF2 inhibition as a therapeutic strategy for RCC. PT2385 has been shown to reduce HIF2α-HIF1β binding at nanomolar concentrations in 786-O cells, and was able to reduce HIF2-driven expression of VEGFA, CCND1, PAI1 and GLUT1 genes with no effect on HIF1 target genes *PGK1* and *PDK1* in renal cell line models [393]. In addition P2385 treatment reduced the expression of HIF2 target genes in xenograft models, whilst also reducing tumour size, ki67 expression and circulating human VEGF levels, and increasing active caspase-3.

Interestingly, in xenograft models PT2385 was able to reduce HIF2α mRNA and protein, suggesting another level of HIF2α regulation which may occur as a result of its failure to bind HIF1β [393]. Preliminary results from a phase I dose escalation study for PT2385 (NCT02293980) in patients with RCC found no dose limiting toxicities among forty-three patients. At the time when this data was presented they had shown one patient with complete response, three with a partial response and sixteen patients with stable disease [394]. PT2385 is currently part of a phase II trial to assess its effect on response and progression-free survival in VHL mutated RCC (NCT03108066) [395]. Whilst no data is available for the efficacy of PT2385 in other cancer types it is used in this thesis as a highly promising HIF2 specific inhibitor. The structure of PT2385 is shown below.

PT2385

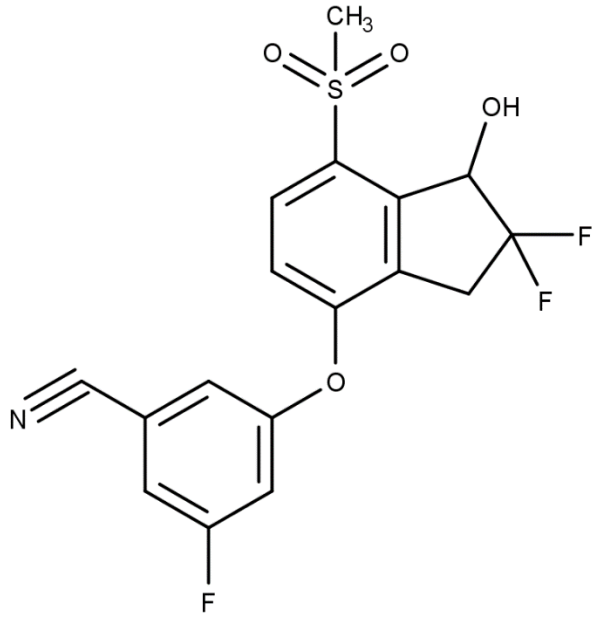

PT2399 is a close analogue of PT2385 currently in preclinical development. Chen et al. 2016 [396] were able to demonstrate that PT2399 had high efficacy in patient-derived xenografts of VHL mutated RCC, suppressing tumorigenesis in 56% of cases. PT2399 was found to be more effective and better tolerated than the angiogenesis inhibitor sunitinib in these experiments. They also determined a HIF2-dependent gene signature which was altered in sensitive but not resistant tumours suggesting a requirement for changes to HIF2-mediated gene transcription for drug efficacy [396].

These promising clinical and preclinical results for HIF2 dimerization inhibitors in RCC suggest that these are clinically viable compounds for treating HIF2-driven cancers. These compounds may provide a good starting point for the assessment of HIF2 inhibition as a therapeutic strategy in other cancer types such as breast cancer.

1.7.4 Targeting HIFs through growth factor signalling

Given that HIFα proteins have been shown to be regulated in normoxia by growth factor signalling, perturbations of growth factor signalling may also be used as an indirect method for targeting HIF-driven cancer pathogenesis. These effects are predominantly seen through inhibition of the PI3K/AKT/mTOR pathway [333]. Several studies have shown that inhibition of mTOR by rapamycin and its derivatives can inhibit HIF1α and HIF2α levels under both normoxia and hypoxia [397-401]. Furthermore, the inhibition of PI3K by well characterised inhibitors LY294002 and wortmannin, as well as by a novel class of HIF1 targeting agents called glyceollins, have been shown to inhibit translation of HIF1α [402, 403]. Resveratrol, a natural compound derived from grapes, has been shown to have anticancer activity in preclinical models of a number of cancer types including breast. Resveratrol has been shown to act through various mechanisms, including through PI3K inhibition, resulting in lowered HIF1α levels [404], and it has been shown to reduce xenograft tumour growth and angiogenesis and VEGF expression in breast cancer cell line models [405], in line with a HIF-dependent mechanism. Studies such as these raise the possibility that targeting growth factor signalling pathways such as the PI3K pathway, perhaps in combination with HIF inhibitors may be a more effective way of reducing HIF-driven cancer progression.

1.8 The HER family of growth factor receptors

The HER receptor family (otherwise known as epidermal growth receptor (EGFR/ErbB) family) is a group of four transmembrane growth factor receptor tyrosine kinases which transduce signals from soluble growth factors outside the cell to downstream signalling pathways inside the cell. The four receptors EGFR (HER1/ErbB1), HER2 (ErbB2), HER3 (ErbB3), and HER4 (ErbB4) have similar structures all consisting of four extracellular

domains (I-IV) with two ligand binding domains (I and III) and two cysteine rich domains (II and IV) (of which domain II is important for receptor dimerization). These are connected by a single pass transmembrane region to the intracellular kinase domain and a C-terminal tail containing a number of phosphorylation sites [406-409]. Upon ligand binding to domains I and III conformational changes in domain III release its dimerization arm [408, 410-412]. This allows receptor monomers to form dimers with other HER receptor members, either as homodimers with equivalent members or as heterodimers with other members of the family [407]. HER receptor dimers then undergo conformational changes which allow the kinase domain to phosphorylate multiple tyrosine residues on the c-terminal tails of themselves (autophosphorylation) and their partnered receptor (transphosphorylation). Phosphorylated tyrosine residues then act as docking sites for a variety of intracellular proteins which recruit signalling molecules to the receptor. This initiates a signalling cascade, the nature of which depends on which tyrosine residues are activated on which receptors [406, 413, 414].

The HER receptors have a large number of growth factor ligands which are able to bind and initiate receptor signalling. Different HER ligands show preference for different HER receptors conferring specificity (Figure 1.7). EGFR has the largest number of known ligands (EGF, TGFα, ARG, BTC, HBEGF and ERG), whilst HER3 and HER4 generally show preference for the neuregulin family of ligands (NRG1, NRG2, NRG3 and NRG4) (an overview of ErbB receptor structures and ligands can be seen in Figure 1.7) [407, 414]. Interestingly, HER2 has no known binding ligands meaning activation of the HER2 receptor under normal physiological conditions requires the ligand activation of another family member and the formation of a heterodimeric receptor with HER2. In contrast, HER3 has an inactive kinase domain meaning in the presence of a HER3 ligand this receptor is also required to dimerise with other HER family members to initiate intracellular signalling. In this way the nature of signalling events downstream of HER signalling depends on the ligand, the dimeric receptor pair which form and the extent of specific tyrosine residue phosphorylation [415].

The two predominant intracellular signalling pathways activated downstream of HER receptor signalling are the Raf/MEK/ERK and PI3K/Akt/mTOR pathways, and over activation of these pathways is a common occurrence in many forms of cancer (Figure 1.8). The Raf/MEK/ERK pathway is typically activated through the Grb2 adapter protein which binds to phosphorylated tyrosine residues on activate HER receptors and recruits the SOS guanine exchange factor. The recruitment of SOS to the cell membrane allows GDP-bound Ras to

exchange GDP for GTP, thereby returning to its active state. Ras in turn activates Raf-1, which is considered the first protein in the kinase cascade which leads to the activation of ERK1 and ERK2. Phosphorylated ERK1/2 is able to translocate to the nucleus and activate transcription factors such as Elk-1 and Ets-1 [416].

PI3K is a kinase consisting of two subunits the catalytic p110 subunit and the regulatory p85 subunit. PI3K signalling is initiated when p85 binds to phosphorylated tyrosine residues on activated HER receptors. This binding dissociates p85 from p110, allowing p110 to catalyse the conversion of PIP2 to PIP3 at the plasma membrane. PIP3 binds Akt allowing its phosphorylation by phosphoinositide dependent kinase 1 and 2 (PDK1/PDK2). The phosphorylation of Akt leads to a number of downstream processes including the inactivation of proapoptotic factors Bad and procaspase-9 (promoting cell survival), the stimulation of cell growth and proliferation by inhibiting β-catenin antagonist GSK3, and the increase in protein synthesis through regulation of mTOR [417].

In cancer cells, the stimulation of the PI3K/AKT or Raf/MEK/ERK pathways is a common contributor to cancer pathogenesis. This can occur through overexpression or activating mutations at the receptor level or at the level of intracellular signalling. In breast cancer perturbations of the PI3K pathway are most commonly caused by activating mutations in the PIK3CA gene (around 25%), but PIK3CA amplification, loss of PTEN function (an enzyme responsible for the reverse catalysis of PIP3 to PIP2), Akt1 mutations and HER2 amplification all promote oncogenic signalling through this pathway [418, 419]. Dysfunction of the Raf/MEK/ERK pathway is also seen in breast cancer, however Ras and Raf mutations are relatively rare (MAP3K1 mutations have been shown to exist in 14% and 5% of luminal A and luminal B breast cancers). Deregulation of gene expression associated with the Raf/MEK/ERK pathway is more common in triple-negative breast cancers, a subtype often characterised by high EGFR activity. Alteration of this pathway is able to promote cancer by allowing growth signal autonomy, insensitivity to antiproliferative signals, inhibiting apoptosis and driving proliferation, angiogenesis and invasion/metastasis [417].

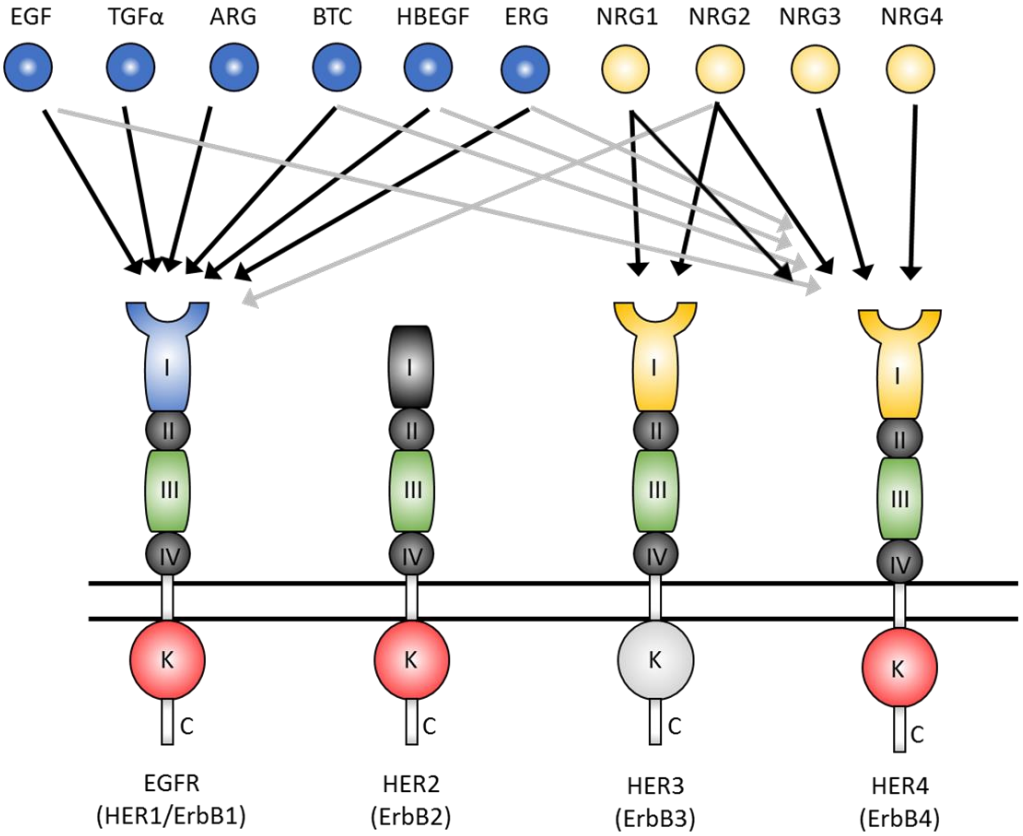

Figure 1.7: HER receptor activation by HER ligands

A schematic representation of HER ligand binding to HER family receptors. Known ligand-receptor interactions are shown by black arrows. Grey arrows represent interactions which induce only moderate signalling. EGFR has the largest number of known ligands, whilst ErbB2 has none. The neuregulins (NRG) show preference for ErbB3 and ErbB4. Ligand binding (domains I and III) induces receptor dimerization leading to phosphorylation of receptor carboxy-terminal tails (C) via the intracellular kinase domain (K). HER3 lacks an active kinase domain and so relies on kinase activity from other receptors to initiate downstream signalling. Epidermal growth factor (EGF), transforming growth factor-α (TGFα), amphiregulin (ARG), betacellulin (BTC), heparin-binding EGF (HBEGF), epiregulin (ERG), Neuregulin (NRG). Figure adapted from Leahy 2004 [407].

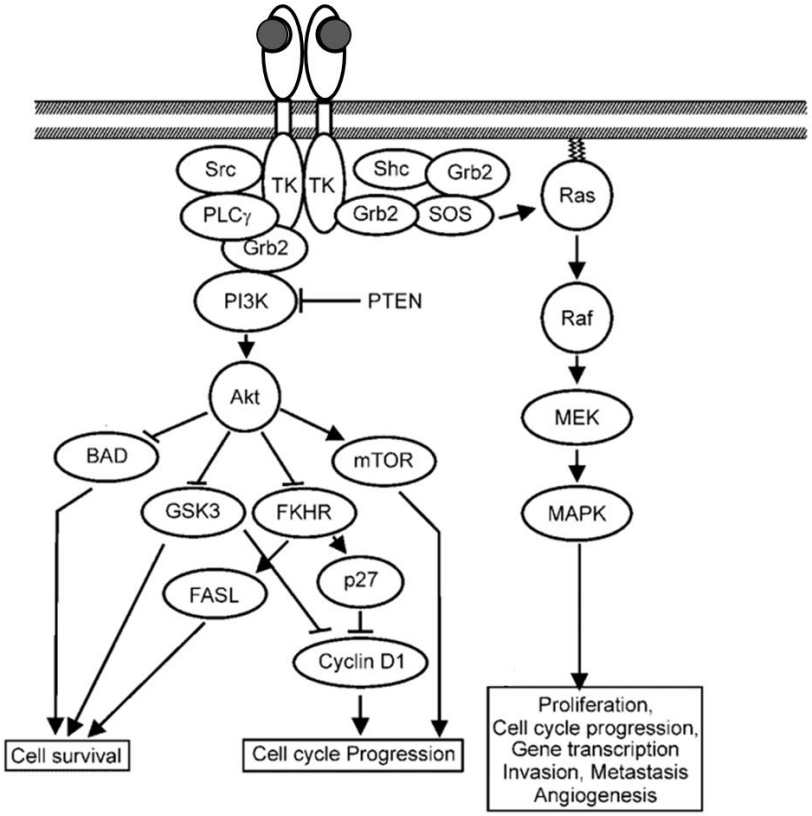

Figure 1.8: PI3K/AKT and Raf/MEK/ERK pathways downstream of RTK signalling

A schematic showing the predominant intracellular signalling pathways downstream of HER signalling. Ligand binding to HER receptors results in receptor dimerization (top). The resulting phosphorylation of c-terminal receptor tails leads to the docking of various proteins such as Shc and Grb2 which mediated the initiation of major cellular signalling pathways. The activation of PI3K/AKT and Raf/MEK/ERK pathways in this way lead to a number of cellular responses which contribute to cancer pathology (bottom). Figure adapted from Saxena and Dwivedi 2012 [503].

1.9 HER-HIF interplay in breast cancer

As discussed above, a number of studies have been conducted to assess the relationship between HIF1α expression and clinical features in breast cancer. Interestingly, a number of these studies were able to demonstrate an association between HIF1α and HER2. A study by Bos et al. in 2003 [285] involving 150 samples from node negative early stage breast cancer found that HIF1α expression was significantly associated with HER2 both in terms of protein expression measured by IHC and in terms of HER2 amplifications determined through FISH. These findings were supported by similar studies showing a significant association between these two factors by Kronblad et al. in 2006 [289] using a cohort of 337 premenopausal stage II breast cancers and by Yamamoto et al. in 2008 in an assessment of 171 invasive breast cancer samples. An association between HER2 and CAIX expression has also been demonstrated [420], suggesting that HER2 is associated with HIF activity. Furthermore, in an investigation into the association between HIF1α and HER2 expression and their connection to patient outcome, Giatromanolaki et al. (2004) [293] were able to demonstrate an interesting relationship; when divided into low and high expression groups for HER2 or HIF1 a cohort of 146 patients with infiltrating carcinoma of the breast (not otherwise specified) demonstrated significantly worse overall survival when either factor was highly expressed in relation to their low expressing counterparts. However, when patients were stratified by both factors, significantly worse overall survival was found for patients with high expression of both factors only. Patients with high expression of HER2 or HIF1α only were shown to have comparable overall survival to those with low expression of both factors. This suggests that HIF1α expression is required for the aggressive characteristic which lead to worse prognosis in HER2-positive breast cancers. Together, these clinical studies demonstrate a clear, pathologically relevant association between HER2-positivity and the expression of HIF1α in breast cancer. Interestingly, similar associations between HER2 and HIF2α [321] and between HIF1α and EGFR [285] have also been shown, suggesting an important relationship between growth factor receptors and HIF signalling pathway in this disease.

In 2001 a study by Laughner et al. [220] demonstrated that HER2 overexpression in mouse 3T3 cells was able to increase the level of HIF1α protein in normoxia leading to the increased expression of VEGF mRNA, and treatment of MCF7 breast cancer cells with the HER3 ligand neuregulin-1β (NRG-1β) was able to elicit a comparable effect. The upregulation

of HIF1α in this study was shown to require PI3K, Akt and mTOR signalling, and be a result of a growth factor driven increase in HIF1α translation. Further work by Li et al. in 2005 [421] supported this mechanism, and was able to demonstrate a HER2-driven increase in HRE transcription in 3T3 cells as well as MDA-MB-453, a breast cancer cell line naturally overexpressing the HER2 receptor. In MDA-MB-453 cells, normoxic HIF1α expression was reduced by the transfection of cells with a dominant-negative form of Akt, demonstrating that HIF1α levels were constitutively driven by Akt signalling, and could be inhibited [421].

Since these initial mechanistic studies describing the normoxic expression of HIF1α a handful of studies have investigated this relationship in preclinical models, providing evidence for the pathological role of HER-HIF interplay in breast cancer. In 2006, a study by Peng et al. [422] was able to demonstrate that the treatment of breast cancer cell lines with EGF, the natural ligand for EGFR, was able to increase HIF1α expression in normoxia, and that in this context HIF1α contributed to EGF-mediated resistance to docetaxel through the expression of the anti-apoptotic gene survivin (BIRC5). In 2013, Whelan et al. [423] demonstrated that knocking out HIF1α expression in HER2-overexpressing cell lines resulted in increased apoptosis in 3D culture models and that tumours grown in a HIF1 knock-out MMTV-Neu mice model had significantly reduced tumour volume, compared to HIF1α wild-type mice. Finally, a study by Kazi et al. in 2014 [424] was able to demonstrate an increase in the normoxic expression of HIF1α associated with AI resistance in long-term letrozole treated (LTLT) breast cancer cells. This increase in HIF1α was shown to be driven by the increased expression and activity of the HER2 receptor and lead to an increase in the expression of multidrug resistance gene BCRP1. To further corroborate this role for HIF1α in AI resistance the authors were also able to demonstrate that the stabilisation of HIF1α using $CoCl_2$ was able to increase the resistance of AI-sensitive cells to letrozole, and this effect was ablated by co-treatment with HIF1α siRNA.

Whilst little research has investigated whether the normoxic upregulation of HIF2α by growth factor signalling can occur in breast cancer, a number of studies have highlighted a role for hypoxia and HIF2α activity in promoting the expression and activity of growth factor receptors, predominantly EGFR. It has been shown in a number of cell lines, including MCF7 and MDA-MB-231 breast cancer lines, that hypoxia can increase EGFR expression [425-427]. This was shown by Franovic et al. in 2007 [425] to be a result of a HIF2α-driven increase in EGFR translation, and in a later study they were able to show that HIF2α drives EGFR and

IGFR expression and activity, and that transfection with a dominant-negative variant of HIF2α resulted in reduced growth in a diverse panel of cell lines [428]. Furthermore, an investigation into tamoxifen and fulvestrant resistance in ER-positive cell lines implicated a bidirectional relationship between HIF2α and EGFR. Alam et al. 2016 [426] demonstrated, using MCF7 and antioestrogen resistant MCF7 lines, that HIF2α (but not HIF1α) was increased in response to the antioestrogens tamoxifen and fulvestrant, and was constitutively higher in antioestrogen resistant cell lines. Inhibition of HIF2α was also able to restore sensitivity to tamoxifen and fulvestrant. Since EGFR activation is believed to contribute to antioestrogen resistance in breast cancer [429], the relationship of HIF2α and EGFR was investigated and expression in these cell lines was found to be interdependent. Knockdown of either factor with siRNA resulted in a reduction of the other in antioestrogen resistant cell lines [426].

Together these studies have demonstrated important roles for HER-HIF interplay in breast cancer, suggesting that in the context of growth factor activation both HIF1α and HIF2α contribute to pathogenesis even in normoxia. The potential for HIF signalling to drive breast cancer progression in hypoxia has been well-documented (Section 1.6.6), but still little is known about how growth factor receptor expression may contribute to this role in hypoxia. Further work is required to understand the different roles of HIF1α and HIF2α under conditions of high growth factor signalling such as in HER2-positive breast cancers, how they alter cell behaviour in normoxia and hypoxia, and whether HIFs represent a targetable pathway in growth factor-driven tumours.

1.10 Aims and objectives

Given the negative consequences of hypoxia and HIF signalling shown to be associated with worse prognosis in cancer, the emerging differences between HIF1α and HIF2α signalling and regulation, and the novel understanding that HIF1α can be modulated in normoxia by growth factor signalling through HER family receptors, this thesis hypothesises that growth factor signalling will have important consequences for the normoxic regulation of HIF2α as well as HIF1α, that the overexpression of the HER2 receptor in HER2-positive breast cancer cells will affect HIF signalling as a result of this growth factor–mediated regulation, and that modulation of HIFs through HER2 signalling will also alter the cellular response to hypoxia in terms of HIF upregulation and HIF-driven gene transcription.

This signalling relationship between HIFs and HER2 may have important consequences for breast cancer progression and aggressiveness in both normoxic and hypoxic tumour regions. The work presented in this thesis aims to further our understanding into the nature of HER-HIF interactions in breast cancer and their role in HER2-positive breast cancer, with a particular focus on the less well understood HIF2α. This was achieved by means of the following objectives:

- To investigate the effect of HER2 overexpression on the hypoxic regulation of HIF1α and HIF2α, and downstream targets in 2D and 3D breast cancer cell line models
- To characterise the role of HER2 overexpression on the transcriptional response to hypoxia by assessing gene expression changes in acute and chronic hypoxia in low-HER2 and HER2-overexpressing breast cancer cell lines
- To further investigate the potential for growth factor signalling to drive the upregulation of HIF1α or HIF2α in breast cancer cell lines by monitoring HIF1α and HIF2α changes induced by ligand stimulation or HER2 overexpression and investigate the pathways involved
- To evaluate the efficacy of HIF2 inhibition in low-HER2 and HER2-positive breast cancer cell lines through HIF2α knockdown and HIF2-specific molecular inhibitors.
- To use publically available gene expression and clinical datasets to understand the role of HIF2α expression and activity in breast cancer survival

Chapter 2: Materials and methods

2.1 Materials

(Materials were obtained from Sigma-Aldrich unless otherwise stated)

2.1.1 Cell lines

A number of human breast cancer cell lines were used in this study. A full list and description of cell lines can be seen in Table 2.1. All cell lines were acquired from the ATCC (American Tissue Culture Collection) with the exception of MCF7-HER2/18 and MCF7-Neo, which are genetically modified lines derived from MCF7 in Kent Osborne's laboratory [430]. Short Tandem Repeat (STR) profiling (performed by Public Health England Culture Collections Cell Line Authentication Service) was used to verify cell line identities at the start of the project.

Table 2.1: Cell Lines

Cell Line	Origin	Molecular Subtype	Receptors
BT474	Primary site of IDC	Luminal	ER+, PgR+, HER2+
HBL100	Derived from the milk of a healthy woman	Basal B	ER-, PgR-, HER2- (Triple Negative)
MCF7	Pleural effusion of IDC	Luminal	ER+, PgR+, HER2-
MCF7-HER2/18	Derived from MCF7 in the Osborne lab [430]	Luminal	ER+, PgR+, HER2+
MCF7-Neo	Derived from MCF7 in the Osborne lab [430]	Luminal	ER+, PgR+, HER2-
MDA-MB-231	Pleural effusion of AC	Basal B	ER-, PgR-, HER2- (Triple Negative)
MDA-MB-361	Primary site of AC	Luminal	ER+, PgR-, HER2+
SKBR3	Pleural effusion of AC	HER2+	ER-, PgR-, HER2+
T47D	Pleural effusion of IDC	Luminal	ER+, PgR+, HER2-
ZR751	Ascites fluid of IDC	Luminal	ER+, PgR-, HER2-

2.1.2 Genetically modified cell lines

Two genetically modified cell lines were used in this study: MCF7-HER2 and MCF7-Neo, both of which are derived from wild-type MCF7 cells by Benz et al. [430]. MCF7-HER2 was genetically modified to overexpress the HER2 receptor by the stable transfection of a pRK5 expression plasmid containing full length HER2 cDNA under the control of the cytomegalovirus promoter/enhancer. This was co-transfected with a second pRK5 plasmid containing the selection gene neomycin phosphotransferase (neo) under the control of the SV40 promoter to allow selection with the antibiotic G418. The control cell line, MCF7-Neo, was created by transfection with the selection plasmid alone. Cell lines were selected with G418 treatment and assayed for HER2 overexpression. Subclones MCF7-HER2-18 and MCF7-Neo-3 were identified by Benz et al. as successfully transfected cells and used for further study. These are the two cell lines that have been used for this study and are referred to in this report as MCF7-HER2 and MCF7-Neo for simplicity [430].

Two processes were used to verify the characteristics of these cell lines: at the start of the project STR profiling (at ECACC) was used to confirm they were of MCF7 origin, and western blotting was used to assess the expression of important receptor proteins (including HER2). STR profiling demonstrated that MCF7-HER2 was, as expected, derived from MCF7 cells. However MCF7-Neo did not match MCF7 lines, suggesting this cell line has been misidentified. This was further confirmed in the western blotting experiment, which demonstrated receptor expression inconsistent with MCF7. MCF7-Neo was therefore recognised as an unsuitable control for the MCF7-HER2 cell line in this study and instead MCF7 (wild-type) and MCF7-HER2 were used together as a cell line model for HER2 overexpression.

2.1.3 Antibodies

	Table 2.2. List of antibodies				
Target	**Company (Catalogue number)**	**Species (Clonality)**	**Observed Molecular Weight**	**Dilution – Western Blotting**	**Dilution - IHC**
Total (Pan) AKT	Cell Signalling Technology #2920	Mouse (Monoclonal)	60 KDa	1:1000	N/A*
Phospho-AKT (Ser472)	Cell Signalling Technology #9271	Rabbit (Polyclonal)	60 KDa	1: 1000	N/A
Alpha Tubulin	Abcam Ab7291	Mouse (Monoclonal)	50 KDa	1: 10,000	N/A
Beta Actin	Abcam Ab8227	Rabbit (Polyclonal)	42 KDa	1: 10,000	N/A
Carbonic Anhydrase IX	Bioscience Slovakia M75	Mouse (Monoclonal)	54 KDa	1: 6000	1: 1000
CD44	Cell Signalling Technology #3570	Mouse (Monoclonal)	80 KDa	1: 500	1: 50
CXCR4	Abcam Ab124824	Rabbit (Monoclonal)	43 KDa	N/A	1: 500
Cyclin D1	Abcam Ab134175	Rabbit (Monoclonal)	34 KDa	1: 10,000	1: 200
EGFR	Cell Signalling Technology #2239	Mouse (Monoclonal)	175 KDa	1: 1000	N/A
EGFR	Cell Signalling Technology #4267	Rabbit (Monoclonal)	175 KDa	1: 1000	N/A
Phospho-EGFR (Tyr1148)	Cell Signalling Technology #4404	Rabbit (Polyclonal)	175 KDa	1: 1000	N/A
Oestrogen receptor alpha	Neomarkers (AER314)	Mouse (Monoclonal)	66 KDa	1:250	N/A
HER2	Cell Signalling Technology #2242	Rabbit (Polyclonal)	185 KDa	1: 1000	N/A
HER2	Cell Signalling Technology #2248	Mouse (Monoclonal)	185 KDa	1: 1000	N/A
Phospho-HER2 (Tyr1221/1222)	Cell Signalling Technology #2243	Rabbit (Monoclonal)	185 KDa	1: 1000	N/A
HER3	Cell Signalling Technology #4754	Rabbit (Monoclonal)	185 KDa	1:1000	N/A

HIF1α	BD Transduction Laboratories 610958	Mouse (Monoclonal)	120 KDa	1: 250	1: 100
HIF2α	Novus Bio NB100-122	Rabbit (Polyclonal)	118 KDa	1: 1000	1: 200
HIF2α	Cell Signalling Technology #7096	Rabbit (Monoclonal)	120 KDa	N/A	1: 200
Hypoxyprobe-1 (Anti-pimonidazole)	Hypoxyprobe Inc.	Mouse (Monoclonal)	N/A	N/A	1:1000
Lamin B1	Abcam Ab133741	Rabbit (Monoclonal)	70 KDa	1: 10,000	N/A
Lamin B1	Abcam Ab8982	Mouse (Monoclonal)	67 KDa	1: 1000	N/A
Lactate Dehydrogenase A	Cell Signalling Technology #3582	Rabbit (Monoclonal)	37 KDa	1: 4000	1: 400
C-Myc	Abcam Abcam32072	Rabbit (Monoclonal)	57 KDa	1: 10,000	1: 500
Progesterone receptor	Epitomics 5132-1	Rabbit (Monoclonal)	118 KDa	1:250	N/A
VEGF	Novus Bio NB100-664	Mouse (Monoclonal)	30 KDa	1: 500	1: 50

* N/A = Not applicable

2.2 Methods

2.2.1 Routine culture of adherent cell lines

All cell lines were cultured in Dulbecco's Modified Eagle Medium (DMEM) (Gibco) containing low glucose (1 g/L), sodium pyruvate (110 mg/L) and phenol red (15 mg/L). This was supplemented with 10% heat-inactivated foetal bovine serum (FBS) (Gibco), 100 U/ml penicillin and 100 μg/ml streptomycin (Gibco) (referred to as complete DMEM). Cell lines were grown in a humidified atmosphere maintained at 37 °C, 5% CO_2 and atmospheric O_2 (approximately 20%). Genetically modified cell lines MCF7-HER2 and MCF7-Neo were cultured with the addition of 1 mg/ml G418 (Sigma) to select for cells expressing the neomycin phosphotransferase gene. 1 mg/ml G418 was used as this concentration was effective at preventing the proliferation of regular MCF7 cells in SRB assays, whilst permitting the growth of both genetically modified cell lines (Figure 2.2).

Upon reaching 70-90% confluence, cell lines were passaged into new flasks. To do this, old media was discarded and cells were washed in phosphate-buffered saline (PBS). Cells were detached from the surface of flasks by 5 min incubation at 37 °C with 5 ml 0.05% trypsin-EDTA solution (Gibco). Trypsin activity was halted by the addition of 5-10 ml complete DMEM. Cell suspensions were then transferred to suitable tubes and centrifuged at 2,500 rpm for 5 min in a Heraeus Labofuge 200. The supernatant was discarded whilst cell pellets were re-suspended in fresh DMEM and the desired proportion of cells seeded into new flasks.

All FBS was heat-inactivated prior to use. This was warmed at 37 °C for 15 min then heated to 56 °C for 30 min. This was then aliquoted and stored at -20 °C for later use.

Cryopreservation of cells in liquid nitrogen

To prepare cells for long term storage in liquid nitrogen, cells were grown to 70-90% confluence, trypsinised as above and re-suspended in freeze mix (FBS containing 10% DMSO (Sigma Aldrich)). These were transferred as 1 ml aliquots into cryovials suitable for liquid nitrogen storage. These were then kept at -70 °C for at least 24 hrs before being placed into liquid nitrogen tanks. To resume culture after storage in liquid nitrogen, 1 ml cell aliquots were quickly thawed in warm complete DMEM and seeded into a new flask.

Hypoxic cell culture

To culture cells at reduced oxygen tensions, cells were transferred to a Whitley H35 hypoxystation. The hypoxystation contains a humidified atmosphere at 37 °C, with CO_2 maintained at 5% and O_2 held at 0.5% (balance with N_2).

Charcoal stripping of foetal bovine serum

Charcoal-stripped serum was used for experiments requiring reduced basal levels of hormones, growth factors and cytokines found in unstripped FBS [431]. This was obtained pre-prepared (Sigma Aldrich), or prepared in house for comparison with unstripped FBS. Stripped serum was prepared in house as follows: 1 litre of FBS was incubated for 2 hrs at 37 °C with 2000 units of type IV sulphatase (Sigma Aldrich) and the pH adjusted to 4.2. Charcoal (5g) and dextran T70 (25mg) (Sigma Aldrich) were mixed in 50 ml of distilled water at 4 °C. The charcoal mix was added to the heat-inactivated FBS and left overnight at 4 °C. This was centrifuged at 4500 rpm for 1 hr at 4 °C using a Rotina 420R centrifuge. The FBS supernatant

was decanted off and re-adjusted to a pH of 4.2. A second batch of activated charcoal was added overnight as before and centrifuged again to remove as much FBS from the charcoal pellet. Centrifugation was repeated one last time to remove residual charcoal, FBS was decanted and pH adjusted to 7.2. Charcoal stripped FBS was filter-sterilised by passing through a 0.45 µm PDVF membrane filter (Thermo Fisher). This was aliquoted and stored at -20 °C for later use.

For experiments where low basal stimulation by endogenous factors was required, 2.5% charcoal-stripped serum was added to phenol-red free DMEM. Phenol red is known to have low level oestrogenic activity [432, 433] and therefore its exclusion from media allows growth conditions with as little basal stimulation as possible.

2.2.2 Multicellular spheroids

To form multicellular spheroids, cells were grown in T175 flasks until 70-90% confluent. These were then trypsinised, centrifuged and re-suspended in complete DMEM (as above), before syringing at least 3 times through a 21 gauge needle to form a homogenous single cell suspension. Cell suspensions were put in spinner flasks which use magnetic rods to constantly stir the media (VWR). These flasks were placed on a Cellspin stirring plate (Integra Biosciences) to maintain a constant stirring speed of 30 rpm. Spinner flasks were kept in standard cell culture conditions (humidified atmosphere of 5% CO_2 at 37 °C) for 1-2 weeks, with fresh DMEM added every 3-5 days. Once spheroids had reached an approximate size of 1-2 mm in diameter they were decanted into petri dishes and processed as required.

Hypoxyprobe labelling of spheroids

To allow hypoxic areas of spheroids to be visualised by IHC, spheroids first had to be stained with Hypoxyprobe-1 (HP1). HP1 is a commercially available pimonidazole based probe for detecting cellular hypoxia. Pimonidazole is activated by reduction exclusively at low oxygen concentrations and covalently binds to thiol groups in cellular proteins [434, 435]. This protein adduct can then be detected using antibodies directed towards the pimonidazole probe. The reduction of HP1 which is required for protein binding is completely

inhibited at concentrations of oxygen ≥14 µM, and half maximal inhibition occurs at 4 µM oxygen [434].

Spheroids were washed with warm PBS and then incubated for 1 hr in DMEM containing 100 µM HP1. Spheroids were then transferred to a 1.5 ml Eppendorf tube and washed again with warm PBS. These were then fixed in 4% formaldehyde for at least 24 hrs ready for further processing.

2.2.3 Sulforhodamine B proliferation assay

Sulforhodamine B (SRB) assays were used to compare cellular proliferation by direct measurement of cellular protein-bound SRB dye over a designated time course. To do this, cells were first seeded at 500-4000 cells per well in a 96-well plate in 200 µl of complete DMEM. The cell seeding density was dependent on the cell line as well as the experimental design. Typically, cells were allowed to grow for 48 hrs before being treated with the desired compounds. This was done for an individual 96-well plate for each time point. If treatment in low serum or stripped serum media was required, cells were first seeded in full DMEM and allowed to settle for 48 hrs before being washed with PBS and the desired media added. These would be incubated for another 48 hrs before being treated. After treatment, plates were fixed at the indicated time points by the addition of 50 µl of 25% trichloroacetic acid directly to the media and left at 4 °C for 1 hr, before being washed 10 times with H_2O and being dried in a 50°C oven. 50 µl of 0.4% SRB solution (made up in 1% acetic acid solution) was added to each well and plates left on a rocker for 30 min at room temperature. Excess SRB solution was tipped off and wells were washed 4 times in 1% acetic acid. Plates were allowed to dry in an oven at 50 °C. Bound SRB dye was solubilised by the addition of 150 µl 10 mM Tris solution (pH 10.5) and left on a rocker at room temperature for 30 min. Absorbance was measured at 540 nm on a BP800 biohit plate reader giving OD values proportional to cell number [436].

2.2.4 Whole cell lysate acquisition

Whole cell lysates were acquired from adherent cell lines and were used to examine protein expression by western blotting. Cells were grown and treated according to the desired experimental comparison; an appropriate number of cells were seeded so that lysates could be collected at 70-90% confluence. Before lysate collection, whole cell lysis buffer was prepared as follows: 30 ml 500 mM Tris (pH7.5), 30 ml of 50 mM EGTA (pH 8.5) and 90 ml of 500 mM NaCl were combined and mixed with a further 150 ml of dH_2O. This was separated into 10 ml aliquots and stored at -20 °C for future use. Preparation of lysis buffer was completed by the addition of detergent, protease and phosphatase inhibitors no more than half an hour before use. To a single 10 ml aliquot, 100 µl Triton X-100 (Sigma), 50 µl of Aprotinin (Sigma), 100 µl of Phosphatase inhibitor cocktail 2 (Sigma), 100 µl of Phosphatase inhibitor cocktail 3 (Sigma) and one Complete mini protease inhibitor tablet (Roche) were added and mixed by vortexing until completely solubilised. To collect lysates, cells were washed with ice-cold PBS and all subsequent steps were completed on ice to minimize protein degradation. PBS was removed and 400 µl of the complete lysis buffer was added to 160 mm dishes; this was reduced to 200 µl and 100µl for 100 mm dishes or 6-well plates respectively. Cells were lysed on ice for 10 min before plates were scraped and lysates transferred to a 1.5 ml Eppendorf tube. Samples were centrifuged at 13,300 rpm at 4 °C for 6 min in a Heraeus Fresco17 bench top centrifuge. Sample supernatants contain the cellular protein and were stored at -80 °C for future use.

2.2.5 Nuclear and cytoplasmic cell lysate acquisition

Lysates containing the nuclear or cytoplasmic fractions were collected for later use in western blot experiments. Solution A [10 mM HEPES pH 7.8, 10mM KCl, 2 mM $MgCl_2$, 0.1 mM EDTA], solution B [10% IGEPAL CA-630 (sigma) in dH_2O] and solution C [50 mM HEPES pH 7.8, 2 M KCl, 3 M NaCl, 0.5 M EDTA, 10% Glycerol] were prepared in advance. Solutions A and C were stored at -20 °C whilst solution B was stored at 4 °C until needed. Solutions A and C were completed by the addition of 50 µl of Aprotinin (Sigma), 100 µl of Phosphatase inhibitor cocktail 2 (Sigma), 100 µl of Phosphatase inhibitor cocktail 3 (Sigma) and one Complete mini protease inhibitor tablet (Roche) to each; these were mixed by vortexing until solubilised. To collect lysates, cells were washed with ice-cold PBS before being scraped in 1

ml of ice-cold PBS and transferred to a 1.5 ml Eppendorf tube. Samples were centrifuged at 13,300 rpm at 4 °C in a Heraeus Fresco17 bench top centrifuge for 1 min. Supernatant was discarded and cellular pellets were re-suspended in 400 µl, 200 µl or 100 µl of completed solution A for 160 mm, 100 mm or 6-well plates respectively. Samples were left on ice for 15 min and 15 µl, 7.5 µl or 3.75 µl of solution B added. These were mixed by vortexing for 30 secs before being centrifuged at 13,300 rpm at 4 °C for 1 min. The supernatant was removed and stored at -70 °C as the cytoplasmic fraction. To the pellet 50 µl (160 mm dishes) or 25 µl (100 mm or 6-well plates) of solution C was added. Samples were left on a rotating table at 4 °C for 20 min. These were then centrifuged at 13,300 rpm at 4 °C for 5 min. Supernatant was removed and stored at -70 °C as the nuclear fraction.

2.2.6 Bicinchoninic acid protein quantification assay

The bicinchoninic acid (BCA) assay allows the quantification of protein in cellular lysates. 5 µl of each lysate was diluted 1:10 in dH_2O and a standard curve of protein concentrations was created by the dilution of 1 mg/ml protein standard (Sigma) in dH_2O. BCA reaction mix was created by 1:50 dilution of copper sulphate II solution (Sigma) in BCA solution (Sigma). 1 ml of reaction mix was added to each lysate and protein standard sample before being vortexed briefly and incubated at 60 °C for 15 min. After this incubation, 200 µl of each sample was pipetted in duplicate into a 96-well plate and the absorbance of samples at 540 nm was read using a Biohit BP800 plate reader. The comparison of the absorbance in protein lysates with protein standards of known concentration allowed the determination of lysate concentration.

2.2.7 SDS polyacrylamide gel electrophoresis

SDS polyacrylamide gel electrophoresis was used to separate denatured proteins within cellular lysates according to size, facilitating the downstream detection of proteins of interest.

Quantified protein lysates were diluted to 40 µg of protein in 30 µl of lysis buffer (although for some experiments different amounts of protein were used). 10 µl of 4x loading buffer [32 mM Tris, 4% SDS, 20% β-mercaptoethanol, 0.016% bromophenol blue, and 40%

glycerol in distilled H_2O] was added to each sample and these were denatured at 95 °C for 3 min. Tubes were spun down in a bench-top microcentrifuge (Eppendorf minispin) and stored on ice until they were loaded onto gels for electrophoresis.

Polyacrylamide gels were prepared immediately before running SDS-PAGE. 7.5% acrylamide resolving gel mix was made with 10 ml of 30% acrylamide solution, 15 ml of 1 M Tris (pH8.85), 400 µl of 10% SDS and 14.6 ml of dH_2O. To initiate the setting of the gel mix, 100 µl of TEMED (National Diagnostics) and 100 µl of 10% ammonium persulphate (Sigma) were added and the solution was immediately mixed and pipetted into the glass moulds. A layer of isopropanol was added to the top to avoid drying out of the gel, and this was left for 20 min or until set. A 3.6% stacking gel solution was made with 3.6 ml of 30% acrylamide, 10 ml of 0.375M Tris (pH 6.8) and 16 ml of dH_2O. Isopropanol was removed and the resolving gel washed gently with dH_2O. 100 µl of TEMED and ammonium persulphate were added to the stacking gel, which was immediately mixed and added to the top of the stacking gel. 10 or 15-well combs were placed into the stacking gel and this was left for 20 min or until set.

Set gels were placed into the Bio Rad Mini Protean electrophoresis cell with 1 litre of running buffer (25 mM Tris, 192 mM glycine, 0.1% (w/v) SDS). 40 µl denatured protein samples were loaded into wells alongside 10 µl molecular weight ladder (prestained protein marker, broad range (11-190 KDa), Cell Signalling Technology) and gels were run at 80 V for 15 min followed by 150 V for 45 min or until proteins were adequately resolved.

2.2.8 Protein transfer to PVDF membrane and probing

Resolved proteins were transferred onto methanol-activated Immobilon-P transfer PVDF membrane (Merck Millipore) by running at 100 V for 1.5 hrs at 4 °C using the Protean Transfer Cell equipment (Bio Rad) filled with 1 litre of transfer buffer (192 mM Glycine, 25 mM Tris). Once transferred, the membranes were removed and blocked in suitable blocking buffer for 1 hr at room temperature. Membranes were probed with primary antibodies diluted in blocking buffer overnight at 4 °C. For a complete list of antibodies, including their dilutions and buffers used, please see Table 2.2 in section 2.1.3. Primary antibodies were discarded and membranes washed 3 times in PBS with the addition of 0.1% Tween20 (PBST) for 5 min on a rocker. Membranes were incubated with fluorescently-labelled secondary

antibodies (Li-Cor IRDye 800cw and IRDye 680LT) with separate wavelengths targeted against the species-specific domain of individual primary antibodies, thus allowing two primary antibodies from different species to be labelled and distinguished from one another. Secondary incubations were performed for 45 min on a rocker at room temperature, whilst protecting the blots from light to avoid loss of signal strength. Secondary antibody mixes were then removed and blots were washed 3 times in PBST on a rocker for 5 min, followed by 3 similar washes in PBS. Membranes were scanned using a Li-Cor Odyssey scanner, and the levels of proteins quantitatively compared using the Image Studio software suite (Li-Cor). Proteins of interest were routinely probed for alongside a loading control which could be used to normalise target expression across samples.

2.2.9 Immunohistochemistry of paraffin embedded tissue

Embedded tissues were sectioned and mounted onto glass slides. Tissue sections were de-waxed in xylene for 5 min (x2) and rehydrated in 100%, 100%, 80% and then 50% ethanol for 2 min each, before gently washed in running water. Antigen retrieval solution (82 mM Sodium citrate, 18 mM Citric acid) was placed in a pressure cooker and pre-heated in a microwave on full power for 10 min. Rehydrated slides were then placed into the antigen retrieval solution and the pressure cooker placed in the microwave for 5 min. This was left to cool for 20 min and slides were then washed twice for 5 min in PBST on an orbital shaker. Endogenous peroxidase activity was blocked by a 10 min incubation with 3% H_2O_2 solution on an orbital shaker at room temperature before being washed for 5 min in PBST. Slides were removed from the PBST and tissue sections were blocked from non-specific protein binding by the addition of Total Protein Block (Dako); these were left at room temperature for 10 min. Protein block was removed and primary antibodies diluted in Dako Antibody Diluent were added and left at room temperature for 1 hr (See Table 2.2 for a list of antibody dilutions used). Slides were washed twice for 5 min in PBST before the addition of Envision labelled polymer (Dako) directed towards either rabbit or mouse primary antibodies depending on the primary antibody used. Slides were incubated at room temperature for 30 min before being washed twice more for 5 min with PBST. DAB chromophore was diluted 1:50 in DAB substrate buffer (Dako) and 50 µl was added to tissue sections for 10 min to allow staining to develop. Counterstaining was performed by placing slides in haemotoxylin for 45 secs, washing in running water for 30 secs, placing in Scott's Tap Water Substitute (STWS) for 30 secs and back into running water for 30 secs. Tissue sections were dehydrated by placing

slides in 50% then 80% ethanol for 30 secs each, followed by 100% ethanol twice for 2 min and xylene twice for 5 min. Slides were mounted with coverslips using DPX mountant.

High resolution images were taken using the Hamamatsu Nanozoomer slide scanner.

2.2.10 Wound healing assays

Wound healing assays were performed using 35 mm µ-dishes with 2-well culture-inserts (Ibidi). These allowed cells to be grown to confluence before the removal of an insert which leaves a defined 500 µm cell-free gap. This allows cell migration into the gap to be measured over a time course of 1-4 days.

Briefly, 70 µl of a 7 x 10^5 cells per ml cell suspension was seeded into each well of the culture-insert dishes. Cells were seeded in complete 10% FBS DMEM, left for 24 hrs or until confluent, before the culture-insert was removed and cells were gently washed with PBS and changed into 0.2% FBS DMEM. Dishes were imaged at 0, 6, 24 hrs and every 24 hrs thereafter up to 96 hrs. Images were taken using brightfield microscopy on a Zeiss Axiovert S100 inverted microscope with a 2.5x objective. For experiments with inhibitory compounds, these were added at the desired concentration at the time of media change.

2.2.11 Collagen invasion assays

3D multicellular spheroids were grown as described above (Section 2.2.2). Spheroids were transferred to a petri dish and individual spheroids taken up into a pipette tip. The spheroid was mixed in the pipette tip with 500 µl of collagen mix [25% type-I collagen, 3 mg/ml (Alphalabs), 45% 1:1000 acetic acid, 10% FBS, 10% 0.22 M NaOH, 10% 10x DMEM]. This was gently pipetted into 24-well plates and allowed to set at 37 °C in a cell culture incubator for 1 hr. Once the collagen mix had set, a P200 tip was used to run around the edge of the well, thereby releasing the set collagen gel. 0.5 ml of complete DMEM was added to each well. Spheroids were imaged at 0 hrs and every 24 hrs thereafter, using brightfield microscopy on a Zeiss Axiovert S100 inverted microscope with a 2.5x objective. Scoring of invasion was performed manually by taking area measurements using the image J software.

2.2.12 siRNA knockdown experiments

Transfection of cells with siRNA oligonucleotides was performed for the targeted knockdown of HIF2α expression. Oligonucleotides and transfection reagents were purchased from Dharmacon and used as per the manufacturer's instructions. Knockdown was performed with four individual oligonucleotides targeted to HIF2α, as well as a pool of these four combined into a 'SMART pool' product. Details of siRNA oligonucleotides can be seen in Table 2.3.

Cells were seeded at a density of $2.5x10^5$ cells per well in 6-well plates (or 1000 cells per well in 96-well plates) in antibiotic-free medium. For 6-well plates the protocol was performed as follows: after 24 hrs, cells were 50-70% confluent and ready to be transfected. 20 µM siRNA solutions were reconstituted in 1x siRNA buffer (Dharmacon), aliquoted and stored at -20°C ready for use. On the day of transfection, 20 µM siRNA solution was added to 200 µl of antibiotic-free/serum-free DMEM, such that final concentration would equal 25 nM for single siRNAs and 5–100 nM for SMARTpool siRNA. In a separate tube, 4 µl of Dharmafect transfection reagent 1 was diluted in 196 µl of antibiotic-free/serum-free DMEM. These tubes were gently mixed and both left at room temperature for 5 min before being combined and mixed gently again. These transfection mixes were incubated at room temperature for 20 min. The seeded cells were washed once in PBS before the addition of 1 ml antibiotic-free 10% FBS DMEM. Transfection mixes were made up to 1 ml by the addition of 600 µl antibiotic-free 10% FBS DMEM, mixed gently and added dropwise to the desired cells. Transfected cells were left for 24 hrs before being changed to antibiotic-containing media. Cells were then treated as desired before the collection of protein lysates for western blotting. Transfections were always performed alongside untreated, mock (transfected without siRNA) and non-targeting (transfected with a non-specific siRNA oligomer) controls. For 96-well plates the protocol was performed in the same way using 0.14 µl of transfection reagent per well. All other reagents were scaled down to produce a final volume of 200 µl per well; details of siRNA oligonucleotides can be found in Table 3.

Table 2.3 : List of siRNA oligonucleotides			
Name	Target/Role	Sequence	Catalogue Number
HIF2α #1	HIF2α	GGCAGCACCUCACAUUUGA	J-004814-06
HIF2α #2	HIF2α	GAGCGCAAAUGUACCCAAU	J-004814-07
HIF2α #3	HIF2α	GACAAGGUCUGCAAAGGGU	J-004814-08
HIF2α #4	HIF2α	GCAAAGACAUGUCCACAGA	J-004814-09
HIF2α SMARTpool	A pool of 4 individual siRNAs targeting HIF2α	A combination of the 4 above oligonucleotides	L-004814-00
Non-targeting Control Pool	Set of 4 oligonucleotides with no target, used as a negative control in siRNA transfection experiments	A pool of 4 non-targeting oligonucleotide sequences. Specific sequences not provided.	D-001810-10

2.2.13 Gene expression analysis

The gene expression microarray experiment was performed in collaboration with Arran Turnbull, Carlos Martinez, James Meehan and Chrysi Xintaropoulou.

Sample collection

MCF7 and MCF7-HER2 cell lines were cultured in complete DMEM and seeded into T-175 flasks. Normoxic samples were grown to 80% confluence and trypsinised (described in Section 2.2.1). Cell suspensions were counted and centrifuged at 1,200 rpm in a Heraeus Fresco17 bench top centrifuge for 5 min to form pellets of at least $3x10^6$ cells. Three biological replicates were collected for each cell line and stored at -70° C until ready for RNA extraction. Hypoxic and cobalt chloride ($CoCl_2$) treated samples were collected in the same way after the appropriate treatment. Acute hypoxic samples were cultured at 0.5% O_2 in a Whitley H35 hypoxystation (as described in Section 2.2.1) for 24 hrs before collection. Chronic hypoxic samples were continually cultured at 0.5% O_2 for 10 weeks before collection. This included

weekly passaging of cells for which media and reagents were all acclimatised to hypoxia prior to use. $CoCl_2$ samples were treated with 400 µM of $CoCl_2$ for 24 hrs before collection.

RNA extraction

RNA extraction from cell pellets was performed using the miRNeasy Mini Kit (Qiagen) as per the manufacturer's instructions. Pellets were mechanically homogenised in 1 ml of QIAzol lysis reagent using a Tissuelyser LT (Qiagen) at 50 Hz for 5 min. 240 µl of chloroform was added and samples were centrifuged at 13,000 rpm for 15 min at 4°C (Heraeus Fresco17 benchtop centrifuge). The upper aqueous phase was removed and added to 750 µl of ethanol. Samples were added to the RNeasy Mini columns and centrifuged at 13,000 rpm for 15 secs at room temperature. Flow-through was discarded and columns were washed with 350 µl RWT buffer and centrifuged again for 15 secs, discarding the flow-through. Columns were incubated with 80 µl of DNase mix (Qiagen) for 15 min at room temperature. Columns were washed with 350 µl of RWT buffer and twice with 500 µl of RPE buffer with centrifugation and flow-through removal after each step. RNA was then eluted from the columns by the addition of 30ul RNase-free water. RNA concentration and quality was assessed using a Nanodrop 2000c spectrophotometer. RNA samples were stored at -70°C for later use.

Reverse transcription and amplification of cRNA

RNA was reverse transcribed, labelled and amplified using the Illumina TotalPrep RNA Amplification Kit as per the manufacturer's instructions. RNA samples were diluted in 11 µl of nuclease-free water to a total amount of 500 ng and incubated with 9 µl of Reverse Transcription Master Mix for 2 hrs at 42°C to form cDNA oligomers. This could then be incubated with 80 µl of Second Strand Master Mix at 16°C for 2 hrs, which allowed the formation of double-stranded complementary DNA, as well as the degradation of remaining RNA. 250 µl of cDNA Binding Buffer was then added to each sample and applied to a cDNA Filter Cartridge and centrifuged for 1 min at 13,300 rpm, discarding the flow-through. 500 µl of Wash Buffer was applied and the cartridges were centrifuged again at 13,300 rpm (flow-through was once again discarded). cDNA was eluted with 20 µl of nuclease-free water (pre-heated to 55°C), left for 2 min at room temperature before being centrifuged for 1 min at 13,300 rpm and the eluate collected. The *in vitro* transcription of cDNA was used to create biotin-labelled cRNA. cDNA eluates were added to 7.5 µl of IVT Master Mix and mixed thoroughly by pipetting. Samples were incubated at 37°C for 14 hrs. The reaction was

stopped with the addition of 75 µl nuclease-free water. cRNA was then purified as follows: 350 µl of cRNA binding buffer was added to each sample along with 250 µl of 100% ethanol and these were mixed by pipetting. Samples were transferred to cRNA filter cartridges and centrifuged at 13,300 rpm for 1 min (flow-through was discarded). Cartridges were washed with 650 µl Wash Buffer and centrifuged again, once again discarding the flow-through. Cartridges were then transferred to collection tubes, 200 µl of pre-heated (55°C) nuclease-free water was added, and samples were incubated at 55°C for 10 min. Finally samples were centrifuged at 13,300 rpm for 1.5 min and the labelled cRNA was collected in the eluate. The concentration and quality of the cRNA was then assessed with a Nanodrop 2000c spectrophotometer.

Hybridisation to HT-12 v4 beadchip array and data normalisation

Biotin-labelled cRNA was sent to Hologic, a healthcare and diagnostics company in Manchester, who performed the hybridisation to the beadchip array and the scanning of the slides. Each chip held 12 samples, each sample being hybridised to an array of 47,000 probes derived from the National Centre of Biotechnology Information (NCBI) reference sequence (release 38, 2009). Samples were distributed over 4 chips, with the location of each sample chosen to reduce the bias of chip batch effects and processed using Illumina GenomeStudio to generate a raw dataset showing expression intensity of each probe. Undetected probes were excluded if they did not reach a minimum detection value in more than 3 samples. This detection value was defined by the Illumina probe detection P-value, with a P-value of greater than 0.05 being deemed as undetected. Probe expression was Log_2 transformed and quantile-normalised using the Lumi Bioconductor package within R. Probes were mapped to Ensembl genes and annotated with Ensembl gene identifiers. Repeat samples were compared using multi-dimensional scaling (MDS) (Appendix 1.1) and assessed for consistency by hierarchical clustering (Appendix 1.2).

2.2.14 Quantitative real-time PCR

RNA was extracted from cellular pellets and quantified as described above. RT-PCR was performed using an applied Biosystems StepOnePlus Real-Time PCR System. Reverse transcription and amplification were performed in one step using the Taqman RNA-to-CT 1-Step Kit and Taqman primers targeting genes of interest or 'housekeeping' genes. RNA was

quantified using a 5-point standard curve for each primer set. Comparison of gene expression between samples was done after normalisation of all values to the geometric mean of three 'housekeeping' genes: PUM1, TBP and RPL37A. Details on individual gene assays for RT-PCR can be seen in Table 2.4 below.

Table 2.4 : RT-PCR Taqman gene expression assay information

Target	Assay ID	Context Sequence	Amplicon length
HIF1α	Hs_00153153_m1	TACACACAGAAATGGCCTTGTGAAA	76
HIF2α	Hs_01026149_m1	TCACCAGAACTTGTGCACCAAGGGT	70
PUM1	Hs_00472881_m1	TGGGGAACATCAGATCATTCAGTTT	77
RPL37a	Hs_01102345_m1	GTGCCTGGACGTACAATACCACTT	125
TBP	Hs_00427620_m1	GCAGCTGCAAAATATTGTATCCACA	91

2.2.15 Survival analysis

Survival analysis using the METABRIC dataset

The METABRIC (Molecular Taxonomy of Breast Cancer International Consortium) breast cancer dataset was downloaded (cbioportal.org) and used for survival analysis performed in R. The METABRIC dataset consists of over 2,000 fresh-frozen breast cancer samples with gene expression and associated clinical data, providing a large dataset without the need for integrating multiple studies into a meta-analysis. Gene expression data for these samples was collected using an Illumina HT-12 V3 array [437]. Patient treatments used in this study were relatively homogenous within clinically relevant subtypes; oestrogen receptor (ER)-positive and lymph node (LN)-negative samples generally did not receive chemotherapy, whilst ER-negative/LN-positive patients did and HER2-positive patients did not receive trastuzumab. This means that the effect of differential treatment types on gene expression is minimized, at least within these subgroups, allowing more simplistic interpretation of the data [437].

Analysis using Kmplot

Kmplot is an online tool for the rapid assessment of survival data in cancer. This tool includes a large dataset for breast cancer survival with gene expression and associated clinical outcome data for 5,143 breast cancer samples covering 22,277 genes [438-440].

These samples were combined and normalised from a number of experiments using Affymetrix HG-U133A and HG-U133 Plus 2.0 arrays available at the online repository GEO, as well as gene expression datasets taken from the European genome-phenome archive (EGA) and The Cancer Genome Atlas (TCGA) [440]. This tool is able to produce Kaplan-Meier curves displaying log rank p-values and hazard ratio with a 95% confidence interval for cohorts stratified into high or low for single or multiple gene expression values, with clinical data available for overall survival (OS), recurrence-free survival (RFS) and distant metastasis-free survival (DMFS). Optimum cut-points for analysis are selected by computing each expression quartile between the upper and lower quartiles of gene expression and selecting the most significant [440]. The gene expression and clinical data used by Kmplot was compiled by combining analyses performed on two compatible Affymetrix platforms (HG-U133A and HG-U133A Plus 2.0 arrays) available for download from GEO. Thirteen studies were selected which included at least 30 patients and provided raw expression data from these arrays as well as clinical survival information. Gene expression values were subjected to quality control and normalisation as described in Györrfy et al. 2009 [438].

SurvivALL

SurvivALL is a package for R (developed by Dominic Pierce, IGMM, University of Edinburgh) which allows the analysis of survival data using continuous data such as gene expression. A basic approach to survival analysis would typically select an appropriate cut-point of gene expression data to compare survival in low vs high expressing samples, but this single cut-point approach does not give any indication of the robustness of any differences found (i.e. whether a significant difference is only seen when cohorts are defined in a very specific way). To improve on this approach, the SurvivALL package performs survival analysis on all possible cut-points, giving survival statistics including p-values and hazard ratios for each. This allows a greater understanding of survival differences as the position and number of significant cut-points is made clear. The SurvivALL package was therefore used alongside all survival analyses performed in R. This package was not used for Kmplot survival analysis, as data from this meta-analysis is not available outside of the online tool.

2.3 Characterisation of cell line models

2.3.1 Confirmation of receptor expression by western blotting

Breast cancers can be broadly categorised by their expression of several key nuclear receptors (ER and PgR) and cell surface receptors (HER2 and EGFR); the relative expression of ERα, PgR and HER2 is used to define tumours as Luminal (A or B), HER2+ or Triple Negative. These subtypes exhibit different characteristics in terms of tumour aggressiveness and prognosis; cell biology, including differences in cell signalling pathway activation and gene expression; as well as differing sensitivities to targeted therapies. In order to understand the implications of HIF signalling in breast cancer it is important to recognise these differences, and as such I intend to use a panel of cell lines which represent these subtypes through a broad range of receptor expression patterns. Initial characterisation of this panel involved the comparison of cell surface and nuclear receptor protein expression through western blotting (Figure 2.1). The expression of EGFR, HER2, HER3, ERα and PgR was compared in untreated whole cell lysates. With the exception of MCF7-Neo (discussed in Section 3.2.2) all cell lines showed expression patterns consistent with their subtype and the literature. EGFR was highly expressed in the triple negative cell lines MDA-MB-231 and HBL100, which both showed low expression of all other receptors. HER2-positive cell lines BT474, MDA-MB-361 and SKBR3 all have moderate to high expression of HER2, but have differing expression of the other receptors; BT474 has relatively high ERα and PgR, SKBR3 shows moderate EGFR expression and MDA-MB-361 has high HER3. Whilst considered an ER-positive cell lines, ER was not detectable in MDA-MB-361, this may be due to an intermediate level of expression in this cell line [441] not detectable with the antibody used. Other ER-driven cell lines MCF7, T47D and ZR751 show predominantly high ERα expression as well as low EGFR and HER2. As expected MCF7-HER2 shows a similar expression profile to MCF7, with the exception of increased HER2 expression. This characterisation demonstrates two important points about this cell line panel. First of all, these cell lines represent the range of receptor expression profiles expected of the different molecular subtypes seen in breast cancer. Secondly, the categorisation of these cell lines by subtype alone is not sufficient in describing their receptor profiles and by extension their biology. This point is best demonstrated by the HER2-positive cell lines. These cell lines show a diversity of receptor levels alongside their high HER2 expression. This is an important consideration when comparing cell lines broadly by subtype,

but the inclusion of such cell lines in this panel means that comparisons within the HER2-positive group may be just as interesting as a broader comparison of subtypes.

2.3.2 Confirmation of the effects of selection antibiotic G418 on wild-type and genetically modified MCF7 cells

Preliminary SRB assays were performed to determine optimum concentration of G418 to be used in cell culture for the growth of genetically modified MCF7-HER2 and MCF7-NEO cell lines (Figure 2.2). Cells were seeded and grown in complete DMEM containing 0–5 mg/ml G418 for 10 days. It was expected that wild-type MCF7 cells lacking any form of resistance cassette would be sensitive to G418 treatment, whilst genetically modified MCF7-HER2 and MCF7-Neo cell lines should show high resistance conferred by the expression of the Neomycin resistance gene. MCF7 cells showed reduced growth rate at concentrations as low as 0.5 mg/ml, and cell growth was completely ablated by 5 days at concentrations of 1 mg/ml and above. In contrast, MCF7-HER2 and MCF7-Neo showed the expected resilience against G418, showing no reduction in growth rate at concentrations of up to 2 mg/ml. These cells were still able to grow at 5 mg/ml, the highest concentration tested, but the growth rate was marginally reduced. Therefore, a concentration of 1 mg/ml was selected as this was able to effectively stop MCF7 growth with no discernible effects on genetically modified cell lines.

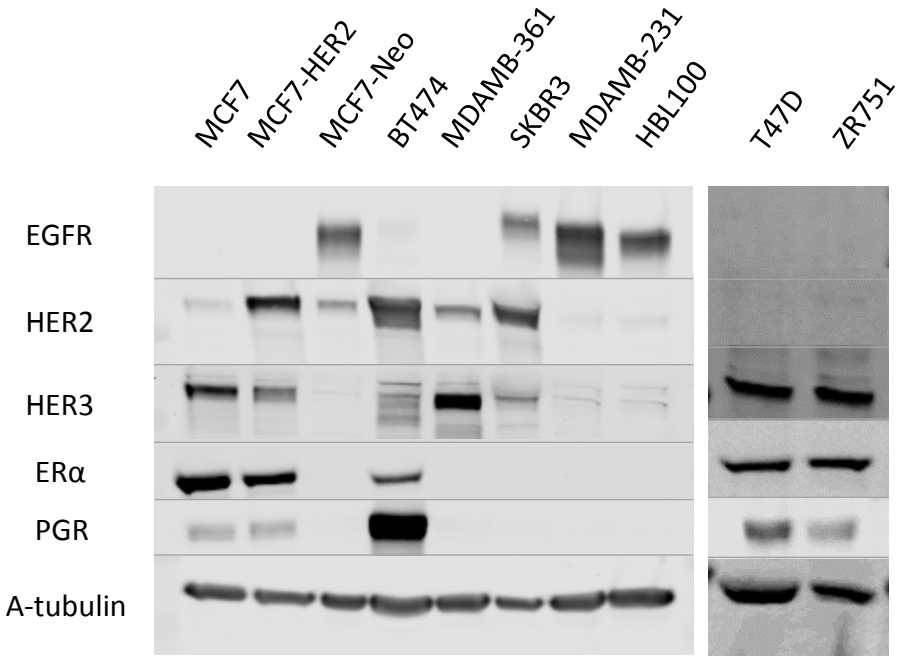

Figure 2.1: Characterisation of cell line receptor expression

Whole cell lysates from a panel of cell lines were run on a 7.5% bis-acrylamide gel. After membrane transfer, blots were probed for various cell surface receptors as well as α-Tubulin as a loading control.

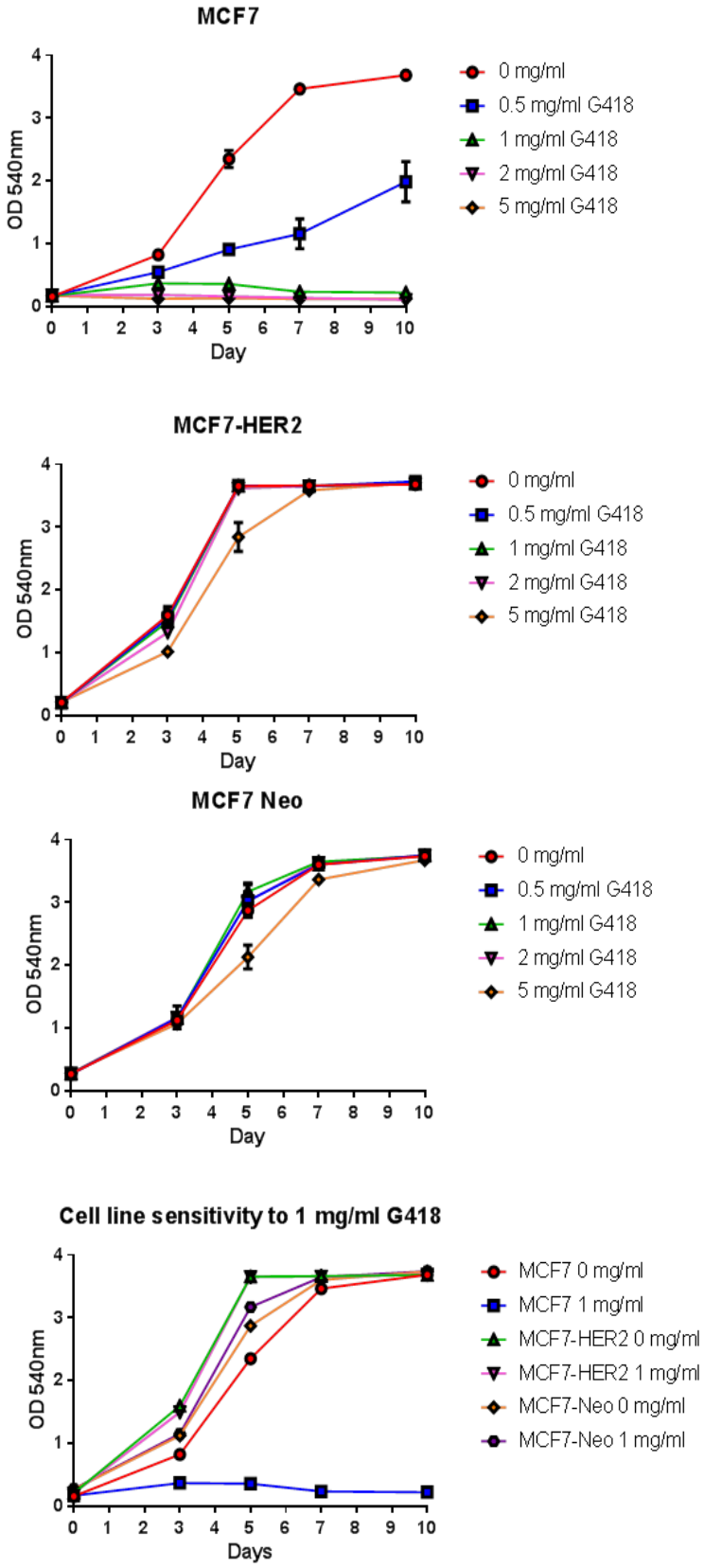

Figure 2.2: G418 sensitivity in MCF7 and genetically modified MCF7 derivative lines

Sulforhodamine B assays were used to compare cell growth in MCF7, MCF7-HER2 and MCF7-Neo cell lines treated with G418. The top 3 panels show how cell proliferation is affected by a range of G418 concentrations in individual cell lines over a 10 day period. The bottom panel shows a comparison of how the 3 cell lines respond to 1 mg/ml, the concentration used for routine cell culture.

Chapter 3: HER2 overexpression in MCF7 cells drives an increased response to hypoxia

3.1 Introduction

The ability of growth factor signalling to modulate hypoxia-inducible factor α-subunit levels in normoxia has demonstrated that the control of HIFα upregulation and HIF transcriptional activity is more complex than the canonical oxygen-dependent mechanism originally proposed. Growth factor stimulation by neuregulin-1β treatment, or activation of the HER2 receptor signalling pathway has been shown to increase HIF1α levels in breast cancer cell lines [220, 421, 424], and the ability of HER2 and EGFR receptor signalling to act through HIF1α or HIF2α has been demonstrated in the context of aromatase inhibitor or anti-oestrogen resistance [424, 426]. In patient tumour samples, HIF1α expression has been shown to correlate with HER2 expression [285, 289, 442] and also poor clinical outcome [284, 286, 287, 443] in a number of studies [444]. The role of HIF2α has been less extensively studied, however its correlation with HER2 expression [321] as well as poor outcome and distant metastasis [261] in breast cancer has also been demonstrated. In addition to an established role in survival and outcome, these studies suggest that both HIF1α and HIF2α may have a relationship with HER2 signalling in breast cancer.

Despite recognition of growth factor-HIF interplay in breast cancer, this has been largely treated as a separate mechanism to the hypoxic regulation of HIFs, with little research into how growth factor signalling modifies the cellular response to hypoxia. In this chapter I aim to determine whether the expression of the HER2 growth factor receptor affects the upregulation of HIFα subunits in response to hypoxia by assessing the extent of HIF1α and HIF2α in a panel of cell lines as well as in an isogenic cell line model of HER2 overexpression. Beyond this, I will use this isogenic cell line model to investigate the effect of HER2 on the expression of important hypoxic response genes in 2D and 3D culture models. Using this approach I am able to provide initial evidence of the importance of HER2 receptor expression in driving an enhanced cellular response to hypoxia. This includes the increased hypoxic activation of genes known to drive aggressiveness and invasion characteristics and reduced survival in breast cancer. Previous research (discussed in chapter 1) has shown that breast

cancer cell lines, including MCF7, upregulate HIF1α and drive hypoxic response genes both canonically in response to hypoxia, and in response to NRG1β in normoxia [220, 421]. HER2 overexpression in mouse 3T3 cells has also been shown to increase HIF1α levels in normoxia [220, 421]. With this in mind, it is suspected that HER2 may modify the hypoxic response through HIF1α, and we anticipate that breast cancer cell lines may demonstrate an increased level of HIF signalling in response to hypoxia when HER2 is highly expressed. Additionally, there is some evidence for a bidirectional relationship between HIF2α and growth factor signalling (through EGFR) in breast cancer cell lines [425], it is therefore also anticipated that the hypoxic induction of HIF2α may be dependent on the levels of growth factor receptors in these cell lines.

3.2 HIF induction by hypoxia is highly variable and cell line-dependent

Initially, the hypoxic upregulation of HIF1α and HIF2α was assessed across a panel of breast cancer cell lines. This panel was selected to represent the three main subtypes of breast cancer as well as an array of different growth factor receptor profiles. The hypoxic stabilisation of the oxygen-labile HIF alpha subunits (HIF1α and HIF2α) was compared by western blotting of nuclear lysates collected in normoxia or after 24, 48 or 72 hours at 0.5% O_2. Western blotting and densitometric quantification can be seen in Figure 3.1. This demonstrates the variability of the hypoxic regulation of HIFα subunits across cell lines. As expected, all cell lines showed increased levels of nuclear HIF1α and HIF2α in response to hypoxia, however the extent to which HIFα subunits were increased in response to hypoxia is clearly highly dependent on cellular context. Induction of HIF-α subunits did not obviously correlate with receptor subtypes (defined by the expression of ER, PR and HER2), as a large amount of variation between cell lines was seen both within and between subtype categories. This included no clear difference between cell lines with high HER2 expression versus those with low HER2.

In general, HIF1α appears less variable than HIF2α, with the exceptions of the HER2-positive cell line SKBR3, which showed low HIF1α induction, and the triple-negative cell line HBL100, which showed high HIF1α induction. However, a marked variability between cell lines was observed in the longevity of induced HIF1α in hypoxia. MCF7, MCF7-HER2 and HBL100 all showed high levels of HIF1α protein after 48 hrs and in the cases of MCF7-HER2 and HBL100 relatively low reductions even by 72 hrs. In contrast, ZR751, T47D, BT474, SKBR3

and MDAMB231 all showed a relatively rapid decrease in HIF1α protein levels. This variability did not appear to correlate with molecular subtype, nor did HIF1α longevity correlate with the magnitude of initial induction in hypoxia. HIF2α was commonly induced by 24 hrs and remained at high levels throughout the 72 hr time course. Across cell lines the magnitude of HIF2α induction was highly variable, however the magnitude once again did not correlate with molecular subtypes or the expression of HER2 in this panel. MCF7 and BT474 showed the lowest induction of HIF2α, whilst ZR751, SKBR3 and HBL100 showed the highest (with T47D, MCF7-HER2 and MDA-MB-231 showing moderate induction), although differences in the levels of the TBP control between cell lines means that caution should be taken when directly comparing normalised results. This comparison of cell lines showed no obvious relationship between HIF1α and HIF2α levels in hypoxia, and no definite indication that levels of hypoxic induction are determined by HER2 expression.

In this experiment the high variability of HIFα induction between cell lines meant that no obvious relationship was seen between HER2 expression and HIFα levels across cell lines. Despite this, the inclusion of MCF7 and its HER2-overexpressing isogenic counterpart MCF7-HER2 suggests that HER2 overexpression in this context may alter the upregulation of HIFα subunits, especially HIF2α in response to hypoxia. This two cell line model is used in the following experiments to investigate this effect in more detail.

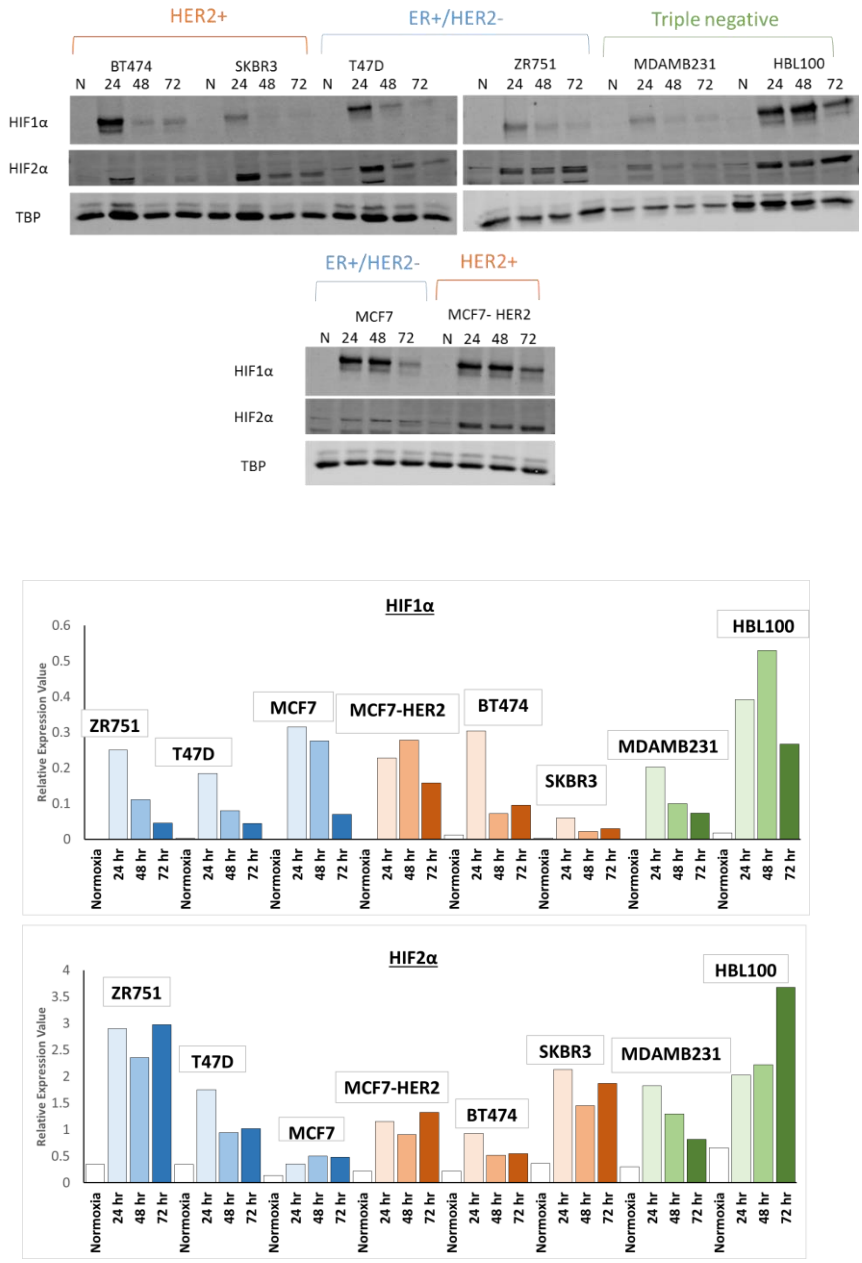

Figure 3.1: Hypoxic upregulation of HIF1α and HIF2α in nuclear fractions across breast cancer cell lines

A panel of breast cancer cell lines representing different molecular subtypes were cultured either in normal culture conditions (20% oxygen) or under hypoxia (0.5% oxygen) for up to 72 hours. Lysates of the nuclear fraction were collected at 24, 48 and 72 hours and after protein quantification, 20 µg of these lysates was loaded and run by gel electrophoresis. Western blotting was performed to detect the expression of HIF1α, HIF2α and Tata-binding protein (TBP). TBP was used as a loading control to which HIF1α and HIF2α densitometry quantification was normalised (n=1).

3.3 The effect of HER2 overexpression on the cellular response to hypoxia in MCF7 and MCF7-HER2

The MCF7 and MCF7-HER2 isogenic cell lines provide a more direct system for studying the effects of HER2 signalling on HIF regulation in breast cancer, as any deviations in cell behaviour can be more directly attributable to the overexpression of the HER2 receptor. As such, differences seen in HIF-upregulation between these two cell lines in Figure 3.1 suggest a role for HER2 in the response to hypoxia. To understand how HER2 overexpression can modify the cell's behaviour in hypoxia, proliferation and motility of these cell lines were compared under normal and hypoxic oxygen concentrations. The hypoxic upregulation of HIF1α and HIF2α was compared between the two cell lines and the upregulation of known hypoxia response genes *CAIX* and *LDHA* examined. Furthermore, the upregulation of these factors in the presence of the EGFR/HER2 inhibitor lapatinib was assessed to determine whether cell line differences could be reversed by the inhibition of growth factor signalling.

3.3.1 Overexpression of the HER2 receptor in MCF7 does not increase cellular growth in response to hypoxia, but increases hypoxic cellular motility

Sulforhodamine B (SRB) assays were used to compare normoxic and hypoxic proliferation between MCF7 and MCF7-HER2 cell lines. These were used to determine the effect of acute and chronic hypoxia on the growth rate of these cell lines. Cells were seeded onto 96-well plates and grown under either normal culture conditions or in 0.5% oxygen for up to 7 days. For chronic hypoxia, cells were continuously passaged in 0.5% oxygen conditions for 10 weeks before being seeded into 96-well plates in hypoxia; 3, 5, or 7 days after seeding, cells were fixed and SRB assay used to determine relative cell densities. No differences between the cell lines under normoxia, acute or chronic hypoxia were observed (Figure 3.2A). Cell number under both hypoxic conditions in both cell lines was reduced relative to normoxia and this was apparent at each time point. This suggests a deleterious effect of hypoxia on cell population growth with no significant differences seen when the HER2 receptor was overexpressed. This is the case when cells are initially exposed to hypoxia, and also after long-term acclimatisation to low oxygen conditions (chronic hypoxia). This

experiment shows that in this model increased HER2 expression does not drive significantly increased proliferation in normoxia or protect against the reduction in proliferative rate seen in hypoxia.

Next, wound healing assays were used to assess the role of HER2 overexpression on cell motility in normoxia and hypoxia. Hypoxia is considered a driver of cellular motility in the tumour microenvironment [315, 445], with the presence of hypoxic regions correlating with increased aggressiveness of the tumour in terms of invasion and metastasis [446]. For this reason, increased cell motility could be considered a more probable phenotypic outcome of an altered response to hypoxia in the presence of HER2 overexpression. To assess this, cells were seeded at confluent levels into plates containing removable inserts. Once the cells had attached, these inserts were removed to create a wound of fixed size (500 μm). The plates were cultured in either normoxia or 0.5% oxygen and the size of the wound at various points along its length was measured daily for 4 days. In normoxia, wound healing in terms of area covered was equivalent between the cell lines, with no significant difference found between them, even though the mean wound coverage was greater in MCF7-HER2 at each time point. Despite this, there were clear phenotypic differences between the cell lines in terms of how they covered the wound; whilst MCF7 remained as an epithelial sheet with strong cell-cell adhesion, MCF7-HER2 invaded as individual cells, with weaker cell-cell adhesion and more obvious lamellapodia (Figure 3.3). This is indicative of an epithelial-to-mesenchymal transition (EMT) phenotype (the role of EMT will be discussed in more detail in Chapter 4). Wound healing in hypoxia demonstrated differences between the two cell lines. In MCF7 cells, wound healing in hypoxia was significantly reduced when compared to normoxia ($p = 0.0013$, two-way ANOVA with Sidak's multiple comparison test), equating to an average of 12% coverage by 96 hrs compared to 46% in normoxia. In MCF7-HER2 wound healing was increased in hypoxia, covering on average 89% of the wound compared to 68% in normoxia. Whilst the differences between normoxia and hypoxia for MCF7-HER2 were not found to be statistically significant, the differences between hypoxic wound healing between cell lines was significant, being higher in MCF7-HER2 ($p<0.0001$, two-way ANOVA with Sidak's multiple comparison test) at 48, 72 and 96 hrs. This demonstrates that motility in hypoxia is higher in MCF7-HER2 despite comparable motility in normoxia.

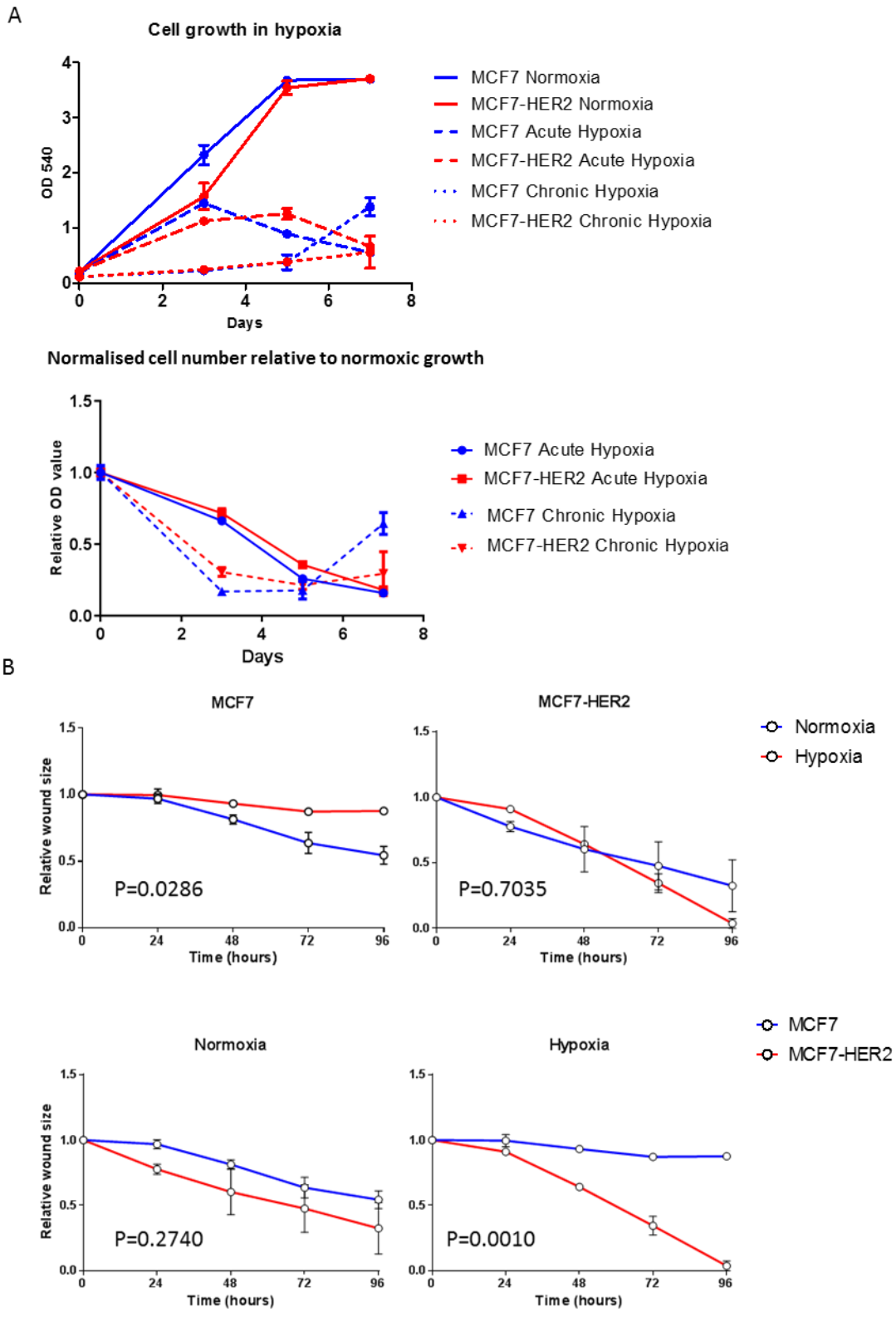

Figure 3.2: The effect of hypoxia on proliferation and wound healing in MCF7 cell lines

A) MCF7 and MCF7-HER2 growth was assessed over 7 days by Sulforhodamine B assay of MCF7 and MCF7-HER2 grown in normoxia (20% oxygen) or hypoxia (0.5% oxygen), chronic hypoxic cells were continually passaged under hypoxia for >10 weeks before the start of the experiment. Both un-normalised OD values over 7 days (top) and growth relative to normoxia (bottom) are shown. Error bars represent the standard deviation (n=6) B) Relative wound area measurements for wound healing assays using MCF7 and MCF7-HER2 under normoxic or hypoxic conditions in 0.2% FBS DMEM. This is a representative example of n=3 biological repeats. Two-way ANOVA was used to determine significance both between cell lines and oxygen conditions. P-values for individual comparisons are displayed for each graph (Two-way ANOVA) (Error bars represent the SEM, n=3).

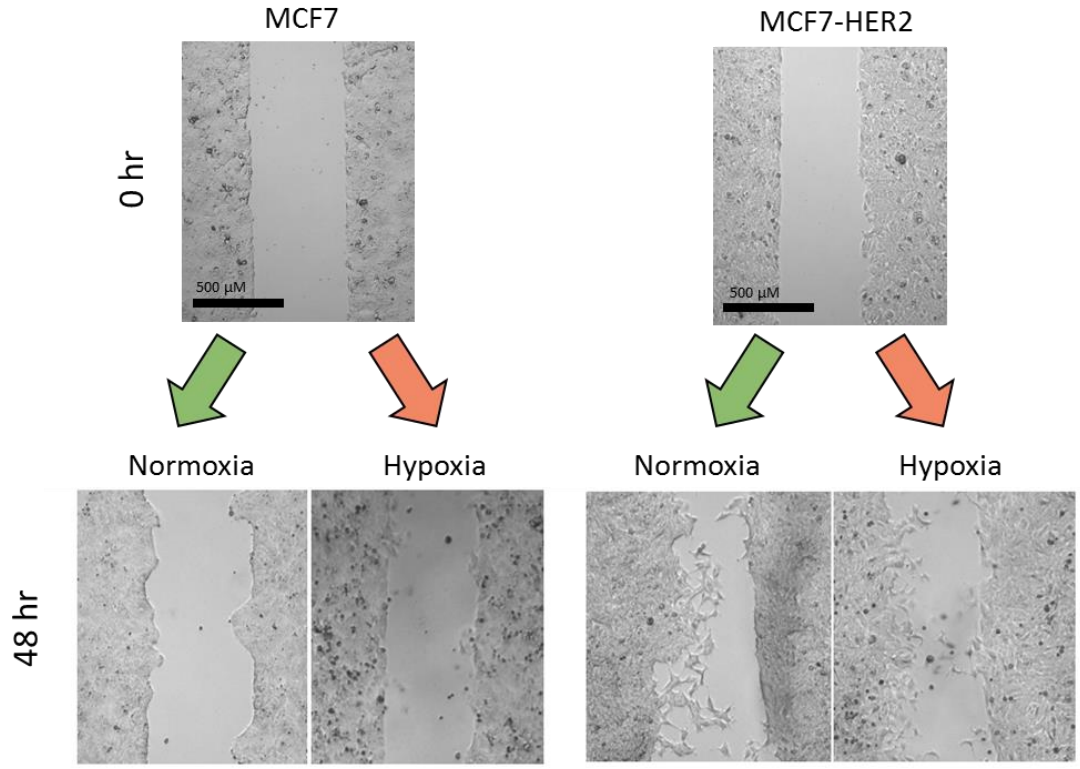

Figure 3.3: Representative images of MCF7 and MCF7-HER2 wound healing assays

Representative images from wound healing assays showing differences between MCF7 and MCF7-HER2 in normoxia and hypoxia. Cells were seeded in complete 10% FBS DMEM until confluent. Media was changed to 0.2% FBS and grown in normoxia or hypoxia after the removal of an insert which obstructs cellular growth over a 500 µM region. Cell movement into this region was assessed over 4 days (Figure 3.2). Images shown are from 0 hrs (top) and 48 hrs (bottom) after the removal of the insert.

3.3.2 HER2 overexpression modifies the hypoxia-mediated stabilisation of HIF proteins in MCF7-HER2 cells

The hypoxic regulation of HIFα subunits was next assessed in the isogenic MCF7 and MCF7-HER2 cell line models to determine whether growth factor signalling could modulate HIF levels under hypoxic conditions. The levels of HIF1α and HIF2α protein were assessed by western blotting of MCF7 and MCF7-HER2 whole cell, nuclear and cytoplasmic lysates grown in normoxia (20% oxygen) or hypoxia (0.5% oxygen). By using both whole cell lysates and lysates enriched for either the nuclear or cytoplasmic cellular fraction the localisation of HIFα protein in normoxia or hypoxia in these cell lines can be assessed. Canonically HIFα protein is understood to translocate to the nucleus when in abundance, and this translocation is required for HIFα to form active transcription factors. Therefore the level of nuclear HIFα is indicative of transcriptionally active protein. Conversely, by looking at the levels of whole cell and cytoplasmic HIFα, we do not overlook the possibility that non-canonical regulation by growth factor signalling might also alter the typical localisation of the protein.

In whole cell lysates, HIF1α levels were comparable between the two cell lines (Figure 3.4). The protein was shown to be below detectable levels in normoxia but increased after 24 hrs in hypoxia. Levels were seen to increase further at 48 hrs before declining partially at 72 hrs. This pattern of stabilisation at early hypoxic time points followed by a decline at later time points has been described in neuroblastoma cell lines [447], and the HIF-associated factor (HAF), which is thought to mediate this effect, has been shown to degrade HIF1α in hypoxia in pancreatic, glioblastoma and RCC cell lines [264]. It was therefore not surprising to see a similar pattern of hypoxic regulation in breast cancer cell lines. No difference in HIF1α induction was seen when HER2 was overexpressed. HIF2α upregulation in MCF7 remained relatively low (close to the detection limit with this antibody) but was seen to increase steadily in response to hypoxia, with the highest levels seen at 72 hrs. While this agreed with the HIF1α and HIF2α dynamics as described in the literature [265], HIF2α expression in the MCF7-HER2 cell line was markedly increased. This included higher levels in normoxia and higher levels in response to hypoxia when compared to wild-type MCF7. Whilst no significant differences were detected between cell lines for HIF1α upregulation, cell line-dependent differences in HIF2α upregulation were shown to be statistically significant ($p=0.0280$, two-way ANOVA), with multiple comparisons showing significant differences between HIF2α levels between the two cell lines after 48 hrs in hypoxia ($p=0.0138$).

As transcription factors, the cellular location of HIF1α and HIF2α is integral to their function. Canonically, HIFα subunits increase in the cytoplasm when oxygen is limiting for the activity of PHD hydroxylases, and dimerise with HIFβ to form active transcriptional units in the nucleus [192, 195, 448]. Thus, in hypoxia the level of HIFs in the nuclear compartment are representative of the active transcription factor. To assess whether increases in HIF2α upregulation in hypoxia coincided with increased nuclear levels of the protein, and to otherwise consider the effect of HER2 expression on the shuttling and cellular location of HIF1α and HIF2α, protein levels over a 72 hr hypoxic time course were assessed in nuclear and cytoplasmic cell lysates of MCF7 and MCF7-HER2 cells (Figure 3.4 C/D).

The expression of HIF1α was strongly upregulated in the nuclear compartment from 24 hrs but remained below detectable levels in the cytoplasmic compartment. Temporally, the pattern of nuclear HIF1α upregulation in response to hypoxia matched that seen in whole cell lysates and is consistent with the pattern described in the literature [265]. Whilst HIF1α levels were comparable between the two cell lines, the decrease in protein seen at 72 hrs appeared reduced in the context of HER2 overexpression. Unfortunately, this could not be confirmed statistically but the potential mechanisms and consequences of this effect will be discussed at the end of this chapter (Section 3.5).

HIF2α expression was detectable in the nuclear and cytoplasmic fractions of both cell lines and upregulated in all cases in response to hypoxia. Upregulation was seen at 24 hrs under hypoxic conditions and remained increased for the 72 hr time course. In agreement with whole cell lysates, HIF2α levels were induced to a greater extent in the MCF7-HER2 cell line when compared to wild-type MCF7. This was the case in both nuclear and cytoplasmic fractions, suggesting an upregulation of the protein in its active nuclear transcription factor role, as well as a build-up in the cytoplasm.

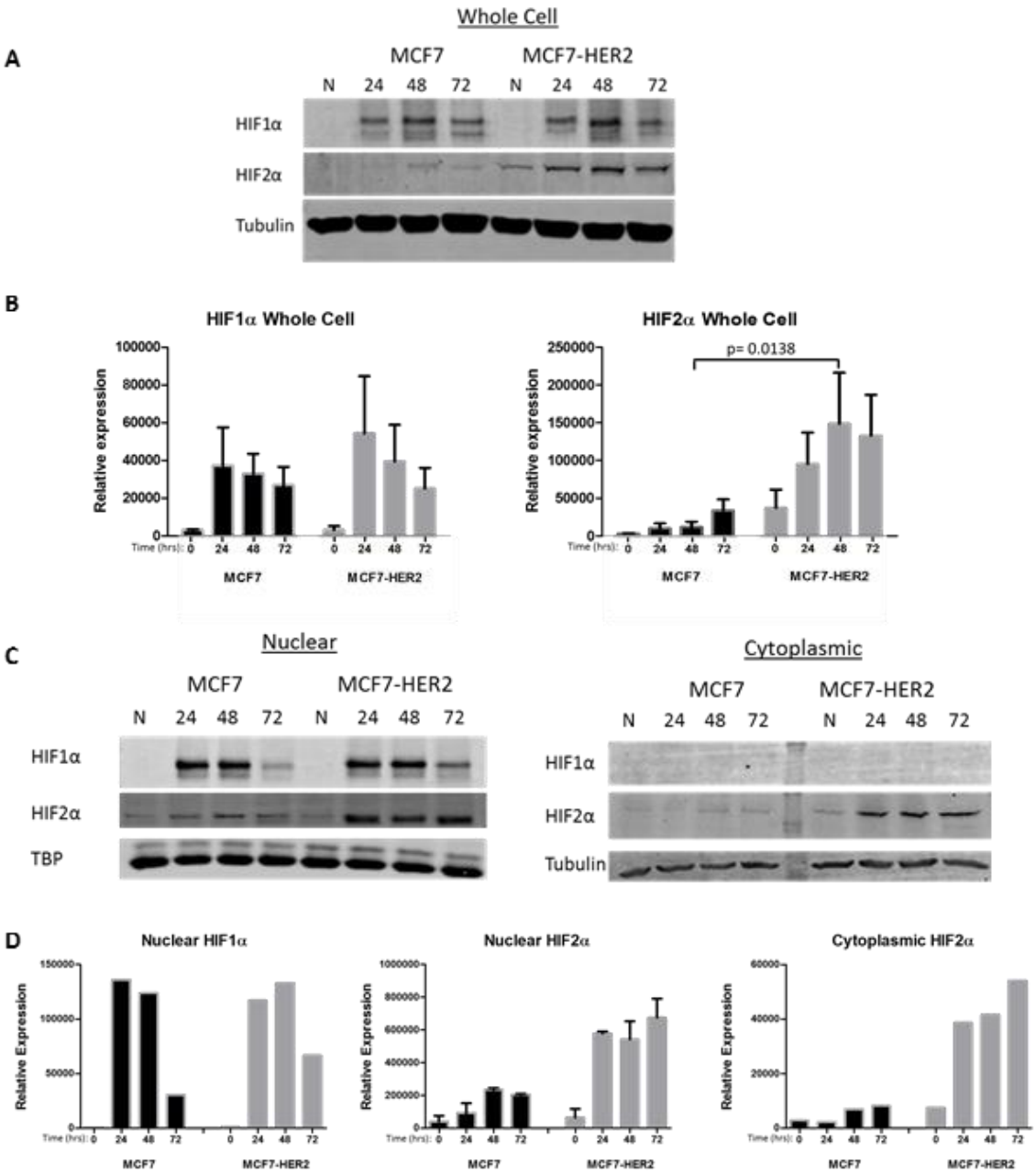

Figure 3.4: The upregulation of HIF1α and HIF2α by hypoxia in MCF7 and MCF7-HER2 cell lines

Western blot analysis of MCF7 and MCF7-HER2 whole cell lysates collected in normoxia (20% oxygen) or hypoxia (0.5% oxygen). Whole cell, nuclear or cytoplasmic lysates were collected at 24, 48 and 72 hours hypoxia; 40 µg of lysates were used for gel electrophoresis. Western blotting for HIF1α, HIF2α, TATA-binding protein (nuclear loading control) and α-Tubulin (whole cell/cytoplasmic loading control) was performed. A) Western images show a representative example of HIF1α and HIF2α hypoxic upregulation in whole cell lysates of MCF7 and MCF7-HER2. B) Graphs display the average densitometry expression values relative to loading control with standard error of the mean (SEM) represented as error bars. The level of HIF2α was found to be significantly different between the two cell lines (two-way ANOVA p=0.0280) with Sidak's multiple comparison showing significantly higher levels in MCF7-HER2 at 48 hrs when compared to MCF7 (p=0.0138); no significant differences were found between cell lines for HIF1α. (n= 5 experiments for HIF1α and n=4 for HIF2α).C) Representative examples of HIF1α and HIF2α in nuclear and cytoplasmic lysates of MCF7 and MCF7-HER2 cell lines. D) Expression of HIF1α in nuclear fractions (n=1), and HIF2α in nuclear (n=2) and cytoplasmic (n=1) fractions normalised to loading controls TBP (nuclear) or α-tubulin (cytoplasmic). Error bars represent the SEM.

3.3.3 Increased hypoxic upregulation of CAIX and LDHA in MCF7-HER2 cells

In addition to HIFα subunit regulation, the hypoxic upregulation of two known HIF target genes, carbonic anhydrase IX (CAIX) and lactate dehydrogenase A (LDHA), was assessed in whole cell lysates by western blotting. Once again, samples were either normoxic (approximately 20% oxygen) or grown in hypoxia (0.5% oxygen) for 24, 48 or 72 hrs. CAIX is a membrane bound version of the enzyme responsible for the conversion of H_2O and CO_2 to HCO_3^- and H^+ ions [449-451]. CAIX is generally associated with hypoxic regions in tumours and considered to be predominantly HIF1 driven. It has been associated with metastasis and poor prognosis in breast cancer [290, 452-454], and its potential as a therapeutic target is the subject of ongoing research [455, 456]. LDH is a glycolytic enzyme responsible for the conversion of pyruvate to lactate. As with numerous glycolytic enzymes LDHA has been shown to be a HIF1 target gene, and thus driven by hypoxia. Overexpression is common in breast cancer, and is associated with poor clinical outcome and resistance to therapy [457-460].

In these experiments CAIX protein levels were shown to be upregulated in hypoxia in both cell lines, with a steady increase seen up to 72 hrs (Figure 3.5). Whilst CAIX was not seen in normoxia in either cell line, the absolute levels at all hypoxic time points were considerably (approximately 4x) higher in the MCF7-HER2 cell line. This suggests that the hypoxic upregulation of the protein is stronger in the context of HER2 overexpression. CAIX upregulation was shown to be significantly different between cell lines ($p=0.0332$ two-way ANOVA), whilst multiple comparisons demonstrated significantly higher CAIX in the MCF7-HER2 cell line at 48 and 72 hrs when compared to MCF7 ($p=0.0204$ and $p=0.0150$ respectively, Sidak's multiple comparisons). LDHA upregulation was seen in response to hypoxia in both cell lines. Protein levels were low in normoxia but induced at 24 hrs, with increasing levels up to 72 hrs. However, no significant difference is seen between MCF7 and MCF7-HER2 cells (Figure 3.5).

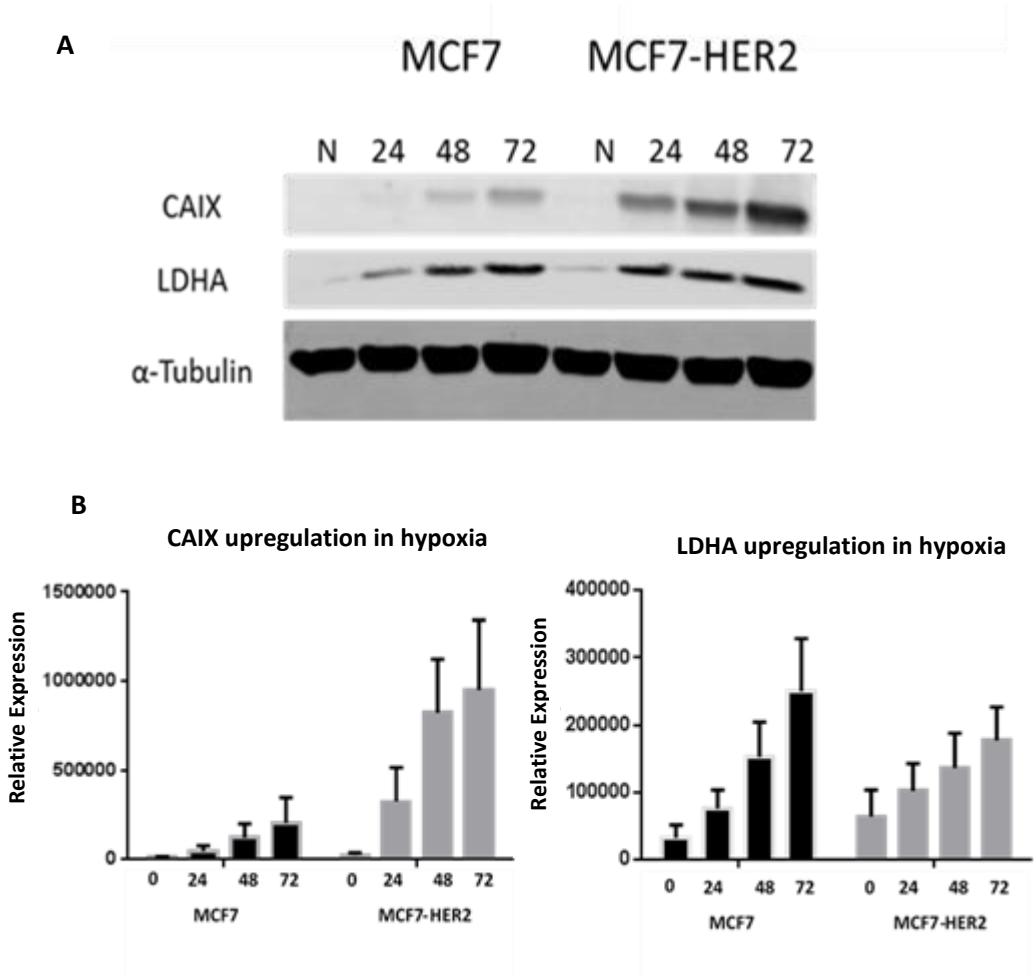

Figure 3.5: Increased upregulation of HIF target genes CAIX and LDHA in hypoxic MCF7-HER2

Western blotting analysis of MCF7-HER2 whole cell lysates collected in normoxia (20% oxygen) or hypoxia (0.5% oxygen). Whole cell lysates were collected at 24, 48 and 72 hours hypoxia. 40 µg of lysates were used for gel electrophoresis. Western blotting for CAIX, LDHA and α-Tubulin (loading control) was performed. A) Representative example of western blotting results. B) Graphs display the average densitometry expression values relative to tubulin, with standard error of the mean (SEM) represented as error bars from n= 5 experiments (HIF2α n=4). Two-way ANOVA with Sidak's multiple comparison test was used to compare expression between cell lines. CAIX expression was significantly higher in MCF7-HER2 (p=0.0332) with multiple comparisons showing significant differences at 48 and 72 hours (p=0.0204 and p=0.0150 respectively).

3.3.4 HER2-mediated CAIX and LDHA upregulation in hypoxia can be reduced by HER2 inhibition with lapatinib

To assess the relationship between HER2 overexpression and increased upregulation of HIF targets in hypoxia, the inhibition of growth factor signalling by lapatinib was investigated. Lapatinib is a small molecular tyrosine kinase inhibitor which blocks the kinase activity of HER1 (EGFR) and HER2 by occupying the ATP-binding pockets of these receptors. This prevents receptor transphosphorylation and thereby inhibits the initiation of the downstream signalling cascade [122]. MCF7-HER2 cells were treated with 1 μM lapatinib or DMSO vehicle only, 30 minutes prior to hypoxia treatment. Whole cell lysates were collected at 24 hr time points and probed for HIF1α, HIF2α, CAIX and LDHA. Whilst western blotting with an antibody specific for phosphorylated tyrosine residues 1221 and 1222 on the HER2 receptor demonstrated successful inhibition of HER2 receptor activation at all time-points (Figure 3.6), effects on the upregulation of HIFα subunits and HIF target proteins were minimal, and no statistically significant effects in this set of experiments were shown. Hypoxic increases in HIF1α and HIF2α appeared mainly unperturbed, however results suggest that any effect from lapatinib on HIF1α may actually increase its upregulation rather than inhibit it. Lapatinib inhibited the upregulation of LDHA, with reduced levels at 48 and 72 hrs hypoxia (Figure 3.6), CAIX levels were also reduced to a small degree after treatment with lapatinib at 24, 48 and 72 hrs, however this effect was not statistically significant.

Multicellular spheroids for both MCF7 and MCF7-HER2 cell lines were grown for 1-2 weeks and fixed in formalin, before being paraffin embedded, sectioned and stained for various targets through immunohistochemistry. The expression of HIF1α and HIF2α, as well as HIF targets were assessed and compared between cell lines (Figure 3.8A-C). This was done alongside staining with hypoxyprobe-1 (Pimonidazole HCl) [461] (see materials and methods), which was able to show the areas of the spheroids that had been exposed to low oxygen conditions (Figure 3.7).

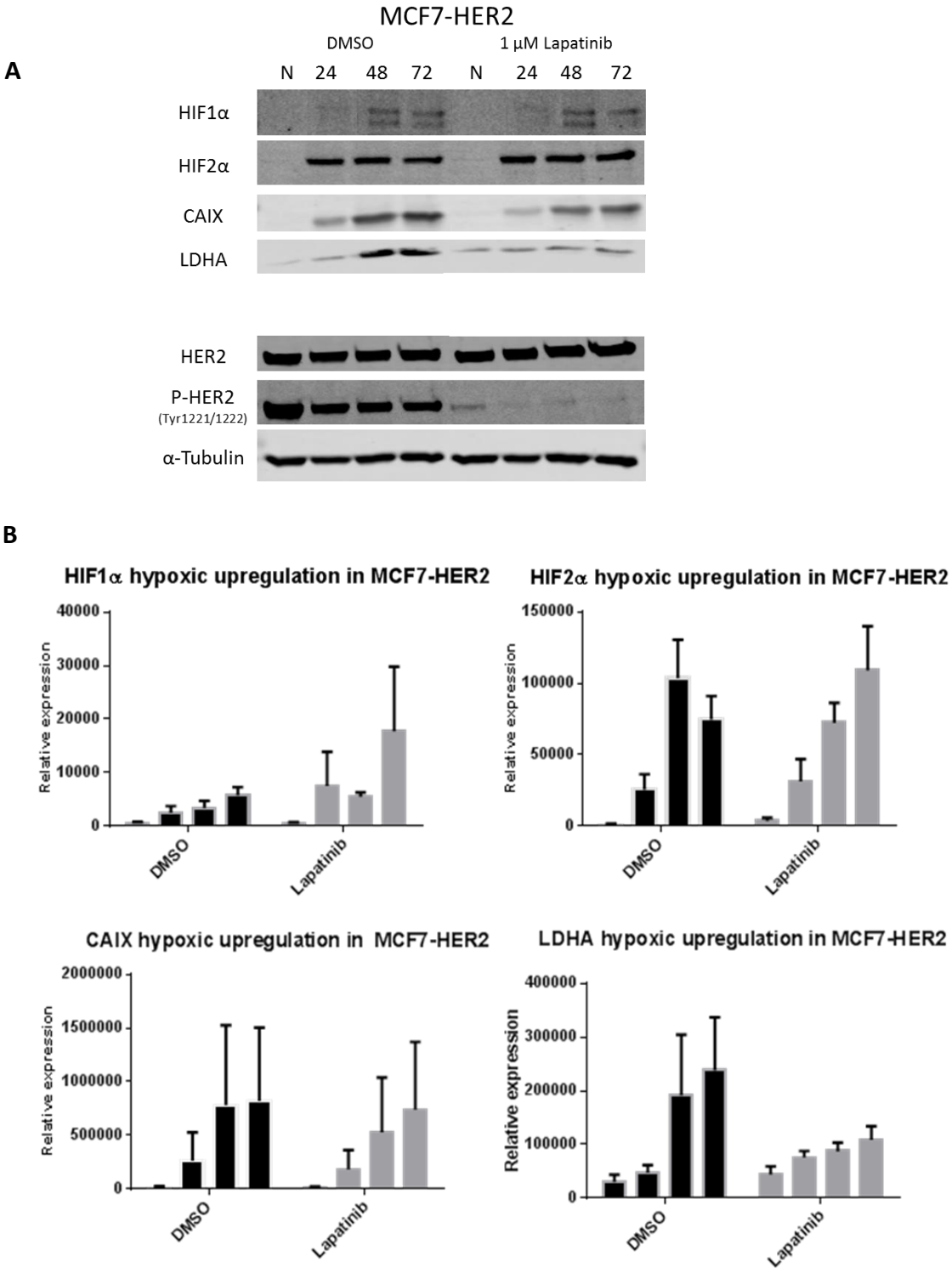

Figure 3.6: The effect of HER2 inhibition with lapatinib on the hypoxic upregulation of HIFα and HIF target genes

A) Representative examples of western blots from the graphs shown above. C) Western blots of HER2 and phospho-HER2 (Tyr1221/1222) were performed to demonstrate the effective inhibition of HER2 phosphorylation by lapatinib. B) Protein expression values relative to loading control (α-tubulin) from western blotting of whole cell collected in normoxia or after, 24, 48 or 72 hrs in hypoxia (0.5% oxygen). Cells were pre-treated with 1 µM of lapatinib or equivalent vehicle (0.01% DMSO) 30 minutes prior to the start of hypoxic treatment. Normoxic samples were treated with lapatinib or DMSO for 72 hrs prior to collection. Error bars represent the SEM of 3 repeat experiments.

Scoring of spheroid staining was done in two different ways; for nuclear staining the percentage of nuclei positively stained in each spheroid was calculated, and for cytoplasmic, membranous or mixed staining patterns, scores between 0 and 6 were assigned based on the area and intensity of the stain. The scoring system first assigned a score of 0-6 for the area of staining coverage (0 = 0-10% staining, 1= 10-25%, 2 = 25-40%, 3 = 40-55%, 4= 55-70%, 5= 70-85% and 6 = 85-100%) and a score of 0-3 for staining intensity, with 0 representing no visible staining, 1 being faint staining and 3 being intense staining (this was scored independently of the area covered). A final score was established by dividing the area score by 2 and adding it to the intensity score. Scoring was performed using only the viable regions of the spheroids and excluding necrotic central areas which were clearly distinguished by a loss of cellularity. The results of this scoring procedure for each target assessed can be seen in Table 3.1.

Staining for HIF1α was seen as nuclear staining in occasional cells, with surprisingly few stained nuclei in either cell line (<10% in all cases) (Figure 3.8A). Staining was not particularly consistent with hypoxyprobe-1 staining, generally occurring most frequently in the central viable region of spheroids rather than directly adjacent to necrotic regions. No discernible differences between cell lines were noted. HIF2α also showed no concordance with hypoxyprobe-1 or any tendency towards staining more centrally within spheroids, where oxygen concentrations would be expected to be lower. Instead, HIF2α staining was largely ubiquitous in terms of cytoplasmic staining, with randomly distributed positively stained nuclei. Staining of HIF2α was more intense in MCF7-HER2 spheroids when compared to wild-type MCF7 spheroids, with a median score of 6 for MCF7-HER2 compared to 2 for MCF7. This difference was most obvious in the cytoplasmic compartment but also included more frequently stained nuclei in the MCF7-HER2 spheroids. In general, HIFα staining patterns seen in these two cell lines in 3D are in agreement with western blotting results. HER2-driven differences are seen in HIF2α but not HIF1α. HIF1α is seen as solely nuclear staining, whereas HIF2α is visibly upregulated in both nuclear and cytoplasmic compartments (Figure 3.8A).

Known HIF targets CAIX, LDHA, VEGF [462] and CD44 [463, 464] were also stained in MCF7 and MCF7-HER2 spheroids (Figure 8 B/C). All four of these proteins were more strongly stained in MCF7-HER2 spheroids when compared to MCF7. CAIX expression was very low in

MCF7 spheroids with essentially no staining being visible. This was expected as MCF7 cells have previously been shown to be low level expressers of CAIX even under hypoxia [456]. On the other hand, MCF7-HER2 showed an increased expression of CAIX with clear membranous staining and a median score of 3 (Figure 3.8B). Areas of staining seemed to develop preferentially on the outside edge of the spheroid as opposed to the hypoxic core and did not appear to correlate to hypoxyprobe-1 staining. LDHA expression was seen fairly ubiquitously in MCF7 cells but was only faintly expressed. In MCF7-HER2, LDHA expression was more highly expressed with higher intensity and more nuclear staining. LDHA was scored with a median value of 4.5 for MCF7 and 6 for MCF7-HER2 (Figure 3.8B). VEGF showed light to moderate cytoplasmic staining apparent across the entire spheroid with the exception of the peri-necrotic region where staining was absent, scoring 3.5 as a median value. MCF7-HER2 showed more intense VEGF staining across the entire spheroid including the peri-necrotic region with a median score of 5.75 (Figure 3.8C). CD44 was the only target tested that appeared to correlate with the hypoxic and peri-necrotic regions of the spheroids, although this was only seen in MCF7-HER2. Expression of CD44 in MCF7 was low, in some cases undetectable, and when present, of low intensity and including small areas of just a few cells (scoring 1.5 as a median score). MCF7-HER2 however showed intense staining, which was not ubiquitous but found primarily in peri-necrotic regions, with less staining observed on the outside of the spheroid (median score of 4.5) (Figure 3.8C). This correlated well with hypoxyprobe-1 expression in these spheroids.

Together IHC in 3D multicellular spheroids demonstrated that the overexpression of HER2 in MCF7-HER2 cells causes the increased expression of HIF targets. This overexpression was not limited to the peri-necrotic regions of the spheroids and most often showed no spatial correlation to hypoxia as determined by hypoxyprobe-1 staining.

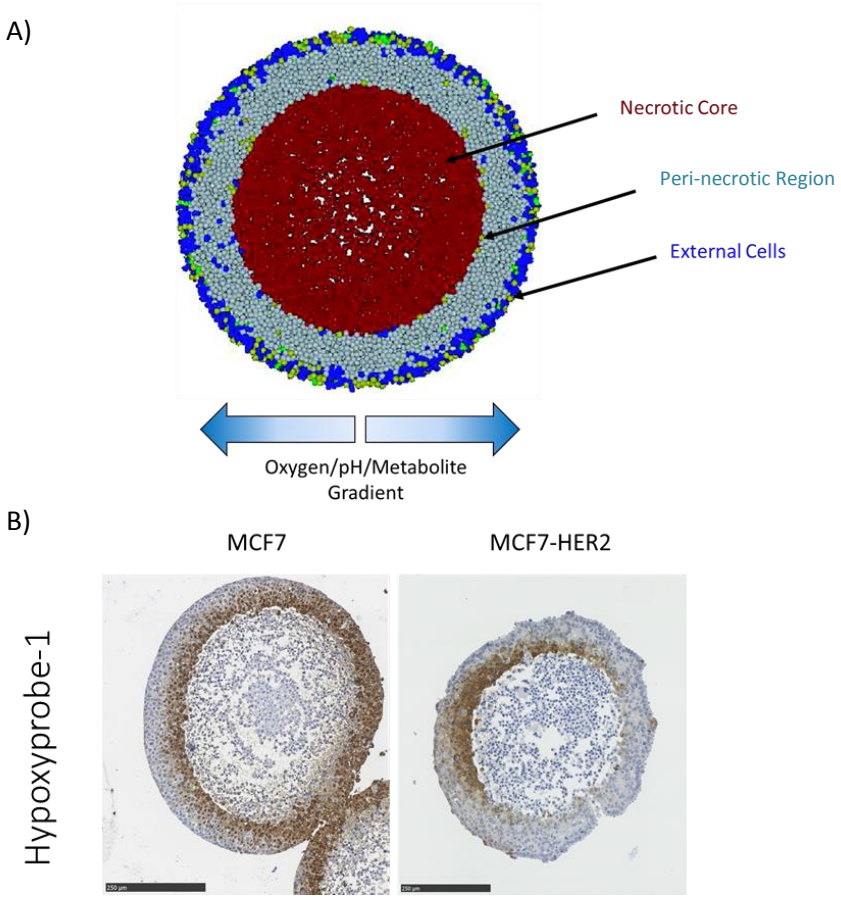

Figure 3.7: Multicellular spheroid structure and hypoxic regions

A) Diagrammatic representation of the structure of multicellular spheroids. Reduced perfusion within the tightly packed spheroid drives the formation of gradients in oxygen, pH and metabolites, resulting in a hypoxic/acidic microenvironment within the spheroid mass. This leads to the formation of a necrotic core (red) and less well oxygenated regions surrounding the necrotic core (the peri-necrotic region(light blue)), with cells on the outside of the spheroid having unimpeded perfusion by the surrounding media (dark blue). B) Multicellular spheroids for MCF7 and MCF7-HER2 cell lines were stained for hypoxyprobe-1. Hypoxyprobe-1 stains any cells which have been hypoxic and demonstrates an inner hypoxic region surrounding a necrotic core, as per Figure A.

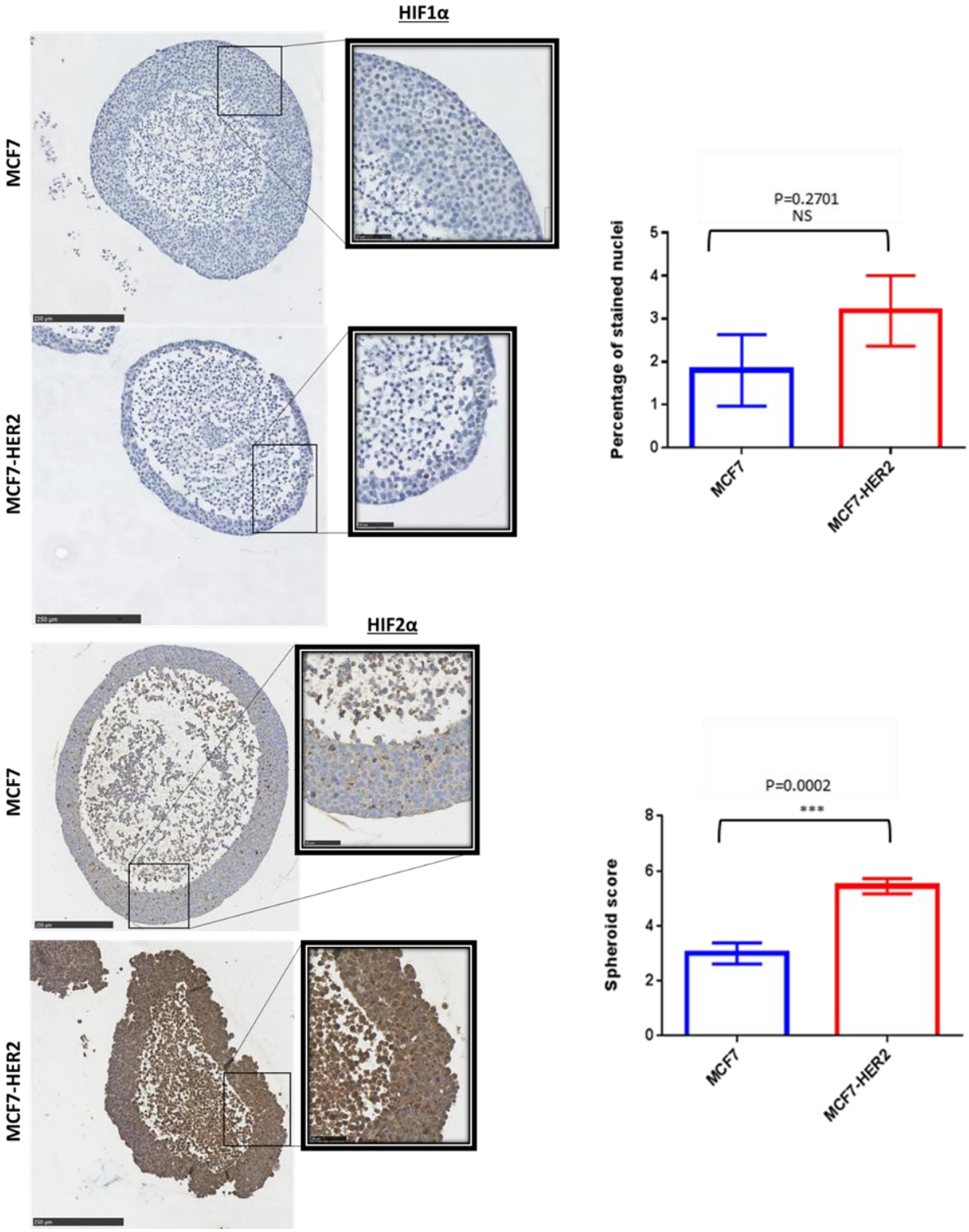

Figure 3.8a: HIF and HIF target gene expression in MCF7 and MCF7-HER2 3D multicellular spheroids

Multicellular spheroids were grown for 1-2 weeks before being formalin fixed and paraffin embedded. Fixed tissue sections were stained by immunohistochemistry with antibodies towards: HIF1α and HIF2α. LHS: The staining pattern of representative spheroids is shown for each antibody in each cell line, with magnified version inset. RHS: Quantification of IHC scoring is shown for each protein. Bars represent mean scores, with error bars representing the SEM. Scores were compared between the two cell lines using a T-test with significance shown for each comparison. Further quantification of spheroid scoring is shown in table 3.1 below.

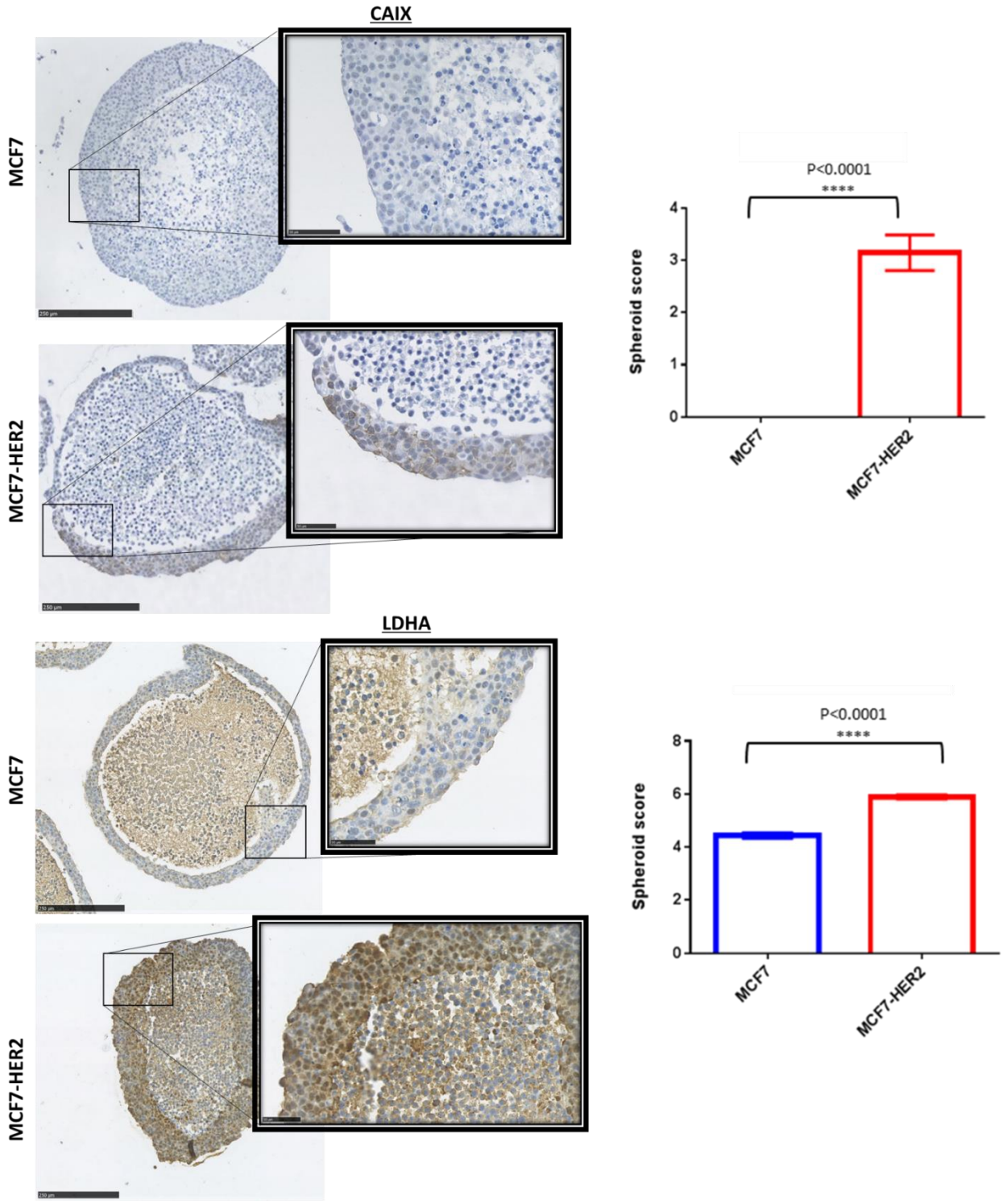

Figure 3.8b: HIF and HIF target gene expression in MCF7 and MCF7-HER2 3D multicellular spheroids

Similar analysis to Figure 3.8a with three additional target proteins: CAIX and LDHA. LHS: the staining pattern of representative spheroids is shown for each antibody in each cell line, with magnified version inset. RHS: quantification of IHC scoring is shown for each protein. Bars represent mean scores, with error bars representing the SEM. Scores were compared between the two cell lines using a T-test with significance shown for each comparison. Further quantification of spheroid scoring is shown in Table 3.1 below.

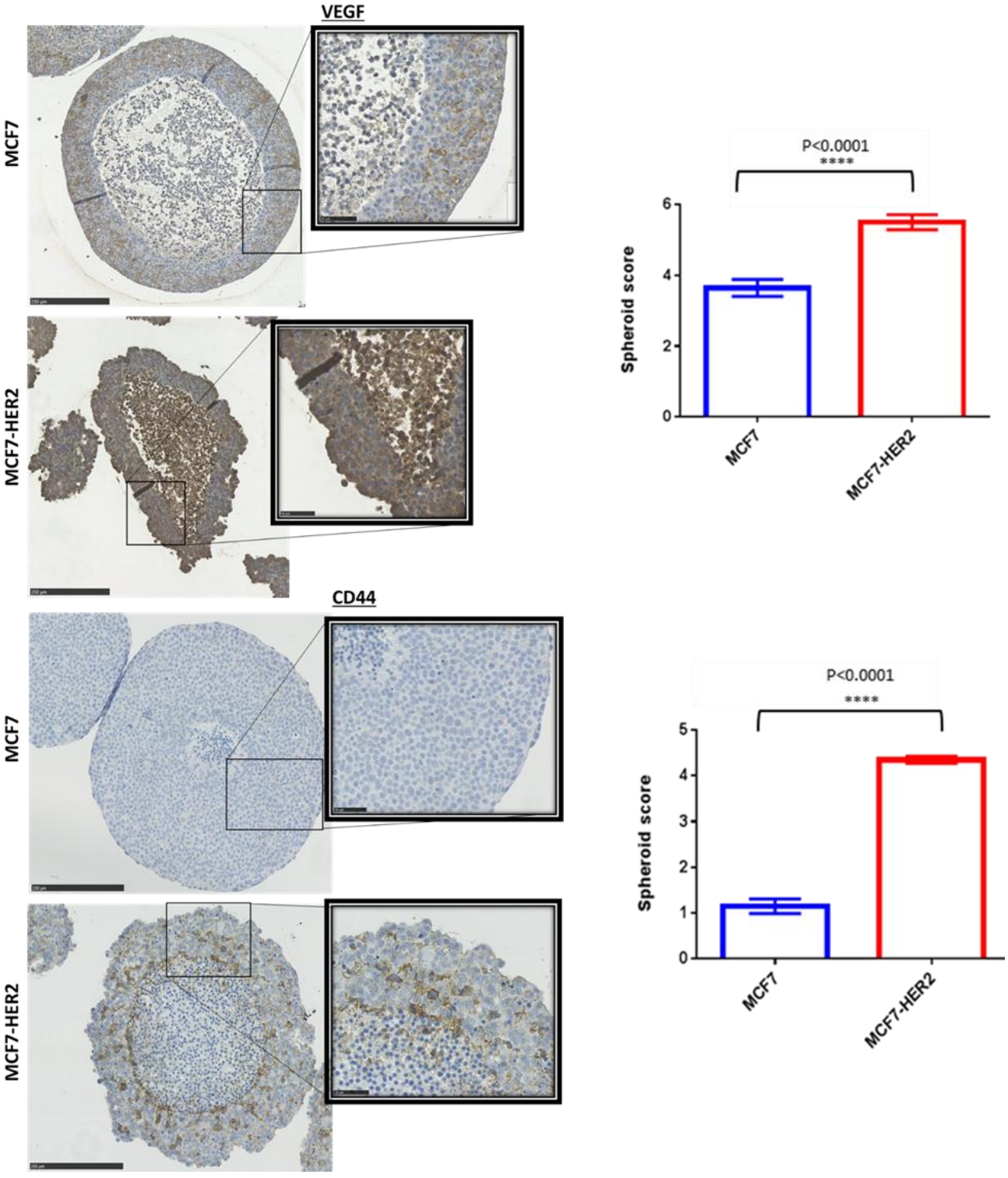

Figure 3.8c: HIF and HIF target gene expression in MCF7 and MCF7-HER2 3D multicellular spheroids

Similar analysis to Figure 3.8a/b with three additional target proteins: VEGF and CD44. LHS: the staining pattern of representative spheroids is shown for each antibody in each cell line, with magnified version inset. RHS: quantification of IHC scoring is shown for each protein. Bars represent mean scores, with error bars representing the SEM. Scores were compared between the two cell lines using a T-test with significance shown for each comparison. Further quantification of spheroid scoring is shown in Table 3.1 below.

Table 3.1: Spheroid IHC Scoring			
HIF1α			
Percentage of stained nuclei	MCF7	MCF7-HER2	P-value (T-test)
Mean %	1.8	3.2	P=0.2701
Range of %	0-8.7%	1.6-6.9%	
Number of Spheroids	10	7	
Combined Area/Intensity Scores (out of 6)	MCF7	MCF7-HER2	
HIF2α			
Mean Score	3	5.4	P=0.0002
Median Score	2	6	
Range	1.5-5.5	3.5-6	
Number of Spheroids	17	9	
LDHA			
Mean Score	4.4	5.9	P<0.0001
Median Score	4.5	6	
Range	3.5-5	5.5-6	
Number of Spheroids	17	9	
CAIX			
Mean Score	0	3.1	P<0.0001
Median Score	0	3	
Range	0	1.5-4.5	
Number of Spheroids	11	7	
CD44			
Mean Score	1.1	4.4	P<0.0001
Median Score	1.5	4.5	
Range	0-1.5	4-4.5	
Number of Spheroids	17	10	
VEGF			
Mean Score	3.6	5.5	P<0.0001
Median Score	3.5	5.75	
Range	1.5-5	4-6	
Number of Spheroids	17	10	

Table 3.1: The results of scoring IHC in multicellular spheroids

Scoring of 3D spheroids for each target and each cell line is shown. Scoring for HIF1α was given as a percentage of stained nuclei from a representative experiment. Other targets were scored out of 6 based on area of staining and intensity. Mean, median and range of scores are shown from one representative experiment from n=3, with the number of spheroids scored shown below.

3.4 Discussion

Previous research has shown a relationship between growth factor receptor signalling and HIF1α expression in normoxia. HER2 overexpression has been demonstrated to be sufficient for the upregulation of HIF1α in normoxia in mouse 3T3 cells [220], and this has been shown to increase the normoxic expression of the hypoxia response gene VEGF [421]. In breast cancer cell lines, treatment with the HER3 ligand neuregulin-1β increased normoxic HIF1α expression in MCF7 cells, and an increase in HER2 expression, caused by either long-term letrozole resistance or transfection of HER2 into MCF7 cells, has also been shown capable of increasing HIF1α levels [424]. In this way HER signalling can increase the levels and activity of HIF1α despite its canonical regulatory mechanisms being dependent on low-oxygen conditions. This novel mechanism demonstrates an important interplay between growth factor signalling and HIF activation, which is known to be a transcription factor for numerous genes involved in breast cancer progression. Despite this, it is unknown how growth factor signalling modifies HIF regulation in hypoxic conditions. The aim of this chapter was to assess how growth factor receptor expression affects HIFα upregulation in response to hypoxia and if changes were evident, to ask whether the upregulation of HIF target genes was also affected.

An initial assessment of hypoxic HIFα protein upregulation across a small panel of breast cancer cell lines demonstrated a high level of variability. The panel showed little or no concurrence between HER receptor expression profiles and the hypoxic induction of HIF1α or HIF2α. This result demonstrated that a comparison of HIFα regulation in the presence or absence of growth factor receptors would not be feasible through the use of a varied cell panel because the numerous differences in the biology of these cells preclude a simple comparison of the hypoxic stabilisation of HIFα subunits. To address the question more directly, the MCF7 and MCF7-HER2 isogenic cell lines were used as a model for HER2 overexpression. With this cell line model we were able to demonstrate that HER2 overexpression can drive an increase in the hypoxic upregulation of HIF2α but not HIF1α and drive the expression of known HIF targets in 2D and 3D models.

Firstly, MCF7 and MCF7-HER2 were compared by SRB and wound healing assays under normoxic and hypoxic conditions to determine whether the overexpression of HER2 provided an advantage in terms of growth rate or cell motility in hypoxia. In SRB assays, MCF7 and MCF7-HER2 growth over 7 days was comparable. Growth rates were similar in normoxia

and were reduced to a similar extent in hypoxia. This included chronically hypoxic cells, which had been adapted to hypoxic growth for 10 weeks prior to the experiment. This work was unable to demonstrate a growth advantage of HER2 overexpression at this oxygen concentration (0.5%) and suggests that HER2 offers no protection from the deleterious effects of hypoxia on proliferation. With this in mind it was decided that investigation of cell motility might be a better way of phenotypically assessing cellular adaptation to hypoxia in the context of HER2 overexpression.

Increased cell motility is considered an accepted outcome of hypoxia in breast cancer. This has been demonstrated through the correlation of tumour hypoxia with increased invasion and metastasis of breast cancers [315, 445, 446] and investigated in terms of HIF1 signalling and the roles of known HIF1 targets [295, 455, 465]. We used our MCF7 isogenic cell line model to investigate whether the overexpression of HER2 affected cellular motility in hypoxia using wound healing assays. Previous research has demonstrated an increased wound healing capacity in MCF7 cells overexpressing the HER2 receptor when compared to wild-type MCF7 cells in normoxia [466], but the effect of HER2 expression on hypoxic cell behaviour is unknown. This reported effect was obtained under different growth conditions, and whilst no significant difference between normoxic MCF7 and MCF7-HER2 cells was seen in the experiments conducted in our lab, average wound healing in MCF7-HER2 was consistently faster than MCF7. It is clear that the capacity of these cell lines for wound healing differs significantly in hypoxia (0.5% O_2). Wound healing was significantly reduced in hypoxia compared to normoxia in the MCF7 cell line only, and was significantly greater in MCF7-HER2 than in MCF7 in hypoxia. This suggests that HER2 overexpression can drive increased motility in response to hypoxia, an effect that could play a significant role in the increased aggressiveness and invasion seen in HER2-positive solid tumours, where tumour hypoxia is often a factor. These wound healing assays were performed in low serum conditions to minimise the contribution of cellular proliferation to wound closure. However, the time required to see wound closure in MCF7 and MCF7-HER2 meant that meaningful comparisons could only be made 48 hrs after the removal of the wound insert, at which point cells are given ample time to divide, therefore cellular proliferation and motility are difficult to distinguish. Despite this, the earlier finding that these cell lines exhibit little difference in cell growth in response to hypoxia suggests that the difference shown in wound healing assays are due to increased motility not proliferation. An additional observation in these wound healing assays was the phenotypic differences in cellular motility between these two

cell lines. Whilst MCF7 covered the wound predominantly as invasive sheets, MCF7-HER2 showed more single cell invasion and cellular characteristics which matched an EMT phenotype. This was seen in normoxia and hypoxia, so is not a direct result of hypoxia, but represents a HER2-driven change which may have consequences for the molecular response to hypoxia, discussed in Chapter 4. The result of these wound healing assays provides initial evidence suggesting that HER2 overexpression in this model may have interesting effects on the cellular response to hypoxia and supports the more detailed investigation into the molecular mechanisms and consequences of HER2-driven hypoxia signalling.

Subsequent experiments on whole cell, nuclear and cytoplasmic cellular lysates collected from MCF7 and MCF7-HER2 were conducted to assess HIF1α and HIF2α upregulation by hypoxia in the context of HER2 overexpression. A comparison of these cell lines showed that HER2 expression had no discernible effect on hypoxic upregulation of HIF1α, however the differences in HIF2α were clear. HIF2α was induced to significantly higher levels in MCF7-HER2 when compared to MCF7, and higher hypoxic levels were also seen in nuclear and cytoplasmic fractionated lysates when compared to MCF7 cells. In whole cell lysates HIF2α levels also appeared to be higher in normoxia in the MCF7-HER2 cell line than in wild-type MCF7. Whilst this level was low compared to hypoxic upregulation of the protein, it poses the question of whether a larger pool of normoxic HIF2α contributes to the increased hypoxic upregulation. This question, as well as the mechanisms behind increased normoxic HIF2α will be investigated and discussed in Chapter 5. In terms of hypoxic upregulation, these data demonstrate that HER2 overexpression is able to enhance the cellular upregulation of HIFs in response to hypoxia, and suggests HIF2α is the major HIF affected. These findings are novel in two respects; firstly, it shows that HER2 overexpression is able to upregulate the normoxic expression of HIF2α in breast cancer, and secondly that in this context the hypoxic upregulation of HIF2α is increased. Whilst previous work has demonstrated an interplay between HER2/HER3 signalling and HIF1α regulation in normoxia, the effects of HER2 on HIF2α were not investigated in these studies and so remain unknown in breast cancer. A relationship between HIF2α levels and EGFR activity in both normoxia and hypoxia has previously been demonstrated in the context of tamoxifen and fulvestrant resistant MCF7 cell lines [426], this supports the notion that growth factor signalling has a meaningful impact on not just HIF1α but also HIF2α levels in breast cancer cell lines. However, the novel finding that this can also occur in the context of HER2 overexpression suggests that the ability of HER family receptors to drive HIF2α may be robust and important in the context of HER2-positive

breast cancers. As described in Figure 3.1, cellular context is extremely important in discerning the relative upregulation of HIF1α and HIF2α in response to hypoxia. Thus, the relative contribution of HIF1α and HIF2α to growth factor-modulated hypoxic responses in breast cancer is also likely to be highly dependent on intrinsic cellular factors. The use of this MCF7 model of HER2 overexpression demonstrates the concept that HIFα regulation by hypoxia is prone to alteration by growth factor signalling, providing clear evidence for a role of HER2 signalling outside of the normoxic regulation of HIFs. In addition, this work provides evidence that in the context of a commonly used model of luminal breast cancer (MCF7), HIF2α may be a contributory factor to this effect, suggesting that the long accepted differences between HIF1α and HIF2α are relevant in the context of growth factor-hypoxia interplay and that further investigation into the role of HIF2α as a driver for the hypoxic response in breast cancer is warranted, especially in the context of HER2-positive breast cancer.

Whilst whole cell levels of HIF1α appeared unaffected by HER2 overexpression in these experiments, subtle changes were seen in nuclear lysates. Specifically, nuclear HIF1α levels were higher in MCF7-HER2 when compared to wild-type MCF7 at 72 hrs only. This increase suggests that whilst the nuclear upregulation of HIF1α in these cell lines was comparable, the downregulation of HIF1α after 48 hrs is inhibited. As this was seen in the nuclear compartment only, one possibility is that the binding of HIF1α with specific nuclear cofactors may be increasing its longevity, and potentially its activity, in the nucleus. Considering the extent of cofactors involved in HIF transcriptional activity and the specificity of cofactors for different HIF proteins [181, 467, 468], this raises the question of whether HER2 overexpression might modulate HIF1 levels and transcriptional activity in the nucleus by altering the expression of relevant cofactors. Considering the non-redundancy of HIF1 and HIF2, and the increasingly recognised role of HIF2α in cancer pathogenesis, this provides an example of how growth factor receptor expression may modulate both HIF1α and HIF2α levels, but in different ways.

The downstream consequences of increased HIF upregulation and hypoxic response were next assessed in terms of HIF target genes *LDHA* and *CAIX*. These are both considered HIF1-specific target genes [469, 470] and were selected because they are well-researched and considered important drivers of pathology in breast and other cancers [454, 458, 459]. As such, it was considered important to investigate whether HER2 modulation of hypoxic

response had an effect on such canonical hypoxia response genes. The investigation of a more varied set of HIF1 and HIF2 target genes to assess the relative contribution of both to HER2-driven hypoxic response has also been carried out as part of this research and is described in Chapter 4. The purpose of this set of experiments was to demonstrate in a more general sense the role of HER2 in modifying hypoxic gene expression. *CAIX* was chosen as a canonical hypoxia response gene, which has been shown to be inducible by hypoxia in a number of breast cancer cell lines. CAIX has been described previously as a driver of tumour aggressiveness and metastasis and has been shown to be a potential therapeutic target in breast cancer [455]. In addition, the expression of *CAIX* in response to hypoxia has been shown to be relatively low in MCF7 cells compared to other breast cancer cell lines, providing a model where increased induction may be more readily detectable [456]. *LDHA* is another canonical hypoxia response gene with important roles in tumorigenesis, being commonly upregulated in breast malignancies and associated with poor clinical outcome [459]. These data demonstrated no change in the normoxic levels of either of these proteins; however a significant increase in hypoxic CAIX upregulation in the HER2 overexpressing cell line was detected. These experiments were able to show the increased expression of known hypoxia response genes in the context of HER2-overexpression. Once again this forms part of the novel finding that HER2 expression exerts important effects on the cellular response to hypoxia, not just increased HIF signalling in normoxia. An important unanswered question is whether the effects of HER2 expression on HIFα regulation directly drives the altered expression of these HIF target genes or whether there are other mechanisms involved. HER2-mediated changes in HIFα were largely limited to HIF2α, whilst HIF1α changes were not seen before the 72 hrs. With the increased upregulation of CAIX present at all time points tested from 24 hrs onwards, this suggests that either increases in HIF2α are responsible for the increased expression of the gene, or that HIF1 transcriptional activity is increased by the presence of HER2 in the absence of any visible increase in HIF1α level; for example this may occur as a result of increased or altered HIF1 cofactor expression in the context of HER2 overexpression leading to increased transcriptional activity. This offers a plausible mechanism by which the increased CAIX and increased nuclear stability of HIF1α in the context of HER2 overexpression may be explained. Despite the literature supporting CAIX as a HIF1 specific gene [470], a role for HIF2α in driving CAIX in MCF7-HER2 cannot be ruled out. HIF1 and HIF2 transcription factors are highly homologous and have both been shown to bind the same HRE consensus sequence, with a large overlap in target genes [239]. Therefore,

alongside the demonstration that HIF2α upregulation in hypoxia is increased by HER2 overexpression in MCF7, it is feasible that increased HIF2 abundance may result in more promiscuous activity and target gene selection. With this in mind it should be acknowledged that research into HIF1 versus HIF2 target specificity in breast cancer has largely been conducted in ER+, HER2- breast cancer models such as MCF7 [239, 240, 243]. With no work having been done to discern how target gene selection may vary in the context of HER2 overexpression, the assignment of HIF target genes as HIF1 or HIF2–specific in the literature may not stringently apply. Naturally, further work is required to determine whether the overexpression of such genes can be driven by HIF2 or whether this is caused by a HER2-mediated increase in HIF1 transcriptional activity.

The dual tyrosine kinase inhibitor lapatinib was used to assess the role of growth factor signalling in driving the hypoxic response in terms of HIF1α, HIF2α, CAIX and LDHA protein levels. The preliminary data work suggests that LDHA and CAIX upregulation may be inhibited (at least partially) by lapatinib. In order to achieve better inhibitory effects in these experiments, longer term inhibition of HER2 may be required. Whilst 1 μM lapatinib was shown to reduce p-HER2 (tyr1221/1222) for the duration of the experiment, the inhibition of p-HER2 just 30 minutes prior to hypoxic exposure might not be sufficient time for transcriptional or secondary effects of HER2 inhibition to occur. It would be interesting to assess whether longer term treatment with lapatinib is able to reduce CAIX and LDHA upregulation to a greater extent, and also assess whether the hypoxic upregulation of HIF2α could be reversed given time for transcriptional effects to come in to play. Further work considering the relationship between HIF2α and HER2 expression is conducted in chapters 5 and 7, providing more evidence supporting the role of HER2 overexpression in the hypoxic effects demonstrated in this chapter.

The majority of work conducted in this chapter was performed in cell lines cultured in 2D. Two-dimensional cell culture is a useful model in the investigation of cell behaviour and cell signalling as the format is highly amenable to experimental manipulation and imaging. The limitation of 2D culture is that it does not accurately represent the behaviour of cancer cells in the tumour microenvironment. 3D multicellular spheroids provide a cell line model which better represents the cellular environment of solid tumours. These spheroids are formed from tightly packed cells, more closely resembling the high level of cell-cell adhesion seen in healthy and cancerous tissue. This close adhesion leads to limited diffusion

of important nutrients and gases, resulting in a necrotic region surrounded by a hypoxic region and increasing oxygen concentration in moving outwards from the necrotic core. This diffusion limitation also leads to additional gradients of carbon dioxide and metabolites, as well as reduced pH in the poorly perfused inner regions. In this way 3D multicellular spheroids provide a model for the poor perfusion and oxygen gradient seen in solid tumours with the benefit of additional microenvironmental stresses, thereby providing a more realistic model of solid tumours. The work in this chapter aimed to use these models to confirm differences in HIFα and HIF target gene expression seen in our isogenic cell line model of HER2 overexpression. This has been used to confirm the increased expression of HIF2α and HIF targets, whilst providing spatial expression patterns, allowing a comparison of expression levels over hypoxic and normoxic spheroid regions, which can be displayed through staining with hypoxyprobe-1.

The IHC analysis of MCF7 and MCF7-HER2 spheroids supported the findings from western blotting of 2D lysates. HIF2α (but not HIF1α) was more highly expressed in MCF7-HER2 when compared to wild-type MCF7, and the expression of CAIX and LDHA was also increased in the HER2-positive cell line. In addition, the assessment of two additional targets, VEGF and CD44, provided additional evidence that the hypoxic response is enhanced by MCF7-HER2. VEGF is a canonical hypoxia response gene which plays an important role in driving angiogenesis and has been shown to be preferentially activated by HIF2α over HIF1α [178, 259, 471-473]. CD44 is a breast cancer surface antigen associated with stem cell characteristics and upregulated by hypoxia. HIF2α is recognised as an upregulator of genes which drive stem cell characteristics [464, 471, 474], and thus the expression of CD44 is an interesting target in the context of increased HIF2α upregulation. The upregulation of CD44 by hypoxia has been previously described [475, 476], as has the fact that it can be directly driven by HIF1α in triple-negative breast cancer [476]. It has also been demonstrated that the intracellular domain of CD44 can increase stability and activity of HIF2α in glioma cells [475]. Additionally, if CD44 expression is increased in the context of high HER2, this provides a potential mechanism by which HIF2α expression may be increased in HER2 overexpressing breast cancer cells. In this study the expression of both VEGF and CD44 was considerably higher in the MCF7-HER2 cell line, implicating HER2-HIF interplay as a mechanism for the upregulation of these genes. Surprisingly, the majority of these HIF target genes showed little concordance with hypoxyprobe-1 expression. This may be due to a disparity between the level of hypoxia required for hypoxyprobe-1 to form its detectable substrate and the level

required for the upregulation of hypoxia-inducible gene transcription. In the context of the multicellular spheroid, tight packing of cells with a large amount of cell-cell adhesion might limit oxygen perfusion enough to permit the expression of HIF-driven genes even when close to the extremities of the spheroid. Alternatively, HER2 may promote the expression of these genes even in normoxia in the context of tightly packed multicellular spheroids. Either way, the higher expression of such genes in HER2-overexpressing cells in this 3D model demonstrate that HER2-driven increases in hypoxic protein expression can still occur in a more structurally accurate representation of the tumour microenvironment.

In overview this chapter has approached the question of whether growth factor receptor expression is able to modulate the cellular response to hypoxic conditions in terms of HIFα upregulation and HIF target expression. A HER2-mediated increase in HIF2α and HIF targets CAIX and LDHA was demonstrated, and the increased expression of HIF target genes was shown in a 3D spheroid model system. This provides evidence that HER2 may act through direct effects on HIF2α in breast cancer and may be responsible for a generalised increase in hypoxic response in terms of HIF target gene expression. As mentioned, the closer investigation of the consequences for HER2 overexpression for the cellular response to hypoxia will be investigated in Chapter 4, whilst the mechanisms underlying the increased expression of HIF2α will be further investigated in Chapter 5.

Chapter 4: HER2 overexpression in MCF7 cells drives an increased transcriptional response to hypoxia

4.1 Introduction

The MCF7 and MCF7-HER2 cell lines provide a useful comparative tool for investigating the effect of HER2 overexpression on the hypoxic response. This model was next used to investigate the effect of HER2 signalling on the transcriptional response to hypoxia using microarray analysis. Global gene expression was assessed in these two cell lines in normoxia, acute hypoxia and chronic hypoxia, and microarray analysis was performed using the Illumina HT12v4 beadchip array. This chip includes over 47,000 probes which provide genome-wide coverage of transcript expression. Using this technology, a detailed analysis was performed to assess how gene transcription is regulated in response to hypoxia and how this response varies in the context of HER2 overexpression. Investigating the global transcriptional response allows important pathways to be identified in terms of their transcript levels in normoxia and hypoxia in both cell lines. The genes and pathways involved in the HER2-driven hypoxic response were investigated in terms of both a generalised response, as well as a response of HIF1 and HIF2 target genes, to understand how these factors play a role in the exacerbated response to hypoxia.

4.2 A comparison of hypoxia metagenes in MCF7 and MF7-HER2 cells

Hypoxia is a well-established indicator of poor prognosis in a number of solid tumour types [477]. As such, past research has sought to better identify where tumour hypoxia may be present so that more accurate prognoses may be made [478, 479]. One such method has been the development of hypoxia metagenes: a set of genes whose combined expression profile can be used to indicate when hypoxia-driven gene expression changes have occurred. In this section I used three published hypoxia metagenes [480-482] to assess the relative expression of hypoxia response in MCF7 and MCF7-HER2. To do this, RNA was extracted from MCF7 and MCF7-HER2 cells grown under normoxic conditions (20% O_2), after 24 hr in hypoxia

(0.5% O_2), or after 10 weeks continual growth in hypoxia. Samples were collected in triplicate and hybridized to the Illumina beadchip array to provide global gene expression data for each condition (full method can be found in Section 2.2.13), this data could then be used to compare the expression of hypoxic gene signatures. All three metagenes had been designed to assess hypoxic gene expression changes, but each had been determined through different methods. Therefore, the combined analysis of each of these metagenes in our microarray data provides a more robust assessment of hypoxic response in MCF7 and MCF7-HER2, so that the role of HER2 in this response can be broadly established.

The three metagenes used in this analysis have all been previously described [480, 481, 483]. These include a 99 gene signature created by Winter et al. (2007)[481], of which 94 genes were available in our microarray dataset, a 51 gene signature from Buffa et al. (2010)[480] of which 50 genes are available in our dataset, and a complete 15 gene signature from Toustrup et al. (2011)[482, 483]. A full list of genes can be found in Appendix 1.1. Other hypoxic gene expression signatures are available ([484-487]), but these three were selected as they represent a varied set, with little overlap in the genes contained within them (Figure 4.1). Additionally, due to the varied approaches taken in their design, each provided its own benefits for this analysis. The Winter et al. [481] metagene was selected as it has been demonstrated as a prognostic indicator in breast cancer and contains a relatively large number of genes which cluster with well-known hypoxic response genes. The metagene from Buffa et al. [480] was designed to be broadly applicable to multiple cancer types and so was chosen here for its robustness. It was developed *in silico* through co-expression networks of hypoxia-regulated genes in a combined analysis of 8 datasets, including 5 from breast cancer patients. The signature from Toustrup et al. [483] is a small (15 gene) signature; these genes were determined to be the optimum set able to differentiate tumours based on the oxygen level read by an electrode. The inclusion of this signature is important as it was verified by oxygen readings as opposed to the expression with expected hypoxia-response genes, which can be highly varied and context dependent. Additionally, the Toustrup signature considers the issue that a number of hypoxia response genes are also pH-dependent in their expression. By starting with predetermined hypoxia-responsive but pH-independent genes, their signature is potentially able to detect hypoxia more specifically. Whilst the Toustrup signature provides a highly specific hypoxia detecting gene set, the Winter and Buffa sets are included to provide a broader set of hypoxia response genes with proven applicability to breast cancer.

Gene expression data from normoxic, acute hypoxic (24 hr) and chronic hypoxic (>10 week) MCF7 and MCF7-HER2 cells from our HT12v4 beadchip array was used to compare the upregulation of hypoxia metagenes in response to hypoxia. Log_2 expression values for hypoxic metagenes were mean centred and subject to hierarchical clustering by Pearson correlation. This was performed individually for the three metagenes. This demonstrated an increased hypoxic response in MCF7-HER2 when compared to wild-type MCF7 cells in both acute and chronic hypoxia (Figure 4.1). Clusters could be broadly placed into three categories, and these are colour-coded in Figure 4.1 (Genes in each cluster are indicated in Appendix 2.1). Red clusters represent genes which are increased in hypoxia in both cell lines. These clusters were present in all three metagenes, making up the entirety of the 15-gene signature. Importantly, red clusters in each gene set showed a greater change in expression in response to hypoxia in MCF7-HER2 when compared to wild-type MCF7, despite these cell lines having comparable levels in normoxia. Blue clusters were present in the two larger metagenes, though these represented a smaller number of genes than the red cluster in each set. Blue clustered genes were generally downregulated by hypoxia in MCF7, but interestingly were expressed at constitutively low levels in MCF7-HER2. Finally, an additional cluster (labelled in green) was seen in the largest dataset (Winter et al.). Expression of these genes did not change markedly in response to hypoxia in these samples but were constitutively more highly expressed in MCF7-HER2.

A statistical comparison of gene expression within the red clusters was carried out for each metagene. A one-way ANOVA was used to compare the mean gene expression values of each treatment category. This was able to confirm a stronger upregulation of these gene clusters in MCF7-HER2 when compared to wild-type MCF7. A significant upregulation of genes in both acute and chronic hypoxia was seen for both MCF7 (acute: $p<0.0172$, chronic: $p<0.007$) and MCF7-HER2 (acute: $p<0.0008$, chronic: $p<0.0008$) cell lines in all three metagenes. However, whilst no significant differences were seen between normoxic MCF7 and normoxic MCF7-HER2 gene expression, gene expression in hypoxia was significantly higher in the HER2 overexpressing cell line when compared to hypoxic MCF7 cells. This was seen in acute hypoxia for all three metagenes (Winter: $p=0.0241$, Buffa: $p= 0.0027$, Toustrup: $p=0.004$), and in the Buffa ($p=0.0266$) and Toustrup ($p=0.0032$) metagenes under chronic hypoxia. The online bioinformatics tool DAVID [488] was used to analyse these red clusters and the enrichment of gene ontology terms relating to biological processes was assessed. Whilst no significant enrichment was seen in the blue or green clusters, in the red clusters

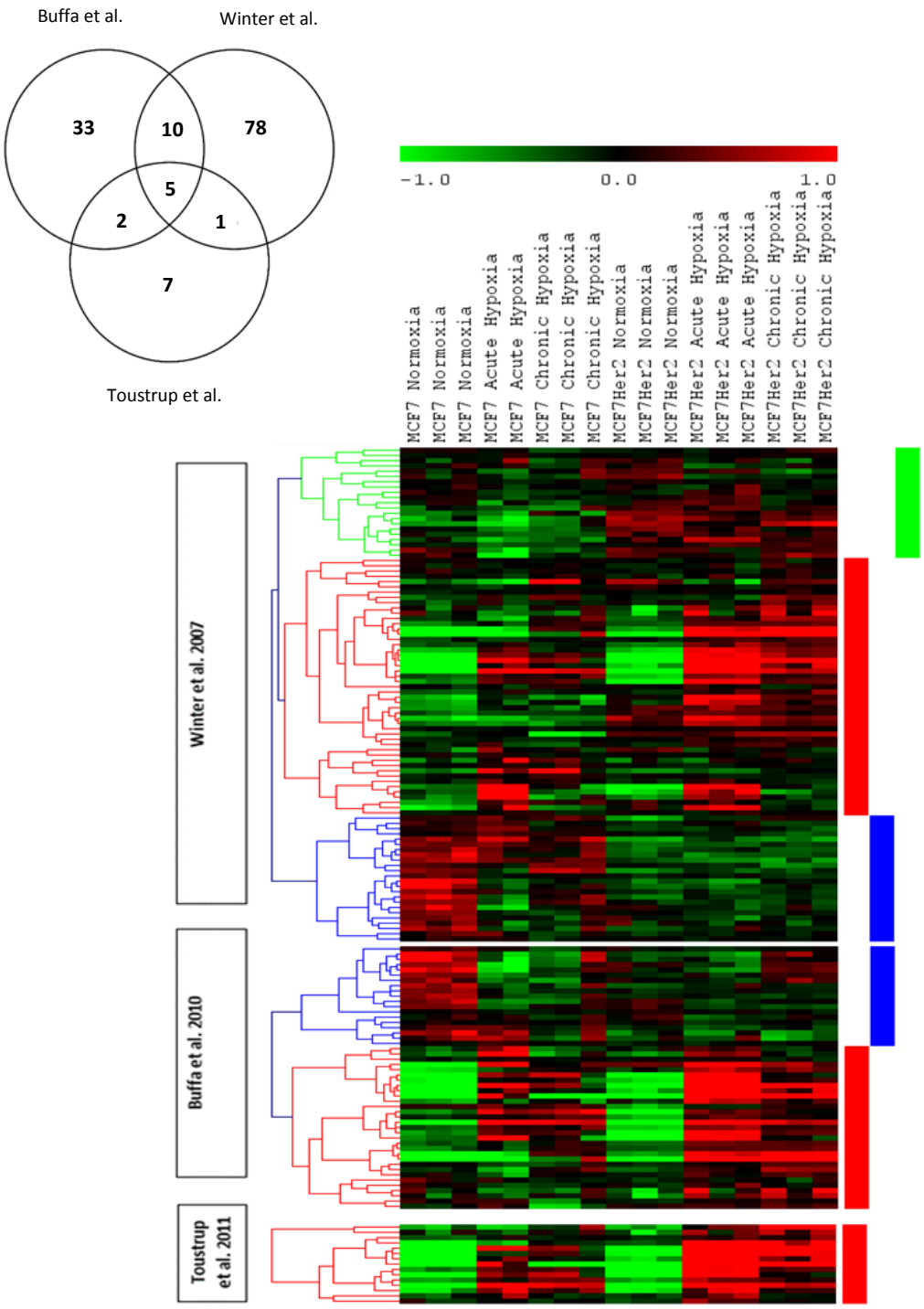

Figure 4.1: Gene expression analysis of three hypoxia metagenes to determine hypoxic response

(Top Left) Venn diagram showing the overlap of genes between these three metagenes and the proportion of said genes in each group. (Main) Hierarchical cluster analysis of mean-centred log_2 expression values of three metagenes in MCF7 and MCF7-HER2 cell lines treated in normoxia (20% O_2), acute hypoxia (0.5% O_2 for 24 hours), and chronic hypoxia (0.5% O_2 for 10 weeks). The notable gene clusters are colour-coded on the right hand side. Green represent clusters constitutively higher in MCF7-HER2, red clusters are generally induced by hypoxia more strongly in MCF7-HER2 and blue clusters are downregulated by hypoxia and constitutively lower in MCF7-HER2. Complete gene sets for each cluster in these metagenes can be found in Appendix 2.1.

this showed a significant increase ($p<0.001$) in a number of GO terms pertaining to hypoxic response and glycolysis in all three metagenes, with glycolytic processes and glucose metabolism highly represented in the red clusters of the Buffa and Winter metagenes. Genes in these clusters include a large proportion of known glycolysis genes (*ALDOA, PDK1, PFKFB3, PFKP, ENO1, PGK1, GPI, HK2* and *PGAM1*) in addition to non-glycolytic genes known to drive hypoxia-mediated cancer pathology (*CAIX, VEGFA, LDHA, LOX, P4HA1, P4HA2* and *ANGPTL4*). Full gene lists for each cluster can be seen in Appendix 2.1.

4.3 The global transcriptional response to hypoxia in MCF7 and MCF7-HER2 shows that HER2 primes cells for hypoxia.

Having determined that HER2 overexpression is able to increase the hypoxic response in terms of recognised hypoxia signatures, the effect of HER2 overexpression on the complete cellular transcriptional response to hypoxia was investigated. Rank product analysis of our microarray data was used to identify significantly changed genes across the entire transcriptome in MCF7 and MCF7-HER2 after acute or chronic hypoxic exposure. Lists of significantly upregulated genes were created by comparing each hypoxic condition to normoxia in each cell line (see Appendix 2.2). In addition a list of constitutively highly expressed genes was created for each cell line by directly comparing normoxic gene expression in MCF7 with MCF7-HER2. These gene lists were compared to assess the overlap of the hypoxic response from these cell lines and represented as Venn diagrams (Figure 4.2). In this figure genes significantly more highly expressed in either MCF7 or MCF7-HER2 are categorised based on whether they are significantly upregulated by hypoxia in MCF7 or MCF7-HER2 alone, in both cell lines, or are not increased by hypoxia in either. This gives a visual representation of transcriptional changes in response to hypoxia in these two cell lines, and has been shown independently for both acute and chronic hypoxia. This initial analysis demonstrates a large difference in the hypoxic response of these two cell lines, both after acute (24 hrs) or chronic (>10 weeks) hypoxic exposure. A small proportion of the total genes upregulated in hypoxia were seen to increase in both cell lines; this equates to just 13.8% of hypoxia responsive genes in acute hypoxia and 14.2% in chronic hypoxia (yellow region Figure 4.2). In addition, it was found that some hypoxia responsive genes were more highly expressed in the MCF7-HER2 cell line than the MCF7 line in normoxia. 14.4% of genes upregulated in acute hypoxia and 18.6% in chronic hypoxia were also constitutively higher in

normoxia in MCF7-HER2 (red region in Figure 4.2), with only 1.2% (acute) and 7.6% (chronic) being constitutively higher in normoxic wild-type MCF7 cells (blue region). This suggests that a number of hypoxic response genes can be driven in normoxia by HER2 overexpression, and this may represent a mechanism by which HER2 primes cells for hypoxia.

The genes involved in the increased hypoxic response of MCF7-HER2 were investigated in more detail with a focus on genes which were specifically upregulated by hypoxia in MCF7-HER2 only (HER2-specific hypoxia genes) and those which were constitutively more highly expressed in MCF7-HER2 in normoxia (HER2-primed hypoxia genes). These genes, determined from the Venn analysis in Figure 4.2, were assessed for important drivers of breast cancer. Genes involved in glycolysis, invasion/metastasis, angiogenesis, tumour microenvironment regulation, and proliferation were identified in acute hypoxia, with an additional upregulation of DNA repair/maintenance and treatment resistance genes shown in chronic hypoxia. Interestingly, a large number of genes associated with notch signalling were also found in acute and chronic hypoxia, suggesting this may promote an epithelial to mesenchymal transition phenotype in these cells under hypoxia. A summary of these findings, including the pathways in which they are involved, can be seen in Figure 4.8 and full gene lists can be found in Appendix 2.2.

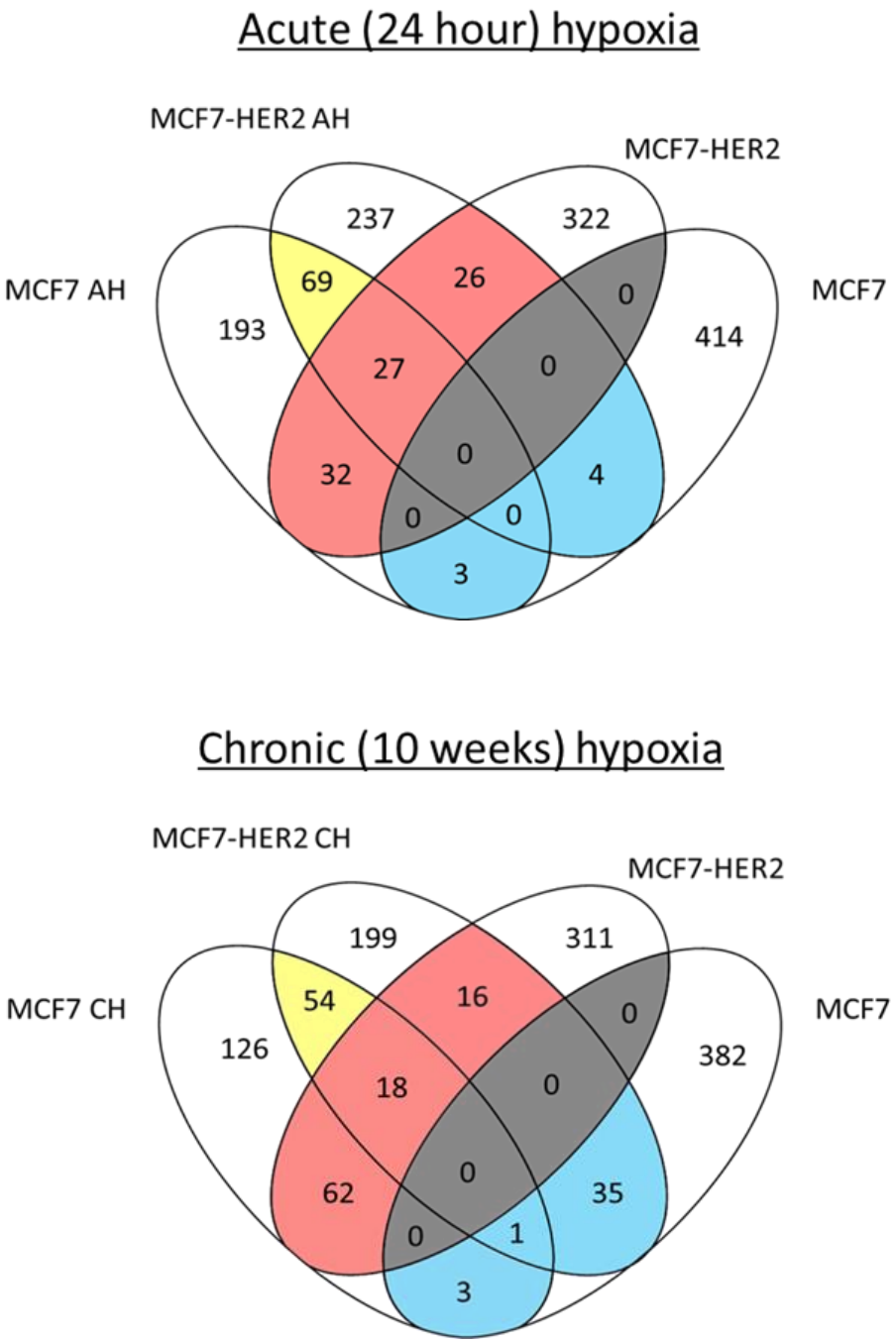

Figure 4.2: Venn analysis of gene lists from rank product comparison of upregulated genes in hypoxia or normoxia in MCF7 and MCF7-HER2

Venn diagram showing the rank product-determined genes upregulated in hypoxia (determined as a comparison between normoxia and hypoxia done individually for each cell line and for acute (AH) or chronic (CH) hypoxia), or genes more highly expressed under normoxia in comparison to the other cell line. Venn diagrams are shown separately for acute hypoxia (top) and chronic hypoxia (bottom). Colour-coding is used to denote areas of interest referred to in the text.

4.4 The role of HIF1 and HIF2 target genes in the HER2-driven hypoxic response.

Having established that HER2 overexpression in MCF7 can intensify the hypoxic response and prime genes for response to hypoxia, subsequent analysis focussed on the behaviour of HIF1 and HIF2 target genes in these two cell lines. HIF1 and HIF2 target gene sets were first established by combining published gene lists of HIF target genes designated through chromatin immunoprecipitation experiments in MCF7 cells [239, 240]. This provided a list of 370 HIF1 targets and 158 HIF2 targets, with 80 of these being assigned to both HIF1 and HIF2. This HIF gene list is used when referring to 'HIF genes' in the following set of analyses; the specific strengths and weaknesses of how this list was defined and its applicability to this research will be discussed later (Section 4.6). Full gene lists can be found in Appendix 2.3.

4.4.1 HER2 overexpression in MCF7 increases HIF target gene expression in normoxia and in response to hypoxia

An overview of HIF target behaviour in these two cell lines is provided by hierarchical clustering of these genes across hypoxia treated MCF7 and MCF7-HER2 cell lines (Figure 4.3). These analyses have been divided into acute and chronic hypoxia for HIF1 specific, HIF2 specific and dual HIF1/HIF2 target genes. Clusters of similarly behaving genes have been colour-coded according to the Figure legend. In both acute and chronic hypoxia the majority of genes fell into one of three clusters: stronger hypoxic response in MCF7-HER2 (red), constitutively higher in MCF7-HER2 (green) or downregulated by hypoxia/constitutively lower in MCF7-HER2 (blue). Genes which behaved similarly in terms of overall expression and hypoxic induction formed relatively small clusters (pink), with additional small clusters showing higher induction by hypoxia in MCF7 (black). In general, the majority of HIF target genes for both HIF1, HIF2 or non-specific gene sets fall into categories equivalent to those seen with hypoxia metagenes in Figure 4.1 (red, green and blue clusters), suggesting a similar HER2-mediated modification in terms of hypoxic response (red) and the normoxic expression (green and blue) in both generalised hypoxic response and HIF target gene expression.

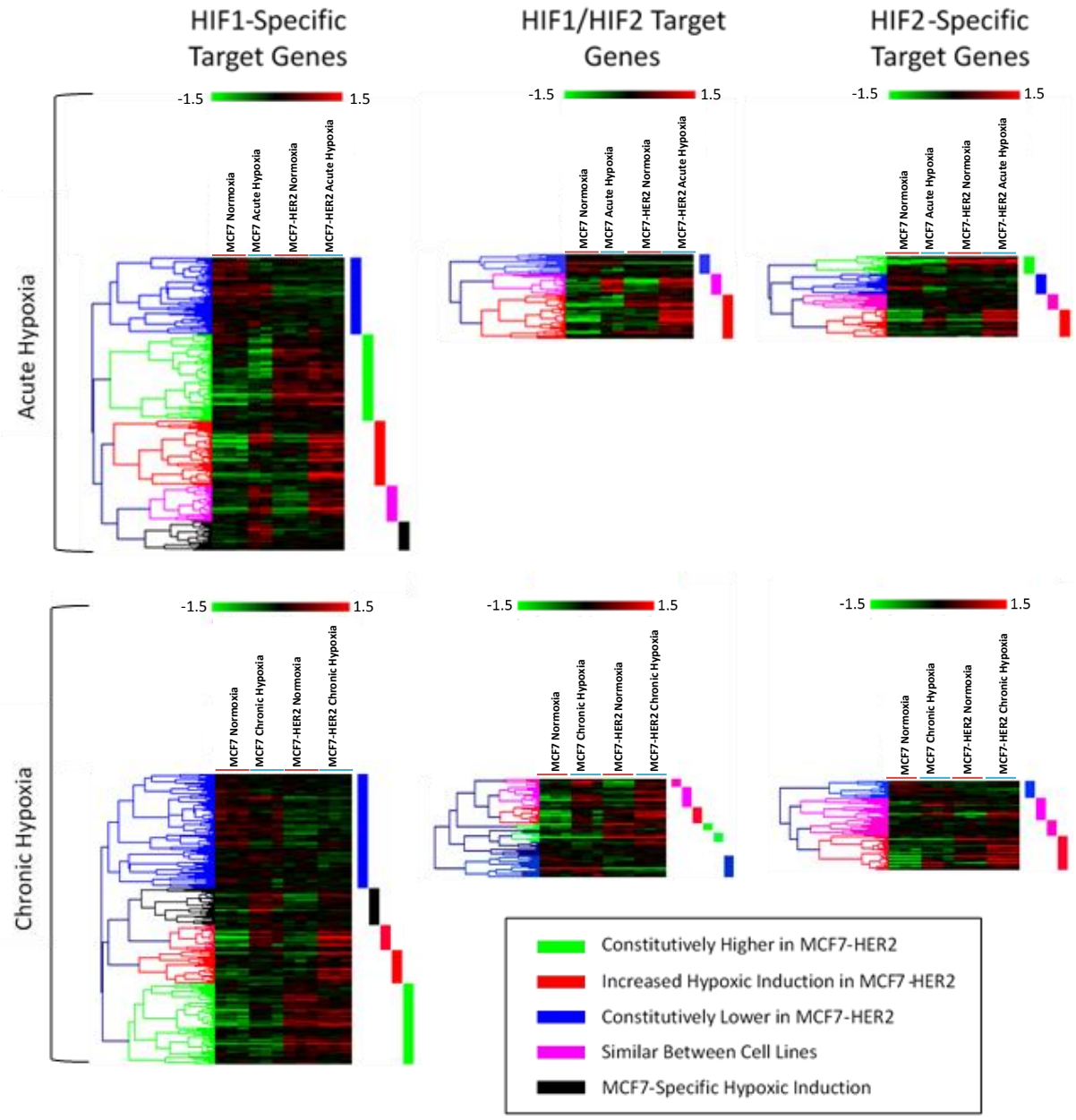

Figure 4.3: Hierarchical clustering of HIF target genes in normoxic and hypoxia treated MCF7 and MCF7-HER2

HIF target genes were compared by hierarchical clustering analysis in hypoxia treated MCF7 and MCF7-HER2. This was done individually for HIF1 target genes, HIF2 target genes and target genes driven by both HIF transcription factors, as well as for a comparison of normoxia with acute and chronic hypoxia. Colour-coding is used to indicate interesting gene clusters, with definitions of colours in the legend above.

4.4.2 HIF1 and HIF2 targets form part of the HER2-specific and HER2-primed response to hypoxia and are involved in breast cancer pathology

HIF target genes were next identified in the rank product gene lists used in Figure 4.2. This was done to see whether general differences in the hypoxic response between MCF7 and MCF7-HER2 included differences in the expression of HIF1 and HIF2 target genes, and to determine whether there were differences in the roles of HIF1 and HIF2 in this effect. Figures 4.4 and 4.5 show this analysis for acute and chronic hypoxia respectively. The proportion of HIF1, HIF2 and non-specific HIF target genes has been shown in each section of the Venn diagrams used in Figure 4.2. In addition, the number of HIF genes is shown as a percentage of the total number in each section. The proportion of HIF target genes in the HER2-mediated response to hypoxia increased. This involved a higher number of both HIF1 and HIF2 targets being increased by hypoxia in MCF7-HER2 only (HER2-specific response), as well as a greater proportion of HIF target genes constitutively expressed in MCF7-HER2 when compared to wild-type MCF7. Importantly, this includes an increase in constitutively overexpressed genes shown to respond to hypoxia (HER2-primed genes). Once again, these effects were seen for both acute and chronic hypoxia.

Within these HER2-modified HIF target genes a number of disease drivers were found in both HER2-specific and the HER2-primed hypoxic response, supporting the suggestion that HER2-overexpression may drive cancer progression in the context of tumour hypoxia. The most interesting HIF target genes from this analysis are shown in Figures 4.6 (acute hypoxia) and 4.7 (chronic hypoxia) and full gene lists can be found in Appendix 2.2. In accordance with hypoxia metagenes in Figure 4.1, we saw a large number of glycolytic genes which behaved as either HER2-specific responders or were primed for hypoxic response in the context of acute and chronic hypoxia (*GLUT1, ALDOA, ALDOC, ENO1, ENO2* etc.). In addition, a number of genes which facilitate cell survival and cancer progression in hypoxia were noted; these included microenvironmental regulators (*CAIX, PDGFB, PXDN),* cell adhesion molecules (DSP, NECT4) and stress response genes (*BNIP3L, NDRG1, DRAM1, DAPK*).

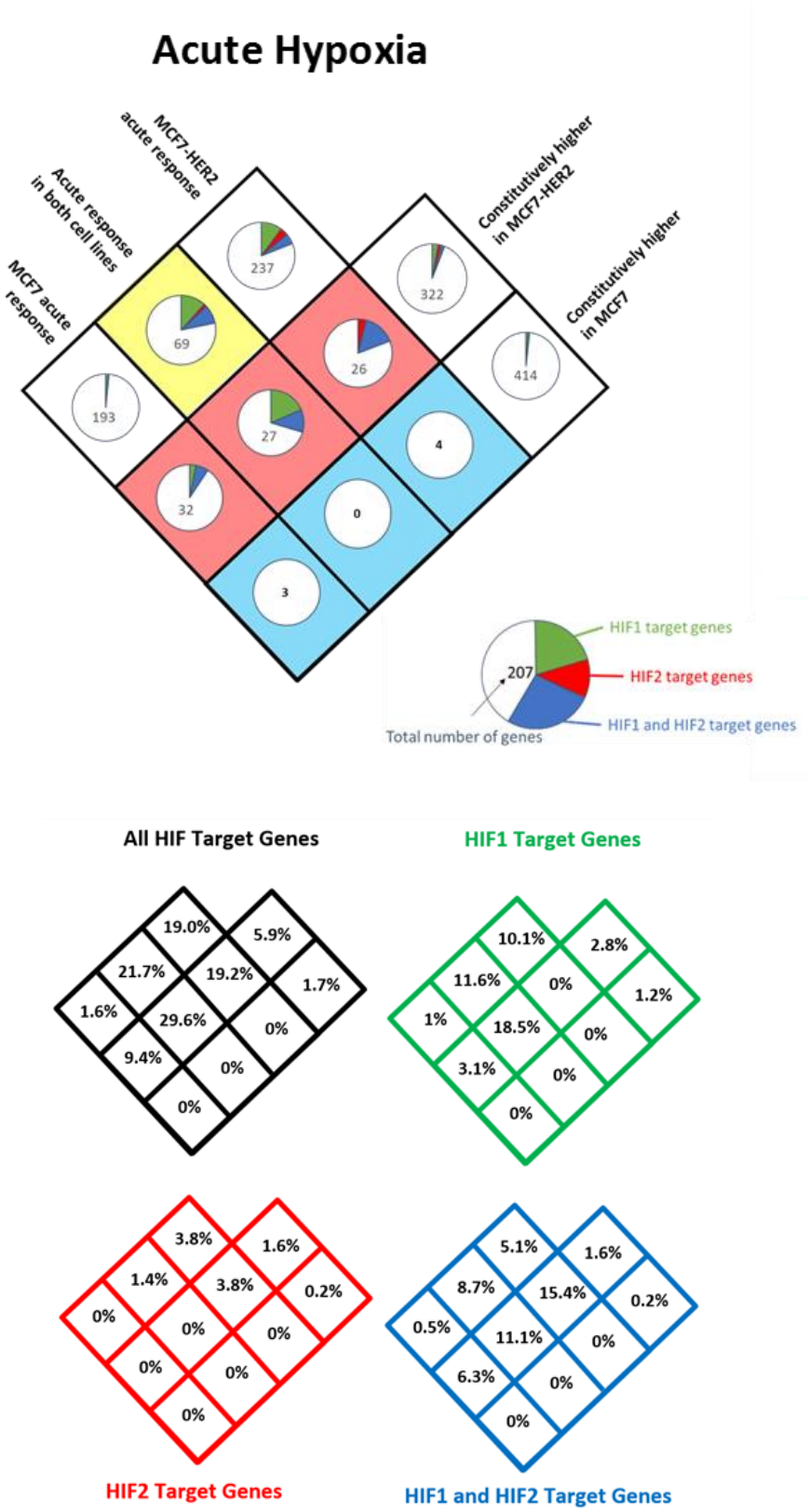

Figure 4.4: Analysis of HIF gene representation in Venn analysis of genes induced by acute hypoxia

Mole and Schödel HIF gene sets were used to determine the representation of HIF target genes in the Venn analysis from Figure 4.2. (Top) A square representation of the Venn diagram from Figure 4.2. Pie charts have been included to display the total number of genes in that sections, as well as the proportion of that section that is represented by HIF target genes. A legend for the pie charts is shown at the lower centre of the image, whilst the percentage of HIF target genes in each category is shown in the bottom half of the figure.

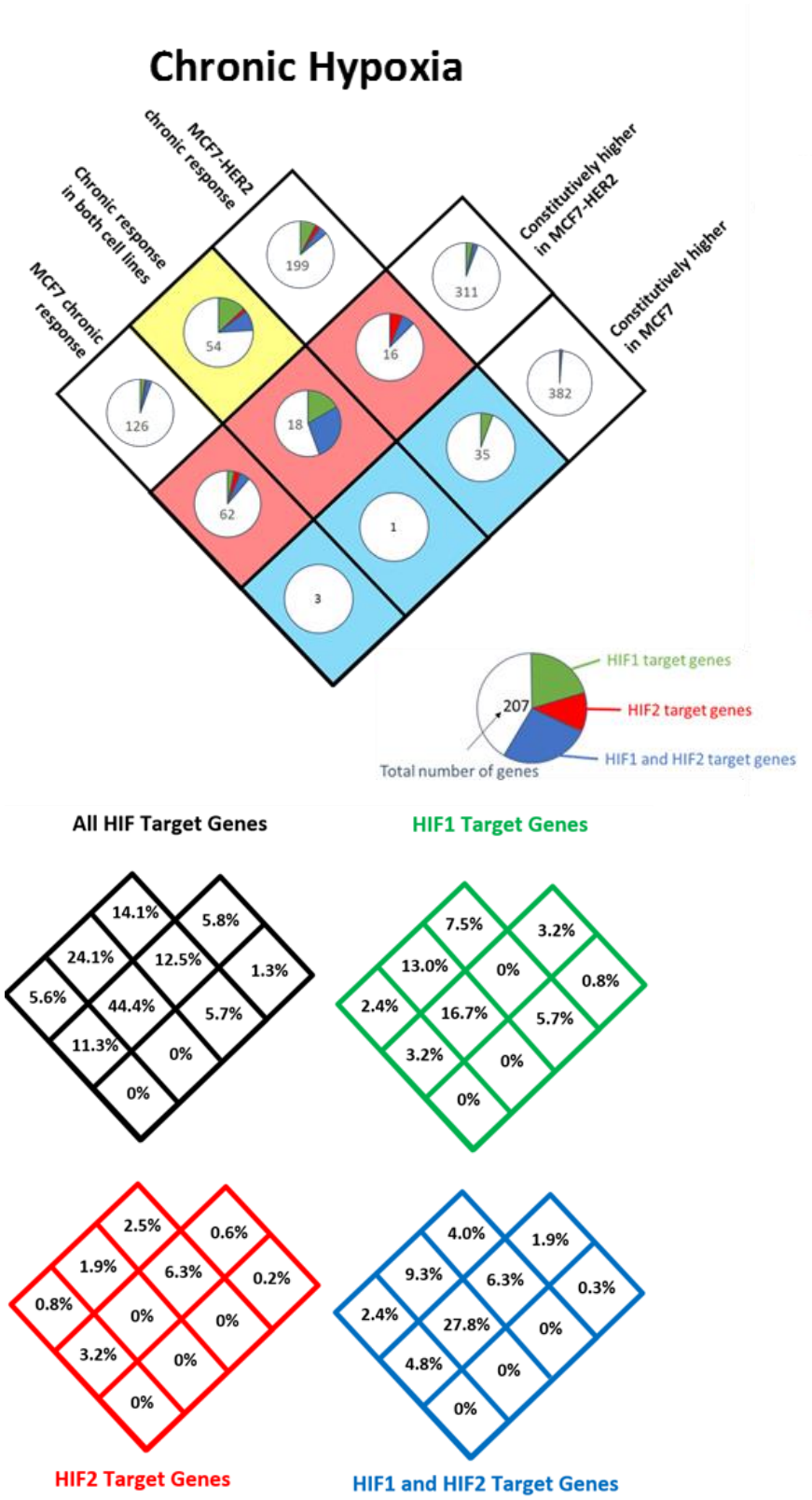

Figure 4.5: Analysis of HIF gene representation in Venn analysis of genes induced by chronic hypoxia

Mole and Schödel HIF gene sets were used to determine the representation of HIF target genes in the Venn analysis from Figure 4.2. (Top) A square representation of the Venn diagram from Figure 4.2. Pie charts have been included to display the total number of genes in that sections, as well as the proportion of that section that is represented by HIF target genes. A legend for the pie charts is shown at the lower centre of the image, whilst the percentage of HIF target genes in each category is shown in the bottom half of the figure.

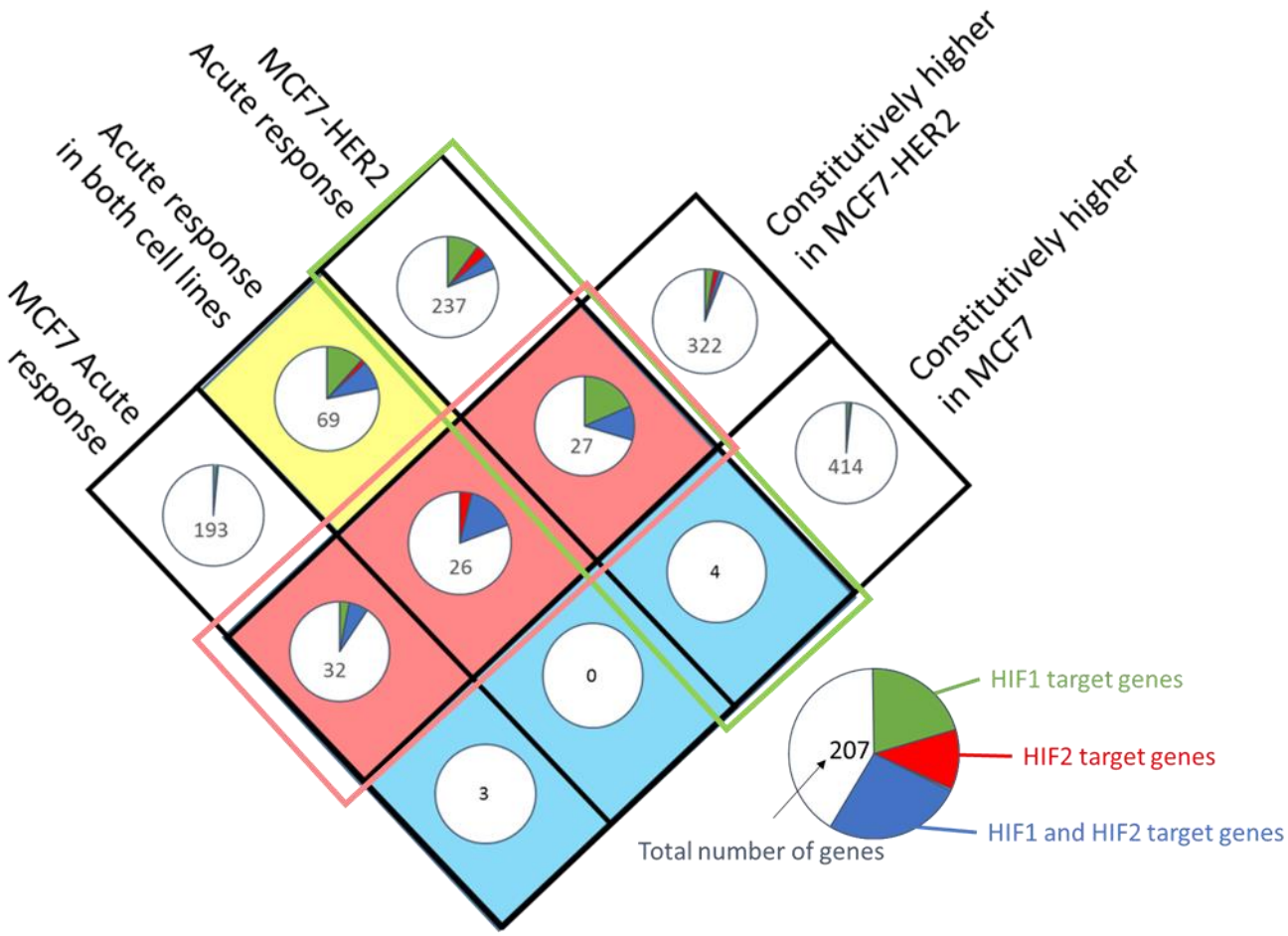

MCF7-HER2 specific HIF targets

Gene product	Driver	Function
Glucose-6-phosphate isomerase	HIF1/HIF2	Glycolytic enzyme
Glucose transporter 1	HIF1/HIF2	Membrane glucose transporter
Hexokinase 2	HIF1/HIF2	Glycolytic enzyme
Enolase 1	HIF1	Glycolytic enzyme
Phosphoglycerate kinase 1	HIF1	Glycolytic enzyme
Lactate dehydrogenase A	HIF1	Anaerobic glycolysis
Aldolase A	HIF2	Glycolytic enzyme
GBE1	HIF1	Glycogen metabolism
BCAS1	HIF1	Candidate oncogene
Carbonic anhydrase IX	HIF1	pH regulation
Platelet derived growth factor B	HIF1/HIF2	Angiogenesis
Desmoplakin	HIF1	Cellular adhesion
Nectin 4	HIF1/HIF2	Cellular adhesion
DAPK2	HIF2	Apoptosis
CITED2	HIF1/HIF2	Transcriptional regulator

Primed for hypoxia in MCF7-HER2

Gene product	Driver	Function
Aldolase C	HIF1	Glycolytic enzyme
Enolase 2	HIF1	Glycolytic enzyme
6-phosphofructo-2-kinase	HIF1	Glycolytic enzyme
PPP1R3C	HIF1/HIF2	Glycogen biosynthesis
S100P	HIF1/HIF2	Cell cycle/differentiation
KDM5B	HIF1	DNA methylase
Stanniocalcin 2	HIF1/HIF2	Proliferation
BNIP3L	HIF1/HIF2	Apoptosis
NDRG1	HIF1/HIF2	Stress response
SPRY1	HIF1/HIF2	Cellular differentiation

Figure 4.6: HIF1 and HIF2 target genes modified by HER2 overexpression in acute hypoxia

ChIP determined gene lists for HIF1 and HIF2 target genes in MCF7 (from Mole and Schödel) were used to identify HIF1 and HIF2 target genes which were either specifically upregulated by acute hypoxia in MCF7-HER2 and not MCF7 (green box), or were constitutively overexpressed in MCF7-HER2 and part of the acute hypoxic response in either cell line (red box). This was done using rank product gene list from the Venn diagram in Figure 4.2. (Top) A representation of the Venn diagram from Figure 4.4 showing the total number of genes in each category and the proportion of HIF genes represented as pie charts. (Bottom) A list of HIF target genes from 'HER2-specific' (green box) or 'HER2-primed' (red box) categories with important cellular functions. Gene/protein name, whether the gene is described as a HIF1 or a HIF2 target and the general function of the protein are shown.

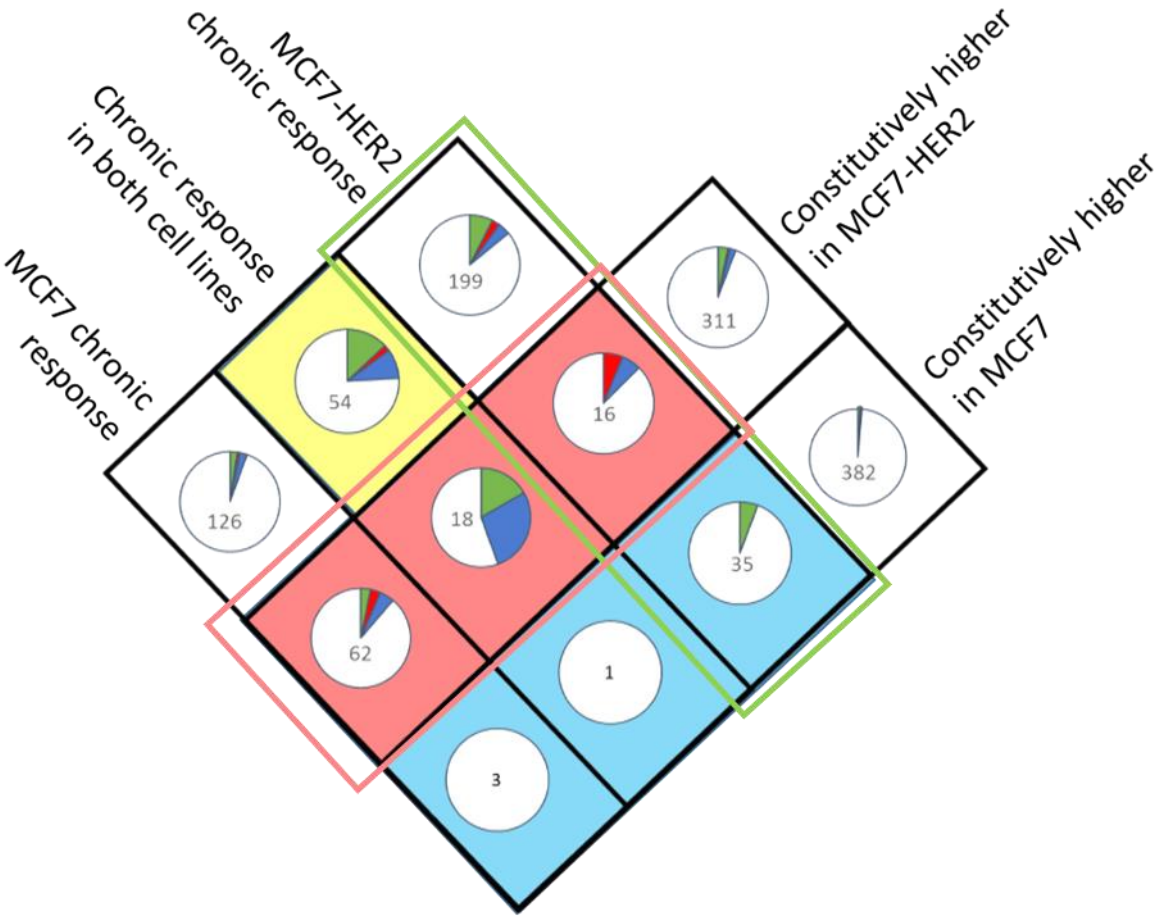

MCF7-HER2 specific HIF targets

Gene product	Driver	Function
Glucose transporter 1	HIF1/HIF2	Membrane glucose transporter
Enolase 1	HIF1	Glycolytic enzyme
Aldolase A	HIF2	Glycolytic enzyme
Pyruvate kinase (muscle)	HIF1	Glycolytic enzyme
Lactate dehydrogenase A	HIF1	Anaerobic glycolysis
Phosphoglycerate mutase 1	HIF1	Glycolytic enzyme
Desmoplakin	HIF1	Cellular adhesion
CITED2	HIF1/HIF2	Transcriptional regulator

Primed for hypoxia in MCF7-HER2

Gene product	Driver	Function
Aldolase C	HIF1	Glycolytic enzyme
Enolase 2	HIF1	Glycolytic enzyme
6-phosphofructo-2-kinase	HIF1	Glycolytic enzyme
Stanniocalcin 2	HIF1/HIF2	Hypoxic proliferation
C-FOS	HIF1/HIF2	Proto-oncogene
S100P	HIF1/HIF2	Proliferation/metastasis
KDM5B	HIF1	Histone demethylase
PXDN	HIF2	Extracellular matrix formation
DRAM1	HIF2	Autophagy
BNIP3L	HIF1/HIF2	Apoptosis
NDRG1	HIF1/HIF2	Stress response
SPRY1	HIF1/HIF2	Cellular differentiation

Figure 4.7: HIF1 and HIF2 target genes modified by HER2 overexpression in chronic hypoxia

ChIP determined gene lists for HIF1 and HIF2 target genes in MCF7 (from Mole and Schödel) were used to identify HIF1 and HIF2 target genes which were either specifically upregulated by chronic hypoxia in MCF7-HER2 and not MCF7 (green box), or were constitutively overexpressed in MCF7-HER2 and part of the chronic hypoxic response in either cell line (red box). This was done using rank product gene list from the Venn diagram in Figure 4.2. (Top) A representation of the Venn diagram from Figure 4.5 showing the total number of genes in each category and the proportion of HIF genes represented as pie charts. (Bottom) A list of HIF target genes from 'HER2-specific' (green box) or 'HER2-primed' (red box) categories with important cellular functions. Gene/protein name, whether the gene is described as a HIF1 or a HIF2 target and the general function of the protein are shown.

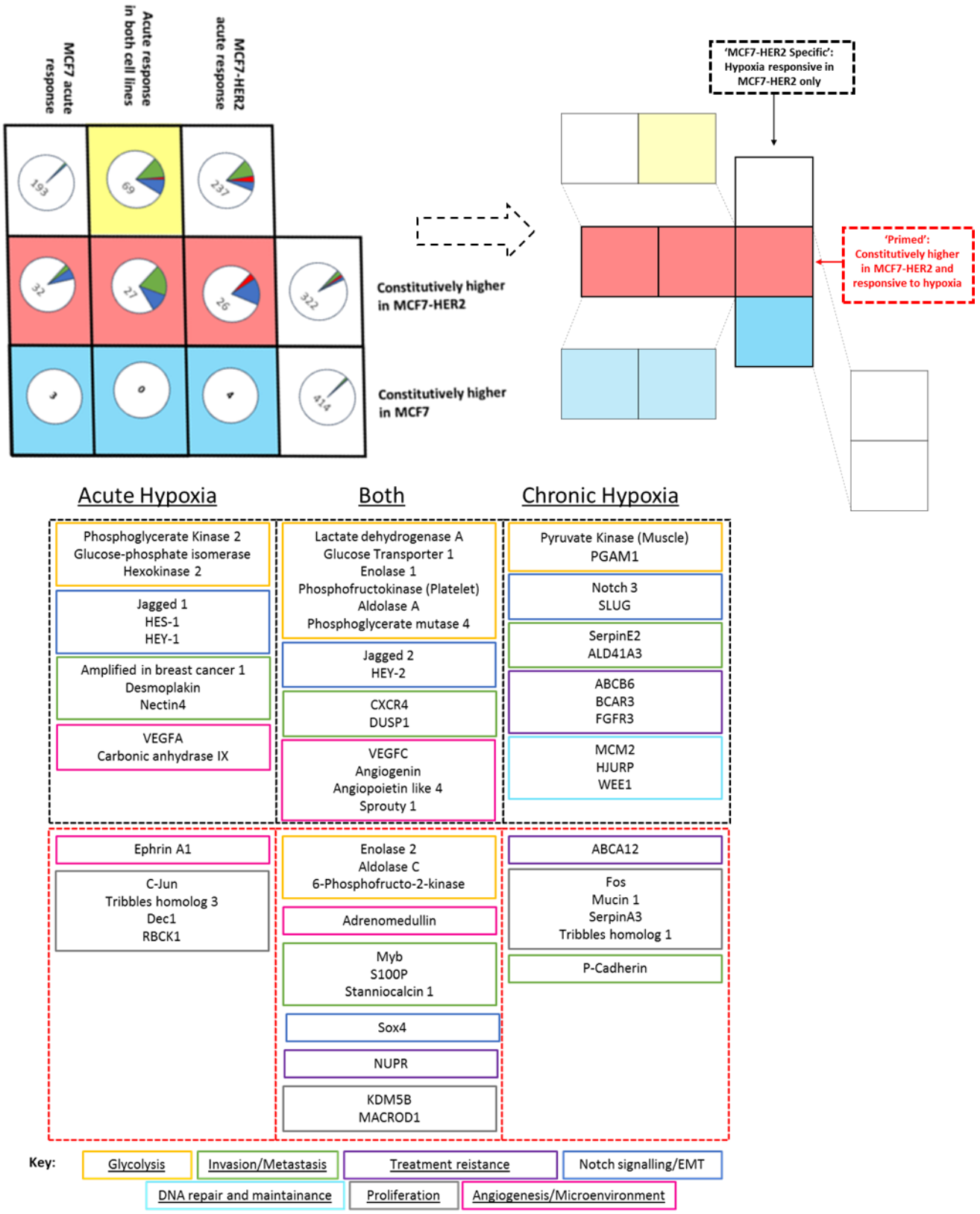

Figure 4.8: Pathologically important genes which form part of the 'HER2-specific' or 'HER2-primed' response to acute and/or chronic hypoxia

Rank product tested gene lists from chronic or acute hypoxia were assessed for important genes which form part of the 'HER2-specific' or 'HER2-primed' hypoxic response in MCF7-HER2 cells. Top left) A representation of the Venn diagrams shown in figures 4.4 and 4.5 comparing genes which are significantly upregulated only in MCF7 in hypoxia, in both cell lines in hypoxia or only in MCF7-HER2 in hypoxia, with genes constitutively more highly expressed in MCF7 or MCF7-HER2 when compared to the other cell line. Top right) A demonstrative deconstruction of the Venn diagram showing which sections constitute the 'HER2-specific' (black dotted box) and the 'HER2-primed' (red dotted box) hypoxic responses. (bottom) Important genes in each of these categories for both acute and chronic hypoxia are shown. Colour-coding is used to show the cellular functions of these genes which may contribute to cancer pathology.

4.5 The expression of primed hypoxic response genes correlates with HER2 expression across breast cancer cell lines

Whether HER2 expression could prime cells and increase response to hypoxia across breast cancer cell lines was next assessed. To do this we took the genes determined to be primed for hypoxia in MCF7-HER2 from our microarray data (n=85 in acute hypoxia and n=96 in chronic hypoxia) and compared their expression with that of HER2 using publically available microarray gene expression data from 172 samples representing 77 different breast cancer cell lines [489]. This produced a reduced list (n=25 acute hypoxia, n=33 chronic hypoxia) of genes with significant ($P<0.05$) Pearson's correlation to HER2 in this dataset. The expression of these genes in the cell line dataset and their correlation with HER2 expression can be seen in Figure 4.9. The top 5 correlating genes specifically primed in acute hypoxia or chronic hypoxia and the top 5 correlators primed in both conditions were determined and their expression in MCF7 and MCF7-HER2 in response to hypoxia is also shown in Figure 4.9. Notably, these included a number of genes with poor implications for breast cancer such as *EFNA1* (angiogenesis), *NUPR1* (metastasis), *S100P* (tumour aggression), *TRIB3*, *WSB1* (poor prognosis) and *RBCK1* (cellular proliferation).

4.6 Discussion

The aim of this chapter was to assess the consequence of HER2 overexpression on the transcriptional response to hypoxia in the MCF7 and MCF7-HER2 breast cancer cell lines. These cell lines provide a model to study the effect of HER2 overexpression without the high variation normally seen between cell lines of differing origins, and have been used in Chapter 3 to demonstrate a HER2-mediated increase in the hypoxic upregulation of HIF2α, CAIX and LDHA. Here we were able to compare the hypoxic response of these cell lines in more detail by measuring the expression levels of the entire transcriptome using an Illumina beadchip array.

This microarray experiment was first used to compare the regulation of pre-determined hypoxia response genes in acute and chronic hypoxia using a series of hypoxia metagenes. The aim of this approach was to broadly assess how the expression of predefined and verified hypoxia response genes differed in the context of wild-type MCF7 and HER2

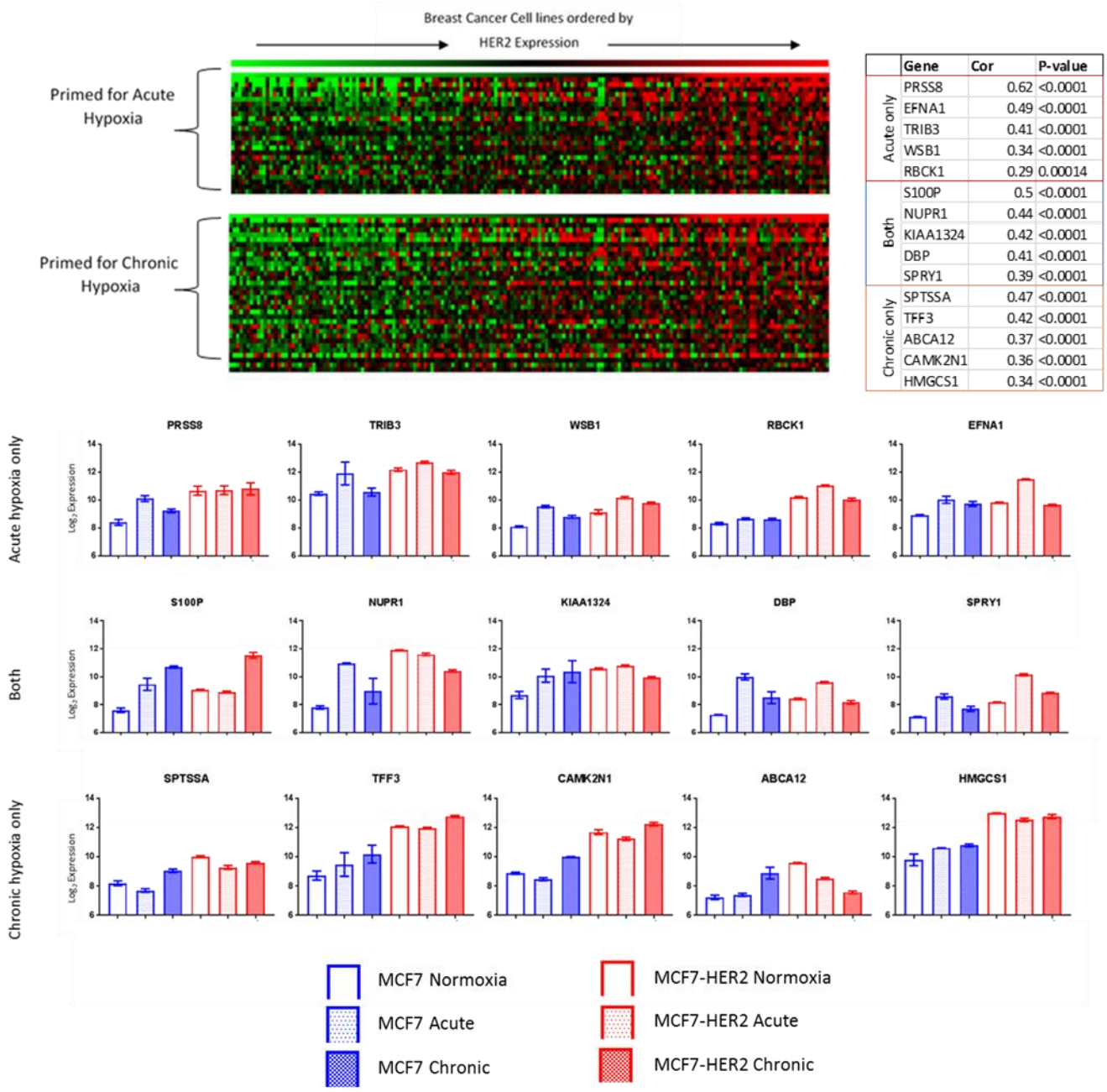

	Gene	Cor	P-value
Acute only	PRSS8	0.62	<0.0001
	EFNA1	0.49	<0.0001
	TRIB3	0.41	<0.0001
	WSB1	0.34	<0.0001
	RBCK1	0.29	0.00014
Both	S100P	0.5	<0.0001
	NUPR1	0.44	<0.0001
	KIAA1324	0.42	<0.0001
	DBP	0.41	<0.0001
	SPRY1	0.39	<0.0001
Chronic only	SPTSSA	0.47	<0.0001
	TFF3	0.42	<0.0001
	ABCA12	0.37	<0.0001
	CAMK2N1	0.36	<0.0001
	HMGCS1	0.34	<0.0001

Figure 4.9: Hypoxia response genes primed for hypoxia correlate with HER2 expression across breast cancer cell lines

Genes which were primed for either acute or chronic hypoxia by HER2 overexpression in MCF7-HER2 were compared to HER2 expression in a dataset containing gene expression data from 172 samples representing 77 different breast cancer cell lines. This resulted in 25 genes upregulated by acute hypoxia and 33 upregulated by chronic hypoxia which correlated with HER2 expression ($p<0.005$), with 16 genes represented in both acute and chronic hypoxia. Top) The expression of these genes is shown in a heat map with cell lines ordered by HER2 expression to demonstrate concordance of gene expression. Top right) The top 5 correlating genes primed for acute, chronic or both types of hypoxia are shown along with Pearson's correlation to HER2 across cell lines and the p-value. Bottom) The $\log_2$ expression values of top correlating genes in MCF7 and MCF7-HER2 from our HT12v4 beadchip array show the hypoxic regulation of these genes (error bars represent the SEM). A full list of genes used in this analysis can be found in Appendix 2.4.

overexpression after acute and chronic hypoxia. Three different hypoxia metagenes were used, each of which offered various strengths and weaknesses.

The Winter et al. metagene was determined by hierarchical clustering of Affymetrix gene expression data with known hypoxic response genes in 59 head and neck squamous-cell carcinoma biopsies. This was deemed an appropriate metagene for two reasons. Firstly, it was derived from clustering with key hypoxia response genes, many of which are known to be regulated by hypoxia in a number of cancers including breast cancer. These genes included CAIX, which was shown to be more strongly induced by hypoxic in MCF7-HER2 (Chapter 3). Secondly, this metagene was shown by Winter et al. to be a significant prognostic indicator for overall survival in a published breast cancer dataset, demonstrating the relevance of the expression of this metagene to breast cancer progression.

The metagene derived by Buffa et al. was included in this analysis as a robust metagene designed to detect hypoxia in various cancer types. This metagene was determined *in silico* through the assessment of co-expression with known hypoxia response genes (including both *CAIX* and *LDHA*, investigated in Chapter 3). Importantly this meta-analysis was performed in 8 datasets including 5 from breast cancer patients, and was validated in independent breast, lung and head and neck cancer datasets. The use of breast cancer datasets in the creation and validation of this metagene make it highly applicable to this work, and a preference for metagenes designed for breast cancer is clearly required in this study. However, choosing metagenes recognised for their robustness and applicability to multiple cancer types provides broader coverage for investigating the role of HER2 in hypoxic response, especially considering that breast cancer samples used to determine hypoxia response genes would likely have had a larger proportion of HER2-negative samples than HER2-overexpressed samples (if they represent the standard frequencies of HER2 overexpression in breast cancer), and thus may bias themselves against recognising hypoxic gene upregulation which only occurs in the context of HER2 overexpression. With this in mind, a combination of metagenes from various sources, not just those designed specifically for breast cancer, is clearly preferable.

The Toustrup signature was included in this analysis as it was designed to be stringent for hypoxia response genes. Whilst not verified prognostically in breast cancer, a couple of different approaches were used, giving it a potential advantage over the other signatures; thus it was included. Firstly, genes were chosen specifically to be pH-independent. In the

tumour microenvironment hypoxia and acidosis often occur in parallel; there is an intrinsic link between the cellular response to hypoxia and to reduced pH, and thus pH level has been shown to affect the expression level of genes previously thought to be hypoxia responsive [490, 491]. The use of pH-independent genes in the creation of this metagene was considered to provide higher specificity for hypoxia and allowed a more stringent gene set to be developed. Secondly, rather than discovering genes through the co-expression with known hypoxia responsive 'seed' genes, Toustrup et al. determined an optimum gene set able to differentiate between high and low oxygen tumours. Tumour oxygen levels were measured using an oxygen electrode and so the final gene expression signature is based on gene expression in hypoxia directly, as opposed to through what would be expected from the literature.

Additional hypoxia metagenes are available [484-487], but the three chosen here were selected to provide a suitably robust overview of hypoxic response. This meant that hypoxic response could be assessed broadly, whilst also focussing on stringently determined hypoxia response genes. For these reasons the use of these three metagenes was deemed to be an appropriate way of robustly analysing hypoxic gene expression in MCF7 and MCF7-HER2.

This analysis clearly demonstrated a modified hypoxic response in MCF7-HER2. Hierarchical clustering showed three predominant patterns of expression, with the vast majority showing an increased response to hypoxia in the HER2-overexpressing cell line. This included the majority of genes being more vigorously upregulated by both acute and chronic hypoxia, and these clusters were shown to be enriched for genes involved in glucose regulation and glycolysis. This demonstrates a clear role for HER2 in driving an increased hypoxic response in MCF7-HER2 cells and shows that this effect is not limited to the target genes shown in Chapter 3, but instead represents a broad change to the hypoxic response. In addition, this analysis showed that the HER2-enhanced response to hypoxia also includes genes which are downregulated by hypoxia, and in these metagenes such genes appear to be constitutively lower in MCF7-HER2. This suggests that in some cases HER2 overexpression in these cell lines might not only increase the response to hypoxia, but prime cells with gene expression changes normally associated with hypoxia being present even in normoxia. Finally, the presence of a small cluster in the Winter gene set showed that some genes were not responsive to hypoxia in MCF7. Whilst this is not in itself particularly surprising, it is

interesting to note that these genes were also more highly expressed in MCF7-HER2, despite no visible response to hypoxia in either cell line. This suggests that the role of HER2 in hypoxic gene expression is not limited to genes which are hypoxia inducible in MCF7.

Having shown a broad modification of hypoxic gene expression in MCF7-HER2, the transcriptional response of these cell lines was assessed by comparison of the entire transcriptome (Figure 4.2). This work validated the vast difference in response to acute and chronic hypoxia seen when HER2 is overexpressed. The most striking difference between these cell lines was the disparity in the number of genes constitutively higher in each cell line that were also responsive to hypoxia. This occurred in both acute and chronic hypoxia but the difference was greatest in acute hypoxia. The expression of hypoxia responsive genes in normoxia suggests that cells may be primed to respond to hypoxia and may play a role in the exacerbated hypoxic response of MCF7-HER2 cells. Additionally, this suggests once again that HER2 overexpression may lead to the expression of genes associated with hypoxia even in normoxia, potentially increasing traits such as metastasis and angiogenesis, which are associated with tumour hypoxia.

Using this data we were also able to directly assess the role of HIFs in this increased response to hypoxia. This was achieved using a set of HIF target genes taken from the literature. The finalised list used was a combined gene set from two papers, these being the full set of identified HIF1 and HIF2 target genes from Mole et al. 2009 supplemented with the top 30 binding sites identified by Schödel et al. 2011. Both these papers used ChIP-seq of HIF1α or HIF2α to determine binding sites for these transcription factors in MCF7 cells treated with 2 mM dimethyloxalylglycine (DMOG), a prolyl-4-hydroxylase inhibitor which leads to the upregulation of HIFα subunits. The fact that these binding sites were determined in MCF7 means there should be a high level of concordance with our dataset. Being sequence dependent, HIFα binding sites would be largely expected to remain similar across cell types, however it should be acknowledged that the HIF targets are likely to vary to some extent in the context of HER2 overexpression. HER2-driven changes in cofactor expression and chromatin structure could play important roles in determining novel binding sites for HIFα subunits, and these would naturally not be included in the gene list used in this dataset. More importantly, it should be recognised that HER2-driven changes in HIF2α expression discussed in Chapter 3 are likely to have profound effects on HIF1 vs HIF2 target binding, and thus the categorisation of these genes as HIF1, HIF2 or HIF1/HIF2 target genes (based solely on ChIP

data in wild-type MCF7s) may not represent the transcription factor responsible for the expression of the gene in MCF7-HER2. With this in mind, HIF2 may play a more vital role in the increase of HIF target genes, as this is the isoform whose expression and hypoxic upregulation was markedly increased by HER2 expression. However, to determine this would require further work looking into how the transcriptional response to hypoxia in MCF7-HER2, either by ChIP-seq in this cell line or further expression experiments in the context of HIF1α or HIF2α inhibition. Despite this limitation, we were able to show a significant increase in HIF target gene expression in the MCF7-HER2 cell line. This was shown by both hierarchical clustering of HIF genes and by the assessment of HIF target genes in rank product gene lists via Venn analysis. In general, a large number of HIF targets were shown to be specifically or more intensely upregulated by hypoxia in the context of HER2 overexpression. This was most notable in the contrast between HIF genes which were not shown to be constitutively higher in either cell line but were upregulated specifically in acute hypoxia in MCF7 (1.6% n=3) or in MCF7-HER2 (19%, n=45). This pattern was repeated in chronic hypoxia (MCF7= 5.6% n= 7, MCF7-HER2=14.1% n=28). This, combined with the finding that the increased number of hypoxia responsive genes seen in the MCF7-HER2 constitutively overexpressed group contained a high proportion of HIF genes, allowed us to conclude that HER2 overexpression modified the hypoxic response in at least two key ways: firstly, by increasing the activity of HIF transcription factors in response to hypoxia, and secondly, by driving the constitutive expression of hypoxia response genes. This appeared to have no specificity for HIF1 or HIF2 target genes, but a role for HIF2α is presumed due to its increased expression in this cell line.

Our investigation into the genes involved in the modified hypoxic response of MCF7-HER2 demonstrated a strong role for glycolysis. This was the case both when HIF target genes were analysed as well as when a non-HIF-centric approach was taken. With the non-HIF-centric approach a wide variety of pathologically important genes were shown to be HER2 regulated, with a number of important pathways represented. The majority of these are known to drive pathways associated with hypoxia-mediated pathology, including angiogenesis, metastasis/invasion and treatment resistance. This strongly suggests that the HER2-mediated increase in hypoxia response may be a strong driver of tumour progression and may contribute to the increased aggression of HER2-positive tumours. In addition to expected pathways, a number of notch signalling genes were noted in the HER2-specific response to hypoxia. Jagged1 and Jagged2 are both notch ligands associated with driving metastasis (especially to the bone) in breast cancer [492, 493]. Jagged1 has previously been

shown to be associated with worse tumour grade, vascular invasion as well as HER2 expression when assessed by IHC in breast cancer [493], whilst Jagged2 has been shown to contribute to stem cell self-renewal and epithelial-to-mesenchymal transition (EMT) in breast cancer [494]. As well as notch ligands, the Notch3 receptor was also included in these genes. *HES-1*, *HEY-1*, *HEY-2*, *SLUG* and *SOX4* are all known downstream targets of notch signalling. The HES/HEY transcription factors have been shown to promote the transcription of a number of genes in response to notch pathway activation. These include important cell cycle regulators (*P21*, *CCND1*), transcription factors (Myc and NFKB2), angiogenic factors (VEGFR1 and VEGFR2) as well as the HER2 receptor [495]. Slug and Sox4 are both recognised drivers of EMT and metastasis in breast cancer [496-498]. In general, hypoxia is recognised as a driver of notch signalling [328], and notch signalling has also been recognised as an important driver of hypoxia mediated metastasis [499]. Notch signalling appears to be a predominant pathway in the HER2-enhanced transcriptional response to hypoxia in MCF7, suggesting that HER2 expression and hypoxia may cooperate in breast cancer to drive EMT and metastasis through notch signalling. This may contribute to the increased cellular motility of MCF7-HER2 cells and their greater potential for migration in hypoxia when compared to wild-type MCF7 (Chapter 3).

Having demonstrated a significant role for HER2 in driving an increased hypoxic response in MCF7-HER2 cells, we next used a cell line dataset to see whether genes primed for hypoxia in MCF7-HER2 correlated with HER2 expression across breast cancer cell lines. Whilst this publically available dataset provided gene expression data for a large number of breast cancer cell lines, samples were all collected under normoxic culture conditions, meaning the direct comparison of gene upregulation in hypoxia was not possible. Instead, genes shown to be primed for hypoxia were tested, as these genes were, by definition, more highly expressed in normoxia when HER2 was overexpressed. This allowed a set of genes which are hypoxia-inducible in our microarray data and which correlate to HER2 expression across breast cancer cell lines to be established, suggesting that such genes may form part of a HER2-driven hypoxic response which is generally applicable to a large number of breast cancer cell lines. Whilst similar experiments in patient tumour samples would have provided more clinical relevance to this work, cell line work was favoured as it would not have been possible to accurately determine the extent of hypoxia in clinical datasets. This would have meant that larger, poorly vascularised tumours might have been present with a stronger expression of hypoxia response genes and it would be impossible to form accurate

conclusions on whether this is driven by HER2 expression or simply variations in hypoxic intensity. For this reason, the combined analysis in breast cancer cell lines and discovery of numerous important drivers of cancer pathogenesis, which are involved in the increased response in MCF7-HER2, was used to propose a significant role for HER2-driven hypoxic activation in breast cancer.

In summary this chapter has investigated the role of HER2-expression in modifying the transcriptional response to hypoxia in breast cancer cell lines. Multiple approaches to analyse this data all demonstrate the increased hypoxic expression of HIF and non-HIF hypoxia response genes and an increased expression of hypoxia response genes under normoxia, suggesting a HER2-mediated priming of cells for hypoxia. Whilst a role for HIF1 and HIF2 is suggested, this is with the understanding that the definition of HIF1 or HIF2 target genes is context dependent. This work supports the data shown in Chapter 3, with an increased hypoxic response in HER2 overexpressing MCF7 cells demonstrated at both protein and transcription levels, with a likely role for HER2-driven HIF2α expression. One caveat of these findings is that care must be taken with the direct comparison of MCF7 and MCF7-HER2 cell lines. Whilst isogenic, these are from disparate clones which may have accumulated some differences. This issue has been partially addressed by the comparison of HER2-primed hypoxic response genes in a panel of breast cancer cell lines, providing some evidence that these changes in gene expression are more broadly attributable to HER2 expression and not just unrelated differences between MCF7 and MCF7-HER2 cell lines. However, future work assessing the effect of HER2 expression on hypoxic response in additional breast cancer models would be valuable. The next chapters will investigate more directly the relationship of HER2 and HIF2α expression.

Chapter 5: Investigating the normoxic upregulation of HIF1α and HIF2α by growth factor signalling

5.1 Introduction

Neuregulin-1β (NRG) is a ligand for HER3 and HER4 receptors [500, 501]. It drives growth factor signalling by binding to either one of these receptors and permitting the formation and subsequent activation of HER receptor dimers (discussed in Chapter 1). Previous research has demonstrated that NRG treatment of MCF7 cells can increase the levels of HIF1α in normoxia through the PI3K/AKT/mTOR signalling pathway, leading to increased protein translation, and also by reducing the protein degradation rate caused by increased binding of HIF1α to HIF1β [220, 421]. These findings show that the HIF pathway is relevant to tumour cell signalling in normoxia if HER growth factor signalling is activated. Despite this, there is still little understanding of how HER2 receptor overexpression (found in 20% of breast cancers), might drive HIFα levels in normoxic conditions, or whether the overexpression of this receptor modifies the way in which cells respond to NRG in terms of HIFα pathway activation.

In this chapter, I describe studies investigating the effect of growth factor receptor signalling on the normoxic regulation of HIF1α and HIF2α and explore the effect of HER2 overexpression on HIFα levels with and without NRG-driven pathway activation. Using molecular inhibitors of various signalling pathways, I investigated possible mechanisms involved in growth factor driven HIFα regulation and obtained evidence of important differences between HIF1α and HIF2α with respect to their roles in normoxia.

5.2 Investigating the growth factor-mediated upregulation of HIF1α and HIF2α in breast cancer cell lines

The first aim of this chapter was to evaluate how NRG stimulation modified HIF1α and HIF2α levels in normoxia in MCF7 and MCF7-HER2 cells. This was to provide further understanding on two important aspects of growth factor-HIF interactions in breast cancer; firstly, to assess the differential capability of growth factors to drive HIF1α vs HIF2α, which has not previously been investigated but is important to consider in the light of our increased understanding of their differential roles in cancer biology, and secondly, to establish whether HER2 overexpression is sufficient to drive HIFα in normoxia or to intensify upregulation in response to NRG, as this may have important implications for the role of normoxic HIF activity in HER2-positive breast cancers.

5.2.1 Growth factor-mediated HIF1α upregulation is not affected by HER2 overexpression in MCF7 cells

To assess the potential for HIF1α upregulation by NRG in MCF7 and MCF7-HER2 cells, cells were treated with 25-400 ng/ml of NRG EGF domain (the HER receptor activating domain of the NRG protein) for 1 – 24 hrs. This was initiated after 20 hrs growth in low serum media to allow the addition of NRG to elicit a strong signalling response. Western blotting of whole cell lysates collected from these cells showed that HIF1α was upregulated by NRG addition (Figure 5.1a), even with low concentrations (25 ng/ml) across the time course in both cell lines. Whilst this demonstrates the potential for NRG-driven upregulation of HIF1α, a quantitative comparison was difficult as levels of HIF1α protein were highly variable. To provide a model for comparison, the upregulation of nuclear HIF1α over a 6 hr time course was assessed (Figure 5.1b). As a transcription factor, nuclear levels of HIF1α are more representative of the active protein, and the isolation of the nuclear fraction where relative levels of transcription factors will be higher allows for better signal to noise ratio when immunoblotting to reduce variability. Figure 5.1b shows HIF1α levels in the nuclear and cytoplasmic compartments after treatment with 200 ng/ml NRG EGF-domain. This experiment clearly indicated upregulation of the protein, with levels steadily increasing over time in both cell lines. This result agrees with previously published examples for MCF7 cells [220]. Surprisingly, HER2 overexpression in this cell line had no apparent effect on the response to NRG stimulation.

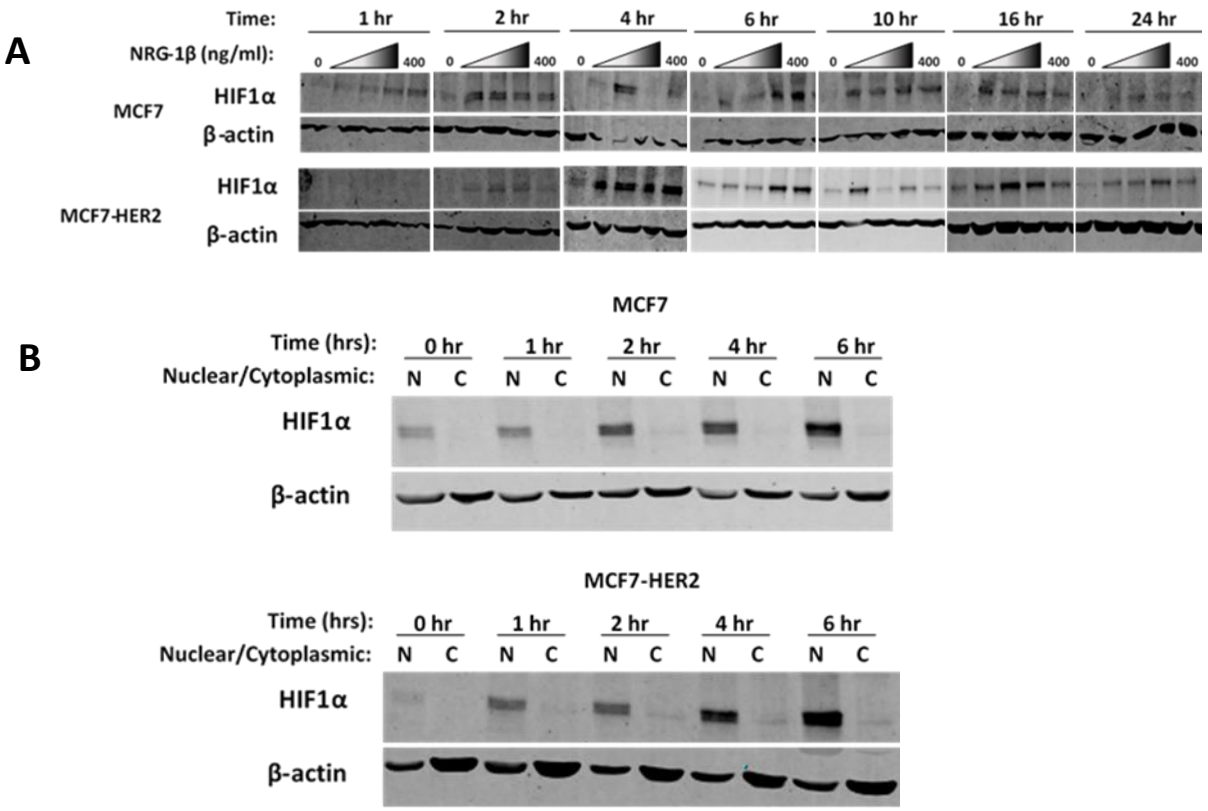

Figure 5.1: HIF1α can be upregulated by neuregulin-1β (NRG) and is similarly induced when HER2 is overexpressed

A) Western blotting of NRG treated MCF7 and MCF7-HER2 whole cell lysates showing the expression of HIF1α and β-actin (loading control). Cells were first serum starved (0% FCS) in phenol red-free media for 20 hrs before the addition of 0, 25, 100, 200 or 400 ng/ml of NRG. Cells were grown in treatment conditions for 1-24 hrs before protein lysates were collected. Probing for HIF1α in 40 µg of these lysates shows that NRG treatment is able to induce normoxic HIF1α levels in both cell lines with no clear indication of a modified effect in the context of HER2 overexpression. B) Similarly, nuclear and cytoplasmic cellular lysates were collected for MCF7 and MCF7-HER2 cells treated with 200 ng/ml of NRG for 1-6 hrs (also after 20 hrs in 0% FCS phenol red-free serum). This demonstrated the nuclear upregulation of HIF1α by NRG in both cell lines. Both figures A and B show representative western images from n=2 experimental repeats.

5.2.2 HIF2α is not upregulated by neuregulin-1β but is constitutively higher in the context of HER2 overexpression

Next, we assessed the effects of NRG treatment on HIF2α levels in normoxia in these two cell lines (Figure 5.2a). Whole cell lysates from MCF7 and MCF7-HER2 cells treated with 200 ng/ml NRG over a 6 hr time course were used for western blotting of HIF2α. In contrast to HIF1α, we saw no change in HIF2α levels in either cell lines over the time course. Interestingly however, we saw constitutively higher expression of HIF2α in the MCF7-HER2 cell line. This suggests that HER2 overexpression may be sufficient to drive HIF2α upregulation in normoxia despite no apparent NRG driven differences. This constitutively higher HIF2α level in MCF7-HER2 was confirmed in further western blotting experiments of whole cell lysates, and combined densitometry values were used to quantitatively compare HIF2α protein in these two cell lines (Figure 5.2b). HIF2α was approximately 7-fold higher in normoxic MCF7-HER2 cells than in wild-type MCF7 cells. In MDA-MB-361, BT474 and SKBR3 cell lines varying basal levels of HIF2α expression were seen, and in concordance with MCF7 and MCF7-HER2 cell lines, no changes in response to NRG were seen.

This work demonstrates that ligand driven HIF1α upregulation is robust and may be independent of HER2 expression. The expression of HIF2α however, appears unaffected by NRG stimulation, whilst HER2 expression is sufficient to drive its upregulation in MCF7 cells, even in normoxia. These findings highlight once again the importance of taking differences between HIF1α and HIF2α into account when considering their implications in breast cancer. The importance of HIF1α vs HIF2α in growth factor-driven HIF regulation appears to be dependent on cellular context, and may have important implications for HER2-positive breast cancers. Importantly, there appears to be more than one mechanism by which HER signalling can drive HIFα upregulation and in this cell line model HIF1α and HIF2α are independently modulated by these different mechanisms. The rest of this chapter will focus on understanding the mechanism of HIF2α upregulation in MCF7-HER2 cells.

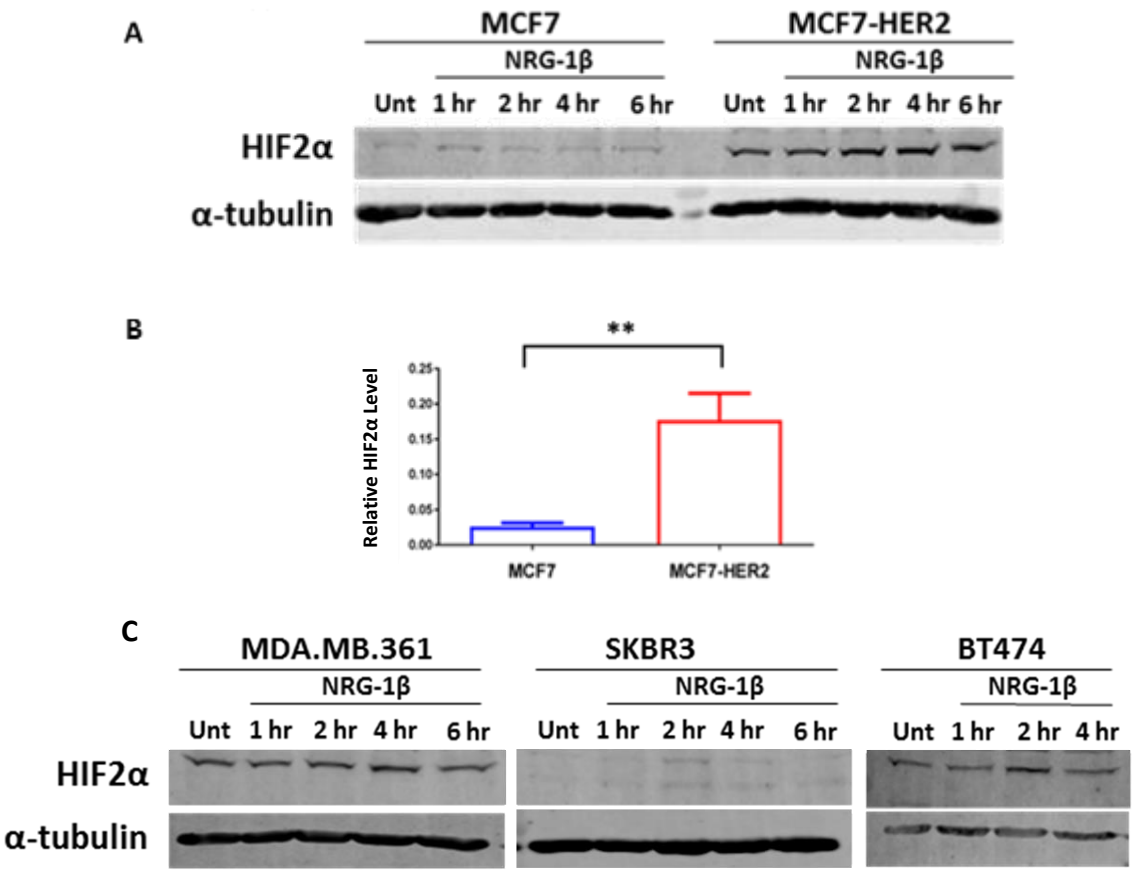

Figure 5.2: HIF2α protein is upregulated by HER2 expression despite no effect from NRG treatment

*A) Western blotting of HIF2*α and α-tubulin in *MCF7 and MCF7-HER2 cell lines treated with 200 ng/ml NRG for 1-6 hrs after 20 hrs serum starvation (0% FCS in phenol red-free media). Whilst HIF2*α is constitutively more highly expressed in the MCF7-HER2 there is no visible effect from NRG treatment in either cell line. B) Bar graph representation of HIF2α protein levels as determined by densitometry readings normalised to tubulin control values in untreated cell lines. This was done in n=5 experiments with the mean value shown for each cell line (error bars represent the SEM) (p=0.0041, unpaired t-test). C) Similar western blotting experiments were performed in breast cancer cell lines MDA.MB.361, SKBR3 and BT474, showing that despite differences in the levels of HIF2α no, or little change in normoxic protein level were seen in these three cell lines (n=2).

5.3 Increased HIF2α levels in MCF7-HER2 are reduced by HER2 inhibition

To establish the role of HER2 driven signalling in the overexpression of HIF2α in MCF7-HER2 cells, we used a selection of receptor tyrosine kinase (RTK) inhibitors to assess how inhibition of HER signalling would affect the constitutive levels of HIF2α in this cell line. In these experiments small molecular inhibitors lapatinib, gefitinib and mubritinib were used. Lapatinib is a dual inhibitor of both HER2 and EGFR. By binding the ATP-binding pocket of these receptors lapatinib is able to prevent autophosphorylation by the receptor kinase domain, inhibiting signal initiation from these receptors [502, 503]. Gefitinib is a reversible inhibitor EGFR which, similar to lapatinib, inhibits kinase activity by binding to the ATP-binding pocket of this receptor. Whilst, reportedly an EGFR inhibitor, gefitinib can also bind other HER family receptors, although the binding affinity of gefitinib to HER2 has been shown to be 200-fold lower than to EGFR [503-505]. Mubritinib (TAK-165) is a HER2 specific kinase inhibitor showing >4000-fold selectivity over other RTKs, and has been shown to have antiproliferative effects on HER2 overexpressing cells *in vitro* and *in vivo* [506, 507].

Initial experiments using lapatinib (a dual HER1/HER2 kinase inhibitor) demonstrated a significant reduction (approximately 50%) in normoxic HIF2α levels when treated with lapatinib when compared to a vehicle control (DMSO) (Figure 5.3) and this effect was similar over 8, 24 and 48 hr treatment durations. As lapatinib is an inhibitor of both HER1 (EGFR) and HER2 activity, we next performed equivalent experiments to compare the effects of lapatinib with EGFR-specific inhibitor gefitinib (Figure 5.4), as well as with a HER2-specific inhibitor mubritinib (Figure 5.5). Whole cell lysates of MCF7-HER2 cells treated with lapatinib (10 μM), gefitinib (2 μM) or a vehicle control (0.1% DMSO) for 8, 24 or 48 hrs were immunoblotted for HIF2α as well as for overall and phosphorylated HER2 and EGFR. This demonstrated a consistent reduction of HIF2α by lapatinib and gefitinib over the 48 hrs. This effect is consistent with the inhibition of HER2 phosphorylation (tyr1221/1222) in these experiments. Phospho-HER2 levels were reduced below detectable levels for cells treated with lapatinib or gefitinib. Additionally, phosphorylated EGFR (tyr1148) appeared reduced by lapatinib and gefitinib. As such, a role for EGFR in HIF2α regulation cannot be ruled out. To demonstrate a specific role for HER2 in HIF2α upregulation, we used a mubritinib, a highly HER2 specific RTK inhibitor. MCF7-HER2 lysates treated with 0.1 to 100 nM concentrations of mubritinib or a

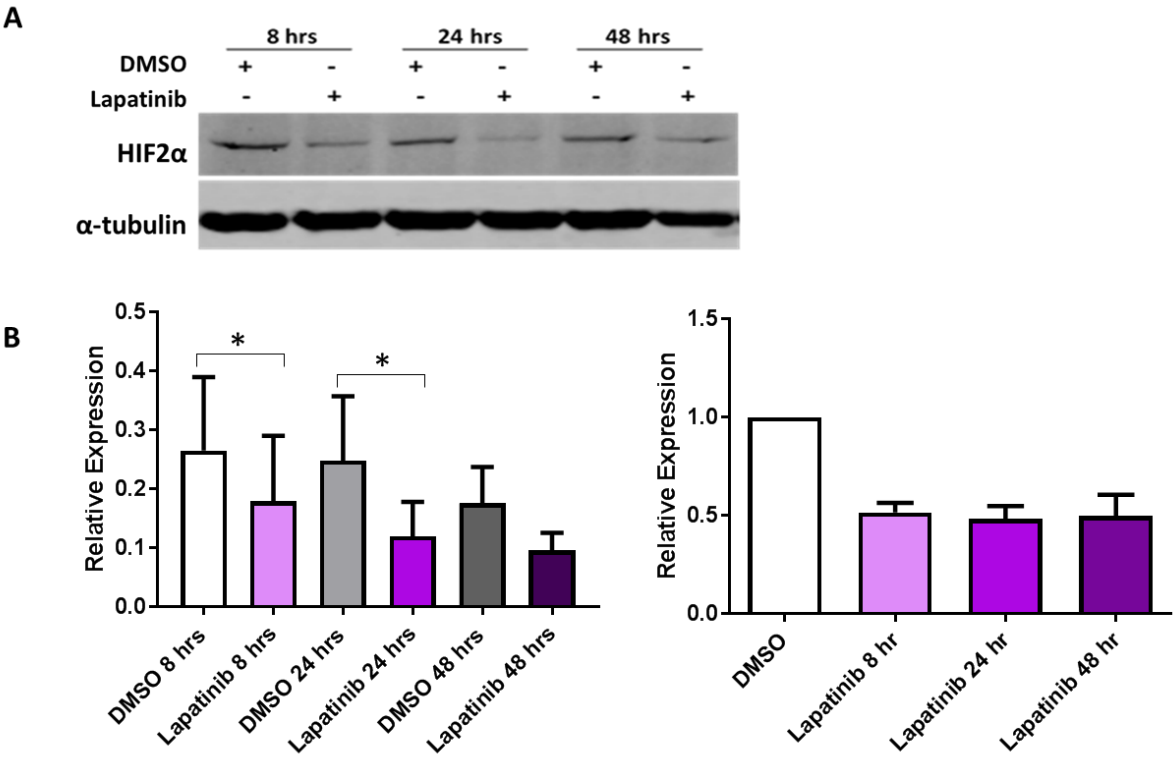

Figure 5.3: Inhibition of RTK signalling with lapatinib reduces the normoxic expression of HIF2α in MCF7-HER2

A) Representative western blot from n=4 experiments showing HIF2α and α-tubulin levels in whole cell lysates of MCF7-HER2 cells treated with 10 μM of lapatinib or vehicle control (0.1% DMSO) for 8, 24 or 48 hrs after 24 hrs growth in 2.5% DCSS in phenol red-free media. B) Mean densitometry values for HIF2α normalised to α-tubulin for each condition (error bars represent the SEM). Ratio paired t-tests of individual time points shows a significant reduction in HIF2α levels at 8 and 24 hrs (p=0.0314 and p=0.0148 respectively). C) Each experiment (n=4) was normalised to its own DMSO control to remove the inter-experimental variability, which resulted in high standard error. This demonstrates a consistent reduction (approximately 50%) in normoxic HIF2α levels across time points.

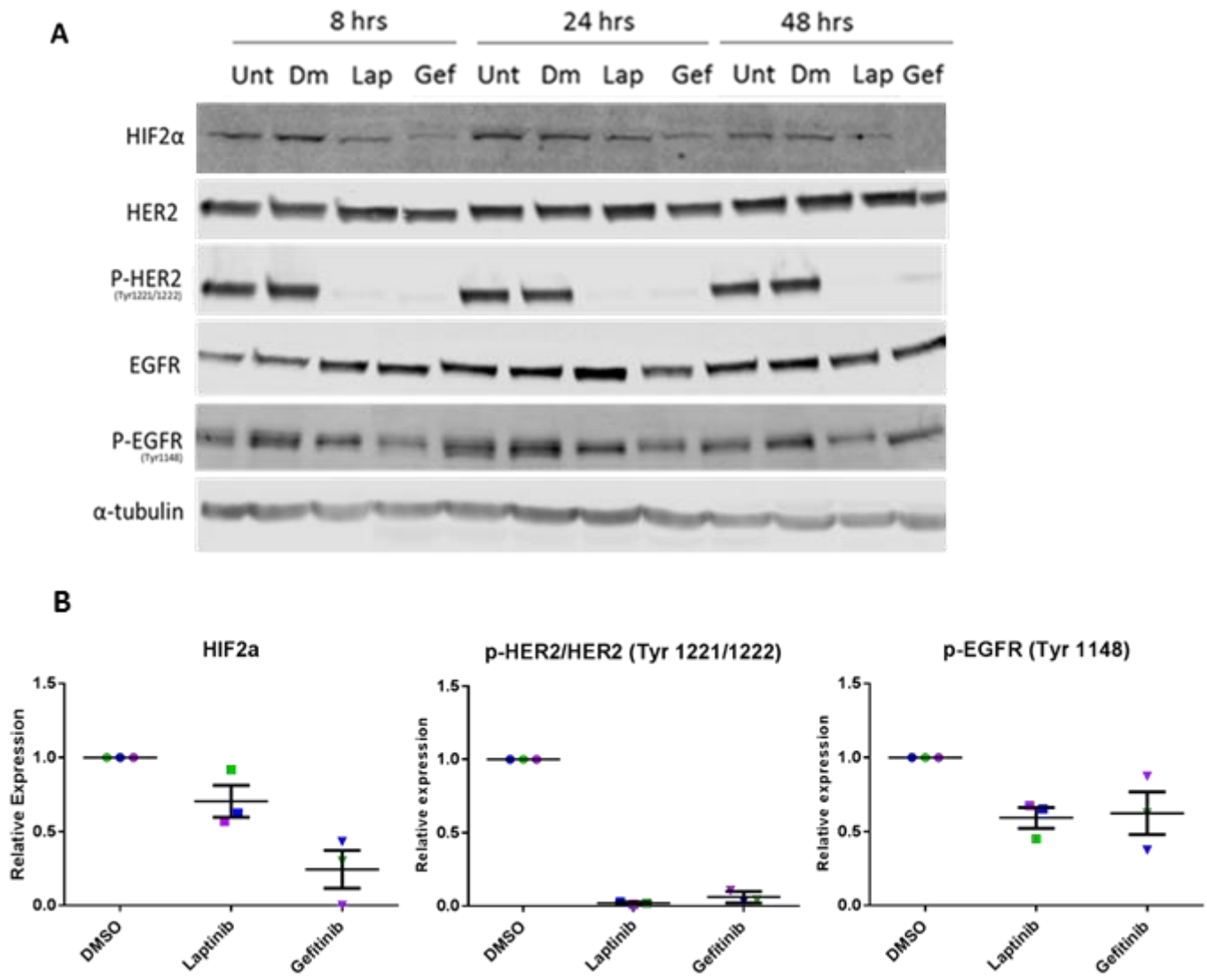

Figure 5.4: Normoxic HIF2α protein level in MCF7-HER2 is reduced after lapatinib or gefitinib treatment

A) Western blotting experiment of whole cell lysates of MCF7-HER2 cells treated with 0.1% DMSO (Dm), 10 µM lapatinib (lap) or 2 µM gefitinib (gef) for 8, 24 or 48 hrs after 24 hrs in reduced serum conditions (2.5% DCSS with phenol red-free media). The same lysates were probed for HIF2α, α-tubulin (loading control, HER2, EGFR as well as phosphorylated forms of the HER2 (tyrosine 1221/1222) and EGFR (tyrosine 1148) receptors. The ratio of these phosphorylated receptors to the overall level of the receptor was used as a surrogate for receptor activation and compared to HIF2α levels. B) The densitometry values for HIF2α (normalised to tubulin), phospho-HER2 (normalised to total HER2) and phosphor-EGFR (normalised to total EGFR) are shown relative to DMSO for each time point. The downregulation of HIF2α coincides with a reduction in both HER2 and EGFR phosphorylation at the selected residues.

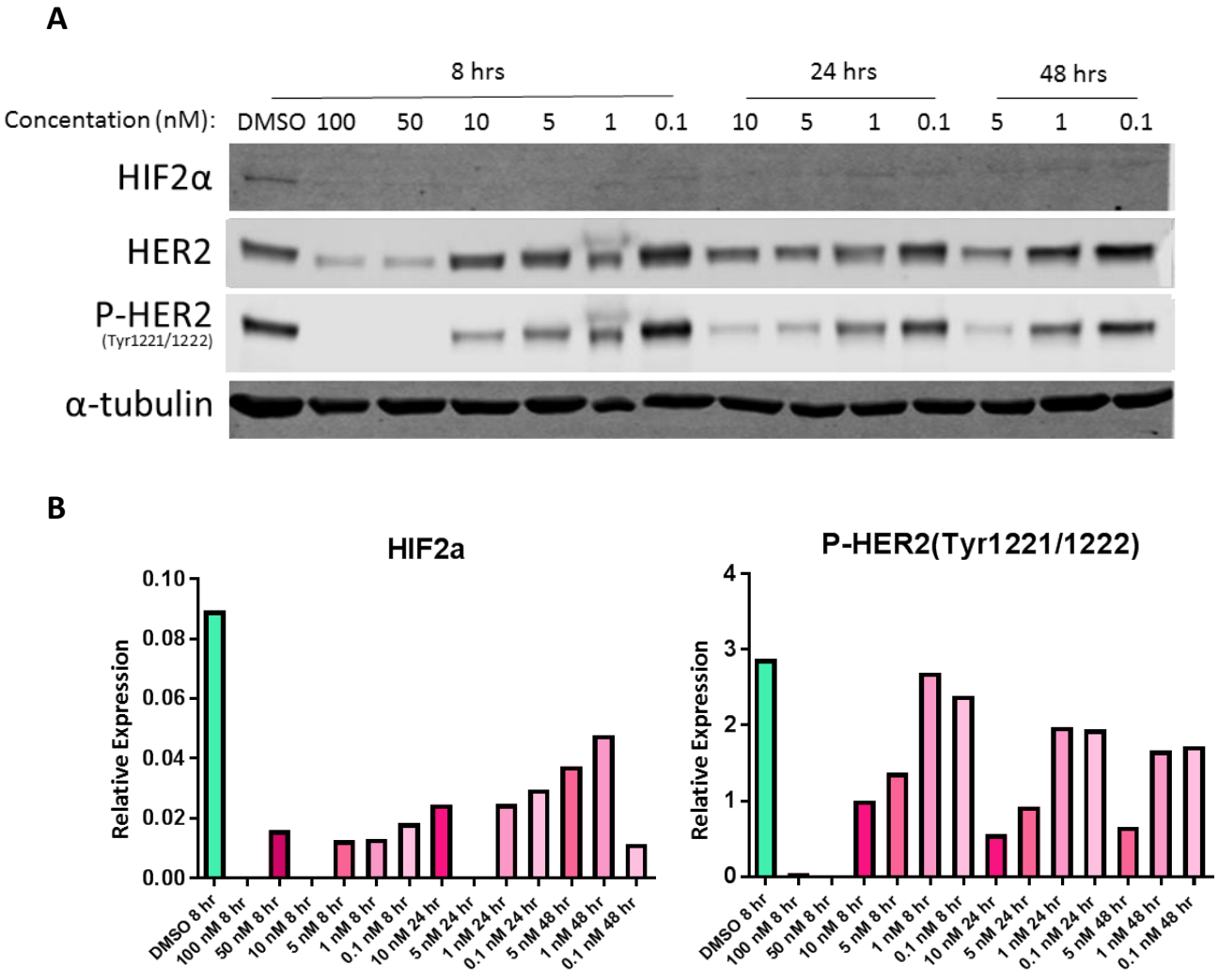

Figure 5.5: HER2-specific tyrosine kinase inhibitor mubritinib reduces HIF2α levels in MCF7-HER2 in normoxia

*A) Western blotting of MCF7-HER2 whole cell lysates treated for 8, 24 or 48 hrs with 0.1% DMSO or 0.1 – 100 nM mubritinib. B) Densitometry values for HIF2*α (normalised to α-tubulin) and phospho-HER2 (normalised to total HER2) are shown. This demonstrates a dose-dependent reduction in both HER2 activation and HIF2α levels (n=1).

vehicle control (DMSO) (treated for 8, 24 or 48 hrs) were immunoblotted for HIF2α, HER2 and p-HER2 (Figure 5.5a). Mubritinib was effective at reducing normoxic HIF2α levels in MCF7-HER2 even at the lowest concentration tested across the time course. This effect was partially dose-dependent and correlated to reduced phosphorylation of HER2 (Figure 5.5b). Some concentrations at later time points were excluded due to visible cytotoxicity.

5.4 High HIF2α levels in MCF7-HER2 are driven at the transcriptional level

The NRG-mediated upregulation of HIF1α has previously been established as a post-transcriptional effect, with increased translation of the protein through PI3K/AKT/mTOR signalling and increased heterodimer stability being demonstrated as the mechanisms driving the increased protein levels in normoxia. In Section 5.2 we demonstrated that differential mechanisms exist for HIF1α and HIF2α upregulation by growth factor signalling in MCF7 and MCF7-HER2 cell lines; therefore, we next wanted to assess whether the upregulation of HIF2α by HER2 overexpression was also mediated at the transcriptional or post-transcriptional level. Having obtained gene expression microarray data for MCF7 and MCF7-HER2 in normoxia and hypoxia (Chapter 4), we used this to compare transcript levels of HIF2α between these cell lines. HIF1α was also included in this comparison so that the differences in regulatory mechanisms of these two factors could be confirmed. Figure 5.6 shows gene expression values (n=3) for HIF1α and HIF2α in MCF7 (blue) and MCF7-HER2 (red) in normoxia, acute and chronic hypoxia as well as after 24 hrs cobalt chloride treated (400 μM). Treatment with cobalt chloride leads to the stabilisation of HIFα subunits even in the presence of oxygen. This is achieved as cobalt ions are able to bind to the iron binding domain of HIF hydroxylases, preventing HIF hydroxylation and subsequent ubiquitination and degradation. Additionally, cobalt is able to bind directly to hydroxylated HIFα proteins and prevent their interaction with VHL [508]. In this way cobalt chloride offers a mechanism of inducing HIF activity without the requirement of hypoxia. Both the treatment of cells in hypoxia and the use of cobalt chloride will induce some HIF-independent effects. By showing gene expression changes occur both in response to hypoxia and cobalt chloride treatment, more evidence is provided that these effects are HIF driven, and not a HIF-independent response to hypoxia.

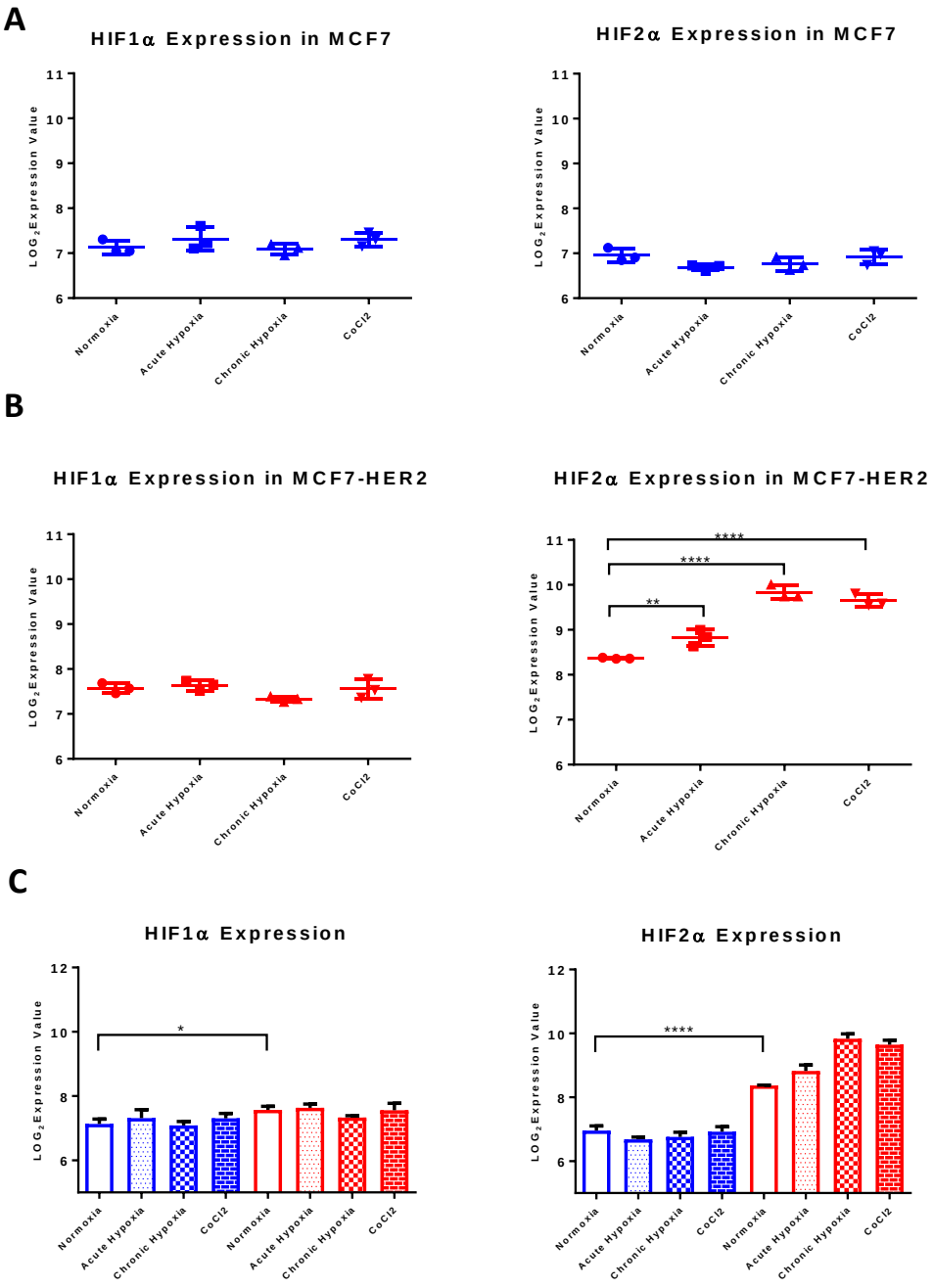

Figure 5.6: Microarray analysis of HIF1α and HIF2α gene expression in response to hypoxia in MCF7 and MCF-HER2

*Log_2 expression values from HT-12v4 Illumina beadchip array for HIF1α and HIF2α in MCF7 (blue) and MCF7-HER2 (red) cell lines grown in normoxia, acute hypoxia (0.5% oxygen for 24 hrs), chronic hypoxia (0.5% oxygen for 10 weeks) or treated with 400 µM cobalt chloride ($CoCl_2$). Panels A and B show mean and standard deviation of HIF1α or HIF2α in MCF7 (A) and MCF7-HER2 (B) cell lines individually, with individual data points shown n=3. One-way ANOVA with Dunnett's multiple comparison to the normoxic group was used to assess any significant effects of hypoxia on expression level. C shows the mean expression (with standard deviation) of HIF1α or HIF2α with the two cell lines plotted on the same axis for comparison. A two-tailed T-test was performed to compare normoxic samples between the two cell lines only. *= p< 0.05, **= p< 0.01, ***= p<0.005, ****= p<0.0001.*

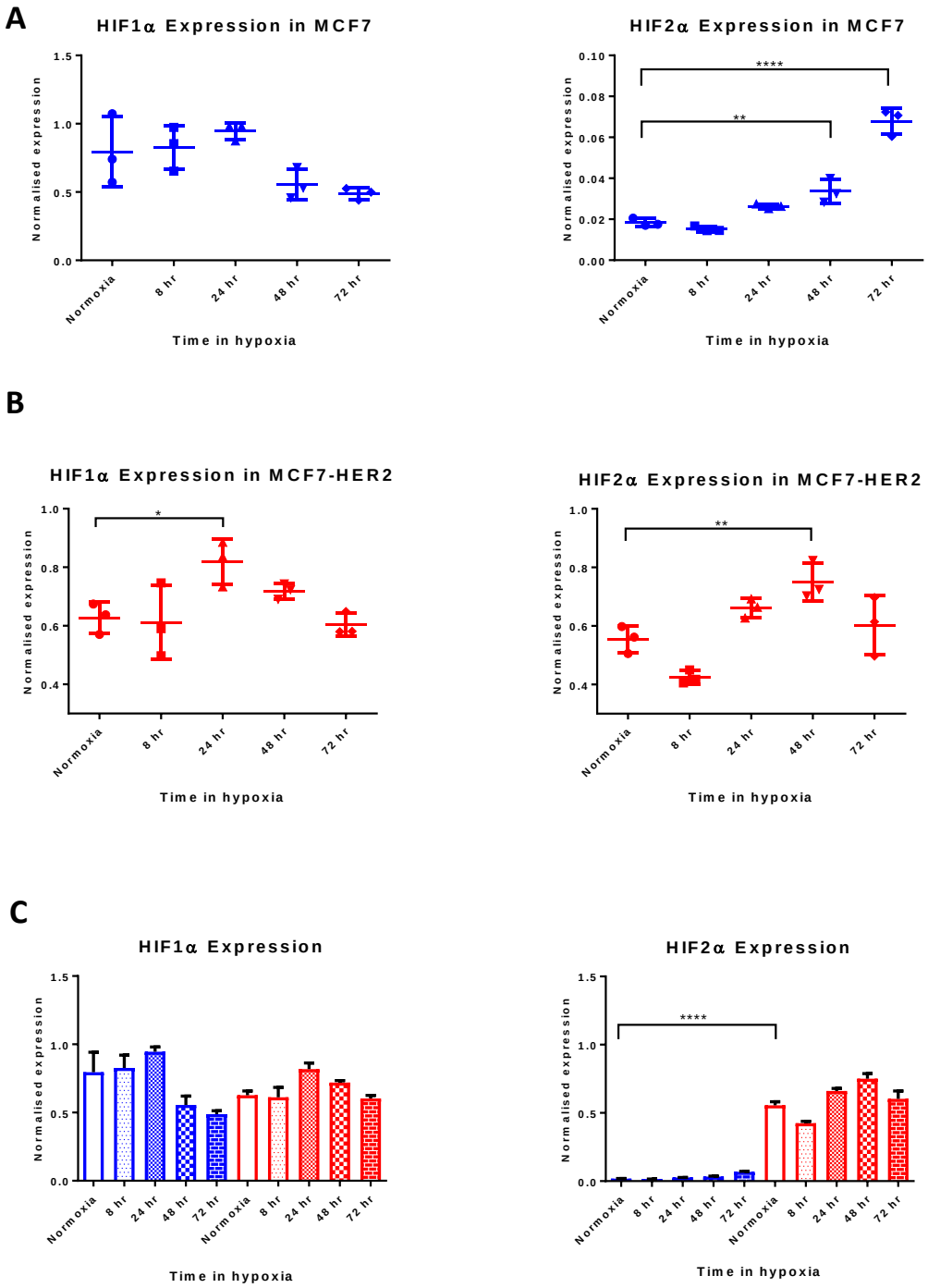

Figure 5.7: RT-PCR analysis of HIF1α and HIF2α gene expression in response to hypoxia in MCF7 and MCF7-HER2

*Real-time-PCR quantification of HIF1α and HIF2α expression in MCF7 and MCF7-HER2 cells in normoxia and 8, 24, 48 and 72 hours hypoxia. Panels A and B show the mean expression values with standard deviation of individual cell lines over the hypoxic time course with individual data points also shown. Statistically significant differences are indicated by asterisks (one-way ANOVA with Dunnett's multiple comparison). Panel C shows a comparison of expression levels in the two cell lines on the same axis to demonstrate cell line differences in expression level, with mean and standard deviation shown. T-test was performed to compare normoxic expression values between cell lines. For both types of statistical test *= p< 0.05, **= p< 0.01,***= p<0.005, ****= p<0.0001.*

This gene expression analysis provided evidence for important differences in the regulation of HIF1α and HIF2α in these cell lines. Transcript levels of both proteins in MCF7 cells were comparable and stable. HIF1α and HIF2α had similar basal levels of expression and no changes were seen in hypoxia or after cobalt chloride treatment. In MCF7-HER2 cells, HIF1α expression was comparable to MCF7 cells. However, HIF2α expression was significantly higher in normoxia when compared to MCF7 cells, and was significantly increased in hypoxia. This included increases in acute and chronic hypoxia, as well as by cobalt chloride treatment.

To validate these findings, quantitative RT-PCR was used to assess the mRNA levels of HIF1α and HIF2α in MCF7 and MCF7-HER2 cells over a 72 hr hypoxia time course. RT-PCR experiments were able to validate a significant increase in mRNA levels of HIF2α in MCF7-HER2 cells when compared to wild-type MCF7, with a > 10-fold increase in transcript levels which remained across the hypoxic time course (Figure 5.7). Differences in the hypoxic upregulation of HIF2α were modest but increased in both cell lines, with a greater effect in MCF7 cells when assessed by RT-PCR. A significant change in HIF1α expression after 24 hrs hypoxia was noted in MCF7-HER2 cells, however this was not apparent in later hypoxic time points or in microarray data. Thus, the key results from assessing transcript levels of HIF1α and HIF2α in these RT-PCR experiments are that HIF2α is more highly expressed in MCF7-HER2 when compared to MCF7 cells, and that HIF2α but not HIF1α transcription is induced by hypoxia.

5.5 Investigation of the signalling pathways involved in the HER2-mediated increase of HIF2α

In Section 5.2 we were able to characterise differences in growth-factor mediated regulation of HIF1α and HIF2α through a comparison of NRG stimulation and HER2 overexpression, showing a HIF1α-specific upregulation in response to NRG stimulation and a HIF2α-specific effect in the context of HER2 overexpression. To understand the mechanisms driving these responses we considered the differences between these two modes of HER signal activation. NRG is a HER3 ligand and so promotes growth factor signalling through HER3 heterodimers, whilst HER2 overexpression drives signalling down stream of HER2 [509]. Whilst both receptors are capable of driving both pathways, we hypothesised that higher

levels of PI3K/AKT/mTOR activation as a result of NRG binding to HER3 may be responsible for its upregulation of HIF1α, whilst the increased activation of Ras/MEK/ERK signalling through HER2 activation may result in a transcriptional response which drives HIF2α gene expression. As the role of PI3K/AKT/mTOR in driving NRG-induced HIF1α upregulation has been published previously [220, 421], we aimed to test whether HIF2α upregulation was driven specifically by the PI3K or the MEK/ERK pathway. This was achieved by inhibiting these pathways using compounds LY294002 and PD98059 in normoxic MCF7-HER2 cells and testing whole cell lysates for levels of HIF2α. LY294002 is a specific inhibitor of PI3K, and as such is a potent inhibitor of PI3K-mediated AKT and mTOR activation. PD98059 is an inhibitor of both MEK1 and MEK2 and so prevents the activation of ERK1/2 by the MAPK signalling cascade.

In order to understand differences in signal activation which may be responsible for HIF2α upregulation in the context of HER2 overexpression, we next decided to assess differences in ERK and AKT activation in MCF7 and MCF7-HER2 cells. To do this, MCF7 and MCF7-HER2 whole cell lysates were collected after 1-6 hr stimulation with 200 ng/ml NRG and assessed for differences in ERK and AKT phosphorylation by western blotting (Figure 5.8a). Whole cell lysates were probed for phospho-ERK1/2 (T202/Y204) and phospho-AKT (S473), these were compared to the levels of total ERK1/2 or total AKT to demonstrate changes in pathway activation and not just protein abundance. All targets showed clear bands at the expected molecular weights, whilst total AKT showed an unexpected doublet this could be due to the pan AKT antibody picking up multiple members of the AKT family or phosphorylated version of the protein (other than S473). Phosphorylation of ERK was shown to be constitutively higher in MCF7-HER2 whilst AKT phosphorylation was comparable between cell lines. The upregulation of phosphorylated forms of both signalling molecules by NRG treatment was equivalent between cell lines. Next MCF7-HER2 cells treated with LY294002 (10 μM) or PD98059 (50 μM) or equivalent concentrations of vehicle control (DMSO) were collected as whole cell lysates and used for western blotting to compare HIF2α expression with these two pathway inhibitors over a 48 hr time course. A representative western blot (Figure 5.8b) and quantitative analysis of densitometry values for HIF2α from n=4 experiments are shown (Figure 5.8c-d). Both compounds were effective in specifically inhibiting downstream phosphorylation; PD98059 showed specific inhibition of ERK phosphorylation whilst LY294002 showed the specific inhibition of AKT phosphorylation. Whilst HIF2α appeared to be inhibited by both compounds at 8 hrs, this inhibition was only stable and reproducible in the context of PI3K inhibition. Combined experiments showed no

significant inhibition of HIF2α after MEK inhibition, whilst PI3K inhibition was shown to produce a significant reduction in HIF2α protein levels. This effect was modest however, reducing protein expression by less than a third of the DMSO control.

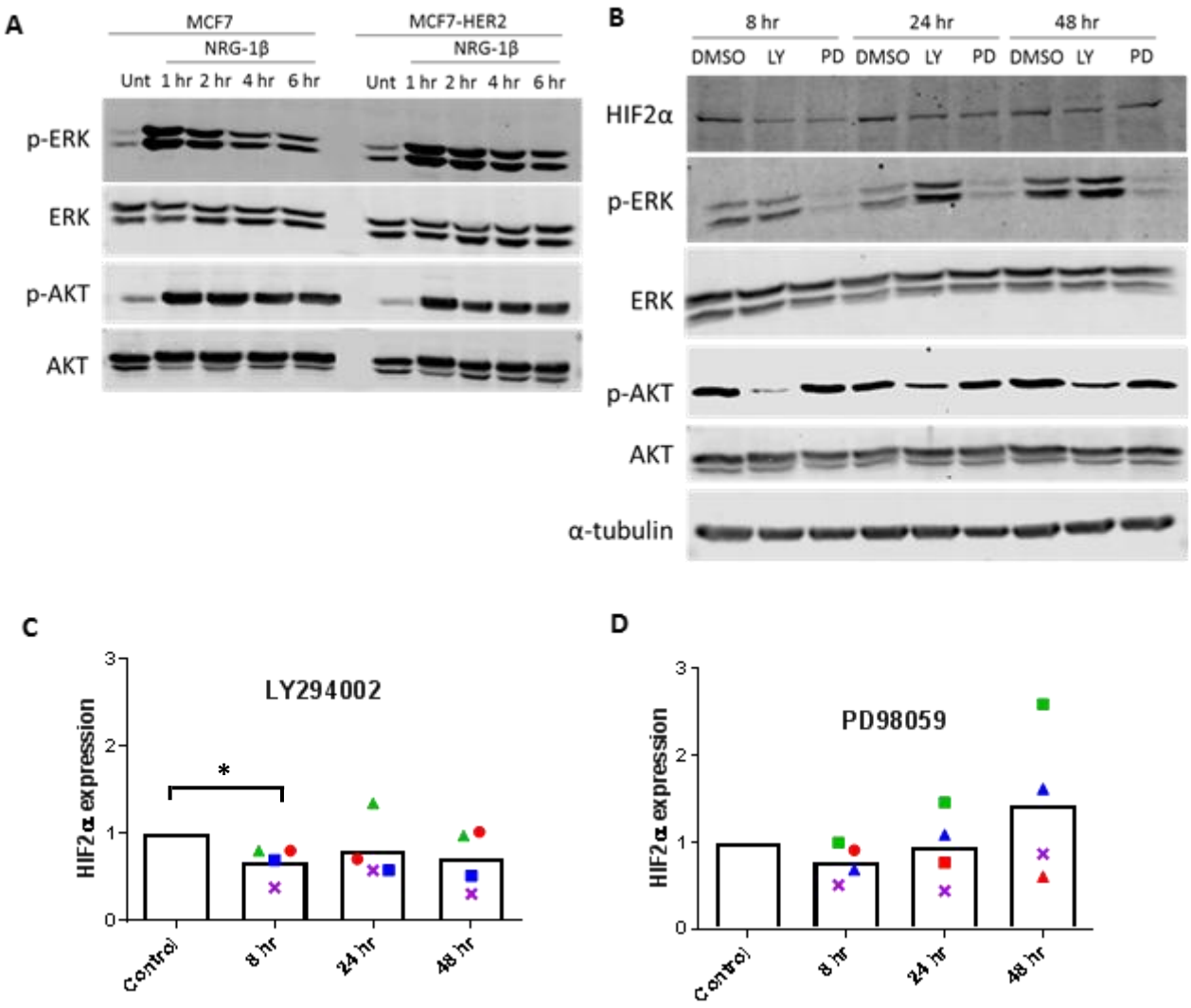

Figure 5.8: Investigating the role of PI3K and ERK downstream signalling on HIF2α expression

A) Western blotting of whole cell lysates from NRG treated MCF7 and MCF7-HER2 cells. Cells were serum starved for 24 hrs (2.5% DCSS, phenol red-free media) prior to treatment with 200 ng/ml NRG for 1-6 hrs. Lysates were probed for ERK1/2, phospho-ERK1/2 (T202/Y204), AKT and phospho-AKT (S473). This is a representative blot of n=4 experimental repeats. B) Western blotting of MCF7-HER2 cells treated with DMSO (<1%), 10 µM PI3K inhibitor LY294002 (LY) or 50 µM MEK inhibitor PD98059. MCF7-HER2 cells were serum starved (2.5% DCSS, phenol red-free media) for 24 hrs before treatment with DMSO, LY294002 or PD98059 for 8, 24 or 48 hrs. Whole cell lysates were collected and probed for HIF2α, ERK1/2, phospho-ERK1/2 (T202/Y204), AKT, phospho-AKT (S473) and α-tubulin. This is a representative western blot from n=4 experimental repeats. Panels C and D show the densitometric quantification of HIF2α protein in these western blots. With individual experimental repeats in each treatment category shown in different colours and mean expression values relative to DMSO controls represented by the bars. Ratio paired t-tests were used to compare the expression of each treatment with DMSO. Here only LY294002 after 8 hrs showed a significant reduction in HIF2α levels (p=0.0445).

5.6 Discussion

In this chapter, I aimed to investigate how HIF1α and HIF2α subunits might be differentially regulated by growth factor signalling in normoxia. Using our isogenic cell line model for HER2 overexpression in MCF7, I was able to demonstrate a HER2-driven upregulation of HIF2α, which differs mechanistically to the ligand-driven HIF1α upregulation previously described [220, 421]. Using western blotting of NRG treated whole cell lysates, I was able to confirm the NRG-driven effects on HIF1α in both our cell lines, whilst demonstrating no equivalent response in HIF2α levels. This is in contrast to the constitutive differences seen in HIFα expression between HER2 overexpressing and wild-type MCF7 cells, where I showed an increased level of HIF2α protein only in the context of highly expressed HER2 receptor. One limitation of this work is it does not address the full complexity of HER signalling, whilst interesting differences between the effects of NRG1β stimulation and HER2 overexpression were seen, the potential for other HER ligands to differentially stimulate HIF1α and HIF2α has not been investigated. Further experiments to assess the possible effects of EGFR signalling, perhaps through stimulation with EGF or other EGFR specific ligands could provide more information on how differences in HIF1α and HIF2α upregulation are governed. Despite this limitation, the differences seen between NRG treatment and HER2 overexpression are of particular interest when considering the HER2-positive subtype of breast cancer. To further understand these differences the mechanisms surrounding constitutive HIF2α expression in MCF7-HER2 were investigated.

The use of small molecular inhibitors which target RTK activity provide a simple means by which specific RTKs can be inhibited to assess downstream functional consequences. Here I used lapatinib, an inhibitor of EGFR/HER2 lapatinib, EGFR-specific inhibitor gefitinib, and HER2 specific inhibitor mubritinib to assess a role for EGFR and HER2 in driving HIF2α in MCF7-HER2. HIF2α was inhibited by lapatinib, gefitinib and mubritinib. Whilst this is not consistent with a specific and independent role for HER2 in this process based on the understood mechanisms of these inhibitors, a strong concordance was seen between HER2 phosphorylation and inhibition of HIF2α in these experiments. Inhibition of EGFR phosphorylation by these molecules was generally weaker but also showed downregulation with lapatinib and gefitinib. Unfortunately, we were unable to provide evidence on whether specific EGFR inhibition would be sufficient to reduce normoxic HIF2α levels, as gefitinib and lapatinib both inhibited HER2 phosphorylation. Nevertheless, the

correlation of HIF2α levels with HER2 phosphorylation, as well as the successful inhibition of HIF2α with the HER2-specific inhibitor mubritinib, provides convincing evidence that HER2 activation is directly responsible for the increases in HIF2α seen in MCF7-HER2 cells. Due to mubritinib's reported specificity for the HER2 receptor, phosphorylation of EGFR was not assessed in experiments using this compound. However, considering the possibility of direct interplay between different members of the HER receptor family, EGFR activation after mubritinib treatment needs to be measured to be sure that a reduction in EGFR signalling is not responsible for reduced HIF2α in these experiments.

Using gene expression data from our microarray experiment (described in Chapter 2) and real-time PCR experiments, I was able to compare the transcriptional regulation of HIF1α and HIF2α in wild-type and HER2 overexpressing MCF7 cells. This provided further evidence that HER2-driven HIF2α upregulation differs from NRG-driven control, which has been shown in the literature to be post-transcriptional [220, 421], relying on a perturbation of protein synthesis and degradation equilibrium to drive the increased protein level. Here we have demonstrated that HIF2α transcript levels are higher in MCF7-HER2, and whilst transcript levels were also significantly increased by hypoxia, this change was small compared to the difference caused by HER2 overexpression. Initially, we had hypothesised that this difference may reflect disparities in downstream pathway activation from NRG stimulation and HER2. However, a comparison of inhibition of the PI3K/AKT and Ras/MEK/ERK pathways suggests that PI3K plays a greater role in HIF2α upregulation, the same pathway demonstrated to drive HIF1α upregulation in response to NRG [220, 421]. Due to the lack of constitutive HIF1α expression in MCF7-HER2 cells and the failure of HIF2α to be stimulated by NRG, it seems unlikely that the same pathway is directly driving expression of these transcription factors. Instead we suggest that the HER2-mediated upregulation of HIF2α is not directly driven by either MEK/ERK or PI3K signalling, and instead may be perturbed as an indirect consequence of PI3K inhibition.

In summary, I have demonstrated a HER2-specific effect on HIF2α levels in normoxia which is likely to contribute to the increased hypoxic response of MCF7-HER2 cells discussed in chapters 3 and 4. The increased transcription of HIF2α drives the higher level of HIF2α protein in normoxia, which in turn provides a larger pool of protein which, when the cells are subjected to hypoxic conditions, allows the normal hypoxic accumulation of protein to be accelerated. This seems a plausible mechanism as parallel differences between HIF1α and

HIF2α are seen in normoxia and hypoxia. HIF1α is similarly expressed in normoxia in both cell lines and similarly upregulated by NRG, as well as showing a similar increase in response to hypoxia. HIF2α however is more highly expressed in the context of HER2 expression and also more vigorously upregulated in hypoxia in this cellular context. The HIF2α specific differences seen when HER2 is overexpressed suggest that alterations in the severity of the hypoxic response (shown in chapters 3 and 4) may be a direct result of HER2-mediated increases in HIF2α transcription.

Chapter 6: Investigating HIF2α as a potential target in breast cancer

6.1 Introduction

As discussed in Chapter 1, research into the role of hypoxia-inducible factors in breast cancer has focussed predominantly on HIF1. The absence of HIF2-focussed research pertaining to breast cancer has extended into investigations of HIF-inhibition as a possible therapeutic strategy for breast cancer. Whilst the apparent benefits of targeting HIFs in breast cancer have resulted in the development of numerous inhibitors which target HIF1 either directly or indirectly [170], the development and investigation of HIF2-specific inhibitors has only progressed due to the recognised role of HIF in other cancer types [510]. In this study, I have demonstrated both the potential for HER2-overexpressing cells to drive HIF2α expression in normoxia (Chapter 5) as well as the increased hypoxic upregulation of a number of pathologically important genes in the context of HER2 overexpression which coincides with HER2-mediated changes to HIF2α but not HIF1α (Chapters 3 and 4). This suggested that HIF2 may be an important driver of breast cancer pathogenesis in the context of HER2 overexpression.

HIF2 inhibitors have been most extensively investigated in ccRCC [511]. Most recent success with HIF2 antagonists has come in the form of small molecule inhibitors designed to inhibit HIF2 dimer formation through binding to the HIF2α PAS domain, which results in the inability of HIF2α to form active dimers with HIFβ subunits [389-391]. These allosteric inhibitors of HIF2 have shown a high level of efficacy in renal cell carcinomas, with PT2399 and its close analogue PT2385 showing great potential in pre-clinical research and phase-1 clinical trials respectively [393, 396, 512]. PT2385 is also currently the subject of a phase II clinical trial for ccRCC [395]. Two such inhibitors were used in this study to investigate their efficacy on breast cancer cell lines, these being the aforementioned PT2385 and HIF2 inhibitory compound 2 [391] (a well-characterised first-generation inhibitor of HIF2 dimerization). In addition to these, compound 76, a specific inhibitor of HIF2α translation [283], was used as an alternative means of HIF2 inhibition. Compound 76 works by promoting the binding of the IRP1 protein to an iron-response element (IRE) in the 5'-UTR of HIF2α

mRNA. Binding of IRP1 to HIF2α mRNA represses basal translation until hypoxic conditions mediate its release through post-translational changes, permitting the translational upregulation of HIF2α in response to hypoxia. Thus compound 76 is a useful tool to assess the effects of HIF2α inhibition in breast cancer through reducing protein levels.

With the potential of HIF2 inhibition in breast cancer being poorly understood, I aimed to assess the efficacy of HIF2-specific inhibition by siRNA and the use of three small molecular inhibitors of HIF2 (PT2385, compound 2 and compound 76) in breast cancer cell lines and investigated whether HER2-positive cell lines showed an increased sensitivity to such treatment.

6.2 Inhibition of HIF2α using siRNA

In initial experiments, I used HIF2α knockdown by siRNA transfection to assess the effects on cell line growth through SRB assays and hypoxic response through western blotting of whole cell lysates. This included some preliminary experiments to establish successful and specific knockdown of HIF2α post-transfection and also to establish an appropriate time frame for HIF2α knockdown.

6.2.1 Preliminary experiments to assess the effectiveness of siRNA transfection in inhibiting HIF2α

As stated above, preliminary experiments were set up to evaluate the specific activity of HIF2α targeting siRNAs. MCF7-HER2 cells were transfected with a panel of siRNA oligonucleotides to assess their ability to knockdown HIF2α. Four unique siRNAs (targeted against HIF2α) at a recommended concentration of 25 μM as well as a SMARTpool siRNA mix (a 1:1:1:1 mix of the four individual siRNAs) at a range of concentrations between 5 and 100 μM were used. To act as controls, additional cells were transfected with either 25 μM non-targeting siRNA (NT), without any siRNA, or left untransfected (unt). Whole cell lysates were collected 96 hrs after transfection and after 24 hrs treatment with 400 μM cobalt chloride. Immunoblotting for HIF1α and HIF2α was performed and is shown in Figure 6.1. This experiment demonstrated that all targeted siRNAs tested were effective at reducing HIF2α levels in this cell line. This effect was weaker at the lowest concentration of SMARTpool siRNA (5 μM), suggesting that this may be a concentration dependent effect. In addition, no

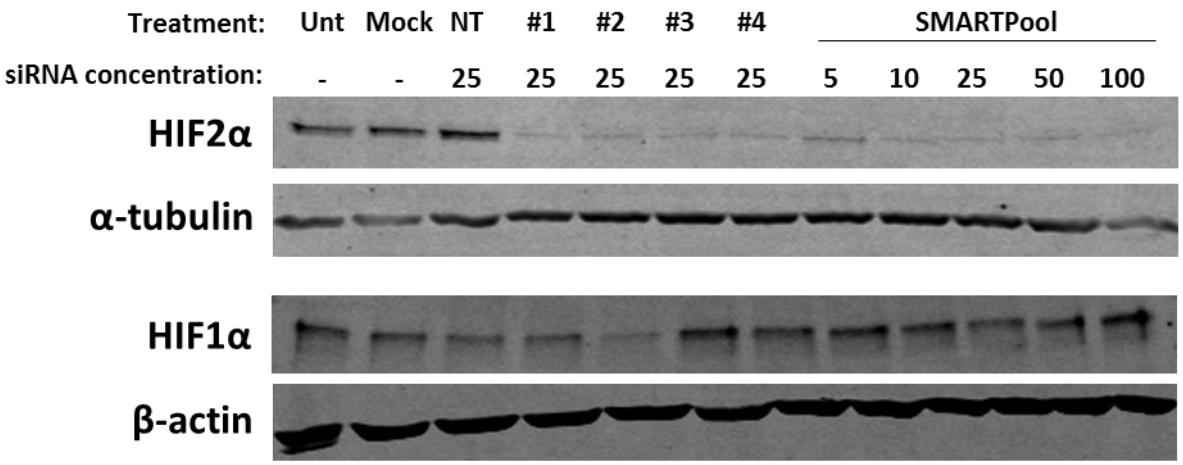

Figure 6.1: Western blotting of a panel of HIF2α siRNAs to determine target specificity

Whole cell lysates were collected after treatment of MCF7-HER2 cells with various HIF2α siRNAs for a total of 96 hrs with 24 hrs cobalt chloride treatment (400 µM) in normoxia. This included 4 siRNAs of various sequences (#1, #2, #3 and #4) all used at a final concentration of 25 µM. As well as SMARTpool siRNA used at concentrations ranging from 5 µM to 100 µM. This was done alongside untransfected cells (Unt), cells transfected with no siRNA (Mock) and cells transfected with a non-targeting siRNA (NT) used at 25 µM. Immunoblotting for HIF2α, HIF1α and loading controls α-tubulin and β-actin (n=1).

reduction in HIF2α levels was seen in mock or NT treatment groups when compared to untransfected cells. In most instances, siRNAs appeared highly specific, as defined by no effect on HIF1α, α-tubulin or β-actin. The main exception to this was siRNA #2 which showed a marked reduction in HIF1α. From this experiment, siRNA #4 and the SMARTpool siRNA used at 10 μM (SP10) were selected for further work, providing two examples of effective yet specific HIF2α knockdown in these cells. SP10 was selected as this was the lowest concentration of SMARTpool siRNA to provide the maximum observed reduction of HIF2α, with the intention of having minimum siRNA induced cellular toxicity.

Having shown that these siRNAs are able to inhibit cobalt chloride stabilised HIF2α in MCF7-HER2 cells, our next experiment aimed to determine whether HIF2α siRNA #4 and SP10 were able to inhibit the hypoxic upregulation of HIF2α. Hypoxic time courses of 0-72 hrs were performed with 96 hrs siRNA treatment to see whether this was sufficient to inhibit the hypoxic upregulation of HIF2α MCF7-HER2. Western blotting of this experiment is shown in Figure 6.2, which demonstrates the expected hypoxic upregulation of HIF2α in untransfected, mock and NT treated samples, but a complete absence of hypoxia upregulated HIF2α after transfection with both #4 and SP10.

Our last preliminary experiment assessed the time frame over which siRNA-mediated inhibition of HIF2α was effective. To do this, MCF7-HER2 cells were treated with #4 or SP10 HIF2a targeting siRNAs alongside mock, NT and untransfected controls. Transfections were performed 24-96 hrs prior to lysate collection and treatment with 400 μM cobalt chloride 24hrs before collection. In this experiment HIF2α levels were particularly low, especially at shorter siRNA time points; despite this HIF2α was reduced at all time points in HIF2α targeting siRNA treated samples, being below the detection limit in these samples (Figure 6.3).

Together these preliminary experiments show that two HIF2α targeting siRNA treatments (#4 and SP10) are effective at reducing HIF2α protein levels with no discernible effects on HIF1α. This knockdown resulted in HIF2α protein levels being reduced by approximately 90% and knockdown was shown to prevent the accumulation of HIF2α protein through cobalt chloride or hypoxia over a 72 hr time course. Knockdown reduced HIF2α levels as early as 24 hrs and up to 96 hrs post-transfections.

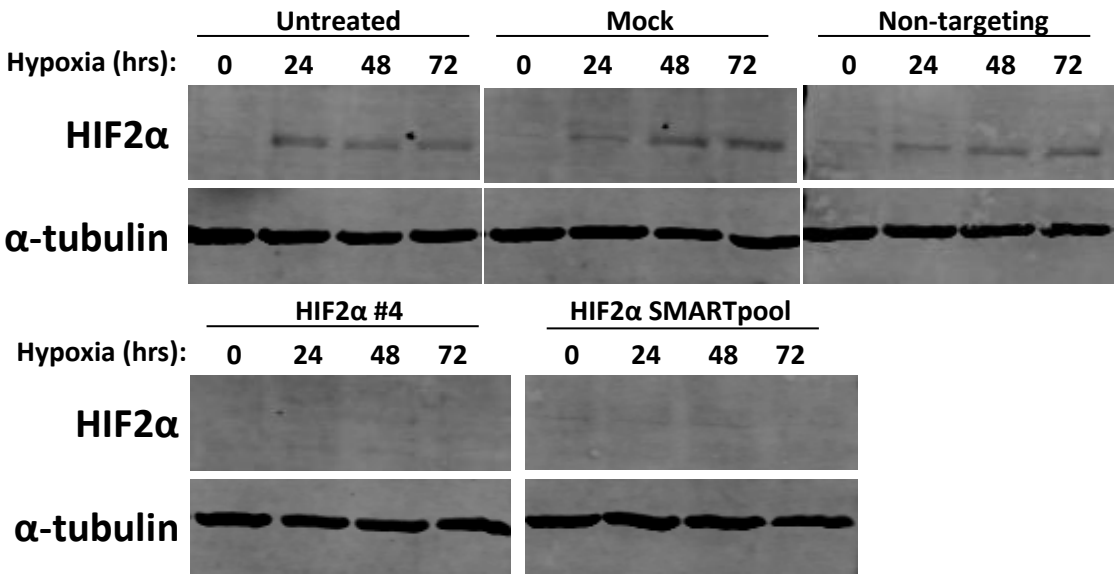

Figure 6.2: Western blotting of siRNA-mediated HIF2α knockdown in MCF7-HER2 in hypoxia

Whole cell lysates were collected after treatment of MCF7-HER2 cells with two HIF2α-specific siRNAs #4 (25 μM) and SMARTpool (10 μM) as well as Untransfected, Mock (no siRNA) and Non-targeting siRNA (25 μM). Cells were treated with siRNAs for a total of 96 hrs, and were either grown in normoxia or in hypoxia for 24, 48 or 72 hrs prior to lysate collection. Immunoblotting for HIF2α or α-tubulin protein (loading control) is shown. Representative repeat of n=2 experiments.

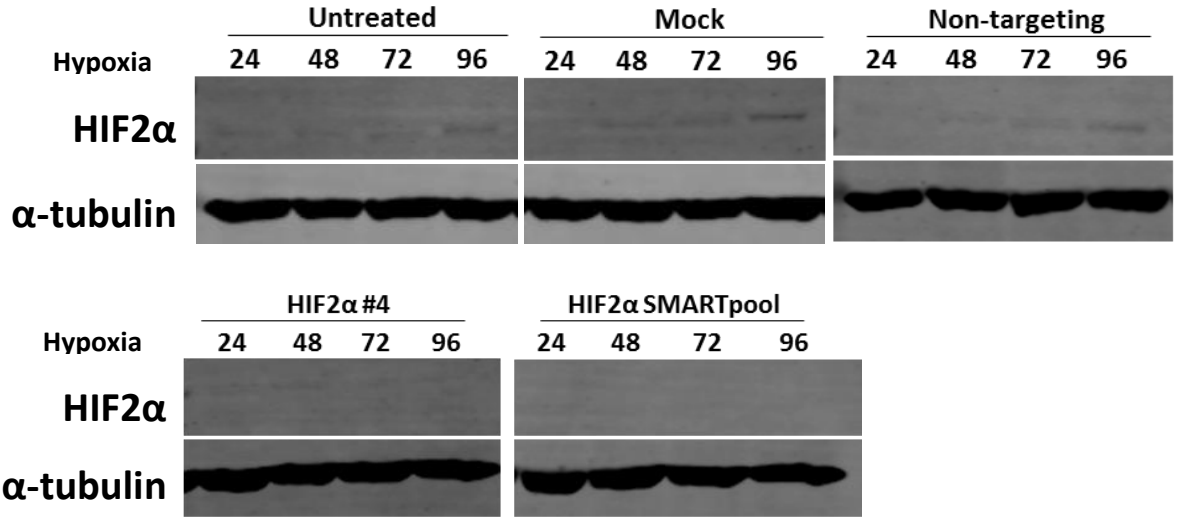

Figure 6.3: Testing the temporal effects of siRNA-mediated HIF2α inhibition

Whole cell lysates were collected from MCF7-HER2 cells untreated or treated with either HIF2α targeting siRNA #4 (25 μM), HIF2α siRNA SMARTpool (10 μM), non-targeting siRNA (25 μM) or transfection reagent without siRNA for 24-96 hrs. All samples were treated with 400 μM cobalt chloride for 24 hrs. Immunoblotting was performed for HIF2α and α-tubulin (loading control) (n=1).

6.2.2 siRNA-mediated HIF2α inhibition reduces cellular growth in normoxia and hypoxia with higher sensitivity in MCF7-HER2 cells

Next, siRNA-mediated knockdown of HIF2α was used to assess the potential for HIF2α inhibition in reducing cellular growth rate as measured by the SRB assay. Relative cell growth was assessed after 5 days treatment with non-targeting, or HIF2α targeting siRNAs #4 and SP10 in normoxia and hypoxia. This was performed with four cell lines, MCF7, MCF7-HER2, MDA-MB-231 and HBL100. HER2 overexpressing and wild-type MCF7 cell lines were used to assess whether HER2 overexpression, which has been associated with increased HIF2α, sensitizes cells to HIF2α inhibition. Triple negative cell lines MDA-MB-231 and HBL100 were used to assess whether cell lines shown to have higher constitutive expression of HIF2α are sensitive to HIF2α inhibition (Figure 3.1). Data from these experiments is shown in Figure 6.4.

A comparison of MCF7 and MCF7-HER2 cells shows that siRNA-mediated HIF2α knockdown had a greater effect on cellular growth in the HER2 overexpressing cell line. In normoxia, MCF7 growth was significantly inhibited by treatment with siRNA #4 ($p<0.0001$) but this was not replicated with the SMARTpool siRNA (SP10). MCF7-HER2 growth was significantly inhibited by both siRNAs ($p<0.0001$) and the level relative growth inhibition was significantly greater in MCF7-HER2 for both siRNAs when compared to wild-type MCF7. Whilst growth was generally inhibited to a lesser extent in hypoxia when compared to normoxia, increased sensitivity of MCF7-HER2 cells when compared to wild-type cells was still observed. No significant inhibition of MCF7 cells was achieved in hypoxia, whilst in MCF7-HER2 both siRNA treatments were once again able to significantly inhibit cellular growth over 5 days ($p<0.0001$ in both cases). Triple-negative cell lines MDA-MB-231 and HBL100 also displayed reduced growth rates with HIF2α siRNA treatment compared to non-targeting controls. In all cases this effect was greater in normoxia. Overall, siRNA #4 was effective at reducing cellular growth in both triple-negative cell lines in normoxia and hypoxia, whilst SP10 transfection was only effective in reducing growth in HBL100 and only in normoxia. Generally, this demonstrates that only MCF7-HER2 cells had a robust sensitivity to HIF2α knockdown. Triple negative cell lines (especially HBL100) did demonstrate higher sensitivity than wild-type MCF7 cells but in these experiments it is unclear whether that is due to being growth factor receptor dependent cell lines or simply due to an increased basal proliferation rate.

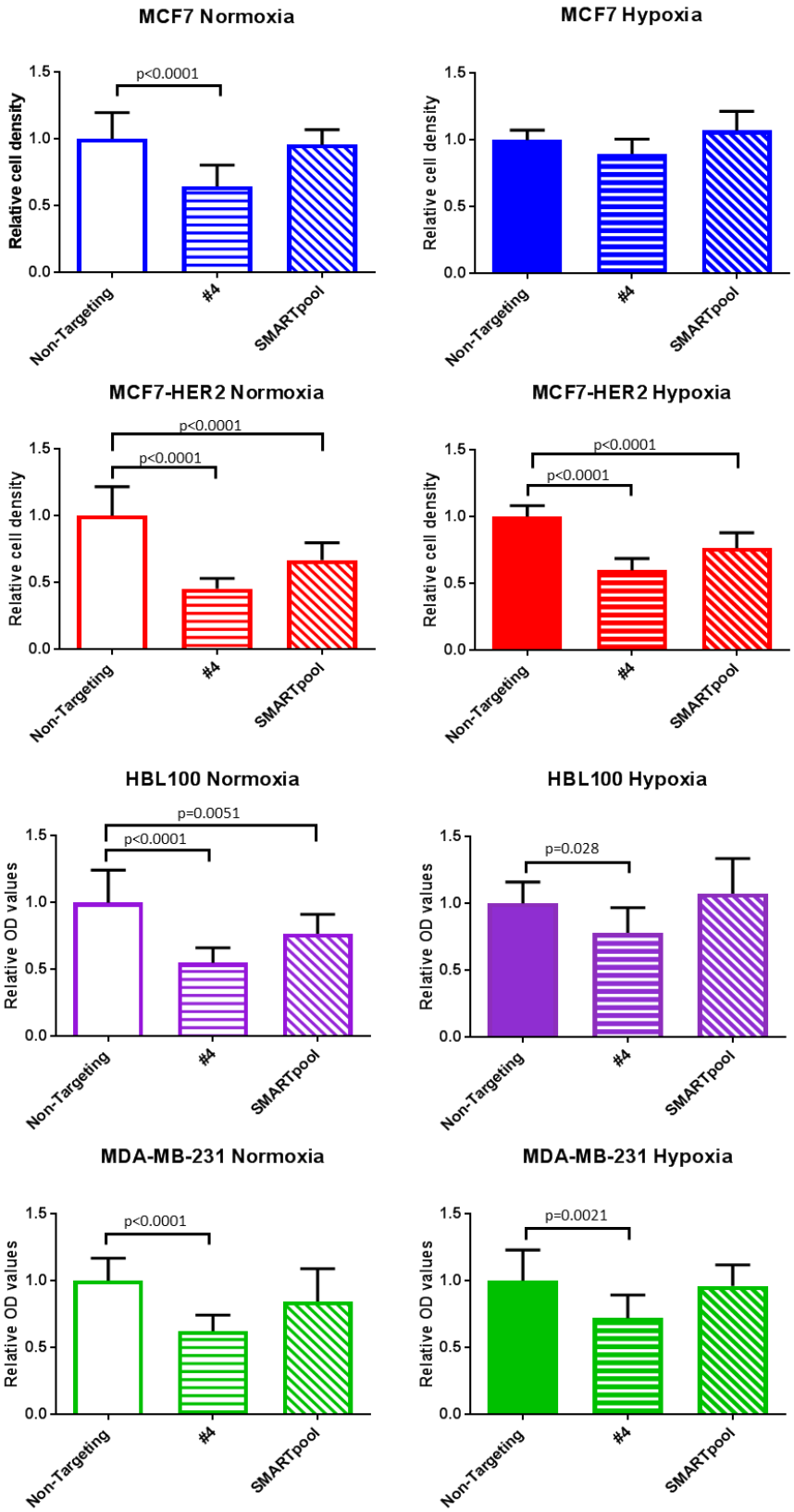

Figure 6.4: The effect of siRNA-mediated HIF2α inhibition on cellular growth

Sulforhodamine B growth assays performed on MCF7 (blue), MCF7-HER2 (red), MDA-MB-231 (green) and HBL100 (purple) cells after 5 days growth in normoxia or hypoxia (0.5% oxygen), following treatment with non-targeting or two HIF2α targeting siRNAs (#4 (25 µM) and SMARTpool (10 µM)). Bars represent mean cell density 5 days after treatment, with standard deviation represented by the error bars (n=12). P-values from all statistically significant results as determined by one-way ANOVA with Dunnett's multiple comparisons are shown.

6.3 Investigating the potential of HIF2 inhibitory compounds in breast cancer cell lines

As discussed in Chapter 1 and the introduction to this chapter, a few HIF2 specific molecular inhibitors have recently become available, and three of these were selected to test whether inhibition of HIF2 through small molecule drugs may be more effective than an siRNA-based strategy at eliciting a cellular response in terms of growth inhibition and inhibition of the upregulation of hypoxic response genes in hypoxia. In the next set of experiments, a HIF2α specific translation inhibitor compound 76 (C76) [283] and two specific inhibitors of HIF2 heterodimer formation, compound 2 (C2) [391] and PT2385 (PT) [393], were used to assess to assess the potential for HIF2 inhibition in breast cancer cell lines. First, these compounds were tested on a range of breast cancer cell lines in SRB growth assays to determine their relative potential for growth inhibition in various subtypes of breast cancer. Compounds were then tested in MCF7-HER2 to assess their potential to inhibit exacerbated hypoxic response in these cells, and finally the potential of these compounds to inhibit cell motility in a selection of cell lines in 2D wound healing assays and 3D collagen invasion assays was examined.

6.3.1 A comparison of cell line sensitivity to HIF2 compounds using SRB growth assays

To assess the effect of these compounds on the growth rate of breast cancer cell lines, two sets of SRB experiments were performed. Firstly, cellular growth over 7 days was assessed using a range of compound concentrations in normoxia and hypoxia in MCF7, MCF7-HER2, MDA-MB-231 and HBL100 cells. Following this, additional experiments were performed on a larger set of cell lines to determine IC_{50} concentrations for each compound in normoxia using cell density measures taken 5 days after treatment.

Figure 6.5 shows SRB growth assay data for MCF7, MCF7-HER2 (6.5a), MDA-MB-231 and HBL100 cells (6.5b) treated with C2, C76 or PT in normoxia or hypoxia over 7 days. A comparison of MCF7 and MCF7-HER2 shows no differences in sensitivity to these compounds

in normoxia or hypoxia. In addition, no clear differences in the effectiveness of compounds were seen between normoxic and hypoxic conditions when compared within cell lines. Treatment with 10 μM C76 did show a stronger relative reduction in growth by 3 days in hypoxia when compared to normoxic equivalents in each cell line, however this was limited to this concentration and results were difficult to interpret due to general reduced proliferation in hypoxia. Whilst no differences between cell lines or oxygen conditions were observed, all three compounds did inhibit cellular growth relative to vehicle (DMSO) controls. With C2 and C76, a clear concentration-dependent effect was seen in both cell lines, with C76 being effective over the range of concentrations tested. PT2385 was generally less effective with a reduction in cellular growth rate only seen at 100 μM (the highest concentration tested). Similar experiments in triple-negative cell lines MDA-MB-231 and HBL100 (Figure 6.5b) suggest that these cell lines may be less amenable to HIF2 inhibition as a strategy for reducing growth rate. Once again, no significant differences were observed between these two cell lines and no differences were observed between normoxia and hypoxia. In contrast to MCF7-derived cell lines however, triple-negative cell lines demonstrated minimal response to C2 and PT treatment. In comparison to DMSO, these cell lines actually showed increased growth rate. However, a dose-dependent reduction in growth rate was still apparent, suggesting that these compounds did not induce cellular growth but rather were less damaging to growth at low concentration than the relatively high concentration of DMSO used as a control in these experiments. This is reflected by the concordance of DMSO controls with 100 μM treatments with both C2 and PT treatment, which represent treatments of the same DMSO concentration. Despite the lack of effects seen using C2 and PT, treatment with the translational inhibitor of HIF2α C76 was still effective at reducing cellular growth in both cell lines in a dose-dependent manner relative to DMSO. This suggests that inhibition of HIF2α protein translation may be a more generally applicable approach than inhibition of HIF2 activity (although non-specific cellular toxicity may reduce its effectiveness as a potential therapeutic).

To further investigate the question of cell line specificity for these compounds, I performed a larger scale experiment in 9 breast cancer cell lines (Figure 6.6). ER-driven cell lines MCF7, T47D and ZR751, HER2-driven cell lines MCF7-HER2, BT474, SKBR3 and MDA.MB.361, and triple-negative cell lines MDA-MB-231 and HBL100 were used. This was done using compound concentrations ranging from 10 nM to 100 μM in normoxia over 5 days, and where possible IC_{50} values were determined for each compound in each cell line

(Figure 6.7 C). In this experiment each compound concentration was compared directly to a DMSO control of equivalent concentration so that compound specific effects could be more easily differentiated from DMSO-mediated toxicity. Graphs for each cell line show the change in cell density over 5 days as a percentage of 5-day growth in the DMSO controls. Across all cell lines C76 had the greatest effect of the three compounds tested. A comparison of C76's effect on each cell line is shown in Figure 6.7 A. This demonstrates that, with the exception of MCF7-HER2, all HER2-overexpressing cell lines (red lines) have increased sensitivity to this compound when compared to ER-positive/HER2-negative (blue) and triple-negative cell lines (green). A comparison of 10 μM C76 treatment after 5 days shows reduced growth in all cell lines tested. However, HER2-overexpressing cell lines BT474, MDA.MB.361 and SKBR3 all showed a significantly greater reduction in growth when compared to ER-driven or triple-negative cell lines ($p<0.0001$ in all cases, one-way ANOVA with Tukey's multiple comparison). The increased sensitivity of these cell lines is also apparent from the reduced IC_{50} values compared to other cell lines (Figure 6.7 C). Compound 2 and PT2385 were both less effective at reducing cellular growth over 5 days and did not show consistently increased activity in HER2-overexpressing cells over the range of concentrations tested (demonstrated by the IC_{50} values shown in Figure 6.7 C). Despite this, C2 did demonstrate significantly greater effects on BT474 ($p<0.0001$), MDA.MB.361 ($p\leq0.0002$) and SKBR3 ($p\leq0.0188$) (one-way ANOVA, Tukey's multiple comparison) compared to HER2-negative cell lines when treated with 50 μM C2.

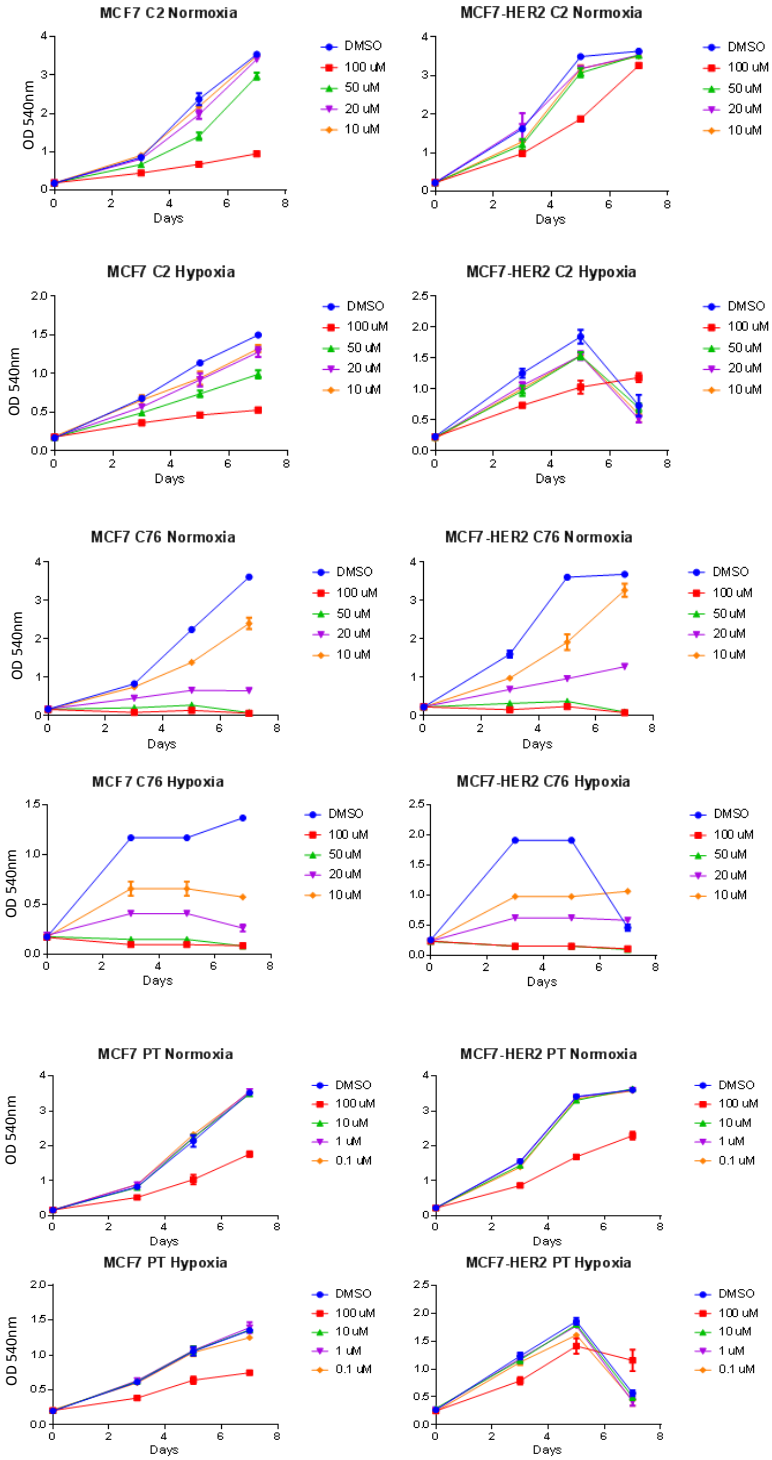

Figure 6.5a: A comparison of cell growth in breast cancer cell lines treated with HIF2 inhibitory compounds

MCF7 and MCF7-HER2 cells were seeded 1000 cells per well in 96-well plates. These were left for 48 hrs before being treated with 0.1-100 µM of compound 2 (C2), compound 76 (C76), PT2385 (PT) or 1% DMSO (vehicle). Cells were grown in normoxia or hypoxia (0.5% oxygen) for 7 days after treatment. Plates were fixed and SRB assays performed to assess cell density at 3, 5 and 7 days post treatment. Graphs showing the absorbance of 540 NM wavelength light as a measure of relative cell density. Error bars show the standard deviations of n=4 repeats.

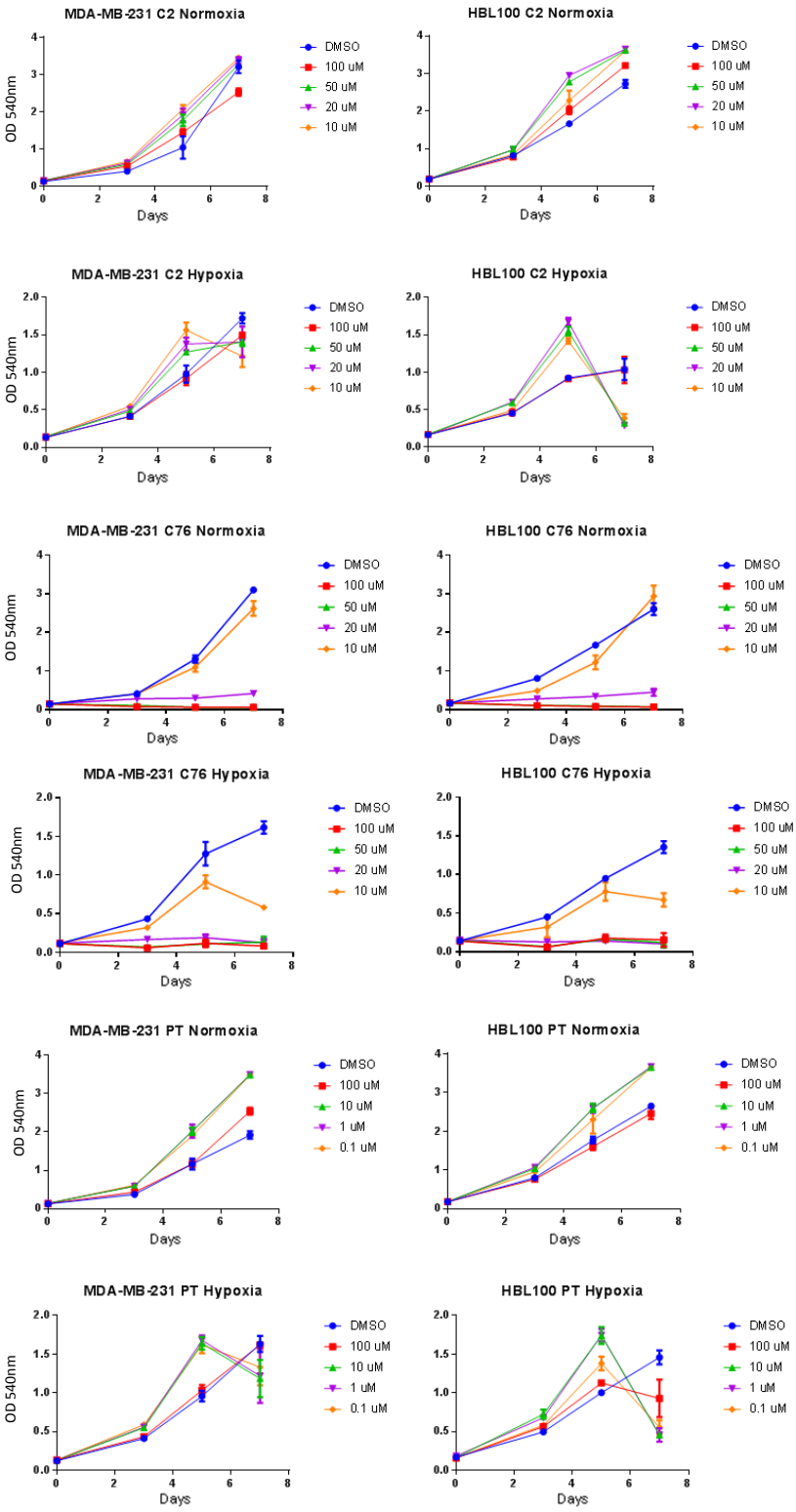

Figure 6.5b: A comparison of cell growth in breast cancer cell lines treated with HIF2 inhibitory compounds

MDA-MB-231 and HBL100 cells were seeded 1000 cells per well in 96-well plates. These were left for 48 hrs before being treated with 0.1-100 µM of compound 2 (C2), compound 76 (C76), PT2385 (PT) or 1% DMSO (vehicle). Cells were grown in normoxia or hypoxia (0.5% oxygen) for 7 days after treatment. Plates were fixed and SRB assays performed to assess cell density at 3, 5 and 7 days post treatment. Graphs showing the absorbance of 540 NM wavelength light as a measure of relative cell density. Error bars show the standard deviations of n=4 repeats.

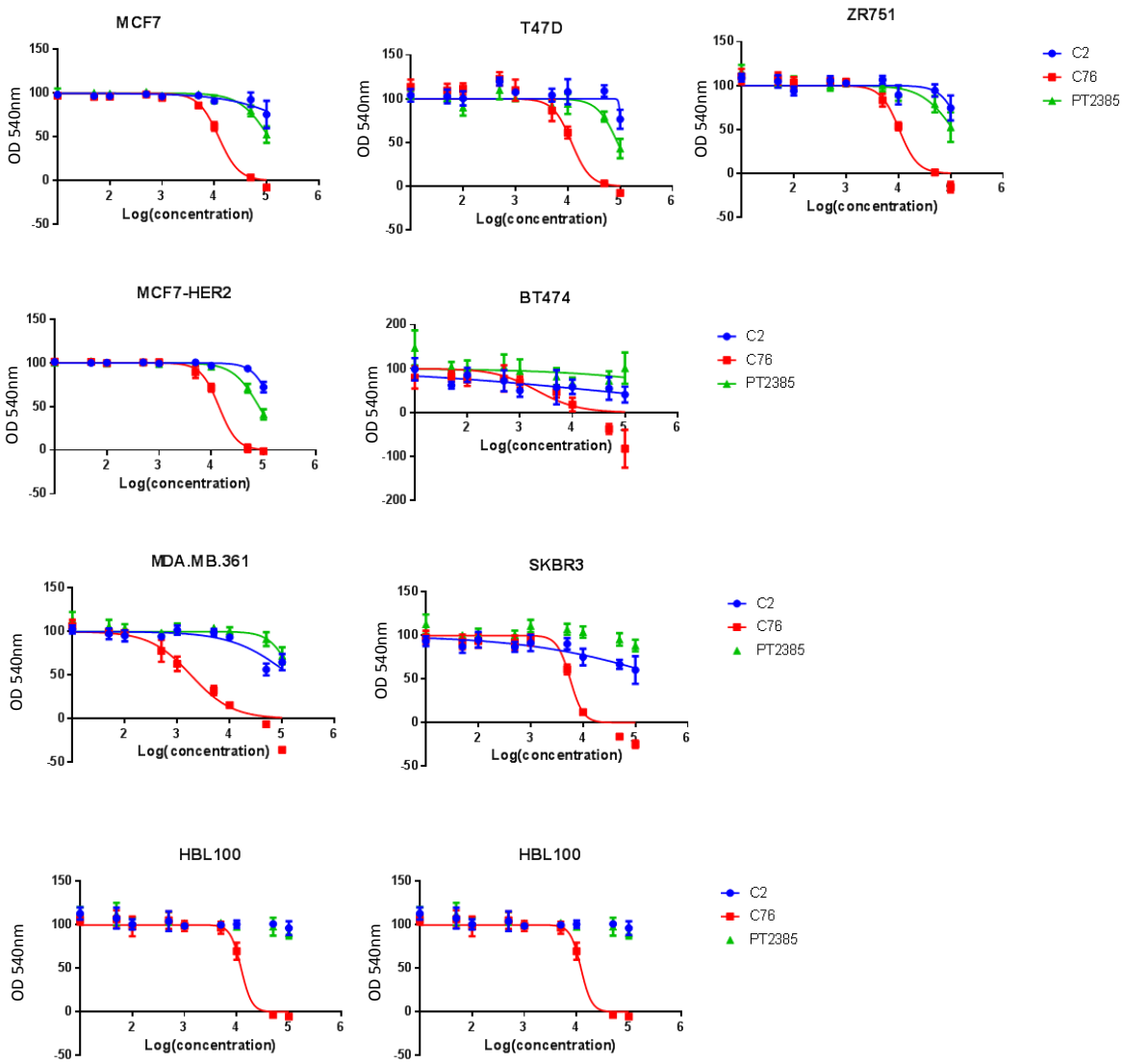

Figure 6.6: Determining IC_{50} values for HIF2 inhibitors in breast cancer cell lines

An expanded panel of breast cancer cell lines was used to determine IC_{50} values for compound 2 (C2), compound 76 (C76) and PT2385 (PT). Cells were seeded into 96 well plates and left for 48 hrs before being treated with 10 nM-100 µM of C2, C76, PT or a range of equivalent concentrations of DMSO (vehicle). Cellular density was assessed after 5 days by SRB assay, and growth curves were normalised to DMSO controls for each cell line. Normalised data was plotted as a percentage of DMSO treated cells. Where possible a non-linear regression model was used to fit curves and determine the value at which cellular growth was reduced by 50%. Error bars represent standard deviation of n=6 repeats.

A

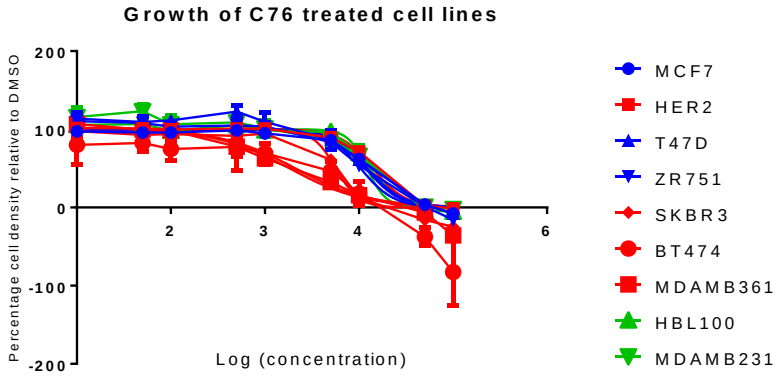

B

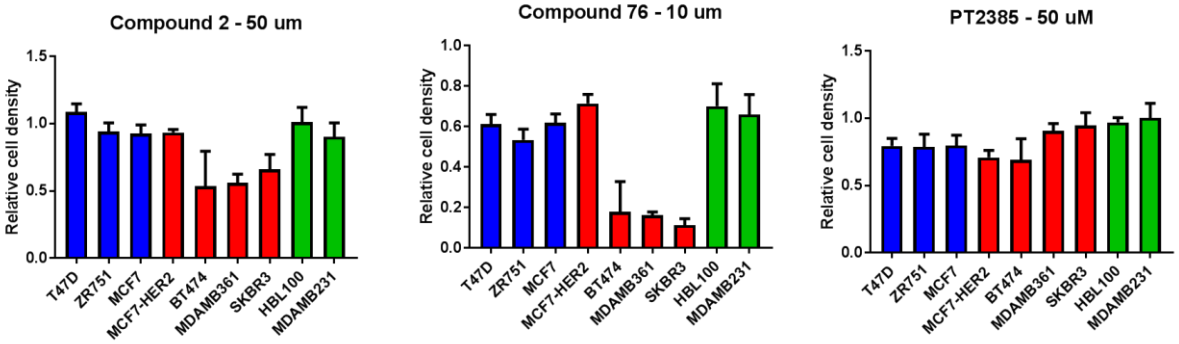

C

Receptor Expression	Cell line	IC_{50} (μM)		
		Compound 2	Compound 76	PT2385
ER-positive/HER2-negative	T47D	104.7	11.9	89.1
	ZR751	158.5	10.4	112.7
	MCF7	798	12.2	120.2
HER2-positive	MCF7-HER2	148.6	14.1	82
	BT474	27.2	2.1	6324.1
	MDA.MB.361	141.9	1.8	158.1
	SKBR3	488.7	5.7	N/A
Triple-negative	HBL100	N/A	12.2	N/A
	MDA.MB.231	93.3	12.8	N/A

Figure 6.7: Summary of IC_{50} growth data for HIF2 inhibitory compounds

A) Five-day cellular growth as a percentage of DMSO control shown for each cell line over a range of concentrations of compound 76 (10 nM-100 μM). All cell lines have been plotted on a single axis for direct comparison. ER-positive/HER2-negative (blue), HER2-positive (red) and triple-negative (green) cell lines are colour coded. Error bars represent the standard deviation of n=6 repeats. B) Bar graphs showing 5-day growth relative to DMSO control for chosen concentrations of each compound, error bars represent the standard deviation from n=6 repeats. C) Table of IC_{50} concentrations of each compound as determined from Figure 6.6.

6.3.2 Inhibition of hypoxic protein upregulation in MCF7-HER2 by HIF2 inhibitory compounds

Western blotting of whole cell lysates was used to assess the effect of HIF2-targeting inhibitors on the hypoxic upregulation of HIF1α, HIF2α, CAIX and LDHA. MCF7-HER2 cells were treated with 50 μM compound 2 (C2), 20 μM compound 76 (C76), 10 μM PT2385 (PT) or vehicle control DMSO (0.5%) for 1 hr before being transferred to and grown in hypoxia for 24, 48 or 72 hrs. The concentrations used were based on previous published research as well as SRB data shown above; both compound 2 [391] and PT2385 [393] have been shown to maximally inhibit HIF2 dimerisation in co-immunoprecipitation experiments in cell line models at concentrations as low as 0.1 and 0.01 μM respectively, with no additional effects seen after 10 μM for compound 2 or 1 μM for PT2385. In addition, PT2385 was shown to reduce the expression of HIF2 target genes in 786-0 cells at concentrations as low as 0.01 μM, with maximal effects seen at 1 μM [393]. The concentration of C76 was chosen as this was the highest concentration which could be used without complete inhibition of cell growth (Figure 6.5a). Western blotting results for this experiment are shown in Figure 6.8. Of the three compounds tested only C76 appeared to have an inhibitory effect on the upregulation of hypoxic response proteins. After treatment with 20 μM C76, the hypoxic upregulation of CAIX was reduced when compared to DMSO control (n=2). This occurred despite no visible reduction in the upregulation of LDHA or HIF2α and an observed increase in the levels of HIF1α in hypoxia when compared to DMSO controls. Treatment with 50 μM C2 had no visible effect on any of the proteins tested, whilst 10 μM PT treatment visibly reduced HIF2α after 72 hrs in hypoxia (n=1) with no concomitant effects on either CAIX or LDHA levels.

A

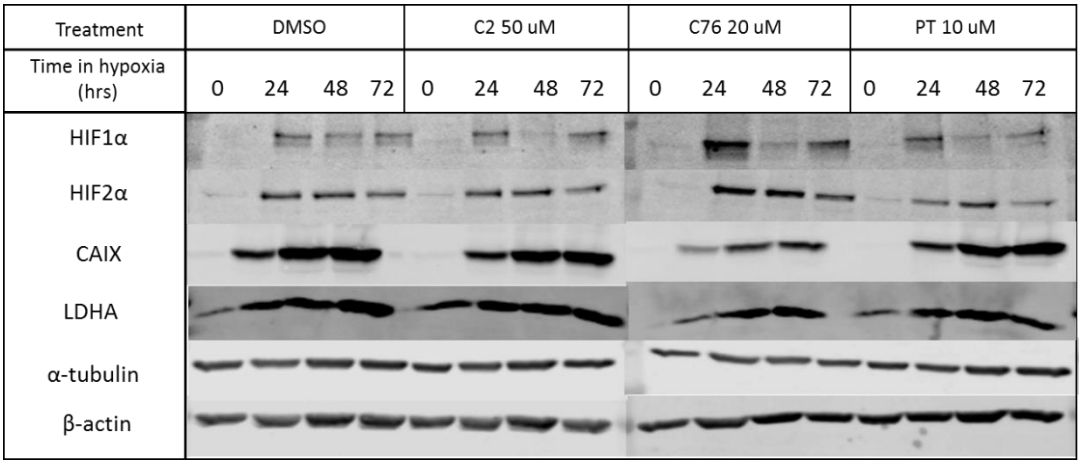

B

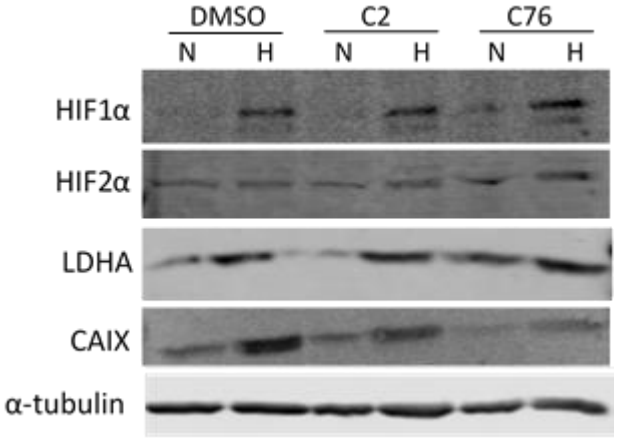

Figure 6.8: Inhibition of hypoxic upregulation with specific inhibitors of HIF2

Immunoblotting of HIF1α, HIF2α, CAIX and LDHA in whole cell lysates of MCF7-HER2 cells treated with HIF2-specific inhibitors (n=2). A) MCF7-HER2 cells were treated with 50 μM compound 2 (C2), 20 μM compound 76 (C76), 10 μM PT2385 (PT) or 0.5% DMSO for 1 hr before being grown in normoxia for 48 hrs or transferred to hypoxia for 24, 48 or 72 hrs before collection. B) Similarly treated MCF7-HER2 cells were grown either in normoxia (N) or hypoxia (H) for 48 hrs (n=2).

6.3.3 Investigating the effect of HIF2 inhibitory compounds on cell motility in 2D and 3D models

Next I wanted to establish whether HIF2α inhibition through treatment with various HIF2 inhibitory compounds could affect the motility of breast cancer cell lines. Initially, cell motility was assessed by 2D wound healing assays in MCF7, MCF7-HER2 as well as in triple-negative cell lines MDA-MB-231 and HBL100, which are both highly motile/invasive cell lines. Cell lines were grown in dishes containing removable inserts. Cells were allowed to reach confluence before inserts were removed and media was changed to low serum media containing either 50 μM C2, 20 μM C76, 10 μM PT or 0.5% DMSO (vehicle control). The removal of the insert produced a uniform 500 μm cell-free gap which closes as cells migrate to occupy the space. By measuring the area of this gap, cell motility was assessed after 24 (MDA-MB-231 and HBL100) or 48 hrs (MCF7 and MCF7-HER2); this was also done with MCF7 and MCF7-HER2 cells cultured in hypoxia for 48 hrs to compare to cell motility in normoxia. Quantitative analysis and representative images from these experiments are shown in figures 6.9 and 6.10.

In normoxia in MCF7 and MCF7-HER2 there was a relatively slow rate of wound closure, whilst no effect was seen in terms of wound closure after C2 or PT (only performed in MCF7-HER2) treatment. However, a significant increase in wound closure rate was seen for both cell lines (MCF7 $p=0.0153$, MCF7-HER2 $p=0.0001$, ANOVA with Dunnett's multiple comparison to DMSO) after treatment with C76. This effect was most pronounced in normoxia, but for MCF7 cells was also noted in hypoxia ($p=0.0002$). In contrast, MDA-MB-231 and HBL100 demonstrated a reduction of wound closure rate when treated with HIF2 inhibitory compounds. MDA-MB-231 wound closure was significantly reduced after treatment with C2 only ($p=0.0033$), whilst HBL100 demonstrated reduced wound closure after treatment with both C76 ($p=0.0037$) and PT ($p=0.0205$), but not C2.

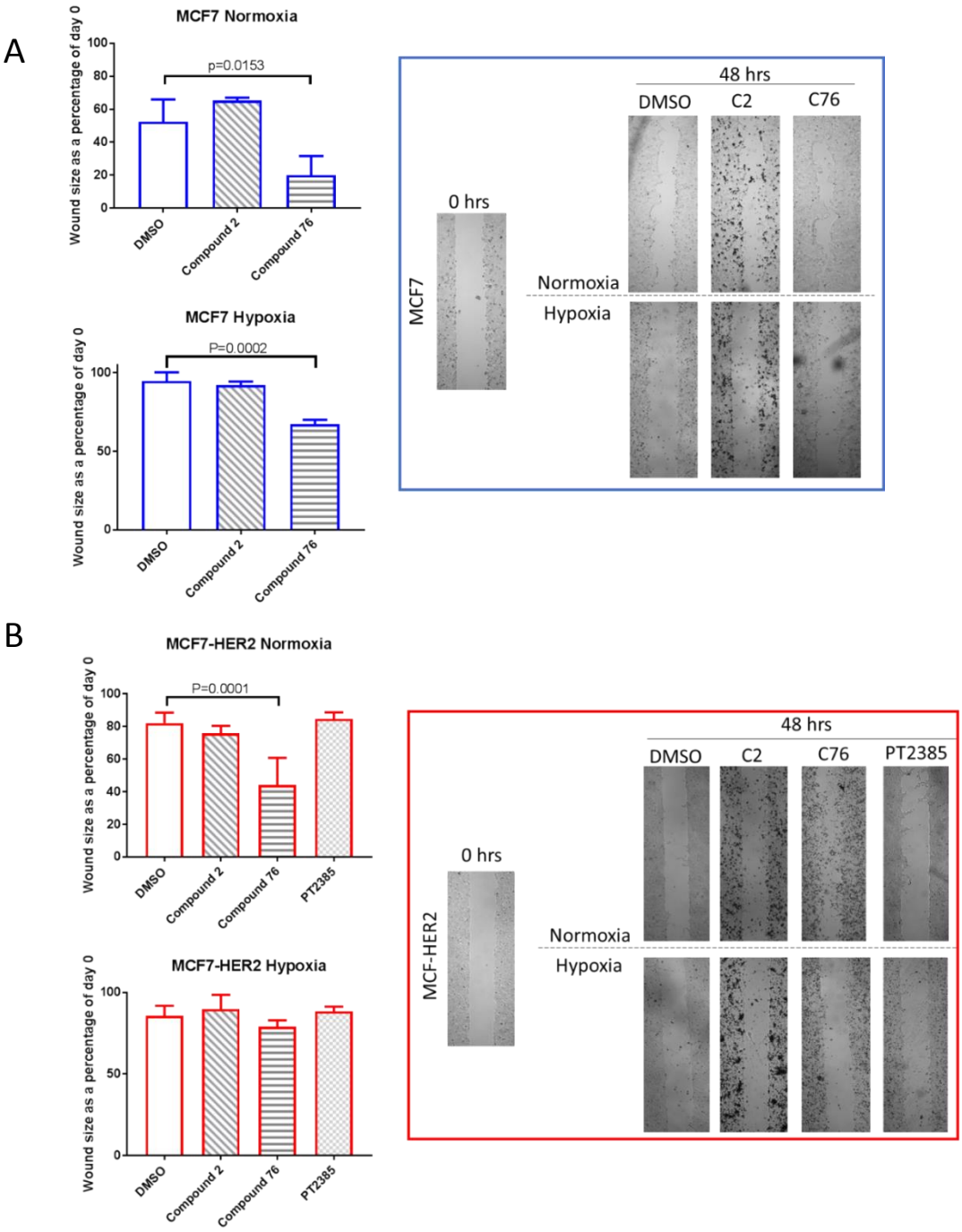

Figure 6.9: 2D wound healing assays for MCF7 and MCF7-HER2 cell lines treated with HIF2 inhibitory compounds

MCF7 (A) and MCF7-HER2 (B) cells were seeded on wound healing plates containing a removable insert. Upon reaching confluence, inserts were removed and media was changed to low serum media containing 0.5% DMSO, 50 µM compound 2 (C2), 20 µM compound 76 (C76) or 10 µM PT2385 (PT) and cultured in normoxia or hypoxia. Plates were imaged and wound area measured at 0 and 48 hrs. (LHS) Quantitative analysis of wound size for each treatment category shown as a percentage of wound size at 0 hrs. Differences were assessed by one-way ANOVA with Dunnett's multiple comparison to the DMSO control (MCF7 n=3, MCF7-HER2 n=6), p-values for significant results are shown (error bars represent the SEM). (RHS) representative images of wound size at 0 hrs and after 48 hrs for each treatment.

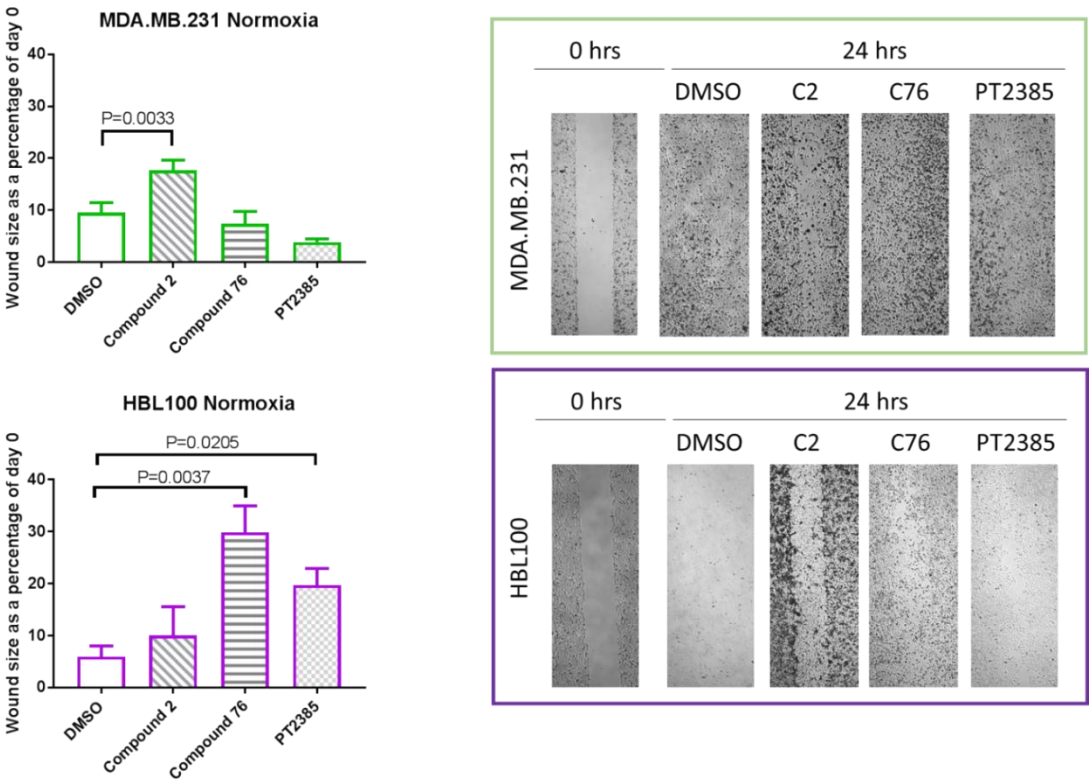

Figure 6.10: 2D wound healing assays for MDA-MB-231 and HBL100 cell lines treated with HIF2 inhibitory compounds

MDA-MB-231 (green) and HBL100 (purple) cells were seeded on wound healing plates containing a removable insert. Upon reaching confluence, inserts were removed and media was changed to low serum media containing 0.5% DMSO, 50 µM compound 2 (C2), 20 µM compound 76 (C76) or 10 µM PT2385 (PT) and cultured in normoxia for 24 hrs. Wound size at 24 hrs was compared to 0 hr wound size for each plate. (LHS) Quantitative analysis of wound size for each treatment category shown as a percentage of wound size at 0 hrs. Differences were assessed by one-way ANOVA with Dunnett's multiple comparison to DMSO control, all significant p-values are shown (error bars represent the SEM) (n=6). (RHS) Representative images of wound size at 0 hrs and 24 hrs for each treatment.

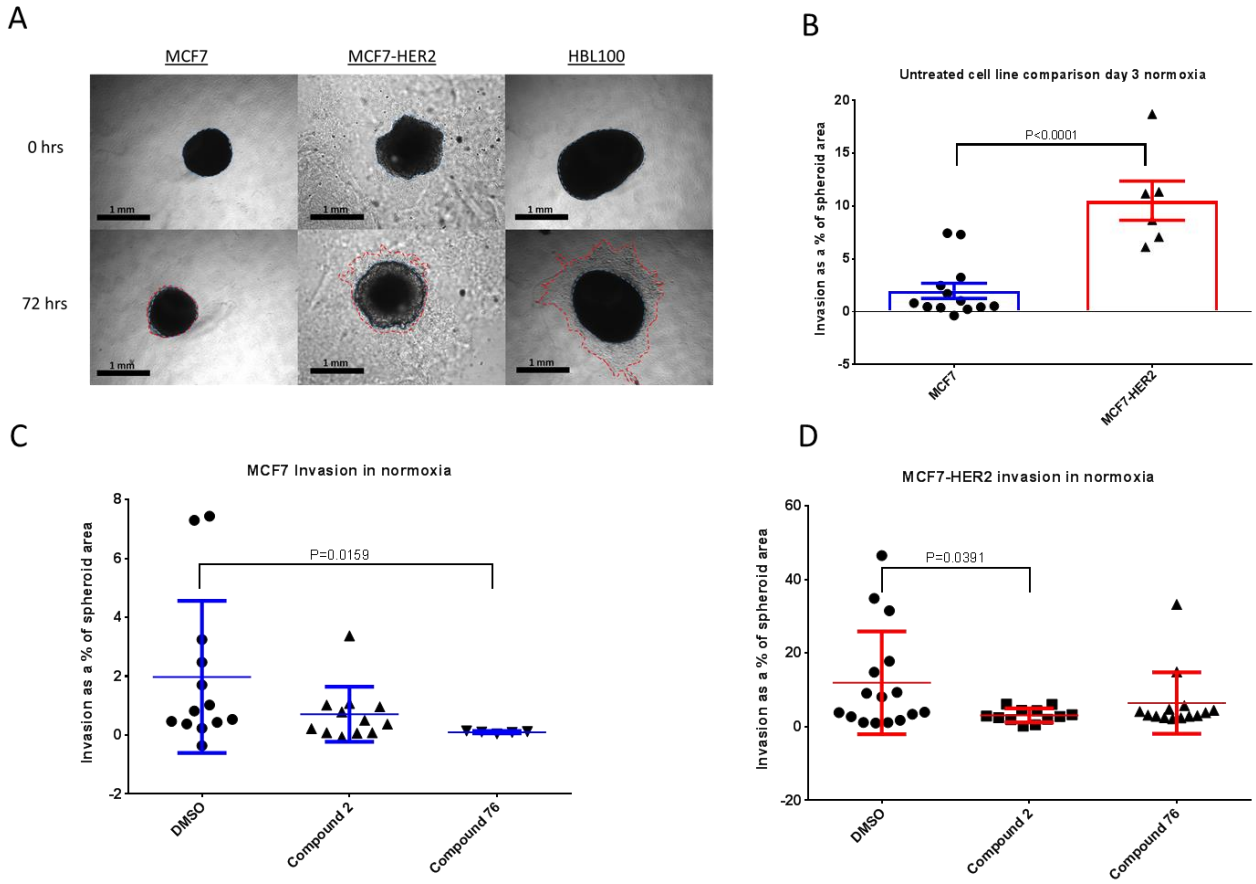

Figure 6.11: Comparison of MCF7 and MCF7-HER2 spheroid invasion with HIF2 inhibitory compounds

A) A representative example of MCF7, MCF7-HER2 and HBL100 spheroids grown for 1 week before being embedded in collagen for 72 hrs. The area of the spheroid (blue lines) and the area covered by invasive cells after 72 hrs (red lines) are shown. B) A comparison of untreated spheroid invasive area relative to spheroid size after 3 days in collagen. MCF7 (blue, n=13), MCF7-HER2 (red, n=6), error bars represent the SEM (p<0.0001, Mann-Whitney unpaired t-test). C & D) Comparison of invasive area from MCF7 (C) or MCF7-HER2 (D) spheroids grown in collagen for 3 days and treated with DMSO (0.5%), HIF2 dimerization inhibitor compound 2 (50 µM) or HIF2α translation inhibitor compound 76 (20 µM). Whisker plots represent mean values with standard deviations. Kruskal-Wallis test with Dunn's multiple comparisons was used to determine significance, p-values for all significant results are shown.

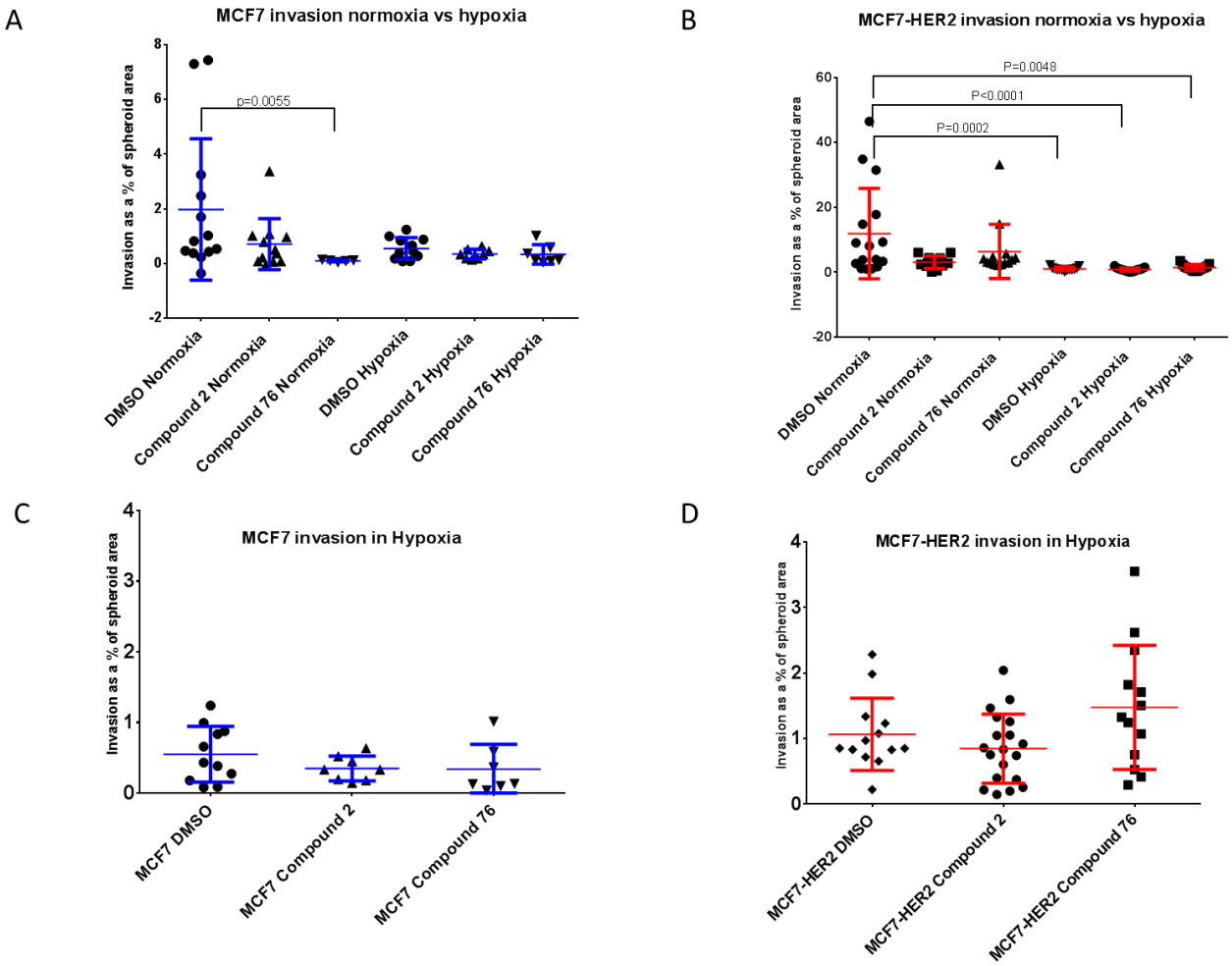

Figure 6.12: Normoxic vs hypoxic invasion in MCF7 and MCF7-HER2 spheroids

MCF7 (blue) and MCF7-HER2 (red) were grown as spheroids for 1 week before being embedded into collagen and left for 3 days in either normoxia (atmospheric oxygen) or hypoxia (0.5% oxygen). Spheroids were treated for the duration with either DMSO (0.5%), HIF2 dimerization inhibitor compound 2 (50 µM) or HIF2α translation inhibitor compound 76 (20 µM). A & B) Comparison of MCF7 (A) or MCF7-HER2 (B) invasion in normoxia and hypoxia. Whisker plots represent mean and standard deviations of multiple spheroid measurements. Kruskal-Wallis non-parametric ANOVA was used to determine significance, the p-values of all significant results are shown. C & D) A comparison of spheroid invasion after 3 days in hypoxia MCF7 (C) and MCF7-HER2 (D) spheroids treated with either DMSO, compound 2 or compound 76. No significant results differences were found using a Kruskal-Wallis non-parametric ANOVA with Dunn's multiple comparisons.

The potential for HIF2 inhibition in reducing cell invasion was assessed using 3D multicellular spheroids for MCF7 and MCF7-HER2 cell lines. Spheroids were grown for one week before being embedded in collagen type-1A. The collagen and surrounding media was treated with 50 μM C2 or 20 μM C76 and spheroids were left for 72 hrs in normoxia or hypoxia. After 72 hrs spheroids were imaged and cellular invasion was assessed by measuring the area covered by cells moving out of the spheroids mass. The invasive area was compared between cell lines and treatment categories to determine the effect of HIF2 inhibition in MCF7 and MCF7-HER2 cells.

MCF7 and MCF7-HER2 spheroids both showed relatively low invasive potential after 72 hrs when compared to HBL100 (used as a positive control for invasion) (Figure 6.11 A). However, MCF7-HER2 did show significantly higher invasion than MCF7 spheroids ($p<0.0001$) (Figure 6.11 B). Despite low invasion, a significant reduction in invasion was seen in MCF7 cells when treated with C76 ($p=0.0159$) when compared to the DMSO control; no effect was seen after C2 treatment (Figure 6.12 C). In MCF7-HER2 a significant reduction in invasion was seen in C2 treated spheroids ($p=0.0391$), but no significant effect was seen after C76 treatment (Figure 6.11 D). Hypoxic experiments demonstrated that spheroid invasion was reduced by growth in hypoxia (Figure 6.12 A and B). In MCF7-HER2, invasion in hypoxic spheroids treated with DMSO ($p=0.0002$), C2 ($p<0.0001$) or C76 ($p=0.0048$) was significantly lower than in normoxic spheroids treated with DMSO. Under hypoxic conditions compound treatment with C2 or C76 was unable to further reduce the invasive potential of either MCF7 or MCF7-HER2 spheroids (Figure 6.12 C and D).

6.4 Discussion

In this chapter, I assessed the potential for HIF2 as a therapeutic target in breast cancer by investigating the effects of HIF2 inhibition through siRNA or treatment with HIF2-specific inhibitory compounds on cellular growth and motility in a panel of breast cancer cell lines.

Using two different siRNAs which were able to specifically reduce HIF2α protein levels in normoxia and hypoxia, I was able to demonstrate an increased sensitivity of HER2-overexpressing cells when compared to their wild-type counterparts. Similar growth assays were able to demonstrate an increased sensitivity of 3 HER2-positive cell lines (SKBR3, BT474

and MDA.MB.361) to C76 and (at 50 μM concentrations only) C2 treatment in normoxia. Together this provides compelling evidence that these cell lines are more sensitive to HIF2-specific inhibition. This would be consistent with the increased sensitivity of HER2-overexpressing cell lines to HIF inhibition being causally linked to the HER2-mediated upregulation of HIF2α demonstrated in Chapter 5. Interestingly, the sensitivity of these cells to both siRNA and small compound-mediated HIF2 inhibition was higher in normoxia than hypoxia. This suggests that the sensitivity to HIF2 inhibition is not due to an inability to respond to hypoxic stress, but instead represents an important non-canonical role for normoxic HIF2α in these cells. Whilst SRB assays were in this way able to demonstrate important differences in cell line growth after HIF2α inhibition, it is important to note that the measurement of total cellular protein by SRB binding does not directly provide information on whether these effects are due to a reduction in proliferation or an increase in cell death. Further work including the use of BrdU incorporation as a measure of DNA synthesis or apoptosis assays (such as the TUNEL assay) would offer more insight into how HIF2α inhibition perturbs cell line growth *in vitro*.

In western blotting experiments treatment with HIF2α-specific translation inhibitor C76 was able to reduce the hypoxic upregulation of CAIX in MCF7-HER2 cells. This was despite an increase in the levels of HIF1α. This effect was limited to 24 hrs, the earliest time point tested, which is likely a result of HIF2α build up in hypoxia. Whilst C76 inhibits translation of HIF2α by promoting binding of IRP1 to the iron response element in the HIF2α 5' UTR, this effect is reduced in hypoxia where binding of IRP is inhibited [283]. This means that C76 was able to reduce normoxic levels of HIF2α, but under hypoxia the re-enabling of HIF2α translation allowed levels to quickly reach those seen in untreated cells. The effect of C76 on CAIX after 24 hrs in hypoxia may be due to a reduced pool of HIF2α at the initiation of hypoxia and a delayed response in terms of CAIX transcription and translation. The inhibition of CAIX upregulation was only seen with C76 and not with either C2 or PT (which are both inhibitors of HIF2 dimerisation with HIFβ). This suggests that canonical HIF2 transcription with HIFβ may not be responsible for CAIX transcription in hypoxia. With this in mind it is likely that HIF2α-mediated upregulation of CAIX in hypoxia occurs through transcriptional actions of HIF2α with other co-factors, or through events which are not reliant on the direct transcriptional activity of HIF2. However, this is only preliminary data as these experiments were only repeated twice, therefore no statistical analysis was possible and more experimental repeats are required to verify these findings.

We also investigated the role of HIF2 inhibitory compounds on cell motility in 2D and cell invasion in 3D spheroids of breast cancer cell lines. In 2D wound healing experiments I was able to demonstrate the inhibition of cell motility by C2 (MDA-MB-231) and both C76 and PT (HBL100) in normoxia, broadly demonstrating the ability of HIF2 inhibition to inhibit motility in highly invasive triple-negative cell lines. Equivalent experiments in MCF7 and MCF7-HER2 were unable to demonstrate a positive effect (presumably due to the low basal level of motility in these cell lines), and contradictory to findings in triple-negative cell lines, motility was increased in both MCF7 and MCF7-HER2 after treatment with C76. This may be due to the effect of C76 on HIF1α, which was shown to be increased even in normoxia by treatment with C76 (Figure 6.9). Despite these findings in 2D, collagen invasion assays using 3D spheroids were able to demonstrate a small inhibition of invasion by HIF2 inhibitory compounds in these cell lines. In MCF7 spheroids, C76 treatment reduced the invasive area after 3 days, however due to the low basal invasiveness of MCF7 spheroids in collagen and the demonstrated cytotoxic effects of C76 in this chapter, it is not currently clear whether this effect is a result of specific inhibition of cell invasion or due to a broader detrimental effect on these cells. In MCF7-HER2 the significant reduction of invasion was seen only after treatment with compound 2. Due to the higher invasive potential of this cell line and the less cytotoxic effect of C2 treatment on these cells, this result provides more convincing evidence that HIF2 inhibition is able to reduce cellular invasion in breast cancer cell lines. 3D spheroids grown in hypoxia showed reduced invasive potential, especially in the case of MCF7-HER2 where normoxic invasive potential was higher. No inhibition of 3D spheroid invasion in hypoxia was seen after treatment with HIF2 inhibitory compounds, but this is probably attributable to the minimal invasive potential seen under these growth conditions.

This investigation of HIF2 inhibition in breast cancer cell lines has demonstrated the possibility that targeting HIF2 may be a therapeutic approach in a subset of breast cancers. SiRNA and compound work demonstrates an increased sensitivity of HER2-overexpressing cells to perturbation of HIF2α, which in concordance with results from chapters 3-5 suggest that the HER2-HIF2 axis may be an important driver of breast cancer pathogenesis and a targetable pathway. That these effects were limited to HER2-overexpressing cells highlights the importance of considering the molecular subtype when investigating potential therapeutic targets in breast cancer. As well as cellular growth, HIF2 inhibition was shown to perturb cell motility and invasion in breast cancer, suggesting that HIF2 contributes to these characteristics in breast cancer. Effects on cell motility in triple-negative cell lines raises the

question of whether HIF2 inhibition would also be an effective strategy in this particularly aggressive subtype of breast cancer, which currently has limited treatment options. Whilst HER2 expression is definitively low in these cell lines, their frequent reliance on EGFR (HER1) driven growth also begs the question of whether EGFR may also result in HIF2α-dependent pathology under certain conditions. Finally, whilst this chapter has provided evidence for HIF2α as an effective means of inhibiting breast cancer cell growth and motility, the fact that C76 can increase cellular motility in MCF7 and MCF7-HER2 cell lines, possibly through the increased levels of HIF1α, demonstrates the importance of considering the role and effect of both HIFα proteins when considering HIF-based therapeutic strategies.

.

Chapter 7: Investigating the role of HIF2α expression in breast cancer survival

7.1 Introduction

The association of HIF1α expression with poor outcome in breast cancer has been demonstrated in a number of studies [284-293, 513, 514]. Despite this the impact of HIF2α in breast cancer is still poorly understood. Whilst a correlation between HIF2α expression and poor prognosis has been shown in various cancer types, including head & neck [515, 516], lung [517], colorectal [518] and bladder [519] cancers, few studies have been conducted in breast cancer and these appear to have conflicting results, with HIF2α expression being associated with both a better [427] and worse [261] prognosis. Having shown that HIF2α is associated with HER2 expression in breast cancer cell lines (chapters 3 and 5), and that HER2 overexpressing cell lines may have increased sensitivity to HIF2α inhibition (chapter 6), we next wanted to ask whether stratifying patients based on HER2 expression may help define the role for HIF2α in breast cancer prognosis.

In this chapter I assessed the relationship between HIF2α expression and patient survival using two publically available datasets; the online tool and associated dataset Kmplot [438] and the METABRIC [437] gene expression dataset, each containing matched clinical and gene expression data. This approach has allowed the role of HIF1α and HIF2α expression in breast cancer survival to be assessed both on complete cohorts and on patients identified as either HER2-positive or HER2-negative in two independent datasets.

7.2 A comparison of HIF1α and HIF2α expression and patient survival using Kmplot

Initially survival analysis for HIF1α and HIF2α was performed using Kmplot [438]. The impact of gene expression on overall survival, recurrence-free survival and distant metastasis-free survival was assessed for both HIF1α and HIF2α. Kaplan-Meier curves were produced to compare survival between patients stratified as having cancers with either high or low expression based on the optimum cut-point, with p-values and hazard ratios for each

analysis provided (Figure 7.1). A comparison of HIF1α and HIF2α shows a clear difference between the two genes; as expected based on previously published research high HIF1α expression was broadly associated with poor survival. Overall ($p<0.0001$), recurrence-free ($p<0.0001$) and distant metastasis-free ($p=0.00012$) survival were all significantly worse in high HIF1α expressing breast cancers. In contrast, high expression of HIF2α had either no significant association with survival (overall and distant metastasis-free survival $p>0.1$) or was weakly associated with an improvement in survival (recurrence-free survival $p<0.05$), showing a clearly differential role for these two factors in breast cancer survival.

The relationship between recurrence-free survival and HIF2α expression in breast cancer patients was shown to vary between high and low grade tumours (Figure 7.2). Survival analysis using Kmplot was performed on patients stratified based on tumour grade; this was only performed for recurrence-free survival as the availability of clinical data precluded a worthwhile analysis in alternative measures of disease progression. This demonstrated a clear difference in the role of HIF2α between low grade and high grade tumours. In grade 1 tumours, high HIF2α expression was associated with an improvement in recurrence-free survival ($p=0.011$), whilst in grade 3 tumours an association with worse recurrence-free survival was seen ($p= 0.0065$). No significant association was seen in grade 2 tumours.

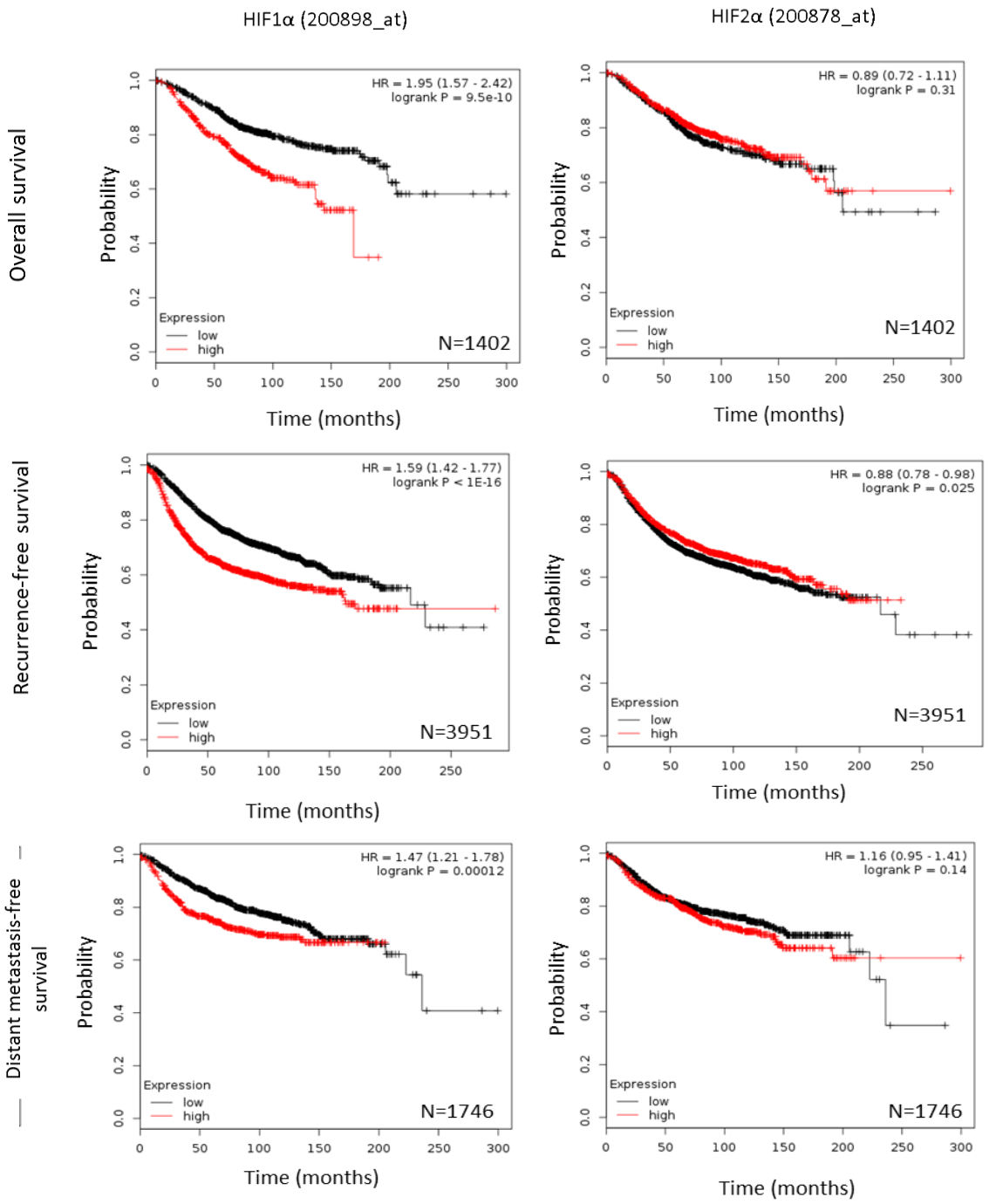

Figure 7.1: HIF1α expression, but not HIF2α, is associated with worse prognosis in a large breast cancer dataset

The online resource Kmplot was used to perform survival analysis for HIF1α and HIF2α expression in a large cohort of breast cancer samples. Kaplan-Meier plots for overall survival, recurrence-free survival and distant metastasis-free survival are shown for each gene. Samples were placed into high and low expression groups based on the optimum cut-point in each individual analysis. Each plot also shows its associated p-value, hazard ratio and the number of patients in the analysis.

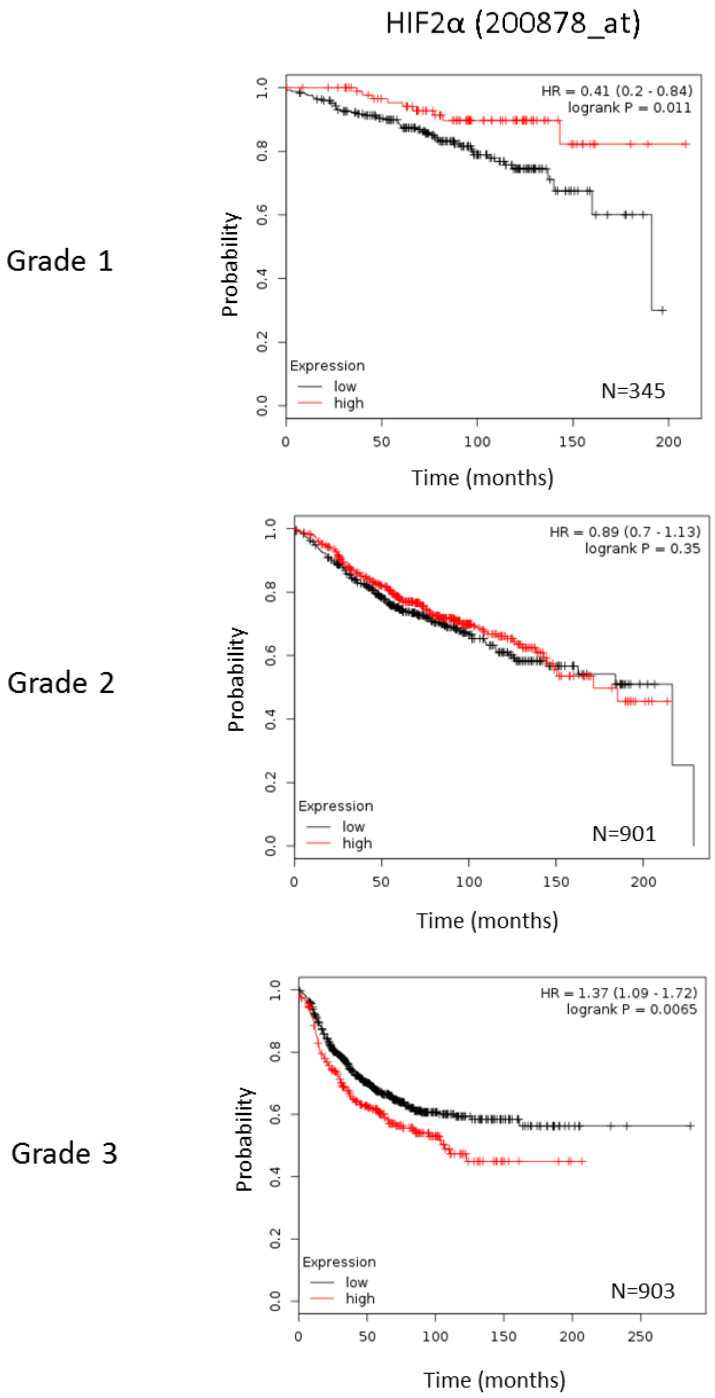

Figure 7.2: HIF2α is associated with worse recurrence-free survival in higher grade tumours

The online resource Kmplot was used to perform survival analysis based on HIF2α expression in a large cohort of breast cancer samples. Kaplan-Meier plots for recurrence-free survival in grade 1, grade 2 or grade 3 tumours. High and low gene expression groups were determined by the optimum cut-point point. Each plot shows its associated p-value, hazard ratio and the number of patients in the analysis.

7.3 HIF2α expression is associated with worse prognosis in HER2–positive breast cancer

Having demonstrated using Kmplot that HIF2α expression has no significant prognostic impact in the full cohort of breast cancer patients, we next stratified this dataset based on HER2 status determined by IHC or FISH, to investigate whether HIF2α was associated with worse survival in HER2-positive patients. A comparison of recurrence-free survival based on HIF1α and HIF2α expression was performed using HER2-positive (n=252) and HER2-negative (n=800) patients (Figure 7.3). Whilst HIF1α demonstrated an association with worse recurrence-free survival in both HER2-positive (HR=1.75, p= 0.011) and HER2-negative samples (HR=1.74, p=<0.0001), HIF2α was only associated with worse survival in HER2-positive samples (HR=1.95, p=0.0023), with no significant association seen in HER2-negative cases (HR=0.83, p=0.16).

To validate the association of HIF2α with poor prognosis in HER2-positive samples, survival analysis was performed using the METABRIC dataset. Patients in this dataset were once again stratified based on clinical HER2 status as determined by IHC and/or FISH analysis. A comparison of disease-specific survival was performed using optimum cut-point values for HIF2α expression in HER2-positive or HER2-negative cohorts (Figure 7.4). This analysis demonstrated, once again, a specific association of HIF2α expression with worse prognosis in HER2-positive patients (HR=6.81, p=0.0197), whilst no significant association was seen in HER2-negative samples (HR=0.46, p=0.0819). The optimum cut-points were determined using the SurvivALL package in R. SurvivALL is an analysis package developed by a collaborative laboratory (Andy Sims/Dominic Pierce) which performs survival analysis based on multiple cut-points to identify all which are significant for a gene of interest. This has allowed us not only to determine the optimum cut-point, but to show a robustness of this effect by demonstrating a range of significant cut-points which all show HIF2α to be associated with worse disease-specific survival in the HER2-positive samples in this dataset. Cut-points with p-values of less than 0.05 are shown by coloured points in SurvivALL graphs (Figure 7.4 A-C) and by grey bars in Kaplan-Meier plots (Figure 7.4 D-E).

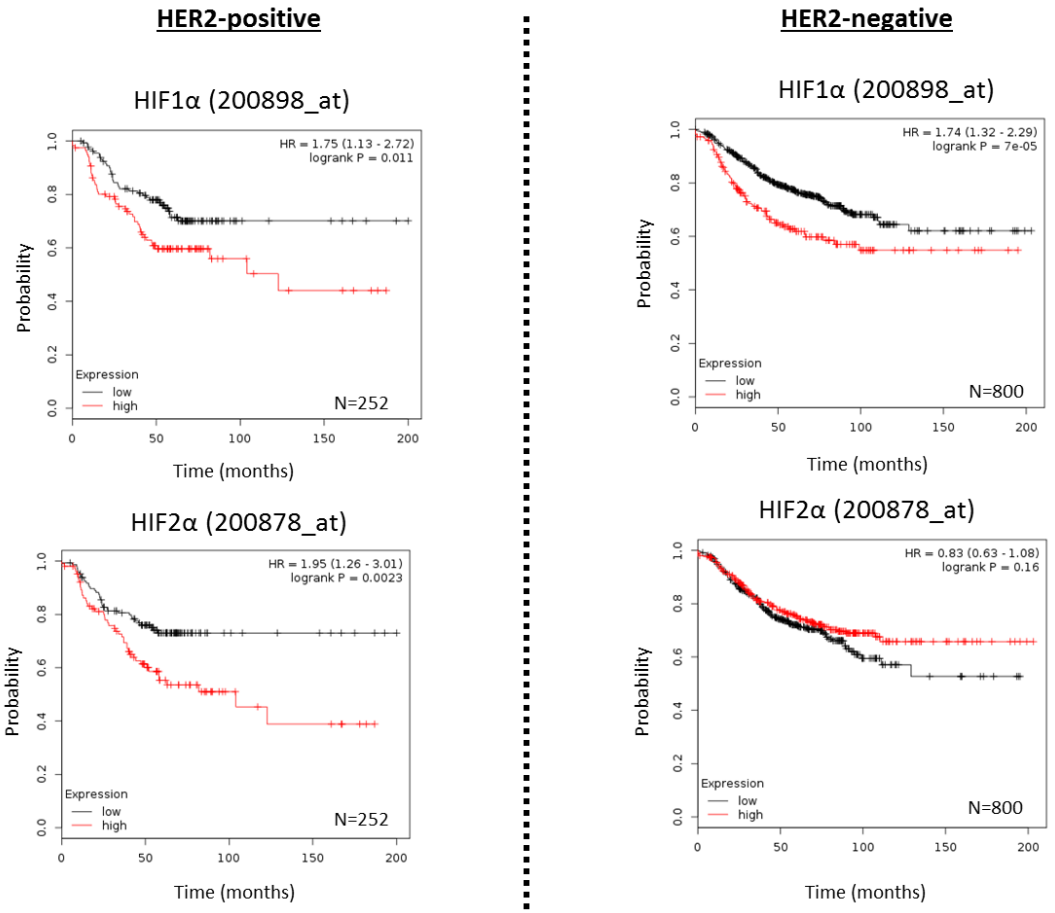

Figure 7.3: HIF2α expression is associated with worse survival specifically in HER2-positive breast cancers

The online resource Kmplot was used to perform survival analysis in breast cancer cohorts divided into HER2-negative and HER2-positive (based on IHC scoring). Recurrence-free survival is shown for HIF1α and HIF2α, with cohorts divided into low and high expression groups by the optimum cut-point. Each plot has its associated p-value, hazard ratio and n number shown.

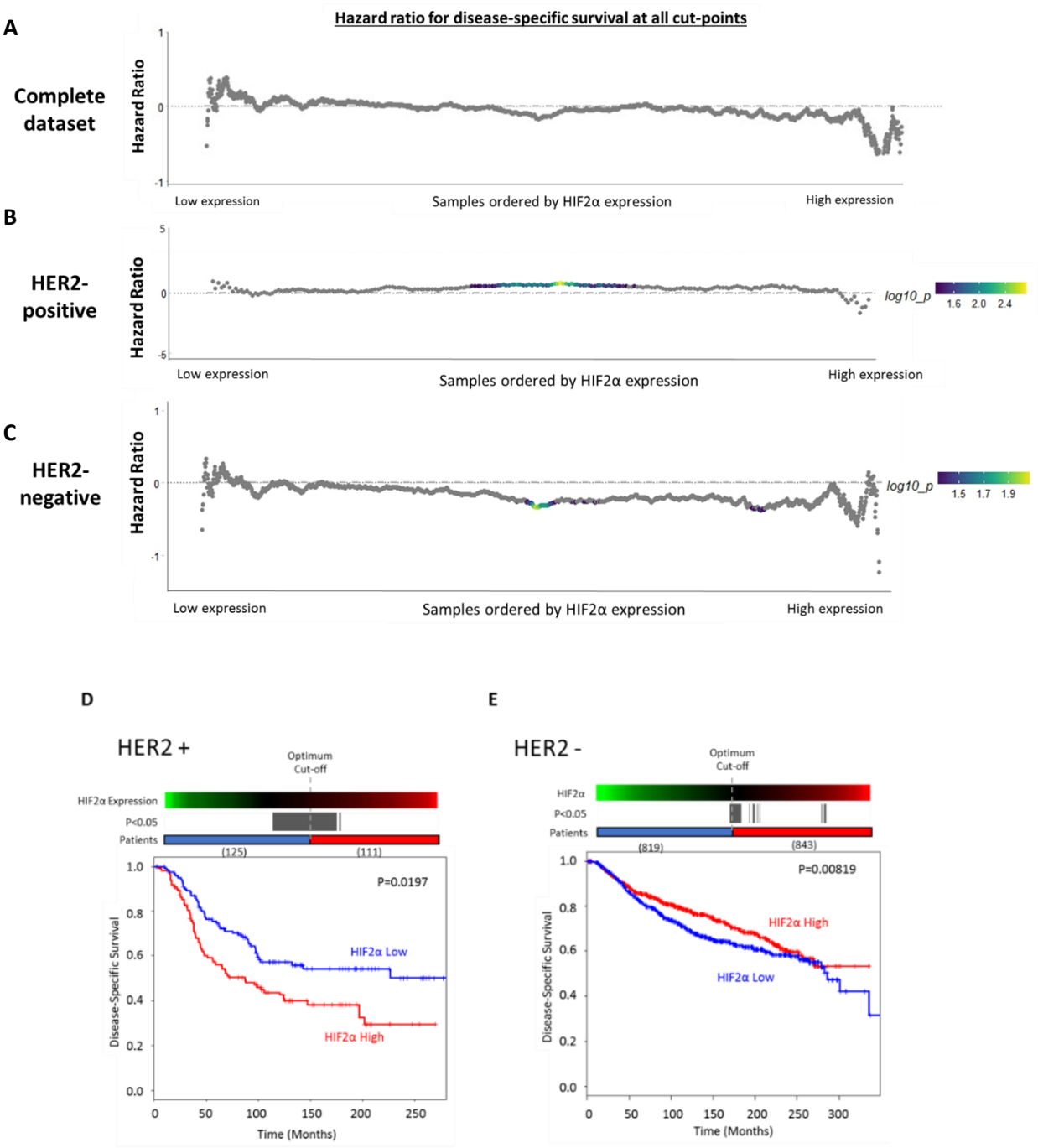

Figure 7.4: Analysis of disease-specific survival (DSS) in the publically available METABRIC dataset demonstrates robust concordance with Kmplot, showing a HER2-specific effect for HIF2α expression

A-C) METABRIC DSS data was assessed for the optimum cut-point in terms of HIF2α expression using the SurvivALL package. The hazard ratio is plotted for survival analysis based on each possible cut point. This is plotted against samples ordered by HIF2α expression (increasing left to right). Cut-points with p-values less than 0.05 are coloured according to the scale shown below for each plot. This analysis has been performed in all samples from the METABRIC dataset (A), HER2-positive samples only (B) and HER2-negative samples only (C). Whilst no significant cut-point was available for the complete sample set, optimum cut-points for HER2-positive and HER2-negative sets have been used to draw Kaplan-Meier curves (D and E). The number and position of significant cut-points according to SurvivALL analysis (grey bar) and how high and low categories are optimally divided (blue and red bar with n numbers below) are displayed for each graph.

7.4 A 10-gene signature for HIF2α activity is associated with worse survival in HER2-positive breast cancer

To further assess the role of HIF2α activity in HER2-specific breast cancer pathogenesis, we next investigated the association of HIF2-specific target gene expression with survival in breast cancer using the Kmplot and METABRIC datasets. A gene set comprising of HIF2α and 9 HIF2-driven genes shown to be HIF2-dependent in MCF7 cells was chosen [243]. These were determined by the siRNA-mediated knockdown of HIF2α followed by microarray expression analysis to find genes whose hypoxic upregulation was dependent on HIF2α expression. The genes included in this set are as follows: *EPAS1*, *CITED2*, *WISP2*, *IGFBP3*, *LOXL2*, *HIST1H4H*, *TBC1D3*, *ILVBL*, *FAM13A1*, and *HEY1*. Kmplot was used to assess overall, recurrence-free and distant metastasis-free survival based on the mean expression of these genes stratified into high and low expression categories based on the optimum cut-point value (Figure 7.5). High expression of this HIF2 gene signature was associated with significantly worse overall (HR= 2.02 p= 0.049), recurrence-free (HR= 2.66, p<0.0001) and distant metastasis-free survival (HR=4.25, p<0.0001) in the HER2-positive group. Significantly worse prognosis was also seen in terms of recurrence-free (HR= 1.18, p=0.0043) and distant metastasis-free survival (HR= 1.28, p=0.016) in the complete dataset without stratification based on HER2 status, and in terms of recurrence-free survival only (HR=1.4, p=0.014) in the HER2-negative patients. All 3 measures of survival demonstrated the greatest association of these genes with poor prognosis when assessed in the HER2-positive group.

The METABRIC study was used as a second dataset to validate a role for HIF2 target genes in poor prognosis in HER2-positive breast cancers. The SurvivALL package was used to determine all significant (p<0.05) cut-points for disease-specific survival based on the mean expression of the 10-gene HIF2 signature. This was done in the complete cohort as well as HER2-positive and HER2-negative cohorts (Figure 7.6 A-C). Significant cut-points in the complete cohort were only seen at particularly high expression levels and so a meaningful comparison of high and low expression groups was not possible. There were no significant cut-points in the HER2-negative cohort, but in HER2-positive samples a robust set of significant cut-points were found. The optimum cut-point value for this group was determined and a Kaplan-Meier plot is shown in Figure 7.4E the expression of these genes is shown as a heat map in Figure 7.4D, and the optimum cut-point used for Kaplan-Meier analysis is shown. In this case, significantly worse disease-specific survival as associated with high mean expression of the 10-gene signature (HR= 5.13, p=0.0176).

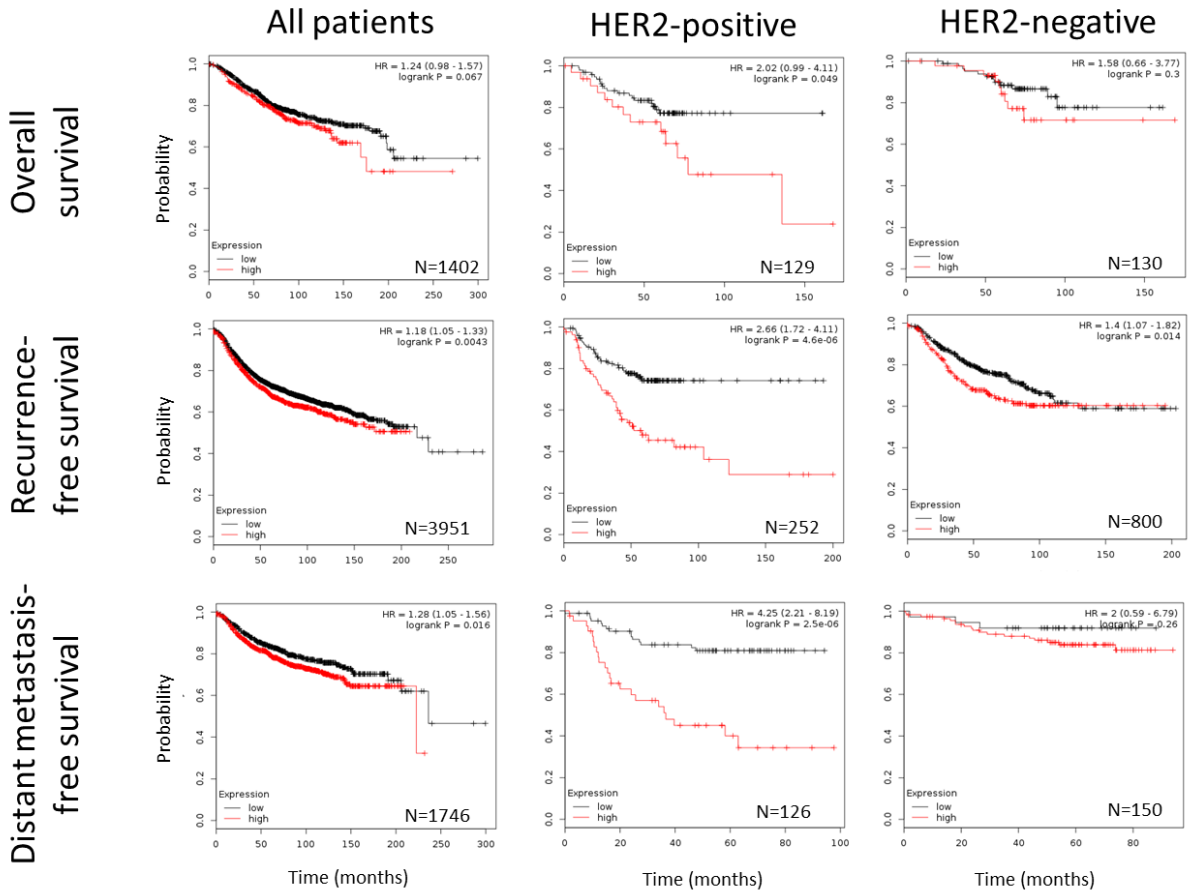

Figure 7.5: A 10-gene HIF2 signature also signifies a worse prognosis in HER2-positive breast cancer

The online resource Kmplot was used to perform survival analysis in breast cancer cohorts divided into HER2-negative and HER2-positive. Survival analysis based on the mean expression of HIF2α and 9 HIF2-specific target genes (CITED2, FAM13A1, HIST1H4H, HEY1, IGFBP3, ILVBL, LOXL2, TBC1D3 and WISP2) is shown in terms of overall survival, recurrence-free survival and distant metastasis-free survival, with cohorts divided into low and high expression groups by the optimum cut-point of mean gene expression. Each plot has its associated p-value, hazard ratio and n number shown.

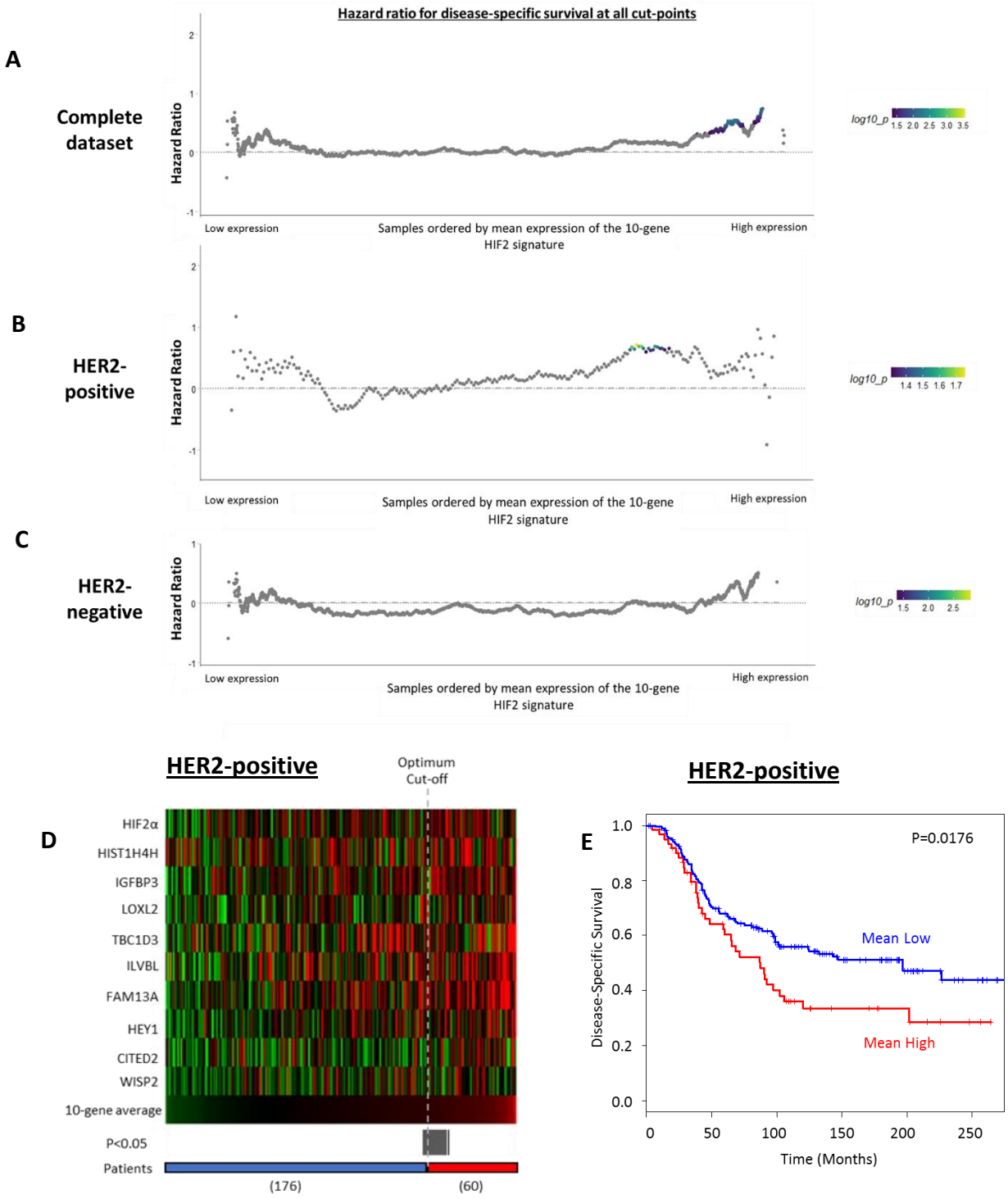

Figure 7.6: Disease-specific survival (DSS) using a 10-gene HIF2 signature in the METABRIC dataset demonstrates concordance with Kmplot, and an association of high HIF2 activity with worse survival in HER2-positive breast cancer

A-C) METABRIC DSS data was assessed for the optimum cut-point in terms of the mean expression of HIF2α and 9 HIF2-specific target genes using the SurvivALL package. The hazard ratio is plotted for survival analysis based on each possible cut-point. This is plotted against samples ordered by the mean expression of genes (increasing left to right). Cut-points with p-values less than 0.05 are coloured according to the scale shown below for each plot. This analysis has been performed in all samples from the METABRIC dataset (A), HER2-positive samples only (B) and HER2-negative samples only (C). The expression of each of the 10 genes ordered by the mean expression is shown for HER2-positive samples (D) with the position of significant cut-points according to SurvivALL analysis (grey bar) and how high and low categories are optimally divided (blue and red bar with n numbers below) both shown. The Kaplan-Meier plot with samples divided by the optimum cut-point in HER2-positive samples is shown (E).

7.5 Discussion

The role of HIF2α in breast cancer prognosis is poorly understood, and the limited studies which have aimed to address this issue have produced conflicting results [261, 427]. Results in chapters 3, 4 and 5 of this thesis have suggested an important relationship between HER2 and HIF2α expression and demonstrate the potential for HER2 overexpression to drive an increased response to hypoxia with the upregulation of a number of genes implicated in breast cancer progression and aggressiveness. With this in mind I have investigated the possibility that the role of HIF2α expression on survival may be directly linked to HER2 expression.

It has been recognised that breast cancers can be broadly defined by their molecular subtype which is determined by the expression of growth factor or hormone receptors, and that molecular subtypes of breast cancer represent distinct diseases with different prognoses and treatment requirements. Here we were able to demonstrate that the role of HIF2α on breast cancer prognosis depends on the expression of HER2. This finding has been shown to be robust as the relationship between HIF2α and poor prognosis was found to be HER2-dependent in two datasets. Whilst optimum cut-points were used for Kaplan-Meier analysis, it was also demonstrated that a range of cut-points are able to show this effect with $p<0.05$. The requirement for HER2 expression for HIF2α's role in worse survival may offer an explanation for the contradictory findings of previous studies [261, 427]. These studies both used IHC of tissue microarrays containing 282 and 691 primary invasive breast cancer samples respectively. Unfortunately, data on HER2 status for these two cohorts has not been published so it is currently unclear whether this could have caused the contradictory outcomes of these studies.

In addition, the role of HIF2 activity in prognosis was shown to be dependent on HER2 expression; the association between the mean expression of a 10-gene HIF2 signature and poor outcome was seen to be greater in HER2-positive cohorts when compared to HER2-negative or complete patient datasets. This was the case for overall survival, recurrence-free survival, and distant-metastasis-free survival, providing further evidence for the robustness of this relationship.

This work once again demonstrates an important difference between HIFα proteins in breast cancer and highlights the need to consider both HIF1α and HIF2α when investigating

HIF-driven cancer pathophysiology. We provide evidence that HIF2α may be a useful prognostic indicator in the context of high HER2 expression and, considering the increased sensitivity of HER2 overexpressing cell lines to HIF2α inhibition discussed in chapter 6, highlight the possibility that HIF2-targeted therapies may be an effective approach for the treatment of HER2-positive breast cancers.

Chapter 8: Final Discussion

8.1 Summary of findings

This project aimed to investigate the role of HER2 and HIF interactions in breast cancer. Specifically, it sought to evaluate how HER2 overexpression may modulate the cellular response to hypoxia through HIFs, and whether any differences could be identified between the roles of HIF1 and HIF2 in growth factor mediated HIF signalling in breast cancer.

First of all, I assessed how HER2 overexpression in an MCF7 cell line model altered the response to hypoxia in terms of cellular growth, motility and the upregulation of hypoxic response proteins including HIF1α and HIF2α. In these experiments I was able to demonstrate an increased upregulation of HIF2α in response to hypoxia, as well as an increased upregulation of the canonical hypoxic response protein CAIX, in the context of HER2 overexpression, providing evidence that HER2 may be an important regulator of HIF2α expression in these cell lines. This coincided with increased motility in hypoxia and the ubiquitous upregulation of HIF2α and hypoxia response proteins VEGF, CAIX and LDHA in 3D spheroid models of these cell lines. I was able to demonstrate that HIF2α upregulation in these cells occurs in normoxia and is driven by HER2 at the level of HIF2α transcription as indicated by both microarray and RT-PCR experiments. In this model I was able to demonstrate that HER2 drives an increase in HIF2α and not HIF1α suggesting a potential role for HIF2α in the differential responses to hypoxia seen in these cell lines, and indicating that the regulation of HIF1α and HIF2α by growth factor signalling occurs through different mechanisms.

In concordance with western blotting and IHC results, Illumina beadchip microarray analysis of MCF7 and MCF7-HER2 cells cultured in both acute and chronic hypoxia was able to demonstrate an increased upregulation of hypoxic response genes when HER2 is overexpressed. When compared to wild-type cells, MCF7-HER2 demonstrated a stronger upregulation of genes known to respond to hypoxia and prognosis in breast cancer. This was seen under conditions of both acute and chronic hypoxia and included a large number of genes known to promote glycolysis and hypoxia-mediated breast cancer progression. An increased hypoxic response was also shown in terms of the upregulation of HIF target genes,

but no clear preference for HIF2 target genes was seen, suggesting that in the context of HER2 overexpression, increased levels of HIF2α can drive the expression of both HIF1 and HIF2 target genes. This highlights the fact that the definition of hypoxic response genes as being either HIF1 or HIF2-driven is malleable and dependent on cellular context, specifically, it appears that high levels of HIF2α might override this target specificity and allow more promiscuous HIF2 target selection. A genome wide analysis of transcripts upregulated by hypoxia in these cell lines demonstrated a role for HER2 overexpression in priming cells for hypoxia. A large proportion of hypoxia responsive genes were seen to be constitutively expressed at higher levels in the context of high HER2 expression. This suggests that the normoxic upregulation of HIF2α might result in an increase in the expression of a number of hypoxia response genes. In addition a larger number of HIF target genes were expressed specifically in the HER2 overexpressing cell line in acute and chronic hypoxia. This demonstrates that HER2 overexpression is able to exacerbate the hypoxic response of MCF7 cells both in terms of HIF and non-HIF target genes and is thereby able to drive glycolysis, angiogenesis, metastasis and cellular proliferation in hypoxia. Having demonstrated that HIF2 and not HIF1 is upregulated and further increased in hypoxia when HER2 is overexpressed in these cells, HIF2 is presumed to play a predominant role in the increased hypoxic response of these cells. This was supported by the inhibition of CAIX upregulation in hypoxia when MCF7-HER2 cells were treated with the HIF2 specific translation inhibitor C76.

In a series of experiments I then demonstrated an increased sensitivity of HER2-positive breast cancer cell lines to HIF2α inhibition. SiRNA-mediated knockdown of HIF2α was able to reduce the growth rate of MCF7-HER2 cells to a higher degree than their HER2-low counterparts, whilst triple-negative cell lines HBL100 and MDA-MB-231 showed intermediate sensitivity. An increased sensitivity of other HER2-positive cell lines was demonstrated using the HIF2α translation inhibitor C76, which was more effective at reducing cell growth in SKBR3, MDA-MB-361 and BT474 cell lines. In addition, HIF2α inhibitors were able to reduce the motility of the highly invasive cell lines MDA-MB-231 and HBL100 in 2D wound healing assays, and despite having a low invasive potential, a small inhibition of MCF7 and MCF7-HER2 invasion into collagen using a 3D spheroid model was also demonstrated. This showed that HIF2 inhibition may be effective at reducing the expression of motility genes, such as those upregulated by hypoxia. Interestingly, in all cell lines, the siRNA-mediated inhibition of cellular growth was greater in normoxia than hypoxia.

This indicates that the role of HIF2α upregulation in normoxia may be important for cell line growth, and targeting HIF2 may not only be applicable to highly hypoxic tumours.

Having demonstrated a HER2-driven mechanism for HIF2α upregulation, and an increased sensitivity of HER2-positive cell lines to HIF2 inhibition, it was hypothesised that HIF2 activity may be an efficacious target in HER2-positive breast cancers. To test whether this HER2-HIF2α relationship may be an important driver of breast cancer I used publically available gene expression and clinical datasets to perform survival analysis based on HIF2α expression and the expression of HIF2 target genes in two large breast cancer cohorts. Here I was able to demonstrate that high HIF2α expression is associated with worse prognosis in breast cancer when HER2 is overexpressed. This suggests that the relationship between HER2 signalling and HIF2α expression demonstrated in this thesis is applicable to breast cancer more generally, and may be an important determinant of survival. In addition, the requirement of HER2 overexpression for the association between HIF2α and poor prognosis offers a potential explanation as to why previous studies [261, 427] have been ambiguous in terms of the relationship between HIF2α and clinical outcome, showing an association of high HIF2α with both worse [261] and with better [427] prognosis. This novel role for HIF2α in HER2-driven breast cancer differs from HIF1α, which was found to be associated with poor prognosis irrelevant of HER2 expression. This, in addition to the differential mechanisms of HIFα regulation by growth factors demonstrated in this thesis, suggests that growth factor regulated HIF1α and HIF2α have differential contributions to breast cancer pathogenesis, and that despite previous findings of HIF1α-growth factor interactions, it appears to be HIF2α which is directly associated with poor prognosis in the context of HER2 overexpression.

8.2 Relevance of findings

Previous work has demonstrated an interplay between growth factor signalling and HIFα proteins. It has been shown, both through the stimulation of growth factor signalling with NRG ligand and the activation of intracellular signalling pathways through the expression of dominant-negative AKT, that these pathways have the capability to increase levels of HIF1α protein and can lead to the increased levels of HIF target VEGF [220, 421]. This work has highlighted a non-canonical relationship between growth factor signalling and HIFα protein regulation in breast cancer cell lines. These findings have important implications

as they demonstrate that the influence of HIF signalling on solid tumours may not be limited to areas of hypoxia, suggesting that HIF-targeted therapies may also be efficacious in solid tumours in the absence of developed hypoxic regions. However, previous work has not reported on how this interaction may contribute to HIF-driven gene expression changes in hypoxia. The work in this thesis has addressed this question by considering how gene expression changes driven by hypoxia are altered in breast cancer cell lines when HER2 is overexpressed. By demonstrating an increase in the expression of hypoxic response genes at low oxygen concentrations in a HER2-overexpressing cell line, we provide evidence that HER2 can promote a more vigorous cellular response to hypoxia, driving a robust set of both HIF and non-HIF genes with a number known to contribute to breast cancer progression. Together with previous studies, this finding provides us with novel insight into how HIF targeted therapies may be best used. Specifically, such compounds may be more effective in the context of high growth factor signalling such as in HER2-positive breast cancers, because in these cancers HIF target genes may play a bigger role in progression and aggressive tumour characteristics due to their increased expression both in normoxia and in response to hypoxia. In these contexts the co-therapies with HIF and HER2 targeting compounds may also be effective as both these factors appear to work together to drive the expression of genes which contribute to disease progression.

One limitation in our understanding of how HIFs contribute to disease has been the different roles of HIF1α and HIF2α. Despite numerous publications on the differences between these two proteins [245, 249, 265], and the exemplar of renal carcinoma; where HIF2α has been shown to be a major contributor to disease progression, in the field of breast cancer much research has been conducted on the presumption that HIF1α is the predominant HIFα protein, or that differences between HIF1α and HIF2α are not important. However, it has now been shown by large scale ChIP experiments that the genes sets driven by HIF1 and HIF2 transcription factors are not the same [239, 240]. With this in mind, one aim of this thesis was to try and understand whether HIF1α and HIF2α are distinct in terms of their regulation by growth factor signalling, and we were able to shown that these two proteins are differentially upregulated by ligand-driven growth factor signalling vs HER2 overexpression in breast cancer cell lines. Whilst the mechanisms governing these differences were not elucidated, this finding contributes to our growing understanding of the specific functions of HIF1α and HIF2α in breast cancer. With previous work already showing that HIF2α gene expression can be driven by EGFR [426], we suggest that EGFR and HER2

driven HIF2α may function through equivalent mechanisms as both result in upregulation at the gene expression level. In contrast, HIF1α upregulated in normoxia by NRG or dominant-negative AKT has been shown to be driven by an increased rate of translation and increased stability of the protein [421]. Therefore the separate mechanisms for the specific upregulation of HIF1α or HIF2α by growth factor signalling shown both in the literature and in this thesis suggest that the context of growth factor signalling and the expression of HER receptors may be an important determinant of which HIFα proteins are highly expressed in breast cancer, and that HIF2α may be predominantly driven in HER2-positive and triple-negative breast cancers.

Most importantly, this thesis has demonstrated the potential for targeting HIF2α specifically in HER2-positive breast cancer. HIF2α targeted therapy has already proven effective in pre-clinical models of RCC [393, 396, 512], and the development of HIF2 dimerisation inhibitors such as PT2385 and PT2399 mean that these compounds can be repurposed for breast cancer if effective. With the current literature having focussed heavily on HIF1α, the potential of specifically targeting HIF2α in breast cancer has not been widely considered. This may be due to HIF1α's clear negative association with survival in breast cancer, which does not appear to be determined by molecular characteristics of the disease. However, by demonstrating that efficacy of targeting HIF2 in MCF7-HER2 and comparing this with survival data stratified by HER2 expression, we provide evidence that HIF2α may be a targetable determinant of disease progression only when HER2 is highly expressed.

8.3 Future work

The findings presented in this thesis provide an exciting new insight into the role of HIF2α in breast cancer. Having demonstrated the pathological relevance of HIF2α expression in HER2-positive breast cancer and provided evidence for mechanistic differences between HIFα protein regulation by growth factors in normoxia and hypoxia, it is now important to further characterise the precise pathways which differentiate between HIF1α and HIF2α signalling in response to growth factor signalling and further assess the potential of targeting specific HIFα proteins in breast cancer. Cellular context seems to be important and understanding these mechanisms may help to stratify patients so that HIF-targeting therapies can be developed specifically for those who would benefit.

HER2 overexpression was able to upregulate HIF2α expression in MCF7-HER2 cells when compared to wild-type MCF7, and this appears to have important implications for the hypoxic response in these cells. Whilst differences in mechanism between HIF1α and HIF2α upregulation by growth factor signalling were demonstrated, it is still unclear how signalling pathways which mediate HIF1α stabilisation in normoxia differ from the pathways driving increased expression of HIF2α. The possible roles of AKT and ERK signalling were investigated, and HIF2α upregulation was shown to rely, at least partially, on AKT signalling; the same pathway reported to promote increased translation and stability of HIF1α in response to the HER3 ligand NRG. A better understanding of these differences may provide important insights into the function of HIF1 versus HIF2 signalling in breast cancers with different forms of signalling dysregulation.

Whilst CAIX upregulation by hypoxia was shown to be increased by HER2 overexpression, there are still some unanswered questions as to the mechanisms responsible. Further work is required to establish how robust this effect is, i.e. can increases in HER2 drive CAIX and other hypoxic targets in other breast cancer cell lines, and whether this effect is driven exclusively by HIF2, or if increases in HIF1 transcriptional activity are also involved. I have demonstrated that the HIF2α translation inhibitor C76 is able to reduce the hypoxic upregulation of CAIX, but due to the nature of the inhibitor it was not particularly amenable to inhibition in hypoxia, and HIF2 transcriptional inhibitors were not able to produce this effect. Additional experiments including a comparison of HIF1α and HIF2α inhibition may be required to determine the contribution of these factors to this response. Similarly, the strong upregulation of hypoxic response genes demonstrated through microarray analysis is presumed to be a result of increased HIF2α in MCF7-HER2, however the relative contributions of HIFα proteins can only be confirmed through further experiments with HIF1α or HIF2α specific inhibition.

The mechanisms driving HIF transcriptional activity in the context of HER2 overexpression also need clarification. The increased expression of HIF2α is likely to contribute but it is still not clear whether HER2-mediated changes in the expression of co-factors may also play a role in HIF target selection. On this note, previous work to understand HIF target selection in breast cancer cell lines has focussed predominantly on MCF7 cells. It is clear from the results presented in this thesis that cellular characteristics such as growth factor expression can contribute to large differences in HIF targets. HIF targets should

therefore be understood as variable and understanding the mechanisms which determine target selection may be more valuable than the identification of HIF1 vs HIF2 targets in a particular context. A number of transcriptional co-factors are known to have specific associations with either HIF1α or HIF2α, thus it may be the expression of these factors as well as the absolute levels of different HIFα proteins which determine HIF gene transcription in normoxia and in response to hypoxia.

Given that HER2-HIF2α interactions have been shown to be associated with breast cancer progression, and HER2-positive cell lines seem to have a distinguishing sensitivity to HIF2 inhibition, further work into the efficacy of HIF2 inhibitors in HER2-positive breast cancers would be highly valuable. HIF2 inhibitors such as PT2385 and its close homologue PT2399 have been shown to be effective at treating ccRCC, with PT2399 currently enrolled on a phase II clinical trial. Whilst heterodimerisation inhibitors C2 and PT2385 did not perform well in growth or motility assays in breast cancer cell lines, it would be worthwhile to understand whether this is due to a failure of these compounds to inhibit HIF2 activity in these models or a failure of HIF2 inhibition to effectively reduce growth or motility. Given the clear relationship between HIF2α expression and poor prognosis in HER2-positive breast cancers, and the efficacy of C76 and HIF2α siRNA in reducing the growth rates of HER2-positive cell lines, it seems sensible that inhibitors such as PT2385 and PT2399, which have been shown to be clinically effective in a different form of cancer, should be more deeply investigated with respect to HER2-positive breast cancer.

Finally, the importance of HIF2α in the context of high HER2 signalling in breast cancer is clear. However, it is still uncertain what role HIF2α may play in breast cancers where growth is promoted by other growth factor receptors such as EGFR (HER1). Triple-negative cell lines showed a moderate sensitivity to HIF2 inhibition in terms of both cell growth and cell motility. As mentioned above, a deeper understanding of the mechanisms governing growth factor-mediated HIF upregulation may provide insight into the relevance of HIF2 in EGFR-driven cancers, and further investigation into the relationship between EGFR and HIF2α expression in breast cancer may implicate HIF2 as a potential target for triple-negative breast cancers, a subtype with currently limited treatment strategies.

8.4 Final remarks

This project aimed to investigate the roles of HIF1α and HIF2α in growth factor driven HIF regulation. With the upregulation of HIF1α by NRG being previously described, I wanted to address the question of whether growth factor signalling is equally able to upregulate HIF1α and HIF2α levels in normoxia, and assess whether growth factor-driven upregulation of HIFα promoted an altered hypoxic response in the context of HER2 overexpression. I have been able to demonstrate that under different conditions growth factor signalling independently drives HIF1α or HIF2α in normoxia, depending on the nature of the signalling pathway. This finding provides a novel role for HIF2α in the non-canonical/normoxic role of HIFs in breast cancer, and demonstrates that differences in HIFα regulation may play an important role in determining their involvement in disease progression. This is reflective of the differences in HIF1α and HIF2α regulation which are already known to exist at the transcriptional, translational and post-translational levels, adding another level of complexity to the differential regulation of these factors.

Whilst the roles of hypoxia and HIF signalling in driving breast cancer have been thoroughly investigated, we still have little understanding of the differential roles that each HIFα protein plays. Previous research has demonstrated an association of HIF1α expression and growth factor signalling both in cell lines and breast cancer samples. Despite this, it was not known to what extent growth factor signalling may affect the cellular response to hypoxia through HIF upregulation, or how different HIFα proteins may be modulated by growth factor signalling. With HER2 overexpression seen in approximately 20% of breast cancers, it is important to understand how HIF signalling in these patients may drive pathogenesis both in normoxic and hypoxic tumour environments. Together this work has shown important differences between HIF1α and HIF2α in terms of their response to growth factor signalling, with a specific role for HIF2α in HER2 overexpressing cells. HIF2α has been implicated as an important player in HER2-positive breast cancer in terms of prognosis, and the increased sensitivity of HER2-positive cells to HIF2 inhibition suggesting that HIF2 may be an effective target in the context of HER2 overexpression. Further work is required to develop these findings, but it is clear that the consideration of both HIF1α and HIF2α as well as the

molecular subtype of the breast cancer is important when contemplating HIF-targeting approaches for this disease. A number of HIF inhibitors are under investigation, and their efficacy in various cancer types has been shown. However, for the majority, little is known about their mechanism of action and their effect on HIF2α. Given the mechanistic differences in growth factor-driven regulation of HIF1α and HIF2α demonstrated in this thesis, I suggest that further work on HIF inhibitors in breast cancer should aim to understand their effects on both. The targeting of individual HIFα proteins such as HIF2α may increase the effectiveness of HIF-targeting therapies. Furthermore, the specific role of HIF2α in HER2-positive breast cancers suggests that HIF2 targeted therapies may be most effective in this subtype, and further work into HIF inhibition as a therapeutic strategy may benefit from the stratification of patients so that the effectiveness of HIF inhibitors can be tested in the context of breast cancers with high growth factor receptor expression. Finally, the role of growth factor signalling in driving HIFα expression raises the question of whether HIF inhibitors may be effective as a co-therapy alongside HER2-targeted therapies for breast cancer. The nature of this relationship suggests that this may be an effective strategy both in normoxic and hypoxic tumour regions. With a range of HIF inhibitory compounds available and the ongoing development of specific HIF2 inhibitors, these considerations may facilitate the use of HIF inhibition as a therapeutic tool for breast cancer.

Bibliography

1. Hanahan, D. and R.A. Weinberg, *Hallmarks of cancer: the next generation.* Cell, 2011. **144**(5): p. 646-74.
2. Hanahan, D. and R.A. Weinberg, *The hallmarks of cancer.* Cell, 2000. **100**(1): p. 57-70.
3. Torre, L.A., et al., *Global cancer statistics, 2012.* CA Cancer J Clin, 2015. **65**(2): p. 87-108.
4. *Cancer statistics in the UK*. [cited 2017 17th May]; Available from: /www.cancerresearchuk.org/health-professional/cancer-statistics.
5. Geddes, D.T., *Inside the lactating breast: the latest anatomy research.* J Midwifery Womens Health, 2007. **52**(6): p. 556-63.
6. Ali, S. and R.C. Coombes, *Endocrine-responsive breast cancer and strategies for combating resistance.* Nat Rev Cancer, 2002. **2**(2): p. 101-12.
7. Brisken, C. and B. O'Malley, *Hormone action in the mammary gland.* Cold Spring Harb Perspect Biol, 2010. **2**(12): p. a003178.
8. Sternlicht, M.D., *Key stages in mammary gland development: the cues that regulate ductal branching morphogenesis.* Breast Cancer Res, 2006. **8**(1): p. 201.
9. *Autophagy in Development and Remodelling of Mammary Gland*, in *Autophagy - A Double-Edged Sword - Cell Survival or Death?*, K.Z.a.T.M. Malgorzata Gajewska, Editor. 2013.
10. Motyl, T., et al., *Apoptosis and autophagy in mammary gland remodeling and breast cancer chemotherapy.* J Physiol Pharmacol, 2006. **57 Suppl 7**: p. 17-32.
11. UK, C.R. *Ductal Carcinoma in Situ (DCIS)*. 2016 [cited 2017 25th May]; Available from: http://www.cancerresearchuk.org/about-cancer/breast-cancer/stages-types-grades/types/ductal-carcinoma-in-situ-dcis.
12. UK, C.R. *Lobular Carcinoma in Situ (LCIS)*. 2016 [cited 2017 25th May]; Available from: http://www.cancerresearchuk.org/about-cancer/breast-cancer/stages-types-grades/types/lobular-carcinoma-in-situ-lcis.
13. Malhotra, G.K., et al., *Histological, molecular and functional subtypes of breast cancers.* Cancer Biol Ther, 2010. **10**(10): p. 955-60.
14. Li, C.I., D.J. Uribe, and J.R. Daling, *Clinical characteristics of different histologic types of breast cancer.* Br J Cancer, 2005. **93**(9): p. 1046-52.
15. Bloom, H.J. and W.W. Richardson, *Histological grading and prognosis in breast cancer; a study of 1409 cases of which 359 have been followed for 15 years.* Br J Cancer, 1957. **11**(3): p. 359-77.
16. Elston, C.W. and I.O. Ellis, *Pathological prognostic factors in breast cancer. I. The value of histological grade in breast cancer: experience from a large study with long-term follow-up.* Histopathology, 2002. **41**(3A): p. 154-61.
17. Genestie, C., et al., *Comparison of the prognostic value of Scarff-Bloom-Richardson and Nottingham histological grades in a series of 825 cases of breast cancer: major importance of the mitotic count as a component of both grading systems.* Anticancer Res, 1998. **18**(1B): p. 571-6.
18. Denoix, P., *Enquete permanente dans les centres anticancereux.* Bull Inst Natl Hyg, 1946. **1**: p. 12-7.
19. *TNM: Classification of Malignant Tumours*. Union Internationale Contre le Cancer. 1968: G. de Buren.

20. Feinstein, A.R. and P.K. Bondy, *A new staging system for cancer, and a re-appraisal of "early" treatment and "cure" by radical surgery.* Trans Assoc Am Physicians, 1967. **80**: p. 111-22.
21. Zeynep Ozsaran, S.D., *Staging of Breast Cancer*, in *Principles and Practice of Modern Radiotherapy Techniques in Breast Cancer*, A.H.a.G. Ozyigit, Editor. 2013.
22. Benson, J.R., et al., *The TNM staging system and breast cancer.* Lancet Oncol, 2003. **4**(1): p. 56-60.
23. Edge, S.B. and C.C. Compton, *The American Joint Committee on Cancer: the 7th edition of the AJCC cancer staging manual and the future of TNM.* Ann Surg Oncol, 2010. **17**(6): p. 1471-4.
24. *Surgery for breast cancer*. 2016 [cited 2017 16th May]; Available from: www.cancer.org/cancer/breast-cancer/treatment/surgery-for-breast-cancer.
25. Blichert-Toft, M., et al., *Long-term results of breast conserving surgery vs. mastectomy for early stage invasive breast cancer: 20-year follow-up of the Danish randomized DBCG-82TM protocol.* Acta Oncol, 2008. **47**(4): p. 672-81.
26. Voogd, A.C., et al., *Differences in risk factors for local and distant recurrence after breast-conserving therapy or mastectomy for stage I and II breast cancer: pooled results of two large European randomized trials.* J Clin Oncol, 2001. **19**(6): p. 1688-97.
27. Kroman, N., et al., *Effect of breast-conserving therapy versus radical mastectomy on prognosis for young women with breast carcinoma.* Cancer, 2004. **100**(4): p. 688-93.
28. Eisen, A., et al., *Prophylactic surgery in women with a hereditary predisposition to breast and ovarian cancer.* J Clin Oncol, 2000. **18**(9): p. 1980-95.
29. Hartmann, L.C., et al., *Efficacy of bilateral prophylactic mastectomy in BRCA1 and BRCA2 gene mutation carriers.* J Natl Cancer Inst, 2001. **93**(21): p. 1633-7.
30. Rhiem, K. and R. Schmutzler, *Impact of Prophylactic Mastectomy in BRCA1/2 Mutation Carriers.* Breast Care (Basel), 2014. **9**(6): p. 385-9.
31. Kunkler, I., *Radiotherapy for breast cancer.* N Engl J Med, 2002. **346**(11): p. 862-4.
32. Kunkler, I., *Adjuvant irradiation for breast cancer.* BMJ, 2000. **320**(7248): p. 1485-6.
33. Overgaard, M., et al., *Postoperative radiotherapy in high-risk premenopausal women with breast cancer who receive adjuvant chemotherapy. Danish Breast Cancer Cooperative Group 82b Trial.* N Engl J Med, 1997. **337**(14): p. 949-55.
34. Ragaz, J., et al., *Adjuvant radiotherapy and chemotherapy in node-positive premenopausal women with breast cancer.* N Engl J Med, 1997. **337**(14): p. 956-62.
35. Klefstrom, P., et al., *Adjuvant postoperative radiotherapy, chemotherapy, and immunotherapy in stage III breast cancer. II. 5-year results and influence of levamisole.* Cancer, 1987. **60**(5): p. 936-42.
36. Overgaard, M., et al., *Postoperative radiotherapy in high-risk postmenopausal breast-cancer patients given adjuvant tamoxifen: Danish Breast Cancer Cooperative Group DBCG 82c randomised trial.* Lancet, 1999. **353**(9165): p. 1641-8.
37. Breastcancer.org. *External radiation*. 2012 [cited 2017 25th May]; Available from: http://www.breastcancer.org/treatment/radiation/types/ext.

38. Cancer.gov. *Radiation Therapy for Cancer*. 2010 [cited 2017 25th May]; Available from: https://www.cancer.gov/about-cancer/treatment/types/radiation-therapy/radiation-fact-sheet.
39. Breastcancer.org. *Types of Radiation*. 2015 [cited 2017 June 16th]; Available from: http://www.breastcancer.org/treatment/radiation/types.
40. *Favourable and unfavourable effects on long-term survival of radiotherapy for early breast cancer: an overview of the randomised trials. Early Breast Cancer Trialists' Collaborative Group.* Lancet, 2000. **355**(9217): p. 1757-70.
41. Clarke, M., et al., *Effects of radiotherapy and of differences in the extent of surgery for early breast cancer on local recurrence and 15-year survival: an overview of the randomised trials.* Lancet, 2005. **366**(9503): p. 2087-106.
42. Fisher, B., et al., *Reanalysis and results after 12 years of follow-up in a randomized clinical trial comparing total mastectomy with lumpectomy with or without irradiation in the treatment of breast cancer.* N Engl J Med, 1995. **333**(22): p. 1456-61.
43. Fisher, B., et al., *Twenty-year follow-up of a randomized trial comparing total mastectomy, lumpectomy, and lumpectomy plus irradiation for the treatment of invasive breast cancer.* N Engl J Med, 2002. **347**(16): p. 1233-41.
44. Poortmans, P., *Evidence based radiation oncology: breast cancer.* Radiother Oncol, 2007. **84**(1): p. 84-101.
45. Blichert-Toft, M., et al., *Danish randomized trial comparing breast conservation therapy with mastectomy: six years of life-table analysis. Danish Breast Cancer Cooperative Group.* J Natl Cancer Inst Monogr, 1992(11): p. 19-25.
46. Partridge, A.H., H.J. Burstein, and E.P. Winer, *Side effects of chemotherapy and combined chemohormonal therapy in women with early-stage breast cancer.* J Natl Cancer Inst Monogr, 2001(30): p. 135-42.
47. Chemocare.com. *Cancer Cells and Chemotherapy*. 2017 [cited 2017 25th May]; Available from: http://chemocare.com/chemotherapy/what-is-chemotherapy/cancer-cells-chemotherapy.aspx.
48. Szulawska, A. and M. Czyz, *[Molecular mechanisms of anthracyclines action].* Postepy Hig Med Dosw (Online), 2006. **60**: p. 78-100.
49. Minotti, G., et al., *Anthracyclines: molecular advances and pharmacologic developments in antitumor activity and cardiotoxicity.* Pharmacol Rev, 2004. **56**(2): p. 185-229.
50. Crathorn, A.R. and J.J. Roberts, *Mechanism of the cytotoxic action of alkylating agents in mammalian cells and evidence for the removal of alkylated groups from deoxyribonucleic acid.* Nature, 1966. **211**(5045): p. 150-3.
51. Siddik, Z.H., *Cisplatin: mode of cytotoxic action and molecular basis of resistance.* Oncogene, 2003. **22**(47): p. 7265-79.
52. Kaye, S.B., *New antimetabolites in cancer chemotherapy and their clinical impact.* Br J Cancer, 1998. **78 Suppl 3**: p. 1-7.
53. Jordan, M.A. and L. Wilson, *Microtubules as a target for anticancer drugs.* Nat Rev Cancer, 2004. **4**(4): p. 253-65.
54. Joerger, M. and B. Thurlimann, *Chemotherapy regimens in early breast cancer: major controversies and future outlook.* Expert Rev Anticancer Ther, 2013. **13**(2): p. 165-78.
55. Early Breast Cancer Trialists' Collaborative, G., *Effects of chemotherapy and hormonal therapy for early breast cancer on recurrence and 15-year survival: an overview of the randomised trials.* Lancet, 2005. **365**(9472): p. 1687-717.
56. McArthur, H.L. and C.A. Hudis, *Breast cancer chemotherapy.* Cancer J, 2007. **13**(3): p. 141-7.

57. Untch, M., et al., *Current and future role of neoadjuvant therapy for breast cancer.* Breast, 2014. **23**(5): p. 526-37.
58. Kirova, Y.M., *Recent advances in breast cancer radiotherapy: Evolution or revolution, or how to decrease cardiac toxicity?* World J Radiol, 2010. **2**(3): p. 103-8.
59. Stewart, J.R., et al., *Radiation injury to the heart.* Int J Radiat Oncol Biol Phys, 1995. **31**(5): p. 1205-11.
60. Stewart, J.R. and L.F. Fajardo, *Radiation-induced heart disease. Clinical and experimental aspects.* Radiol Clin North Am, 1971. **9**(3): p. 511-31.
61. Darby, S.C., et al., *Risk of ischemic heart disease in women after radiotherapy for breast cancer.* N Engl J Med, 2013. **368**(11): p. 987-98.
62. Giordano, S.H., et al., *Risk of cardiac death after adjuvant radiotherapy for breast cancer.* J Natl Cancer Inst, 2005. **97**(6): p. 419-24.
63. Patt, D.A., et al., *Cardiac morbidity of adjuvant radiotherapy for breast cancer.* J Clin Oncol, 2005. **23**(30): p. 7475-82.
64. Kayl, A.E. and C.A. Meyers, *Side-effects of chemotherapy and quality of life in ovarian and breast cancer patients.* Curr Opin Obstet Gynecol, 2006. **18**(1): p. 24-8.
65. Meinardi, M.T., et al., *Long-term chemotherapy-related cardiovascular morbidity.* Cancer Treat Rev, 2000. **26**(6): p. 429-47.
66. Osborne, C.K., H. Zhao, and S.A. Fuqua, *Selective estrogen receptor modulators: structure, function, and clinical use.* J Clin Oncol, 2000. **18**(17): p. 3172-86.
67. Chumsri, S., et al., *Aromatase, aromatase inhibitors, and breast cancer.* J Steroid Biochem Mol Biol, 2011. **125**(1-2): p. 13-22.
68. Miller, W.R., *Aromatase inhibitors and breast cancer.* Minerva Endocrinol, 2006. **31**(1): p. 27-46.
69. Chengalvala, M.V., J.C. Pelletier, and G.S. Kopf, *GnRH agonists and antagonists in cancer therapy.* Curr Med Chem Anticancer Agents, 2003. **3**(6): p. 399-410.
70. Robertson, J.F. and R.W. Blamey, *The use of gonadotrophin-releasing hormone (GnRH) agonists in early and advanced breast cancer in pre- and perimenopausal women.* Eur J Cancer, 2003. **39**(7): p. 861-9.
71. Prowell, T.M. and N.E. Davidson, *What is the role of ovarian ablation in the management of primary and metastatic breast cancer today?* Oncologist, 2004. **9**(5): p. 507-17.
72. Lao Romera, J., et al., *Update on adjuvant hormonal treatment of early breast cancer.* Adv Ther, 2011. **28 Suppl 6**: p. 1-18.
73. Johnston, S.J. and K.L. Cheung, *Fulvestrant - a novel endocrine therapy for breast cancer.* Curr Med Chem, 2010. **17**(10): p. 902-14.
74. Rosalba Torrisi, A.B., Aron Goldhirsch, *Endocrine therapy of breast cancer*, in *Drugs Affecting Growth of Tumours*, C.H.S. Herbert M. Pinedo, Editor. 2016.
75. Stewart, H.J., R.J. Prescott, and A.P. Forrest, *Scottish adjuvant tamoxifen trial: a randomized study updated to 15 years.* J Natl Cancer Inst, 2001. **93**(6): p. 456-62.
76. Fisher, B., et al., *Treatment of lymph-node-negative, oestrogen-receptor-positive breast cancer: long-term findings from National Surgical Adjuvant Breast and Bowel Project randomised clinical trials.* Lancet, 2004. **364**(9437): p. 858-68.
77. Carpenter, R. and W.R. Miller, *Role of aromatase inhibitors in breast cancer.* Br J Cancer, 2005. **93 Suppl 1**: p. S1-5.

78. Smith, I.E., *Aromatase inhibitors in early breast cancer therapy.* Semin Oncol, 2004. **31**(6 Suppl 12): p. 9-14.
79. Dombernowsky, P., et al., *Letrozole, a new oral aromatase inhibitor for advanced breast cancer: double-blind randomized trial showing a dose effect and improved efficacy and tolerability compared with megestrol acetate.* J Clin Oncol, 1998. **16**(2): p. 453-61.
80. Buzdar, A.U., et al., *Anastrozole versus megestrol acetate in the treatment of postmenopausal women with advanced breast carcinoma: results of a survival update based on a combined analysis of data from two mature phase III trials. Arimidex Study Group.* Cancer, 1998. **83**(6): p. 1142-52.
81. Kaufmann, M., et al., *Exemestane is superior to megestrol acetate after tamoxifen failure in postmenopausal women with advanced breast cancer: results of a phase III randomized double-blind trial. The Exemestane Study Group.* J Clin Oncol, 2000. **18**(7): p. 1399-411.
82. Chlebowski, R., et al., *Clinical perspectives on the utility of aromatase inhibitors for the adjuvant treatment of breast cancer.* Breast, 2009. **18 Suppl 2**: p. S1-11.
83. Mouridsen, H., et al., *Phase III study of letrozole versus tamoxifen as first-line therapy of advanced breast cancer in postmenopausal women: analysis of survival and update of efficacy from the International Letrozole Breast Cancer Group.* J Clin Oncol, 2003. **21**(11): p. 2101-9.
84. Bonneterre, J., et al., *Anastrozole versus tamoxifen as first-line therapy for advanced breast cancer in 668 postmenopausal women: results of the Tamoxifen or Arimidex Randomized Group Efficacy and Tolerability study.* J Clin Oncol, 2000. **18**(22): p. 3748-57.
85. Bonneterre, J., et al., *Anastrozole is superior to tamoxifen as first-line therapy in hormone receptor positive advanced breast carcinoma.* Cancer, 2001. **92**(9): p. 2247-58.
86. Paridaens, R.J., et al., *Phase III study comparing exemestane with tamoxifen as first-line hormonal treatment of metastatic breast cancer in postmenopausal women: the European Organisation for Research and Treatment of Cancer Breast Cancer Cooperative Group.* J Clin Oncol, 2008. **26**(30): p. 4883-90.
87. *Ovarian ablation in early breast cancer: overview of the randomised trials. Early Breast Cancer Trialists' Collaborative Group.* Lancet, 1996. **348**(9036): p. 1189-96.
88. Freedman, O.C., et al., *Adjuvant endocrine therapy for early breast cancer: a systematic review of the evidence for the 2014 Cancer Care Ontario systemic therapy guideline.* Curr Oncol, 2015. **22**(Suppl 1): p. S95-S113.
89. Bertelli, G., *Sequencing of aromatase inhibitors.* Br J Cancer, 2005. **93 Suppl 1**: p. S6-9.
90. Hanamura, T. and S.I. Hayashi, *Overcoming aromatase inhibitor resistance in breast cancer: possible mechanisms and clinical applications.* Breast Cancer, 2017.
91. Rondon-Lagos, M., et al., *Tamoxifen Resistance: Emerging Molecular Targets.* Int J Mol Sci, 2016. **17**(8).
92. Gutierrez, C. and R. Schiff, *HER2: biology, detection, and clinical implications.* Arch Pathol Lab Med, 2011. **135**(1): p. 55-62.
93. McArthur, H.L. and C.A. Hudis, *Trastuzumab: a picky partner?* Clin Cancer Res, 2009. **15**(20): p. 6311-3.
94. Roskoski, R., Jr., *The ErbB/HER receptor protein-tyrosine kinases and cancer.* Biochem Biophys Res Commun, 2004. **319**(1): p. 1-11.

95. Hudis, C.A., *Trastuzumab--mechanism of action and use in clinical practice.* N Engl J Med, 2007. **357**(1): p. 39-51.
96. Ahmed, S., A. Sami, and J. Xiang, *HER2-directed therapy: current treatment options for HER2-positive breast cancer.* Breast Cancer, 2015. **22**(2): p. 101-16.
97. Valabrega, G., F. Montemurro, and M. Aglietta, *Trastuzumab: mechanism of action, resistance and future perspectives in HER2-overexpressing breast cancer.* Ann Oncol, 2007. **18**(6): p. 977-84.
98. Perez, E.A., et al., *Four-year follow-up of trastuzumab plus adjuvant chemotherapy for operable human epidermal growth factor receptor 2-positive breast cancer: joint analysis of data from NCCTG N9831 and NSABP B-31.* J Clin Oncol, 2011. **29**(25): p. 3366-73.
99. Perez, E.A., et al., *Sequential versus concurrent trastuzumab in adjuvant chemotherapy for breast cancer.* J Clin Oncol, 2011. **29**(34): p. 4491-7.
100. Gianni, L., et al., *Treatment with trastuzumab for 1 year after adjuvant chemotherapy in patients with HER2-positive early breast cancer: a 4-year follow-up of a randomised controlled trial.* Lancet Oncol, 2011. **12**(3): p. 236-44.
101. Slamon, D., et al., *Adjuvant trastuzumab in HER2-positive breast cancer.* N Engl J Med, 2011. **365**(14): p. 1273-83.
102. Joensuu, H., et al., *Fluorouracil, epirubicin, and cyclophosphamide with either docetaxel or vinorelbine, with or without trastuzumab, as adjuvant treatments of breast cancer: final results of the FinHer Trial.* J Clin Oncol, 2009. **27**(34): p. 5685-92.
103. Moja, L., et al., *Trastuzumab containing regimens for early breast cancer.* Cochrane Database Syst Rev, 2012(4): p. CD006243.
104. Petrelli, F., et al., *Neoadjuvant chemotherapy and concomitant trastuzumab in breast cancer: a pooled analysis of two randomized trials.* Anticancer Drugs, 2011. **22**(2): p. 128-35.
105. Dieras, V. and T. Bachelot, *The success story of trastuzumab emtansine, a targeted therapy in HER2-positive breast cancer.* Target Oncol, 2014. **9**(2): p. 111-22.
106. LoRusso, P.M., et al., *Trastuzumab emtansine: a unique antibody-drug conjugate in development for human epidermal growth factor receptor 2-positive cancer.* Clin Cancer Res, 2011. **17**(20): p. 6437-47.
107. Verma, S., et al., *Trastuzumab emtansine for HER2-positive advanced breast cancer.* N Engl J Med, 2012. **367**(19): p. 1783-91.
108. Krop, I.E., et al., *Trastuzumab emtansine versus treatment of physician's choice for pretreated HER2-positive advanced breast cancer (TH3RESA): a randomised, open-label, phase 3 trial.* Lancet Oncol, 2014. **15**(7): p. 689-99.
109. Hurvitz, S.A., et al., *Phase II randomized study of trastuzumab emtansine versus trastuzumab plus docetaxel in patients with human epidermal growth factor receptor 2-positive metastatic breast cancer.* J Clin Oncol, 2013. **31**(9): p. 1157-63.
110. ASCO. *Phase III MARIANNE Trial Results*. 2015 [cited 2017 June 15th]; Available from: https://am.asco.org/phase-iii-marianne-trial-results.
111. Clinicaltrials.gov. *A Study of Trastuzumab Emtansine (T-DM1) Plus Pertuzumab/Pertuzumab Placebo Versus Trastuzumab [Herceptin] Plus a Taxane in Patients With Metastatic Breast Cancer (MARIANNE)*. [cited 2017 June 15th]; Available from: https://clinicaltrials.gov/ct2/show/NCT01120184.
112. Capelan, M., et al., *Pertuzumab: new hope for patients with HER2-positive breast cancer.* Ann Oncol, 2013. **24**(2): p. 273-82.

113. Cho, H.S., et al., *Structure of the extracellular region of HER2 alone and in complex with the Herceptin Fab.* Nature, 2003. **421**(6924): p. 756-60.
114. Fendly, B.M., et al., *Characterization of murine monoclonal antibodies reactive to either the human epidermal growth factor receptor or HER2/neu gene product.* Cancer Res, 1990. **50**(5): p. 1550-8.
115. Minckwitz, G.V., *APHINITY trial (BIG 4-11): A randomized comparison of chemotherapy (C) plus trastuzumab (T) plus placebo (Pla) versus chemotherapy plus trastuzumab (T) plus pertuzumab (P) as adjuvant therapy in patients (pts) with HER2-positive early breast cancer (EBC).* Journal of Clinical Oncology, 2017. **35**.
116. Clinicaltrials.gov. *A study of pertuzumab in addition to chemotherapy and Herceptin (trastzumab) as adjuvant therapy in patients with HER2-positive primary breast cancer.* . 2014 [cited 2017 June 14th]; Available from: http://clinicaltrials.gov/show/NCT01358877.
117. Schneeweiss, A., et al., *Pertuzumab plus trastuzumab in combination with standard neoadjuvant anthracycline-containing and anthracycline-free chemotherapy regimens in patients with HER2-positive early breast cancer: a randomized phase II cardiac safety study (TRYPHAENA).* Ann Oncol, 2013. **24**(9): p. 2278-84.
118. Gianni, L., et al., *Efficacy and safety of neoadjuvant pertuzumab and trastuzumab in women with locally advanced, inflammatory, or early HER2-positive breast cancer (NeoSphere): a randomised multicentre, open-label, phase 2 trial.* Lancet Oncol, 2012. **13**(1): p. 25-32.
119. FDA.gov. *Perjeta*. 2013 [cited 2017 14th June]; Available from: https://www.accessdata.fda.gov/drugsatfda_docs/label/2013/125409s051lbl.pdf.
120. Moreira, C. and V. Kaklamani, *Lapatinib and breast cancer: current indications and outlook for the future.* Expert Rev Anticancer Ther, 2010. **10**(8): p. 1171-82.
121. Arteaga, C.L., et al., *Treatment of HER2-positive breast cancer: current status and future perspectives.* Nat Rev Clin Oncol, 2011. **9**(1): p. 16-32.
122. Montemurro, F., G. Valabrega, and M. Aglietta, *Lapatinib: a dual inhibitor of EGFR and HER2 tyrosine kinase activity.* Expert Opin Biol Ther, 2007. **7**(2): p. 257-68.
123. Goss, P.E., et al., *Adjuvant lapatinib for women with early-stage HER2-positive breast cancer: a randomised, controlled, phase 3 trial.* Lancet Oncol, 2013. **14**(1): p. 88-96.
124. Piccart-Gebhart, M., *First results from the phase III ALTTO trial (BIG 2-06; NCCTG [Alliance] N063D) comparing one year of anti-HER2 therapy with lapatinib alone (L), trastuzumab alone (T), their sequence (T→L), or their combination (T+L) in the adjuvant treatment of HER2-positive early breast cancer (EBC).* Journal of Clinical Oncology, 2014.
125. Baselga, J., et al., *Lapatinib with trastuzumab for HER2-positive early breast cancer (NeoALTTO): a randomised, open-label, multicentre, phase 3 trial.* Lancet, 2012. **379**(9816): p. 633-40.
126. Guarneri, V., et al., *Preoperative chemotherapy plus trastuzumab, lapatinib, or both in human epidermal growth factor receptor 2-positive operable breast cancer: results of the randomized phase II CHER-LOB study.* J Clin Oncol, 2012. **30**(16): p. 1989-95.
127. Untch, M., et al., *Lapatinib versus trastuzumab in combination with neoadjuvant anthracycline-taxane-based chemotherapy (GeparQuinto, GBG 44): a randomised phase 3 trial.* Lancet Oncol, 2012. **13**(2): p. 135-44.

128. Blackwell, K.L., et al., *Randomized study of Lapatinib alone or in combination with trastuzumab in women with ErbB2-positive, trastuzumab-refractory metastatic breast cancer.* J Clin Oncol, 2010. **28**(7): p. 1124-30.
129. Breastcancer.org. *Targeted Therapies*. [cited 2017 14th June]; Available from: http://www.breastcancer.org/treatment/targeted_therapies.
130. Malumbres, M., *CDK4/6 Inhibitors resTORe Therapeutic Sensitivity in HER(2)(+) Breast Cancer.* Cancer Cell, 2016. **29**(3): p. 243-4.
131. Finn, R.S., et al., *The cyclin-dependent kinase 4/6 inhibitor palbociclib in combination with letrozole versus letrozole alone as first-line treatment of oestrogen receptor-positive, HER2-negative, advanced breast cancer (PALOMA-1/TRIO-18): a randomised phase 2 study.* Lancet Oncol, 2015. **16**(1): p. 25-35.
132. FDA.gov. *Palbociclib (IBRANCE)*. [cited 2017 14th June]; Available from: https://ww.fda.gov/drugs/informationondrugs/approveddrugs/ucm549978.htm .
133. Hortobagyi, G.N., et al., *Ribociclib as First-Line Therapy for HR-Positive, Advanced Breast Cancer.* N Engl J Med, 2016. **375**(18): p. 1738-1748.
134. FDA.gov. *Ribociclib (Kisqali)*. [cited 2017 14th June]; Available from: https://www.fda.gov/Drugs/informationondrugs/approveddrugs/ucm546438.htm.
135. Piccart, M., et al., *Everolimus plus exemestane for hormone-receptor-positive, human epidermal growth factor receptor-2-negative advanced breast cancer: overall survival results from BOLERO-2dagger.* Ann Oncol, 2014. **25**(12): p. 2357-62.
136. Zardavas, D., J. Baselga, and M. Piccart, *Emerging targeted agents in metastatic breast cancer.* Nat Rev Clin Oncol, 2013. **10**(4): p. 191-210.
137. Perou, C.M., et al., *Molecular portraits of human breast tumours.* Nature, 2000. **406**(6797): p. 747-52.
138. Sorlie, T., et al., *Gene expression patterns of breast carcinomas distinguish tumor subclasses with clinical implications.* Proc Natl Acad Sci U S A, 2001. **98**(19): p. 10869-74.
139. Perou, C.M., *Molecular stratification of triple-negative breast cancers.* Oncologist, 2010. **15 Suppl 5**: p. 39-48.
140. Prat, A., et al., *Phenotypic and molecular characterization of the claudin-low intrinsic subtype of breast cancer.* Breast Cancer Res, 2010. **12**(5): p. R68.
141. Cancer Genome Atlas, N., *Comprehensive molecular portraits of human breast tumours.* Nature, 2012. **490**(7418): p. 61-70.
142. Prat, A., et al., *Clinical implications of the intrinsic molecular subtypes of breast cancer.* Breast, 2015. **24 Suppl 2**: p. S26-35.
143. Peppercorn, J., C.M. Perou, and L.A. Carey, *Molecular subtypes in breast cancer evaluation and management: divide and conquer.* Cancer Invest, 2008. **26**(1): p. 1-10.
144. Sorlie, T., *Introducing molecular subtyping of breast cancer into the clinic?* J Clin Oncol, 2009. **27**(8): p. 1153-4.
145. Weigelt, B., et al., *Breast cancer molecular profiling with single sample predictors: a retrospective analysis.* Lancet Oncol, 2010. **11**(4): p. 339-49.
146. Parker, J.S., et al., *Supervised risk predictor of breast cancer based on intrinsic subtypes.* J Clin Oncol, 2009. **27**(8): p. 1160-7.
147. Gyorffy, B., et al., *Multigene prognostic tests in breast cancer: past, present, future.* Breast Cancer Res, 2015. **17**: p. 11.
148. Badve, S.B.a.S., *Prognostic and Predictive Gene Expression Signatures in Breast Cancer*, in *Molecular Pathology of Breast Cancer*. 2016. p. 269 - 281.

149. Reis-Filho, J.S. and L. Pusztai, *Gene expression profiling in breast cancer: classification, prognostication, and prediction.* Lancet, 2011. **378**(9805): p. 1812-23.
150. Dubsky, P., et al., *The EndoPredict score provides prognostic information on late distant metastases in ER+/HER2- breast cancer patients.* Br J Cancer, 2013. **109**(12): p. 2959-64.
151. Yeo, B., et al., *Clinical utility of the IHC4+C score in oestrogen receptor-positive early breast cancer: a prospective decision impact study.* Br J Cancer, 2015. **113**(3): p. 390-5.
152. Turnbull, A.K., et al., *Accurate Prediction and Validation of Response to Endocrine Therapy in Breast Cancer.* J Clin Oncol, 2015. **33**(20): p. 2270-8.
153. Weigelt, B. and J.S. Reis-Filho, *Molecular profiling currently offers no more than tumour morphology and basic immunohistochemistry.* Breast Cancer Res, 2010. **12 Suppl 4**: p. S5.
154. Arranz, E.E., et al., *Gene signatures in breast cancer: current and future uses.* Transl Oncol, 2012. **5**(6): p. 398-403.
155. Mook, S., et al., *Individualization of therapy using Mammaprint: from development to the MINDACT Trial.* Cancer Genomics Proteomics, 2007. **4**(3): p. 147-55.
156. Paik, S., et al., *A multigene assay to predict recurrence of tamoxifen-treated, node-negative breast cancer.* N Engl J Med, 2004. **351**(27): p. 2817-26.
157. Chia, S.K., et al., *A 50-gene intrinsic subtype classifier for prognosis and prediction of benefit from adjuvant tamoxifen.* Clin Cancer Res, 2012. **18**(16): p. 4465-72.
158. Ma, X.J., et al., *A five-gene molecular grade index and HOXB13:IL17BR are complementary prognostic factors in early stage breast cancer.* Clin Cancer Res, 2008. **14**(9): p. 2601-8.
159. McKeown, S.R., *Defining normoxia, physoxia and hypoxia in tumours-implications for treatment response.* Br J Radiol, 2014. **87**(1035): p. 20130676.
160. Vaupel, P., M. Hockel, and A. Mayer, *Detection and characterization of tumor hypoxia using pO2 histography.* Antioxid Redox Signal, 2007. **9**(8): p. 1221-35.
161. Vaupel, P., et al., *Oxygenation gain factor: a novel parameter characterizing the association between hemoglobin level and the oxygenation status of breast cancers.* Cancer Res, 2003. **63**(22): p. 7634-7.
162. Rundqvist, H. and R.S. Johnson, *Tumour oxygenation: implications for breast cancer prognosis.* J Intern Med, 2013. **274**(2): p. 105-12.
163. Weis, S.M. and D.A. Cheresh, *Tumor angiogenesis: molecular pathways and therapeutic targets.* Nat Med, 2011. **17**(11): p. 1359-70.
164. Vaupel, P., et al., *Hypoxia in breast cancer: role of blood flow, oxygen diffusion distances, and anemia in the development of oxygen depletion.* Adv Exp Med Biol, 2005. **566**: p. 333-42.
165. Ribatti, D., et al., *The structure of the vascular network of tumors.* Cancer Lett, 2007. **248**(1): p. 18-23.
166. Hohenberger, P., et al., *Tumor oxygenation correlates with molecular growth determinants in breast cancer.* Breast Cancer Res Treat, 1998. **48**(2): p. 97-106.
167. Cornfield, D.B., et al., *The prognostic significance of multiple morphologic features and biologic markers in ductal carcinoma in situ of the breast: a study of a large cohort of patients treated with surgery alone.* Cancer, 2004. **100**(11): p. 2317-27.

168. Chaudary, N. and R.P. Hill, *Hypoxia and metastasis in breast cancer.* Breast Dis, 2006. **26**: p. 55-64.
169. Vaupel, P., S. Briest, and M. Hockel, *Hypoxia in breast cancer: pathogenesis, characterization and biological/therapeutic implications.* Wien Med Wochenschr, 2002. **152**(13-14): p. 334-42.
170. Ward, C., et al., *New strategies for targeting the hypoxic tumour microenvironment in breast cancer.* Cancer Treat Rev, 2013. **39**(2): p. 171-9.
171. Gatenby, R.A., et al., *Cellular adaptations to hypoxia and acidosis during somatic evolution of breast cancer.* Br J Cancer, 2007. **97**(5): p. 646-53.
172. Keith, B. and M.C. Simon, *Hypoxia-inducible factors, stem cells, and cancer.* Cell, 2007. **129**(3): p. 465-72.
173. Semenza, G.L., *Hypoxia-inducible factors: mediators of cancer progression and targets for cancer therapy.* Trends Pharmacol Sci, 2012. **33**(4): p. 207-14.
174. Wang, G.L. and G.L. Semenza, *Purification and characterization of hypoxia-inducible factor 1.* J Biol Chem, 1995. **270**(3): p. 1230-7.
175. Hogenesch, J.B., et al., *Characterization of a subset of the basic-helix-loop-helix-PAS superfamily that interacts with components of the dioxin signaling pathway.* J Biol Chem, 1997. **272**(13): p. 8581-93.
176. Wang, G.L., et al., *Hypoxia-inducible factor 1 is a basic-helix-loop-helix-PAS heterodimer regulated by cellular O2 tension.* Proc Natl Acad Sci U S A, 1995. **92**(12): p. 5510-4.
177. Flamme, I., et al., *HRF, a putative basic helix-loop-helix-PAS-domain transcription factor is closely related to hypoxia-inducible factor-1 alpha and developmentally expressed in blood vessels.* Mech Dev, 1997. **63**(1): p. 51-60.
178. Ema, M., et al., *A novel bHLH-PAS factor with close sequence similarity to hypoxia-inducible factor 1alpha regulates the VEGF expression and is potentially involved in lung and vascular development.* Proc Natl Acad Sci U S A, 1997. **94**(9): p. 4273-8.
179. Hara, S., et al., *Expression and characterization of hypoxia-inducible factor (HIF)-3alpha in human kidney: suppression of HIF-mediated gene expression by HIF-3alpha.* Biochem Biophys Res Commun, 2001. **287**(4): p. 808-13.
180. Semenza, G.L., *Oxygen sensing, hypoxia-inducible factors, and disease pathophysiology.* Annu Rev Pathol, 2014. **9**: p. 47-71.
181. Lisy, K. and D.J. Peet, *Turn me on: regulating HIF transcriptional activity.* Cell Death Differ, 2008. **15**(4): p. 642-9.
182. Kenneth, N.S. and S. Rocha, *Regulation of gene expression by hypoxia.* Biochem J, 2008. **414**(1): p. 19-29.
183. Duan, C., *Hypoxia-inducible factor 3 biology: complexities and emerging themes.* Am J Physiol Cell Physiol, 2016. **310**(4): p. C260-9.
184. Majmundar, A.J., W.J. Wong, and M.C. Simon, *Hypoxia-inducible factors and the response to hypoxic stress.* Mol Cell, 2010. **40**(2): p. 294-309.
185. Makino, Y., et al., *Inhibitory PAS domain protein is a negative regulator of hypoxia-inducible gene expression.* Nature, 2001. **414**(6863): p. 550-4.
186. Heidbreder, M., et al., *Hypoxia rapidly activates HIF-3alpha mRNA expression.* FASEB J, 2003. **17**(11): p. 1541-3.
187. Makino, Y., et al., *Inhibitory PAS domain protein (IPAS) is a hypoxia-inducible splicing variant of the hypoxia-inducible factor-3alpha locus.* J Biol Chem, 2002. **277**(36): p. 32405-8.

188. Zhang, P., et al., *Hypoxia-inducible factor 3 is an oxygen-dependent transcription activator and regulates a distinct transcriptional response to hypoxia.* Cell Rep, 2014. **6**(6): p. 1110-21.
189. Zagorska, A. and J. Dulak, *HIF-1: the knowns and unknowns of hypoxia sensing.* Acta Biochim Pol, 2004. **51**(3): p. 563-85.
190. Bardos, J.I. and M. Ashcroft, *Negative and positive regulation of HIF-1: a complex network.* Biochim Biophys Acta, 2005. **1755**(2): p. 107-20.
191. Rocha, S., *Gene regulation under low oxygen: holding your breath for transcription.* Trends Biochem Sci, 2007. **32**(8): p. 389-97.
192. Semenza, G.L., *HIF-1 and mechanisms of hypoxia sensing.* Curr Opin Cell Biol, 2001. **13**(2): p. 167-71.
193. Yu, F., et al., *HIF-1alpha binding to VHL is regulated by stimulus-sensitive proline hydroxylation.* Proc Natl Acad Sci U S A, 2001. **98**(17): p. 9630-5.
194. Schofield, C.J. and P.J. Ratcliffe, *Oxygen sensing by HIF hydroxylases.* Nat Rev Mol Cell Biol, 2004. **5**(5): p. 343-54.
195. Semenza, G.L., *Hydroxylation of HIF-1: oxygen sensing at the molecular level.* Physiology (Bethesda), 2004. **19**: p. 176-82.
196. Appelhoff, R.J., et al., *Differential function of the prolyl hydroxylases PHD1, PHD2, and PHD3 in the regulation of hypoxia-inducible factor.* Journal of Biological Chemistry, 2004. **279**(37): p. 38458-38465.
197. Huang, L.E., et al., *Regulation of hypoxia-inducible factor 1alpha is mediated by an O2-dependent degradation domain via the ubiquitin-proteasome pathway.* Proc Natl Acad Sci U S A, 1998. **95**(14): p. 7987-92.
198. Ivan, M., et al., *HIFalpha targeted for VHL-mediated destruction by proline hydroxylation: implications for O2 sensing.* Science, 2001. **292**(5516): p. 464-8.
199. Jaakkola, P., et al., *Targeting of HIF-alpha to the von Hippel-Lindau ubiquitylation complex by O2-regulated prolyl hydroxylation.* Science, 2001. **292**(5516): p. 468-72.
200. Wenger, R.H., *Cellular adaptation to hypoxia: O2-sensing protein hydroxylases, hypoxia-inducible transcription factors, and O2-regulated gene expression.* FASEB J, 2002. **16**(10): p. 1151-62.
201. Mahon, P.C., K. Hirota, and G.L. Semenza, *FIH-1: a novel protein that interacts with HIF-1alpha and VHL to mediate repression of HIF-1 transcriptional activity.* Genes Dev, 2001. **15**(20): p. 2675-86.
202. Baek, J.H., et al., *OS-9 interacts with hypoxia-inducible factor 1alpha and prolyl hydroxylases to promote oxygen-dependent degradation of HIF-1alpha.* Mol Cell, 2005. **17**(4): p. 503-12.
203. Baek, J.H., et al., *Spermidine/spermine-N1-acetyltransferase 2 is an essential component of the ubiquitin ligase complex that regulates hypoxia-inducible factor 1alpha.* J Biol Chem, 2007. **282**(32): p. 23572-80.
204. Yee Koh, M., T.R. Spivak-Kroizman, and G. Powis, *HIF-1 regulation: not so easy come, easy go.* Trends Biochem Sci, 2008. **33**(11): p. 526-34.
205. Li, Z., et al., *VHL protein-interacting deubiquitinating enzyme 2 deubiquitinates and stabilizes HIF-1alpha.* EMBO Rep, 2005. **6**(4): p. 373-8.
206. Jung, C.R., et al., *E2-EPF UCP targets pVHL for degradation and associates with tumor growth and metastasis.* Nat Med, 2006. **12**(7): p. 809-16.
207. Liu, Y.V., et al., *RACK1 competes with HSP90 for binding to HIF-1alpha and is required for O(2)-independent and HSP90 inhibitor-induced degradation of HIF-1alpha.* Mol Cell, 2007. **25**(2): p. 207-17.
208. Liu, Y.V., et al., *Calcineurin promotes hypoxia-inducible factor 1alpha expression by dephosphorylating RACK1 and blocking RACK1 dimerization.* J Biol Chem, 2007. **282**(51): p. 37064-73.

209. Flugel, D., et al., *Glycogen synthase kinase 3 phosphorylates hypoxia-inducible factor 1alpha and mediates its destabilization in a VHL-independent manner.* Mol Cell Biol, 2007. **27**(9): p. 3253-65.
210. Tang, T.T. and L.A. Lasky, *The forkhead transcription factor FOXO4 induces the down-regulation of hypoxia-inducible factor 1 alpha by a von Hippel-Lindau protein-independent mechanism.* J Biol Chem, 2003. **278**(32): p. 30125-35.
211. Zundel, W., et al., *Loss of PTEN facilitates HIF-1-mediated gene expression.* Genes Dev, 2000. **14**(4): p. 391-6.
212. Stiehl, D.P., et al., *Normoxic induction of the hypoxia-inducible factor 1alpha by insulin and interleukin-1beta involves the phosphatidylinositol 3-kinase pathway.* FEBS Lett, 2002. **512**(1-3): p. 157-62.
213. Koumenis, C. and B.G. Wouters, *"Translating" tumor hypoxia: unfolded protein response (UPR)-dependent and UPR-independent pathways.* Mol Cancer Res, 2006. **4**(7): p. 423-36.
214. Liu, L., et al., *Hypoxia-induced energy stress regulates mRNA translation and cell growth.* Mol Cell, 2006. **21**(4): p. 521-31.
215. Braunstein, S., et al., *A hypoxia-controlled cap-dependent to cap-independent translation switch in breast cancer.* Mol Cell, 2007. **28**(3): p. 501-12.
216. Zhou, J. and B. Brune, *Cytokines and hormones in the regulation of hypoxia inducible factor-1alpha (HIF-1alpha).* Cardiovasc Hematol Agents Med Chem, 2006. **4**(3): p. 189-97.
217. Fukuda, R., et al., *Insulin-like growth factor 1 induces hypoxia-inducible factor 1-mediated vascular endothelial growth factor expression, which is dependent on MAP kinase and phosphatidylinositol 3-kinase signaling in colon cancer cells.* J Biol Chem, 2002. **277**(41): p. 38205-11.
218. Zhong, H., et al., *Modulation of hypoxia-inducible factor 1alpha expression by the epidermal growth factor/phosphatidylinositol 3-kinase/PTEN/AKT/FRAP pathway in human prostate cancer cells: implications for tumor angiogenesis and therapeutics.* Cancer Res, 2000. **60**(6): p. 1541-5.
219. Treins, C., et al., *Insulin stimulates hypoxia-inducible factor 1 through a phosphatidylinositol 3-kinase/target of rapamycin-dependent signaling pathway.* J Biol Chem, 2002. **277**(31): p. 27975-81.
220. Laughner, E., et al., *HER2 (neu) signaling increases the rate of hypoxia-inducible factor 1alpha (HIF-1alpha) synthesis: novel mechanism for HIF-1-mediated vascular endothelial growth factor expression.* Mol Cell Biol, 2001. **21**(12): p. 3995-4004.
221. Gorlach, A., *Regulation of HIF-1alpha at the transcriptional level.* Curr Pharm Des, 2009. **15**(33): p. 3844-52.
222. Page, E.L., et al., *Induction of hypoxia-inducible factor-1alpha by transcriptional and translational mechanisms.* J Biol Chem, 2002. **277**(50): p. 48403-9.
223. Bonello, S., et al., *Reactive oxygen species activate the HIF-1alpha promoter via a functional NFkappaB site.* Arterioscler Thromb Vasc Biol, 2007. **27**(4): p. 755-61.
224. Deudero, J.J., et al., *Induction of hypoxia-inducible factor 1alpha gene expression by vascular endothelial growth factor.* J Biol Chem, 2008. **283**(17): p. 11435-44.
225. Tacchini, L., et al., *Hepatocyte growth factor-activated NF-kappaB regulates HIF-1 activity and ODC expression, implicated in survival, differently in different carcinoma cell lines.* Carcinogenesis, 2004. **25**(11): p. 2089-100.

226. Belaiba, R.S., et al., *Hypoxia up-regulates hypoxia-inducible factor-1alpha transcription by involving phosphatidylinositol 3-kinase and nuclear factor kappaB in pulmonary artery smooth muscle cells.* Mol Biol Cell, 2007. **18**(12): p. 4691-7.
227. Rius, J., et al., *NF-kappaB links innate immunity to the hypoxic response through transcriptional regulation of HIF-1alpha.* Nature, 2008. **453**(7196): p. 807-11.
228. Tian, H., et al., *The hypoxia-responsive transcription factor EPAS1 is essential for catecholamine homeostasis and protection against heart failure during embryonic development.* Genes Dev, 1998. **12**(21): p. 3320-4.
229. Scortegagna, M., et al., *The HIF family member EPAS1/HIF-2alpha is required for normal hematopoiesis in mice.* Blood, 2003. **102**(5): p. 1634-40.
230. Peng, J., et al., *The transcription factor EPAS-1/hypoxia-inducible factor 2alpha plays an important role in vascular remodeling.* Proc Natl Acad Sci U S A, 2000. **97**(15): p. 8386-91.
231. Covello, K.L., et al., *HIF-2alpha regulates Oct-4: effects of hypoxia on stem cell function, embryonic development, and tumor growth.* Genes Dev, 2006. **20**(5): p. 557-70.
232. Covello, K.L., M.C. Simon, and B. Keith, *Targeted replacement of hypoxia-inducible factor-1alpha by a hypoxia-inducible factor-2alpha knock-in allele promotes tumor growth.* Cancer Res, 2005. **65**(6): p. 2277-86.
233. Maranchie, J.K., et al., *The contribution of VHL substrate binding and HIF1-alpha to the phenotype of VHL loss in renal cell carcinoma.* Cancer Cell, 2002. **1**(3): p. 247-55.
234. Kondo, K., et al., *Inhibition of HIF2alpha is sufficient to suppress pVHL-defective tumor growth.* PLoS Biol, 2003. **1**(3): p. E83.
235. Raval, R.R., et al., *Contrasting properties of hypoxia-inducible factor 1 (HIF-1) and HIF-2 in von Hippel-Lindau-associated renal cell carcinoma.* Mol Cell Biol, 2005. **25**(13): p. 5675-86.
236. Hu, C.J., et al., *Differential roles of hypoxia-inducible factor 1alpha (HIF-1alpha) and HIF-2alpha in hypoxic gene regulation.* Mol Cell Biol, 2003. **23**(24): p. 9361-74.
237. Warnecke, C., et al., *Differentiating the functional role of hypoxia-inducible factor (HIF)-1alpha and HIF-2alpha (EPAS-1) by the use of RNA interference: erythropoietin is a HIF-2alpha target gene in Hep3B and Kelly cells.* FASEB J, 2004. **18**(12): p. 1462-4.
238. Wang, V., et al., *Differential gene up-regulation by hypoxia-inducible factor-1alpha and hypoxia-inducible factor-2alpha in HEK293T cells.* Cancer Res, 2005. **65**(8): p. 3299-306.
239. Mole, D.R., et al., *Genome-wide association of hypoxia-inducible factor (HIF)-1alpha and HIF-2alpha DNA binding with expression profiling of hypoxia-inducible transcripts.* J Biol Chem, 2009. **284**(25): p. 16767-75.
240. Schodel, J., et al., *High-resolution genome-wide mapping of HIF-binding sites by ChIP-seq.* Blood, 2011. **117**(23): p. e207-17.
241. Dayan, F., et al., *The oxygen sensor factor-inhibiting hypoxia-inducible factor-1 controls expression of distinct genes through the bifunctional transcriptional character of hypoxia-inducible factor-1alpha.* Cancer Res, 2006. **66**(7): p. 3688-98.
242. Hu, C.J., et al., *The N-terminal transactivation domain confers target gene specificity of hypoxia-inducible factors HIF-1alpha and HIF-2alpha.* Mol Biol Cell, 2007. **18**(11): p. 4528-42.

243. Aprelikova, O., et al., *Role of ETS transcription factors in the hypoxia-inducible factor-2 target gene selection.* Cancer Res, 2006. **66**(11): p. 5641-7.
244. Koshiji, M., et al., *HIF-1alpha induces cell cycle arrest by functionally counteracting Myc.* EMBO J, 2004. **23**(9): p. 1949-56.
245. Gordan, J.D., C.B. Thompson, and M.C. Simon, *HIF and c-Myc: sibling rivals for control of cancer cell metabolism and proliferation.* Cancer Cell, 2007. **12**(2): p. 108-13.
246. Zhang, H., et al., *HIF-1 inhibits mitochondrial biogenesis and cellular respiration in VHL-deficient renal cell carcinoma by repression of C-MYC activity.* Cancer Cell, 2007. **11**(5): p. 407-20.
247. Corn, P.G., et al., *Mxi1 is induced by hypoxia in a HIF-1-dependent manner and protects cells from c-Myc-induced apoptosis.* Cancer Biol Ther, 2005. **4**(11): p. 1285-94.
248. Gordan, J.D., et al., *HIF-2alpha promotes hypoxic cell proliferation by enhancing c-myc transcriptional activity.* Cancer Cell, 2007. **11**(4): p. 335-47.
249. Keith, B., R.S. Johnson, and M.C. Simon, *HIF1alpha and HIF2alpha: sibling rivalry in hypoxic tumour growth and progression.* Nat Rev Cancer, 2011. **12**(1): p. 9-22.
250. Vousden, K.H. and C. Prives, *Blinded by the Light: The Growing Complexity of p53.* Cell, 2009. **137**(3): p. 413-31.
251. Lavin, M.F. and N. Gueven, *The complexity of p53 stabilization and activation.* Cell Death Differ, 2006. **13**(6): p. 941-50.
252. Sanchez-Puig, N., D.B. Veprintsev, and A.R. Fersht, *Binding of natively unfolded HIF-1alpha ODD domain to p53.* Mol Cell, 2005. **17**(1): p. 11-21.
253. Chen, D., et al., *Direct interactions between HIF-1 alpha and Mdm2 modulate p53 function.* J Biol Chem, 2003. **278**(16): p. 13595-8.
254. Bertout, J.A., et al., *HIF2alpha inhibition promotes p53 pathway activity, tumor cell death, and radiation responses.* Proc Natl Acad Sci U S A, 2009. **106**(34): p. 14391-6.
255. Roberts, A.M., et al., *Suppression of hypoxia-inducible factor 2alpha restores p53 activity via Hdm2 and reverses chemoresistance of renal carcinoma cells.* Cancer Res, 2009. **69**(23): p. 9056-64.
256. Brugarolas, J., et al., *Regulation of mTOR function in response to hypoxia by REDD1 and the TSC1/TSC2 tumor suppressor complex.* Genes Dev, 2004. **18**(23): p. 2893-904.
257. Li, Y., et al., *Bnip3 mediates the hypoxia-induced inhibition on mammalian target of rapamycin by interacting with Rheb.* J Biol Chem, 2007. **282**(49): p. 35803-13.
258. Gan, B., et al., *Identification of FIP200 interaction with the TSC1-TSC2 complex and its role in regulation of cell size control.* J Cell Biol, 2005. **170**(3): p. 379-89.
259. Wiesener, M.S., et al., *Induction of endothelial PAS domain protein-1 by hypoxia: characterization and comparison with hypoxia-inducible factor-1alpha.* Blood, 1998. **92**(7): p. 2260-8.
260. Lando, D., et al., *Oxygen-dependent regulation of hypoxia-inducible factors by prolyl and asparaginyl hydroxylation.* Eur J Biochem, 2003. **270**(5): p. 781-90.
261. Helczynska, K., et al., *Hypoxia-inducible factor-2alpha correlates to distant recurrence and poor outcome in invasive breast cancer.* Cancer Res, 2008. **68**(22): p. 9212-20.

262. Bracken, C.P., et al., *Cell-specific regulation of hypoxia-inducible factor (HIF)-1alpha and HIF-2alpha stabilization and transactivation in a graded oxygen environment.* J Biol Chem, 2006. **281**(32): p. 22575-85.
263. Koh, M.Y., B.G. Darnay, and G. Powis, *Hypoxia-associated factor, a novel E3-ubiquitin ligase, binds and ubiquitinates hypoxia-inducible factor 1alpha, leading to its oxygen-independent degradation.* Mol Cell Biol, 2008. **28**(23): p. 7081-95.
264. Koh, M.Y., et al., *The hypoxia-associated factor switches cells from HIF-1alpha- to HIF-2alpha-dependent signaling promoting stem cell characteristics, aggressive tumor growth and invasion.* Cancer Res, 2011. **71**(11): p. 4015-27.
265. Koh, M.Y. and G. Powis, *Passing the baton: the HIF switch.* Trends Biochem Sci, 2012. **37**(9): p. 364-72.
266. Koh, M.Y. and G. Powis, *HAF : the new player in oxygen-independent HIF-1alpha degradation.* Cell Cycle, 2009. **8**(9): p. 1359-66.
267. Chen, L., et al., *Mammalian tumor suppressor Int6 specifically targets hypoxia inducible factor 2 alpha for degradation by hypoxia- and pVHL-independent regulation.* J Biol Chem, 2007. **282**(17): p. 12707-16.
268. Marchetti, A., et al., *Int-6, a highly conserved, widely expressed gene, is mutated by mouse mammary tumor virus in mammary preneoplasia.* J Virol, 1995. **69**(3): p. 1932-8.
269. Mayeur, G.L. and J.W. Hershey, *Malignant transformation by the eukaryotic translation initiation factor 3 subunit p48 (eIF3e).* FEBS Lett, 2002. **514**(1): p. 49-54.
270. Berra, E., et al., *HIF prolyl-hydroxylase 2 is the key oxygen sensor setting low steady-state levels of HIF-1 alpha in normoxia.* Embo Journal, 2003. **22**(16): p. 4082-4090.
271. Aprelikova, O., et al., *Regulation of HIF prolyl hydroxylases by hypoxia-inducible factors.* Journal of Cellular Biochemistry, 2004. **92**(3): p. 491-501.
272. Jokilehto, T. and P.M. Jaakkola, *The role of HIF prolyl hydroxylases in tumour growth.* Journal of Cellular and Molecular Medicine, 2010. **14**(4): p. 758-770.
273. Soilleux, E.J., et al., *Use of novel monoclonal antibodies to determine the expression and distribution of the hypoxia regulatory factors PHD-1, PHD-2, PHD-3 and FIH in normal and neoplastic human tissues.* Histopathology, 2005. **47**(6): p. 602-610.
274. Tan, E.Y., et al., *The key hypoxia regulated gene CAIX is upregulated in basal-like breast tumours and is associated with resistance to chemotherapy.* British Journal of Cancer, 2009. **100**(2): p. 405-411.
275. Jokilehto, T., et al., *Overexpression and nuclear translocation of hypoxia-inducible factor prolyl hydroxylase PHD2 in head and neck squamous cell carcinoma is associated with tumor aggressiveness.* Clinical Cancer Research, 2006. **12**(4): p. 1080-1087.
276. Couvelard, A., et al., *Overexpression of the Oxygen Sensors PHD-1, PHD-2, PHD-3, and FIH Is Associated with Tumor Aggressiveness in Pancreatic Endocrine Tumors.* Clinical Cancer Research, 2008. **14**(20): p. 6634-6639.
277. Seth, P., et al., *Novel estrogen and tamoxifen induced genes identified by SAGE (Serial Analysis of Gene Expression).* Oncogene, 2002. **21**(5): p. 836-843.
278. Lu, X.S., et al., *Predicting features of breast cancer with gene expression patterns.* Breast Cancer Research and Treatment, 2008. **108**(2): p. 191-201.
279. Zhang, Q., et al., *Control of Cyclin D1 and Breast Tumorigenesis by the EgIN2 Prolyl Hydroxylase.* Cancer Cell, 2009. **16**(5): p. 413-424.

280. Sanchez, M., et al., *Iron-regulatory proteins limit hypoxia-inducible factor-2alpha expression in iron deficiency.* Nat Struct Mol Biol, 2007. **14**(5): p. 420-6.
281. Mastrogiannaki, M., et al., *HIF-2alpha, but not HIF-1alpha, promotes iron absorption in mice.* J Clin Invest, 2009. **119**(5): p. 1159-66.
282. Morita, M., et al., *HLF/HIF-2alpha is a key factor in retinopathy of prematurity in association with erythropoietin.* EMBO J, 2003. **22**(5): p. 1134-46.
283. Zimmer, M., et al., *Small-molecule inhibitors of HIF-2a translation link its 5'UTR iron-responsive element to oxygen sensing.* Mol Cell, 2008. **32**(6): p. 838-48.
284. Dales, J.P., et al., *Overexpression of hypoxia-inducible factor HIF-1alpha predicts early relapse in breast cancer: retrospective study in a series of 745 patients.* Int J Cancer, 2005. **116**(5): p. 734-9.
285. Bos, R., et al., *Levels of hypoxia-inducible factor-1alpha independently predict prognosis in patients with lymph node negative breast carcinoma.* Cancer, 2003. **97**(6): p. 1573-81.
286. Schindl, M., et al., *Overexpression of hypoxia-inducible factor 1alpha is associated with an unfavorable prognosis in lymph node-positive breast cancer.* Clin Cancer Res, 2002. **8**(6): p. 1831-7.
287. Gruber, G., et al., *Hypoxia-inducible factor 1 alpha in high-risk breast cancer: an independent prognostic parameter?* Breast Cancer Res, 2004. **6**(3): p. R191-8.
288. Generali, D., et al., *Hypoxia-inducible factor-1alpha expression predicts a poor response to primary chemoendocrine therapy and disease-free survival in primary human breast cancer.* Clin Cancer Res, 2006. **12**(15): p. 4562-8.
289. Kronblad, A., et al., *Hypoxia inducible factor-1alpha is a prognostic marker in premenopausal patients with intermediate to highly differentiated breast cancer but not a predictive marker for tamoxifen response.* Int J Cancer, 2006. **118**(10): p. 2609-16.
290. Trastour, C., et al., *HIF-1alpha and CA IX staining in invasive breast carcinomas: prognosis and treatment outcome.* Int J Cancer, 2007. **120**(7): p. 1451-8.
291. Yamamoto, Y., et al., *Hypoxia-inducible factor 1alpha is closely linked to an aggressive phenotype in breast cancer.* Breast Cancer Res Treat, 2008. **110**(3): p. 465-75.
292. Vleugel, M.M., et al., *Differential prognostic impact of hypoxia induced and diffuse HIF-1alpha expression in invasive breast cancer.* J Clin Pathol, 2005. **58**(2): p. 172-7.
293. Giatromanolaki, A., et al., *c-erbB-2 related aggressiveness in breast cancer is hypoxia inducible factor-1alpha dependent.* Clin Cancer Res, 2004. **10**(23): p. 7972-7.
294. Liao, D. and R.S. Johnson, *Hypoxia: a key regulator of angiogenesis in cancer.* Cancer Metastasis Rev, 2007. **26**(2): p. 281-90.
295. Liu, Z.J., G.L. Semenza, and H.F. Zhang, *Hypoxia-inducible factor 1 and breast cancer metastasis.* J Zhejiang Univ Sci B, 2015. **16**(1): p. 32-43.
296. Semenza, G.L., *Regulation of the breast cancer stem cell phenotype by hypoxia-inducible factors.* Clin Sci (Lond), 2015. **129**(12): p. 1037-45.
297. Samanta, D., et al., *Hypoxia-inducible factors are required for chemotherapy resistance of breast cancer stem cells.* Proc Natl Acad Sci U S A, 2014. **111**(50): p. E5429-38.
298. Coradini, D., et al., *Hypoxia and estrogen receptor profile influence the responsiveness of human breast cancer cells to estradiol and antiestrogens.* Cell Mol Life Sci, 2004. **61**(1): p. 76-82.

299. Bos, R., et al., *Levels of hypoxia-inducible factor-1 alpha during breast carcinogenesis.* J Natl Cancer Inst, 2001. **93**(4): p. 309-14.
300. Chaffer, C.L. and R.A. Weinberg, *A perspective on cancer cell metastasis.* Science, 2011. **331**(6024): p. 1559-64.
301. Valastyan, S. and R.A. Weinberg, *Tumor metastasis: molecular insights and evolving paradigms.* Cell, 2011. **147**(2): p. 275-92.
302. Krishnamachary, B., et al., *Hypoxia-inducible factor-1-dependent repression of E-cadherin in von Hippel-Lindau tumor suppressor-null renal cell carcinoma mediated by TCF3, ZFHX1A, and ZFHX1B.* Cancer Res, 2006. **66**(5): p. 2725-31.
303. Moreno-Bueno, G., F. Portillo, and A. Cano, *Transcriptional regulation of cell polarity in EMT and cancer.* Oncogene, 2008. **27**(55): p. 6958-69.
304. Hugo, H.J., et al., *Direct repression of MYB by ZEB1 suppresses proliferation and epithelial gene expression during epithelial-to-mesenchymal transition of breast cancer cells.* Breast Cancer Res, 2013. **15**(6): p. R113.
305. Munoz-Najar, U.M., et al., *Hypoxia stimulates breast carcinoma cell invasion through MT1-MMP and MMP-2 activation.* Oncogene, 2006. **25**(16): p. 2379-92.
306. Duffy, M.J., et al., *Metalloproteinases: role in breast carcinogenesis, invasion and metastasis.* Breast Cancer Res, 2000. **2**(4): p. 252-7.
307. Pritchard, S.C., et al., *Expression of matrix metalloproteinases 1, 2, 9 and their tissue inhibitors in stage II non-small cell lung cancer: implications for MMP inhibition therapy.* Oncol Rep, 2001. **8**(2): p. 421-4.
308. Incorvaia, L., et al., *MMP-2, MMP-9 and activin A blood levels in patients with breast cancer or prostate cancer metastatic to the bone.* Anticancer Res, 2007. **27**(3B): p. 1519-25.
309. Gilkes, D.M., et al., *Hypoxia-inducible factor 1 (HIF-1) promotes extracellular matrix remodeling under hypoxic conditions by inducing P4HA1, P4HA2, and PLOD2 expression in fibroblasts.* J Biol Chem, 2013. **288**(15): p. 10819-29.
310. Zhang, H., et al., *HIF-1-dependent expression of angiopoietin-like 4 and L1CAM mediates vascular metastasis of hypoxic breast cancer cells to the lungs.* Oncogene, 2012. **31**(14): p. 1757-70.
311. Padua, D., et al., *TGFbeta primes breast tumors for lung metastasis seeding through angiopoietin-like 4.* Cell, 2008. **133**(1): p. 66-77.
312. Erler, J.T. and A.J. Giaccia, *Lysyl oxidase mediates hypoxic control of metastasis.* Cancer Res, 2006. **66**(21): p. 10238-41.
313. Erler, J.T., et al., *Hypoxia-induced lysyl oxidase is a critical mediator of bone marrow cell recruitment to form the premetastatic niche.* Cancer Cell, 2009. **15**(1): p. 35-44.
314. Erler, J.T., et al., *Lysyl oxidase is essential for hypoxia-induced metastasis.* Nature, 2006. **440**(7088): p. 1222-6.
315. Wong, C.C., et al., *Hypoxia-inducible factor 1 is a master regulator of breast cancer metastatic niche formation.* Proc Natl Acad Sci U S A, 2011. **108**(39): p. 16369-74.
316. Moeller, B.J. and M.W. Dewhirst, *Raising the bar: how HIF-1 helps determine tumor radiosensitivity.* Cell Cycle, 2004. **3**(9): p. 1107-10.
317. Sullivan, R., et al., *Hypoxia-induced resistance to anticancer drugs is associated with decreased senescence and requires hypoxia-inducible factor-1 activity.* Mol Cancer Ther, 2008. **7**(7): p. 1961-73.
318. Xiang, L., et al., *Hypoxia-inducible factor 1 mediates TAZ expression and nuclear localization to induce the breast cancer stem cell phenotype.* Oncotarget, 2014. **5**(24): p. 12509-27.

319. Talks, K.L., et al., *The expression and distribution of the hypoxia-inducible factors HIF-1alpha and HIF-2alpha in normal human tissues, cancers, and tumor-associated macrophages.* Am J Pathol, 2000. **157**(2): p. 411-21.
320. Leek, R.D., et al., *Relation of hypoxia-inducible factor-2 alpha (HIF-2 alpha) expression in tumor-infiltrative macrophages to tumor angiogenesis and the oxidative thymidine phosphorylase pathway in Human breast cancer.* Cancer Res, 2002. **62**(5): p. 1326-9.
321. Giatromanolaki, A., et al., *Hypoxia-inducible factor-2 alpha (HIF-2 alpha) induces angiogenesis in breast carcinomas.* Appl Immunohistochem Mol Morphol, 2006. **14**(1): p. 78-82.
322. Patel, S.A. and M.C. Simon, *Biology of hypoxia-inducible factor-2alpha in development and disease.* Cell Death Differ, 2008. **15**(4): p. 628-34.
323. Gort, E.H., et al., *The TWIST1 oncogene is a direct target of hypoxia-inducible factor-2alpha.* Oncogene, 2008. **27**(11): p. 1501-10.
324. Staller, P., et al., *Chemokine receptor CXCR4 downregulated by von Hippel-Lindau tumour suppressor pVHL.* Nature, 2003. **425**(6955): p. 307-11.
325. Burger, A.M., et al., *Essential roles of IGFBP-3 and IGFBP-rP1 in breast cancer.* Eur J Cancer, 2005. **41**(11): p. 1515-27.
326. Brantley-Sieders, D.M., et al., *Ephrin-A1 facilitates mammary tumor metastasis through an angiogenesis-dependent mechanism mediated by EphA receptor and vascular endothelial growth factor in mice.* Cancer Res, 2006. **66**(21): p. 10315-24.
327. Ahn, S.G., et al., *LOXL2 expression is associated with invasiveness and negatively influences survival in breast cancer patients.* Breast Cancer Res Treat, 2013. **141**(1): p. 89-99.
328. Chen, J., et al., *Hypoxia potentiates Notch signaling in breast cancer leading to decreased E-cadherin expression and increased cell migration and invasion.* Br J Cancer, 2010. **102**(2): p. 351-60.
329. Elvert, G., et al., *Cooperative interaction of hypoxia-inducible factor-2alpha (HIF-2alpha) and Ets-1 in the transcriptional activation of vascular endothelial growth factor receptor-2 (Flk-1).* J Biol Chem, 2003. **278**(9): p. 7520-30.
330. Jogi, A., et al., *Hypoxia alters gene expression in human neuroblastoma cells toward an immature and neural crest-like phenotype.* Proc Natl Acad Sci U S A, 2002. **99**(10): p. 7021-6.
331. Helczynska, K., et al., *Hypoxia promotes a dedifferentiated phenotype in ductal breast carcinoma in situ.* Cancer Res, 2003. **63**(7): p. 1441-4.
332. Zhang, C., et al., *Hypoxia induces the breast cancer stem cell phenotype by HIF-dependent and ALKBH5-mediated m(6)A-demethylation of NANOG mRNA.* Proc Natl Acad Sci U S A, 2016. **113**(14): p. E2047-56.
333. Wigerup, C., S. Pahlman, and D. Bexell, *Therapeutic targeting of hypoxia and hypoxia-inducible factors in cancer.* Pharmacol Ther, 2016. **164**: p. 152-69.
334. Denny, W.A., *The role of hypoxia-activated prodrugs in cancer therapy.* Lancet Oncol, 2000. **1**(1): p. 25-9.
335. Phillips, R.M., *Targeting the hypoxic fraction of tumours using hypoxia-activated prodrugs.* Cancer Chemother Pharmacol, 2016. **77**(3): p. 441-57.
336. Rischin, D., et al., *Tirapazamine, cisplatin, and radiation versus cisplatin and radiation for advanced squamous cell carcinoma of the head and neck (TROG 02.02, HeadSTART): a phase III trial of the Trans-Tasman Radiation Oncology Group.* J Clin Oncol, 2010. **28**(18): p. 2989-95.
337. Phillips, R.M., et al., *EO9 (Apaziquone): from the clinic to the laboratory and back again.* Br J Pharmacol, 2013. **168**(1): p. 11-8.

338. Hicks, K.O., et al., *Pharmacokinetic/pharmacodynamic modeling identifies SN30000 and SN29751 as tirapazamine analogues with improved tissue penetration and hypoxic cell killing in tumors.* Clin Cancer Res, 2010. **16**(20): p. 4946-57.
339. Borad, M.J., et al., *Randomized Phase II Trial of Gemcitabine Plus TH-302 Versus Gemcitabine in Patients With Advanced Pancreatic Cancer.* J Clin Oncol, 2015. **33**(13): p. 1475-81.
340. Chawla, S.P., et al., *Phase II study of the safety and antitumor activity of the hypoxia-activated prodrug TH-302 in combination with doxorubicin in patients with advanced soft tissue sarcoma.* J Clin Oncol, 2014. **32**(29): p. 3299-306.
341. Liapis, V., et al., *Anticancer efficacy of the hypoxia-activated prodrug evofosfamide (TH-302) in osteolytic breast cancer murine models.* Cancer Med, 2016. **5**(3): p. 534-45.
342. Jiang, B.H., et al., *Dimerization, DNA binding, and transactivation properties of hypoxia-inducible factor 1.* J Biol Chem, 1996. **271**(30): p. 17771-8.
343. Kung, A.L., et al., *Suppression of tumor growth through disruption of hypoxia-inducible transcription.* Nat Med, 2000. **6**(12): p. 1335-40.
344. Semenza, G.L., *Targeting HIF-1 for cancer therapy.* Nat Rev Cancer, 2003. **3**(10): p. 721-32.
345. Rapisarda, A., et al., *Identification of small molecule inhibitors of hypoxia-inducible factor 1 transcriptional activation pathway.* Cancer Res, 2002. **62**(15): p. 4316-24.
346. Sidera, K. and E. Patsavoudi, *HSP90 inhibitors: current development and potential in cancer therapy.* Recent Pat Anticancer Drug Discov, 2014. **9**(1): p. 1-20.
347. Modi, S., et al., *HSP90 inhibition is effective in breast cancer: a phase II trial of tanespimycin (17-AAG) plus trastuzumab in patients with HER2-positive metastatic breast cancer progressing on trastuzumab.* Clin Cancer Res, 2011. **17**(15): p. 5132-9.
348. Kurebayashi, J., et al., *A radicicol derivative, KF58333, inhibits expression of hypoxia-inducible factor-1alpha and vascular endothelial growth factor, angiogenesis and growth of human breast cancer xenografts.* Jpn J Cancer Res, 2001. **92**(12): p. 1342-51.
349. Bohonowych, J.E., et al., *Comparative analysis of novel and conventional Hsp90 inhibitors on HIF activity and angiogenic potential in clear cell renal cell carcinoma: implications for clinical evaluation.* BMC Cancer, 2011. **11**: p. 520.
350. Damaskos, C., et al., *Histone Deacetylase Inhibitors: An Attractive Therapeutic Strategy Against Breast Cancer.* Anticancer Res, 2017. **37**(1): p. 35-46.
351. Luu, T.H., et al., *A phase II trial of vorinostat (suberoylanilide hydroxamic acid) in metastatic breast cancer: a California Cancer Consortium study.* Clin Cancer Res, 2008. **14**(21): p. 7138-42.
352. Yardley, D.A., et al., *Randomized phase II, double-blind, placebo-controlled study of exemestane with or without entinostat in postmenopausal women with locally recurrent or metastatic estrogen receptor-positive breast cancer progressing on treatment with a nonsteroidal aromatase inhibitor.* J Clin Oncol, 2013. **31**(17): p. 2128-35.
353. Hutt, D.M., et al., *The histone deacetylase inhibitor, Vorinostat, represses hypoxia inducible factor 1 alpha expression through translational inhibition.* PLoS One, 2014. **9**(8): p. e106224.

354. Rapisarda, A., et al., *Schedule-dependent inhibition of hypoxia-inducible factor-1alpha protein accumulation, angiogenesis, and tumor growth by topotecan in U251-HRE glioblastoma xenografts.* Cancer Res, 2004. **64**(19): p. 6845-8.
355. Rapisarda, A., et al., *Topoisomerase I-mediated inhibition of hypoxia-inducible factor 1: mechanism and therapeutic implications.* Cancer Res, 2004. **64**(4): p. 1475-82.
356. Rapisarda, A., R.H. Shoemaker, and G. Melillo, *Targeting topoisomerase I to inhibit hypoxia inducible factor 1.* Cell Cycle, 2004. **3**(2): p. 172-5.
357. Kummar, S., et al., *Phase I study of PARP inhibitor ABT-888 in combination with topotecan in adults with refractory solid tumors and lymphomas.* Cancer Res, 2011. **71**(17): p. 5626-34.
358. Pastorino, F., et al., *Tumor regression and curability of preclinical neuroblastoma models by PEGylated SN38 (EZN-2208), a novel topoisomerase I inhibitor.* Clin Cancer Res, 2010. **16**(19): p. 4809-21.
359. Norris, R.E., et al., *Phase 1 evaluation of EZN-2208, a polyethylene glycol conjugate of SN38, in children adolescents and young adults with relapsed or refractory solid tumors.* Pediatr Blood Cancer, 2014. **61**(10): p. 1792-7.
360. Slingerland, M., et al., *Cardiac glycosides in cancer therapy: from preclinical investigations towards clinical trials.* Invest New Drugs, 2013. **31**(4): p. 1087-94.
361. Stenkvist, B., et al., *Cardiac glycosides and breast cancer.* Lancet, 1979. **1**(8115): p. 563.
362. Stenkvist, B., et al., *Evidence of a modifying influence of heart glucosides on the development of breast cancer.* Anal Quant Cytol, 1980. **2**(1): p. 49-54.
363. Stenkvist, B., et al., *Cardiac glycosides and breast cancer, revisited.* N Engl J Med, 1982. **306**(8): p. 484.
364. Zhang, H., et al., *Digoxin and other cardiac glycosides inhibit HIF-1alpha synthesis and block tumor growth.* Proc Natl Acad Sci U S A, 2008. **105**(50): p. 19579-86.
365. Mabjeesh, N.J., et al., *2ME2 inhibits tumor growth and angiogenesis by disrupting microtubules and dysregulating HIF.* Cancer Cell, 2003. **3**(4): p. 363-75.
366. Ma, L., et al., *2-Methoxyestradiol synergizes with sorafenib to suppress hepatocellular carcinoma by simultaneously dysregulating hypoxia-inducible factor-1 and -2.* Cancer Lett, 2014. **355**(1): p. 96-105.
367. LaVallee, T.M., et al., *Significant antitumor activity in vivo following treatment with the microtubule agent ENMD-1198.* Mol Cancer Ther, 2008. **7**(6): p. 1472-82.
368. Zhou, Q., et al., *A phase I dose-escalation, safety and pharmacokinetic study of the 2-methoxyestradiol analog ENMD-1198 administered orally to patients with advanced cancer.* Invest New Drugs, 2011. **29**(2): p. 340-6.
369. Kung, A.L., et al., *Small molecule blockade of transcriptional coactivation of the hypoxia-inducible factor pathway.* Cancer Cell, 2004. **6**(1): p. 33-43.
370. Cook, K.M., et al., *Epidithiodiketopiperazines block the interaction between hypoxia-inducible factor-1alpha (HIF-1alpha) and p300 by a zinc ejection mechanism.* J Biol Chem, 2009. **284**(39): p. 26831-8.
371. Reece, K.M., et al., *Epidithiodiketopiperazines (ETPs) exhibit in vitro antiangiogenic and in vivo antitumor activity by disrupting the HIF-1alpha/p300 complex in a preclinical model of prostate cancer.* Mol Cancer, 2014. **13**: p. 91.

372. Chun, Y.S., et al., *Inhibitory effect of YC-1 on the hypoxic induction of erythropoietin and vascular endothelial growth factor in Hep3B cells.* Biochem Pharmacol, 2001. **61**(8): p. 947-54.
373. Li, S.H., et al., *A novel mode of action of YC-1 in HIF inhibition: stimulation of FIH-dependent p300 dissociation from HIF-1{alpha}.* Mol Cancer Ther, 2008. **7**(12): p. 3729-38.
374. Rankin, E.B., et al., *Hypoxia-inducible factor-2 (HIF-2) regulates hepatic erythropoietin in vivo.* J Clin Invest, 2007. **117**(4): p. 1068-77.
375. Shin, D.H., et al., *Preclinical evaluation of YC-1, a HIF inhibitor, for the prevention of tumor spreading.* Cancer Lett, 2007. **255**(1): p. 107-16.
376. Yeo, E.J., et al., *YC-1: a potential anticancer drug targeting hypoxia-inducible factor 1.* J Natl Cancer Inst, 2003. **95**(7): p. 516-25.
377. Masoud, G.N., et al., *Design, Synthesis and Biological Evaluation of Novel HIF1alpha Inhibitors.* Anticancer Res, 2015. **35**(7): p. 3849-59.
378. Blackledge, M.S. and C. Melander, *Programmable DNA-binding small molecules.* Bioorg Med Chem, 2013. **21**(20): p. 6101-14.
379. Olenyuk, B.Z., et al., *Inhibition of vascular endothelial growth factor with a sequence-specific hypoxia response element antagonist.* Proc Natl Acad Sci U S A, 2004. **101**(48): p. 16768-73.
380. Jacobs, C.S. and P.B. Dervan, *Modifications at the C-terminus to improve pyrrole-imidazole polyamide activity in cell culture.* J Med Chem, 2009. **52**(23): p. 7380-8.
381. Raskatov, J.A., J.O. Szablowski, and P.B. Dervan, *Tumor xenograft uptake of a pyrrole-imidazole (Py-Im) polyamide varies as a function of cell line grafted.* J Med Chem, 2014. **57**(20): p. 8471-6.
382. Hu, Y., J. Liu, and H. Huang, *Recent agents targeting HIF-1alpha for cancer therapy.* J Cell Biochem, 2013. **114**(3): p. 498-509.
383. Dikmen, Z.G., et al., *In vivo and in vitro effects of a HIF-1alpha inhibitor, RX-0047.* J Cell Biochem, 2008. **104**(3): p. 985-94.
384. Greenberger, L.M., et al., *A RNA antagonist of hypoxia-inducible factor-1alpha, EZN-2968, inhibits tumor cell growth.* Mol Cancer Ther, 2008. **7**(11): p. 3598-608.
385. Jeong, W., et al., *Pilot trial of EZN-2968, an antisense oligonucleotide inhibitor of hypoxia-inducible factor-1 alpha (HIF-1alpha), in patients with refractory solid tumors.* Cancer Chemother Pharmacol, 2014. **73**(2): p. 343-8.
386. Lin, D. and J. Wu, *Hypoxia inducible factor in hepatocellular carcinoma: A therapeutic target.* World J Gastroenterol, 2015. **21**(42): p. 12171-8.
387. Van Audenhove, I. and J. Gettemans, *Nanobodies as Versatile Tools to Understand, Diagnose, Visualize and Treat Cancer.* EBioMedicine, 2016. **8**: p. 40-8.
388. Groot, A.J., et al., *Conditional inactivation of HIF-1 using intrabodies.* Cell Oncol, 2008. **30**(5): p. 397-409.
389. Key, J., et al., *Principles of ligand binding within a completely buried cavity in HIF2alpha PAS-B.* J Am Chem Soc, 2009. **131**(48): p. 17647-54.
390. Scheuermann, T.H., et al., *Artificial ligand binding within the HIF2alpha PAS-B domain of the HIF2 transcription factor.* Proc Natl Acad Sci U S A, 2009. **106**(2): p. 450-5.
391. Scheuermann, T.H., et al., *Allosteric inhibition of hypoxia inducible factor-2 with small molecules.* Nat Chem Biol, 2013. **9**(4): p. 271-6.
392. Krieg, M., et al., *Up-regulation of hypoxia-inducible factors HIF-1alpha and HIF-2alpha under normoxic conditions in renal carcinoma cells by von*

Hippel-Lindau tumor suppressor gene loss of function. Oncogene, 2000. **19**(48): p. 5435-43.
393. Wallace, E.M., et al., *A Small-Molecule Antagonist of HIF2alpha Is Efficacious in Preclinical Models of Renal Cell Carcinoma.* Cancer Res, 2016. **76**(18): p. 5491-500.
394. Courtney, K.D., Infante, J.R., Lam, E.T., Figlin, R.A., Rini, B.I., Brugarolas, J., et al., *A phase I dose escalation trial of PT2385, a first-in-class oral HIF-2a inhibitor, in patients with advanced clear cell renal cell carcinoma.* J. Clin. Oncol, 2016. **34**: p. 171054-171176.
395. *PT2385 for the Treatment of Von Hippel-Lindau Disease-Associated Clear Cell Renal Cell Carcinoma*. 2017 [cited 2017 29.8.17]; Available from: https://clinicaltrials.gov/ct2/show/NCT03108066.
396. Chen, W., et al., *Targeting renal cell carcinoma with a HIF-2 antagonist.* Nature, 2016. **539**(7627): p. 112-117.
397. Hudson, C.C., et al., *Regulation of hypoxia-inducible factor 1alpha expression and function by the mammalian target of rapamycin.* Mol Cell Biol, 2002. **22**(20): p. 7004-14.
398. Majumder, P.K., et al., *mTOR inhibition reverses Akt-dependent prostate intraepithelial neoplasia through regulation of apoptotic and HIF-1-dependent pathways.* Nat Med, 2004. **10**(6): p. 594-601.
399. Mohlin, S., et al., *PI3K-mTORC2 but not PI3K-mTORC1 regulates transcription of HIF2A/EPAS1 and vascularization in neuroblastoma.* Cancer Res, 2015. **75**(21): p. 4617-28.
400. Wan, X., et al., *CCI-779 inhibits rhabdomyosarcoma xenograft growth by an antiangiogenic mechanism linked to the targeting of mTOR/Hif-1alpha/VEGF signaling.* Neoplasia, 2006. **8**(5): p. 394-401.
401. Cejka, D., et al., *Everolimus (RAD001) and anti-angiogenic cyclophosphamide show long-term control of gastric cancer growth in vivo.* Cancer Biol Ther, 2008. **7**(9): p. 1377-85.
402. Jiang, B.H., et al., *Phosphatidylinositol 3-kinase signaling controls levels of hypoxia-inducible factor 1.* Cell Growth Differ, 2001. **12**(7): p. 363-9.
403. Lee, S.H., et al., *A group of novel HIF-1alpha inhibitors, glyceollins, blocks HIF-1alpha synthesis and decreases its stability via inhibition of the PI3K/AKT/mTOR pathway and Hsp90 binding.* J Cell Physiol, 2015. **230**(4): p. 853-62.
404. Bishayee, A., *Cancer prevention and treatment with resveratrol: from rodent studies to clinical trials.* Cancer Prev Res (Phila), 2009. **2**(5): p. 409-18.
405. Garvin, S., K. Ollinger, and C. Dabrosin, *Resveratrol induces apoptosis and inhibits angiogenesis in human breast cancer xenografts in vivo.* Cancer Lett, 2006. **231**(1): p. 113-22.
406. Roskoski, R., Jr., *The ErbB/HER family of protein-tyrosine kinases and cancer.* Pharmacol Res, 2014. **79**: p. 34-74.
407. Leahy, D.J., *Structure and function of the epidermal growth factor (EGF/ErbB) family of receptors.* Adv Protein Chem, 2004. **68**: p. 1-27.
408. Garrett, T.P., et al., *The crystal structure of a truncated ErbB2 ectodomain reveals an active conformation, poised to interact with other ErbB receptors.* Mol Cell, 2003. **11**(2): p. 495-505.
409. Burgess, A.W., *EGFR family: structure physiology signalling and therapeutic targets.* Growth Factors, 2008. **26**(5): p. 263-74.
410. Baselga, J. and S.M. Swain, *Novel anticancer targets: revisiting ERBB2 and discovering ERBB3.* Nat Rev Cancer, 2009. **9**(7): p. 463-75.

411. Ward, C.W. and M.C. Lawrence, *Similar but different: ligand-induced activation of the insulin and epidermal growth factor receptor families.* Curr Opin Struct Biol, 2012. **22**(3): p. 360-6.
412. Ward, C.W., et al., *The insulin and EGF receptor structures: new insights into ligand-induced receptor activation.* Trends Biochem Sci, 2007. **32**(3): p. 129-37.
413. Olayioye, M.A., et al., *The ErbB signaling network: receptor heterodimerization in development and cancer.* EMBO J, 2000. **19**(13): p. 3159-67.
414. Citri, A. and Y. Yarden, *EGF-ERBB signalling: towards the systems level.* Nat Rev Mol Cell Biol, 2006. **7**(7): p. 505-16.
415. Citri, A., K.B. Skaria, and Y. Yarden, *The deaf and the dumb: the biology of ErbB-2 and ErbB-3.* Exp Cell Res, 2003. **284**(1): p. 54-65.
416. Roberts, P.J. and C.J. Der, *Targeting the Raf-MEK-ERK mitogen-activated protein kinase cascade for the treatment of cancer.* Oncogene, 2007. **26**(22): p. 3291-310.
417. Fresno Vara, J.A., et al., *PI3K/Akt signalling pathway and cancer.* Cancer Treat Rev, 2004. **30**(2): p. 193-204.
418. Zardavas, D., W.A. Phillips, and S. Loi, *PIK3CA mutations in breast cancer: reconciling findings from preclinical and clinical data.* Breast Cancer Res, 2014. **16**(1): p. 201.
419. Mukohara, T., *PI3K mutations in breast cancer: prognostic and therapeutic implications.* Breast Cancer (Dove Med Press), 2015. **7**: p. 111-23.
420. Bartosova, M., et al., *Expression of carbonic anhydrase IX in breast is associated with malignant tissues and is related to overexpression of c-erbB2.* J Pathol, 2002. **197**(3): p. 314-21.
421. Li, Y.M., et al., *A hypoxia-independent hypoxia-inducible factor-1 activation pathway induced by phosphatidylinositol-3 kinase/Akt in HER2 overexpressing cells.* Cancer Res, 2005. **65**(8): p. 3257-63.
422. Peng, X.H., et al., *Cross-talk between epidermal growth factor receptor and hypoxia-inducible factor-1alpha signal pathways increases resistance to apoptosis by up-regulating survivin gene expression.* J Biol Chem, 2006. **281**(36): p. 25903-14.
423. Whelan, K.A., et al., *The oncogene HER2/neu (ERBB2) requires the hypoxia-inducible factor HIF-1 for mammary tumor growth and anoikis resistance.* J Biol Chem, 2013. **288**(22): p. 15865-77.
424. Kazi, A.A., et al., *Nonhypoxic regulation and role of hypoxia-inducible factor 1 in aromatase inhibitor resistant breast cancer.* Breast Cancer Res, 2014. **16**(1): p. R15.
425. Franovic, A., et al., *Translational up-regulation of the EGFR by tumor hypoxia provides a nonmutational explanation for its overexpression in human cancer.* Proc Natl Acad Sci U S A, 2007. **104**(32): p. 13092-7.
426. Alam, M.W., et al., *HIF2alpha contributes to antiestrogen resistance via positive bilateral crosstalk with EGFR in breast cancer cells.* Oncotarget, 2016. **7**(10): p. 11238-50.
427. Stiehl, D.P., et al., *Non-canonical HIF-2alpha function drives autonomous breast cancer cell growth via an AREG-EGFR/ErbB4 autocrine loop.* Oncogene, 2012. **31**(18): p. 2283-97.
428. Franovic, A., et al., *Human cancers converge at the HIF-2alpha oncogenic axis.* Proc Natl Acad Sci U S A, 2009. **106**(50): p. 21306-11.
429. Frogne, T., et al., *Activation of ErbB3, EGFR and Erk is essential for growth of human breast cancer cell lines with acquired resistance to fulvestrant.* Breast Cancer Res Treat, 2009. **114**(2): p. 263-75.

430. Benz, C.C., et al., *Estrogen-dependent, tamoxifen-resistant tumorigenic growth of MCF-7 cells transfected with HER2/neu.* Breast Cancer Res Treat, 1992. **24**(2): p. 85-95.
431. Welshons, W.V., et al., *Control of proliferation of MCF-7 breast cancer cells in a commercial preparation of charcoal-stripped adult bovine serum.* Breast Cancer Res Treat, 1992. **23**(1-2): p. 97-104.
432. Welshons, W.V. and V.C. Jordan, *Adaptation of estrogen-dependent MCF-7 cells to low estrogen (phenol red-free) culture.* Eur J Cancer Clin Oncol, 1987. **23**(12): p. 1935-9.
433. Berthois, Y., J.A. Katzenellenbogen, and B.S. Katzenellenbogen, *Phenol red in tissue culture media is a weak estrogen: implications concerning the study of estrogen-responsive cells in culture.* Proc Natl Acad Sci U S A, 1986. **83**(8): p. 2496-500.
434. Varia, M.A., et al., *Pimonidazole: a novel hypoxia marker for complementary study of tumor hypoxia and cell proliferation in cervical carcinoma.* Gynecol Oncol, 1998. **71**(2): p. 270-7.
435. Raleigh, J.A. and C.J. Koch, *Importance of thiols in the reductive binding of 2-nitroimidazoles to macromolecules.* Biochem Pharmacol, 1990. **40**(11): p. 2457-64.
436. Vichai, V. and K. Kirtikara, *Sulforhodamine B colorimetric assay for cytotoxicity screening.* Nat Protoc, 2006. **1**(3): p. 1112-6.
437. Curtis, C., et al., *The genomic and transcriptomic architecture of 2,000 breast tumours reveals novel subgroups.* Nature, 2012. **486**(7403): p. 346-52.
438. Gyorffy, B., et al., *An online survival analysis tool to rapidly assess the effect of 22,277 genes on breast cancer prognosis using microarray data of 1,809 patients.* Breast Cancer Res Treat, 2010. **123**(3): p. 725-31.
439. *Kmplot online survival tool*. 2017 [cited 2017 25.8.17]; Available from: http://kmplot.com/analysis/index.php?p=background.
440. Mihaly, Z., et al., *A meta-analysis of gene expression-based biomarkers predicting outcome after tamoxifen treatment in breast cancer.* Breast Cancer Res Treat, 2013. **140**(2): p. 219-32.
441. Yaich, L.E., et al., *Analysis of estrogen receptor (ER) gene, transcript and protein in ER-positive and -negative breast cancer cell lines.* Endocrine-Related Cancer, 1995. **2**(4): p. 293-309.
442. Badowska-Kozakiewicz, A., M. Sobol, and J. Patera, *Expression of Hypoxia-Inducible Factor 1alpha in Invasive Breast Cancer with Metastasis to Lymph Nodes: Correlation with Steroid Receptors, HER2 and EPO-R.* Adv Clin Exp Med, 2016. **25**(4): p. 741-50.
443. Zhong, H., et al., *Overexpression of hypoxia-inducible factor 1alpha in common human cancers and their metastases.* Cancer Res, 1999. **59**(22): p. 5830-5.
444. Mabjeesh, N.J. and S. Amir, *Hypoxia-inducible factor (HIF) in human tumorigenesis.* Histol Histopathol, 2007. **22**(5): p. 559-72.
445. Liao, D., et al., *Hypoxia-inducible factor-1alpha is a key regulator of metastasis in a transgenic model of cancer initiation and progression.* Cancer Res, 2007. **67**(2): p. 563-72.
446. Chang, J. and J. Erler, *Hypoxia-mediated metastasis.* Adv Exp Med Biol, 2014. **772**: p. 55-81.
447. Holmquist-Mengelbier, L., et al., *Recruitment of HIF-1alpha and HIF-2alpha to common target genes is differentially regulated in neuroblastoma: HIF-2alpha promotes an aggressive phenotype.* Cancer Cell, 2006. **10**(5): p. 413-23.

448. Weidemann, A. and R.S. Johnson, *Biology of HIF-1alpha.* Cell Death Differ, 2008. **15**(4): p. 621-7.
449. Imtaiyaz Hassan, M., et al., *Structure, function and applications of carbonic anhydrase isozymes.* Bioorg Med Chem, 2013. **21**(6): p. 1570-82.
450. Swietach, P., et al., *The role of carbonic anhydrase 9 in regulating extracellular and intracellular ph in three-dimensional tumor cell growths.* J Biol Chem, 2009. **284**(30): p. 20299-310.
451. Swietach, P., et al., *New insights into the physiological role of carbonic anhydrase IX in tumour pH regulation.* Oncogene, 2010. **29**(50): p. 6509-21.
452. Wykoff, C.C., et al., *Expression of the hypoxia-inducible and tumor-associated carbonic anhydrases in ductal carcinoma in situ of the breast.* Am J Pathol, 2001. **158**(3): p. 1011-9.
453. Kaya, A.O., et al., *Hypoxia inducible factor-1 alpha and carbonic anhydrase IX overexpression are associated with poor survival in breast cancer patients.* J BUON, 2012. **17**(4): p. 663-8.
454. Potter, C.P. and A.L. Harris, *Diagnostic, prognostic and therapeutic implications of carbonic anhydrases in cancer.* Br J Cancer, 2003. **89**(1): p. 2-7.
455. Ward, C., et al., *Evaluation of carbonic anhydrase IX as a therapeutic target for inhibition of breast cancer invasion and metastasis using a series of in vitro breast cancer models.* Oncotarget, 2015. **6**(28): p. 24856-70.
456. Meehan, J., et al., *Inhibition of pH regulation as a therapeutic strategy in hypoxic human breast cancer cells.* Oncotarget, 2017.
457. Fiume, L., et al., *Inhibition of lactate dehydrogenase activity as an approach to cancer therapy.* Future Med Chem, 2014. **6**(4): p. 429-45.
458. Wang, Z.Y., et al., *LDH-A silencing suppresses breast cancer tumorigenicity through induction of oxidative stress mediated mitochondrial pathway apoptosis.* Breast Cancer Res Treat, 2012. **131**(3): p. 791-800.
459. Miao, P., et al., *Lactate dehydrogenase A in cancer: a promising target for diagnosis and therapy.* IUBMB Life, 2013. **65**(11): p. 904-10.
460. Granchi, C., et al., *Inhibitors of lactate dehydrogenase isoforms and their therapeutic potentials.* Curr Med Chem, 2010. **17**(7): p. 672-97.
461. Pogue, B.W., et al., *Estimation of oxygen distribution in RIF-1 tumors by diffusion model-based interpretation of pimonidazole hypoxia and eppendorf measurements.* Radiat Res, 2001. **155**(1 Pt 1): p. 15-25.
462. Forsythe, J.A., et al., *Activation of vascular endothelial growth factor gene transcription by hypoxia-inducible factor 1.* Mol Cell Biol, 1996. **16**(9): p. 4604-13.
463. Liang, G., et al., *Hypoxia regulates CD44 expression via hypoxia-inducible factor-1alpha in human gastric cancer cells.* Oncol Lett, 2017. **13**(2): p. 967-972.
464. Heddleston, J.M., et al., *Hypoxia inducible factors in cancer stem cells.* Br J Cancer, 2010. **102**(5): p. 789-95.
465. Montagner, M., et al., *SHARP1 suppresses breast cancer metastasis by promoting degradation of hypoxia-inducible factors.* Nature, 2012. **487**(7407): p. 380-4.
466. Asrani, K., et al., *The HER2- and heregulin beta1 (HRG)-inducible TNFR superfamily member Fn14 promotes HRG-driven breast cancer cell migration, invasion, and MMP9 expression.* Mol Cancer Res, 2013. **11**(4): p. 393-404.
467. Loboda, A., A. Jozkowicz, and J. Dulak, *HIF-1 versus HIF-2--is one more important than the other?* Vascul Pharmacol, 2012. **56**(5-6): p. 245-51.

468. Dengler, V.L., M.D. Galbraith, and J.M. Espinosa, *Transcriptional regulation by hypoxia inducible factors.* Crit Rev Biochem Mol Biol, 2014. **49**(1): p. 1-15.
469. Semenza, G.L., et al., *Transcriptional regulation of genes encoding glycolytic enzymes by hypoxia-inducible factor 1.* J Biol Chem, 1994. **269**(38): p. 23757-63.
470. Kaluz, S., et al., *Transcriptional control of the tumor- and hypoxia-marker carbonic anhydrase 9: A one transcription factor (HIF-1) show?* Biochim Biophys Acta, 2009. **1795**(2): p. 162-72.
471. Zhao, J., et al., *The role of hypoxia-inducible factor-2 in digestive system cancers.* Cell Death Dis, 2015. **6**: p. e1600.
472. Akeno, N., et al., *Hypoxia induces vascular endothelial growth factor gene transcription in human osteoblast-like cells through the hypoxia-inducible factor-2alpha.* Endocrinology, 2001. **142**(2): p. 959-62.
473. Xia, G., et al., *Regulation of vascular endothelial growth factor transcription by endothelial PAS domain protein 1 (EPAS1) and possible involvement of EPAS1 in the angiogenesis of renal cell carcinoma.* Cancer, 2001. **91**(8): p. 1429-36.
474. Peng, G. and Y. Liu, *Hypoxia-inducible factors in cancer stem cells and inflammation.* Trends Pharmacol Sci, 2015. **36**(6): p. 374-83.
475. Johansson, E., et al., *CD44 Interacts with HIF-2alpha to Modulate the Hypoxic Phenotype of Perinecrotic and Perivascular Glioma Cells.* Cell Rep, 2017. **20**(7): p. 1641-1653.
476. Krishnamachary, B., et al., *Hypoxia regulates CD44 and its variant isoforms through HIF-1alpha in triple negative breast cancer.* PLoS One, 2012. **7**(8): p. e44078.
477. Brizel, D.M., et al., *Tumor oxygenation predicts for the likelihood of distant metastases in human soft tissue sarcoma.* Cancer Res, 1996. **56**(5): p. 941-3.
478. Vaupel, P., et al., *Oxygenation of human tumors: evaluation of tissue oxygen distribution in breast cancers by computerized O2 tension measurements.* Cancer Res, 1991. **51**(12): p. 3316-22.
479. Stone, H.B., et al., *Oxygen in human tumors: correlations between methods of measurement and response to therapy. Summary of a workshop held November 19-20, 1992, at the National Cancer Institute, Bethesda, Maryland.* Radiat Res, 1993. **136**(3): p. 422-34.
480. Buffa, F.M., et al., *Large meta-analysis of multiple cancers reveals a common, compact and highly prognostic hypoxia metagene.* Br J Cancer, 2010. **102**(2): p. 428-35.
481. Winter, S.C., et al., *Relation of a hypoxia metagene derived from head and neck cancer to prognosis of multiple cancers.* Cancer Res, 2007. **67**(7): p. 3441-9.
482. Toustrup, K., et al., *Development of a hypoxia gene expression classifier with predictive impact for hypoxic modification of radiotherapy in head and neck cancer.* Cancer Res, 2011. **71**(17): p. 5923-31.
483. Toustrup, K., et al., *Hypoxia gene expression signatures as prognostic and predictive markers in head and neck radiotherapy.* Semin Radiat Oncol, 2012. **22**(2): p. 119-27.
484. Denko, N.C., et al., *Investigating hypoxic tumor physiology through gene expression patterns.* Oncogene, 2003. **22**(37): p. 5907-14.
485. Chi, J.T., et al., *Gene expression programs in response to hypoxia: cell type specificity and prognostic significance in human cancers.* PLoS Med, 2006. **3**(3): p. e47.

486. Seigneuric, R., et al., *Impact of supervised gene signatures of early hypoxia on patient survival.* Radiother Oncol, 2007. **83**(3): p. 374-82.
487. Eustace, A., et al., *A 26-gene hypoxia signature predicts benefit from hypoxia-modifying therapy in laryngeal cancer but not bladder cancer.* Clin Cancer Res, 2013. **19**(17): p. 4879-88.
488. Huang da, W., B.T. Sherman, and R.A. Lempicki, *Systematic and integrative analysis of large gene lists using DAVID bioinformatics resources.* Nat Protoc, 2009. **4**(1): p. 44-57.
489. Moleirinho, S., et al., *KIBRA exhibits MST-independent functional regulation of the Hippo signaling pathway in mammals.* Oncogene, 2013. **32**(14): p. 1821-30.
490. Sorensen, B.S., et al., *Influence of oxygen concentration and pH on expression of hypoxia induced genes.* Radiother Oncol, 2005. **76**(2): p. 187-93.
491. Sorensen, B.S., et al., *Identifying pH independent hypoxia induced genes in human squamous cell carcinomas in vitro.* Acta Oncol, 2010. **49**(7): p. 895-905.
492. Sethi, N., et al., *Tumor-derived JAGGED1 promotes osteolytic bone metastasis of breast cancer by engaging notch signaling in bone cells.* Cancer Cell, 2011. **19**(2): p. 192-205.
493. Bednarz-Knoll, N., et al., *Potential Involvement of Jagged1 in Metastatic Progression of Human Breast Carcinomas.* Clin Chem, 2016. **62**(2): p. 378-86.
494. Xing, F., et al., *Hypoxia-induced Jagged2 promotes breast cancer metastasis and self-renewal of cancer stem-like cells.* Oncogene, 2011. **30**(39): p. 4075-86.
495. Al-Hussaini, H., et al., *Notch signaling pathway as a therapeutic target in breast cancer.* Mol Cancer Ther, 2011. **10**(1): p. 9-15.
496. Martin, T.A., et al., *Expression of the transcription factors snail, slug, and twist and their clinical significance in human breast cancer.* Ann Surg Oncol, 2005. **12**(6): p. 488-96.
497. Parvani, J.G. and W.P. Schiemann, *Sox4, EMT programs, and the metastatic progression of breast cancers: mastering the masters of EMT.* Breast Cancer Res, 2013. **15**(4): p. R72.
498. Liang, Y.J., et al., *MiR-124 targets Slug to regulate epithelial-mesenchymal transition and metastasis of breast cancer.* Carcinogenesis, 2013. **34**(3): p. 713-22.
499. Sahlgren, C., et al., *Notch signaling mediates hypoxia-induced tumor cell migration and invasion.* Proc Natl Acad Sci U S A, 2008. **105**(17): p. 6392-7.
500. Montero, J.C., et al., *Neuregulins and cancer.* Clin Cancer Res, 2008. **14**(11): p. 3237-41.
501. Hobbs, S.S., et al., *Neuregulin isoforms exhibit distinct patterns of ErbB family receptor activation.* Oncogene, 2002. **21**(55): p. 8442-52.
502. Gaul, M.D., et al., *Discovery and biological evaluation of potent dual ErbB-2/EGFR tyrosine kinase inhibitors: 6-thiazolylquinazolines.* Bioorg Med Chem Lett, 2003. **13**(4): p. 637-40.
503. Saxena, R. and A. Dwivedi, *ErbB family receptor inhibitors as therapeutic agents in breast cancer: current status and future clinical perspective.* Med Res Rev, 2012. **32**(1): p. 166-215.
504. Ward, W.H., et al., *Epidermal growth factor receptor tyrosine kinase. Investigation of catalytic mechanism, structure-based searching and discovery of a potent inhibitor.* Biochem Pharmacol, 1994. **48**(4): p. 659-66.

505. Wakeling, A.E., et al., *ZD1839 (Iressa): an orally active inhibitor of epidermal growth factor signaling with potential for cancer therapy.* Cancer Res, 2002. **62**(20): p. 5749-54.
506. Nagasawa, J., et al., *Novel HER2 selective tyrosine kinase inhibitor, TAK-165, inhibits bladder, kidney and androgen-independent prostate cancer in vitro and in vivo.* Int J Urol, 2006. **13**(5): p. 587-92.
507. Sugita, S., et al., *Effect of type I growth factor receptor tyrosine kinase inhibitors on phosphorylation and transactivation activity of the androgen receptor in prostate cancer cells: Ligand-independent activation of the N-terminal domain of the androgen receptor.* Oncol Rep, 2004. **11**(6): p. 1273-9.
508. Yuan, Y., et al., *Cobalt inhibits the interaction between hypoxia-inducible factor-alpha and von Hippel-Lindau protein by direct binding to hypoxia-inducible factor-alpha.* J Biol Chem, 2003. **278**(18): p. 15911-6.
509. Yarden, Y. and G. Pines, *The ERBB network: at last, cancer therapy meets systems biology.* Nat Rev Cancer, 2012. **12**(8): p. 553-63.
510. Qing, G. and M.C. Simon, *Hypoxia inducible factor-2alpha: a critical mediator of aggressive tumor phenotypes.* Curr Opin Genet Dev, 2009. **19**(1): p. 60-6.
511. Martinez-Saez, O., et al., *Targeting HIF-2 alpha in clear cell renal cell carcinoma: A promising therapeutic strategy.* Crit Rev Oncol Hematol, 2017. **111**: p. 117-123.
512. Cho, H., et al., *On-target efficacy of a HIF-2alpha antagonist in preclinical kidney cancer models.* Nature, 2016. **539**(7627): p. 107-111.
513. Moon, E.J., et al., *The potential role of intrinsic hypoxia markers as prognostic variables in cancer.* Antioxid Redox Signal, 2007. **9**(8): p. 1237-94.
514. Gilkes, D.M. and G.L. Semenza, *Role of hypoxia-inducible factors in breast cancer metastasis.* Future Oncol, 2013. **9**(11): p. 1623-36.
515. Koukourakis, M.I., et al., *Hypoxia-inducible factor (HIF1A and HIF2A), angiogenesis, and chemoradiotherapy outcome of squamous cell head-and-neck cancer.* Int J Radiat Oncol Biol Phys, 2002. **53**(5): p. 1192-202.
516. Koukourakis, M.I., et al., *Endogenous markers of two separate hypoxia response pathways (hypoxia inducible factor 2 alpha and carbonic anhydrase 9) are associated with radiotherapy failure in head and neck cancer patients recruited in the CHART randomized trial.* J Clin Oncol, 2006. **24**(5): p. 727-35.
517. Giatromanolaki, A., et al., *Relation of hypoxia inducible factor 1 alpha and 2 alpha in operable non-small cell lung cancer to angiogenic/molecular profile of tumours and survival.* Br J Cancer, 2001. **85**(6): p. 881-90.
518. Yoshimura, H., et al., *Prognostic impact of hypoxia-inducible factors 1alpha and 2alpha in colorectal cancer patients: correlation with tumor angiogenesis and cyclooxygenase-2 expression.* Clin Cancer Res, 2004. **10**(24): p. 8554-60.
519. Koga, F., et al., *Prognostic significance of endothelial Per-Arnt-sim domain protein 1/hypoxia-inducible factor-2alpha expression in a subset of tumor associated macrophages in invasive bladder cancer.* J Urol, 2004. **171**(3): p. 1080-4.

Appendix 1: Assessment of microarray data

Appendix 1.1: Multi-dimensional scaling of gene expression microarray data.

Multidimensional scaling of samples from the gene expression microarray displays relative similarity between the samples. Cell line clusters are circled in individual colours, whilst samples are colour-coded for cell line (outside colour) and by treatment category (central colour). Red arrows indicate these samples which have not clustered with their biological repeats. These samples were assessed by hierarchical clustering (appendix 1.2).

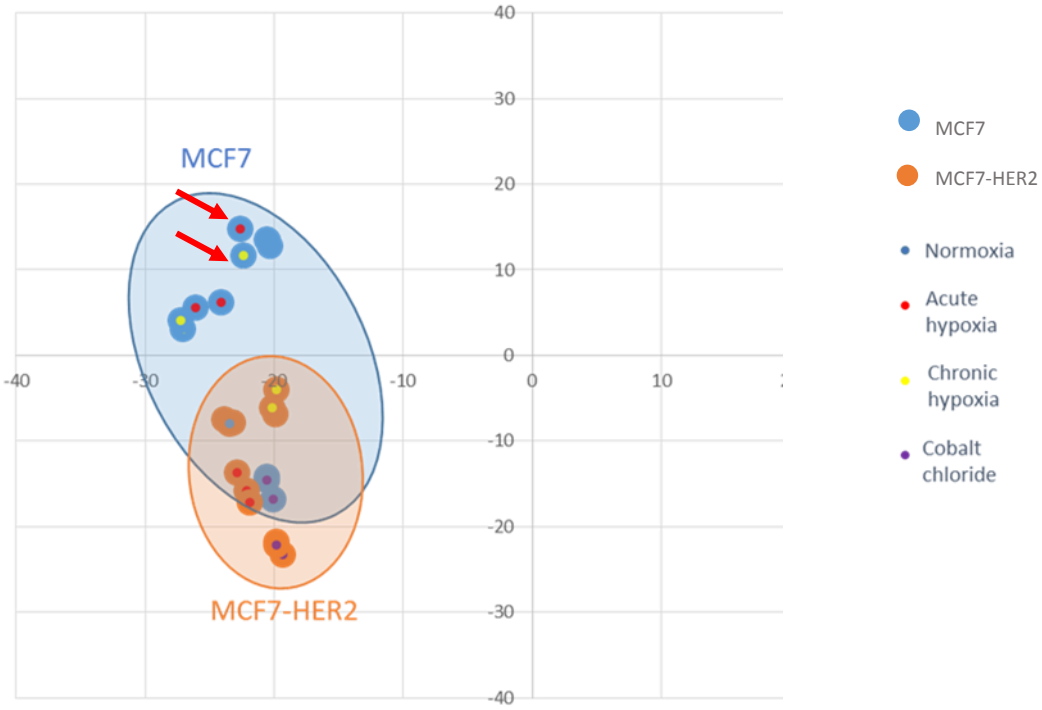

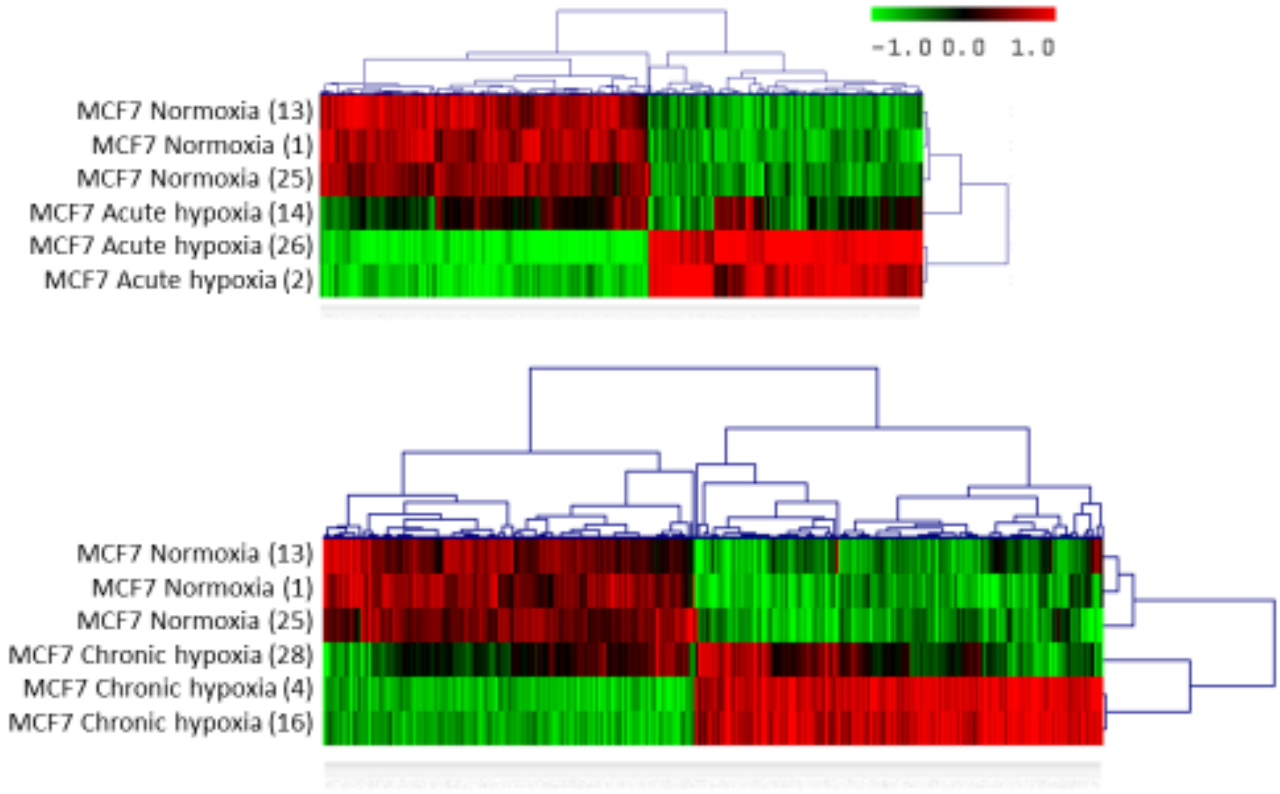

Appendix 1.2: Hierarchical clustering of significantly changed genes in normoxic vs hypoxic samples in MCF7.

Hierarchical clustering of significantly changed genes (as determined by rank product testing FDR=0.05) used to assess the similarity of unsure samples to normoxic or hypoxic samples in MCF7 cells. Samples with ambiguous coordinates in MDS analysis were tested in this way to determine whether they clustered with normoxic or hypoxic samples. MCF7 AH (14) was found to cluster more closely to normoxic MCF7 samples than equivalent hypoxic samples and so was omitted from microarray analysis experiments unless otherwise stated.

Appendix 2: Gene lists

Appendix 2.1: Hypoxia metagenes arranged by clusters from Figure 4.3

Tables show full gene lists from the metagenes used in Figure 4.3. Genes are organised by metagenes (columns) and which clusters they belong to (table titles). Genes which are found in multiple metagene are indicated (rows)

Hypoxia metagene red clusters

Winter		Buffa		Toustrup
NDRG1, SLC2A1, P4HA1, ALDOA, BNIP3	↔	NDRG1,SLC2A1, P4HA1, ALDOA, BNIP3	↔	NDRG1, SLC2A1, P4HA1, ALDOA, BNIP3
MRGBP, PGK1, CA9, GAPDH, TPI1, VEGFA, LDHA, HILPDA, PGAM1	↔	MRGBP, PGK1, CA9, GAPDH, TPI1, VEGFA, LDHA, HILPDA, PGAM1		
		ADM, ANKRD37	↔	ADM, ANKRD37
KCTD11	↔		↔	KCTD11
				P4HA2, BNIP3L, LOX, FAM162A, EGLN3, PDK1, PFKFB3
		PFKP, ENO1, PSMA7, ESRP1, GPI, YKT6, LRRC42, MAD2L2, MAP7D1, SEC61G, CTSV, HK2 AK4, DDIT4, MIF		
VEZT, HES2, MIR7855, PYGL, RNF24, LRP2BP, SLCO1B3, PPARD, PFKFB4, PDZD11, PLAU, VAPB, PLEKHG3, KRT17, MIR6886, SLC6A8, TNS4, PTGFRN, DPM2, TUBB2A, CREBZF, HAUS2, AK3, PPM1J, ANKRD9, ANGPTL4, CXCL8, TANC2, PAWR, NDUFA4L2, S100A10, RNPS1, SLC6A10P, TMEM189				

Hypoxia metagene green cluster

Winter
MNAT1, BCAR1, SNX24, TPD52L2, PSMA7, CORO1C, PGF, RAN, EIF2S1, NUDT15, IMPA2, CNIH4, TPBG, HOMER1, C16orf74, PPP4R1, SLC16A1, TMEM30B, S100A3, COL4A5, GMFB

Hypoxia metagene blue clusters

Winter		Buffa
ANLN	↔	ANLN
METTL22, PVR, CA12, TFAP2C, GEMIN2, GSS, GPN3, B4GALT2, SLIRP, XPO5, PSMB7, ECE2, NTMT1, BMS1, ADORA2B, CDCA4, MTX1, PSMD2, MRPL14, RUVBL2, TEAD4, NME1, MIF		
		KIF4A, ACOT7, CDKN3, CHCHD2, KIF20A, CORO1C, TUBA1B, PSRC1, TUBA1C, PNP, MRPL15, SLC16A1, SLC25A32, SHCBP1, MRPL13, TUBB6, UTP11,MCTS1

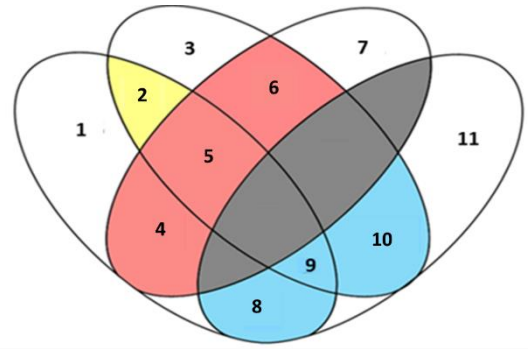

Appendix 2.2: Gene lists for rank product analysis shown in chapter 4 (Figure 4.4)

Full gene lists for rank product testing of MCF7 and MCF7-HER2 cell lines. These are arranged in terms of their position on the Venn diagrams in Figure 4.4. Positions are labelled as shown in the key (LHS). Separate tables for acute and chronic hypoxia are shown.

Acute hypoxia rank product gene lists	
Venn Location	**Gene names**
1	ZNF263, TRAPPC6A, MIR6511B1, AKAP8L, MIR6872, ZRANB1, PNKP, HSPA5, TNPO3, KLF6, MNT, ASNS, MYO3B, KDM5A, FERMT2, RBMS2, XAB2, JADE1, ZCWPW1, PPP1R13B, SPAG7, MFSD11, HDAC6, tspan15, PCNX1, CCNB1IP1, EMD, MAGT1, SLC38A7, HCFC1R1, CLASRP, ERCC2, SF3A2, MIR4750, CCDC130, PIAS4, RABAC1, LHPP, MIR6805, AATF, AIP, EPM2A, DBN1, GALNT3, CACYBP, ARHGEF2, ZBTB17, CTGF, FOXO3, SIL1, NFYB, TBC1D15, Hist1h1a, SPDEF, LRRFIP1, SYMPK, EDN2, krt17, MBD4, DOCK6, MAP1S, JUND, PNPLA7, RBBP8NL, ASS1, ZNF317, PLXNA3, ABCB7, dlg4, RNF122, ERCC5, LOC101927181, ABHD17C, USP8, MAPK8IP3, RNF165, ERBB2, Tmem91, FAM63A, RAB13, GMPPA, SLC25A38, ATG12, TIAM2, ITPRIP, TMEM219, NUBPL, VPS26B, DPYSL4, UBALD1, FLCN, MMS19, PDIA4, RNF20, FUT6, TSC22D3, RHPN1, ZYX, RNASEK-C17orf49, UBXN1, ALPP, ZNF148, PIGX, C1ORF50, CAMLG, USP49, PHAX, PPFIBP2, RNF169, WEE1, TEF, ACSF2, MVD, RAB3IL1, SLC3A2, ADAM9, THBS3, zrsr2, BRD3, IFFO2, CHD3, ADPRM, ZNF581, ZNF524, PTGER4, RAB33B, LAMB2, ZNF738, GOLGB1, NUDT18, NR1D2, ZNF408, c11orf68, WDR25, SGF29, MIR7-3HG, FAM91A1, MIR6785, PCDHB9, DMAP1, ZNF223, KLHL28, GCC1, NLRP8, SSTR2, TMEM136, WASH6P, HIST2H2AA3, DUSP8, zbtb3, FAM83G, ZNF322P1, RPL14, ZNF600, SUPT5H, HIST3H2BB, PDLIM7, FLNA, ZNF433, SPTAN1, Mt1f, GPATCH3, ZNF358, SELENOM, PJA2, ENSG00000199298, ENSG00000199663, ENSG00000202364, RNU4-2, GDI1, ARHGEF35, TERF1P4, LOC285696, ENSG00000215719, LINC01567, DBT, SMCR5, WASH7P, DDAH2, LOC440704, ZDHHC20-IT1, cox19, ENSG00000240652, HIST2H2BB, RN7SL1, ENSG00000251701, ENSG00000255107, SLC5A8, ENSG00000257540, ENSG00000260043, PIR46900, GPS1M, SMG1P7
2	SAMD4A, FOXJ2, PTPN21, EDN1, NFE2L1, MRGBP, RNF24, AVL9, RSRC2, BCL6, FAM162A, PFKFB4, KDM3A, RGS2, RLF, SERGEF, GADD45G, OSER1, DTNA, HILPDA, PHF21A, CIR1, CYR61, TUFT1, ppfia4, CSRNP1, TNIP1, NOCT, C10orf12, EYA3, CIART, DEDD2, ZNF653, ATF3, YEATS2, ARHGEF3, DAPK3, KRT80, ZNF212, KIF5B, BNIP3, VPS37D, PAWR, CLK3, PLD6, MB21D2, RIPK4, ANKRD37, HIST1H1C, FUT11, SERTAD1, Hist1h3d, PIM3, LRIG2, RNA5S9, RN7SKP80, rn7sk, HSPA1A, RNVU1-18, ENSG00000207315, RNU1-3, ENSG00000209804, PPME1, ZNF579, PPP2R2A, EPB41L4A-AS1, LINC01715, ENSG00000248721, F5H5P2
3	WDR54, MYLIP, CSDE1, DAPK2, ZZZ3, CDH10, RIOK2, DLX3, BCAS1, MSANTD3, PFKP, ARHGAP10, P4HA2, SCARB1, ENO1, FNDC3B, PGM1, STK17B, GSK3B, PLOD1, YTHDC1, ATG16L1, UIMC1, ZBTB25, ALKBH5, DSP, SIRT1, RASSF7, LRP5L, PIK3IP1, PACSIN2, PDGFB, PYGL, SUSD6, SLCO4A1, JAG1, RIOK3, PGK1, DHDH, PPP1R13L, SYDE1, GPI, stx1a, C1GALT1, CA9, SHB, DDX50, FBXL20, MANBA, GRPEL1, HSPA8, KMT5B, SLC35F2, LIN7A, LOC100507424, VEGFA, HBEGF, ARRDC3, PRLR, CRBN, HES1, BBX, GBE1, IGFBP5, COQ10B, ID2, DARS, atf2, ARID3A, qsox1, SMG7, GADD45A, CD2, ID3, SLC2A1, FKBP15, CTNNAL1, MXI1, AVPI1, PPP3CC, PAPD5, PSPC1, TMEM39B, CXCR4, HOXC13, KCNS1, ARFGEF2, TRERF1, FOSB, ZNF436, PLEKHG3, DNAJB9, GAD1, EGLN3, SAT1, DNAJB1, PER2, USPL1, SWAP70, PLEKHA8P1, LDHA, CABLES1, ddb2, UBQLN1, HEY2, EGLN1, cep350, c2orf49, WDR33, TEX10, PIM1, SORL1, INTS12, LNX2, VPS37B, USP3, CDR2, PRELID3A, GAREM1, NARF, WDR45B, NECTIN4, RGL1, MALL, OSBPL10, PAM, IGFBP3, PLIN2, ALDOA, VEGFC, FOXO1, NGLY1, CCL28, PELO, CCDC174, ELMSAN1, BRPF1, NCK1, HK2, CCDC107, CRTC2, ITGA5, AK4, DHRS3, RYBP, MEAF6, SAP30, CITED2, SLU7, RP9, SLC29A4, HEY1, GEM, UBAP1, RNF183, DPCD, ARIH1, CYB5A, ZNF143, nab2, patl1, c15orf39, vkorc1, ANGPTL4, FAM83B, ING2, TSPAN5, FEM1B, MAP2K1, SIN3A, GPR37L1, SLC30A1, RALGAPB, ZNF296, PPM1D, KBTBD2, NAIF1, MIR6510, KLF11, ISG20, HINFP, RND1, OVOL1, PPP1R3B, SLCO2A1, ZNF654, UBE2O, ANO6, RIMKLA, NIM1K, AQP11, ZFAND2A, MPI, MIR6883, SERTAD2, LOC284023, TMEM45A, SETD2, c3orf58, BACE2, SPNS2,

	DDX41, BCOR, ENSG00000183900, DENND5A, MAP7D2, FAM110C, JAG2, SEMA4B, IRS2, KPNA4, ZNF395, THSD4, fam47e, TSC22D2, MKL1, RPF2, ERO1A, HELZ, WWP2, FOXJ3, hspa1b, SMG1P2, ANG, LOC399715, CEBPD, HSPA7, PGAM4, TPI1P2, ENSG00000236575, ENSG00000238117, KCNMB3P1, C8orf58, ENSG00000249007, ENSG00000249590, MIR1204, ENSG00000256006
4	SARS, PRSS8, FAM107B, LOC105376575, RGS17, TRIB3, TBL1X, GLTSCR2, RASD1, STC2, FHL2, KIAA1324, SIPA1L2, MYB, RRAS, MACROD1, HOOK1, FAM129A, SAT2, CDK19, VPS28, SPSB3, GBP2, S100P, RASEF, LARP6, KIFC2, ALCAM, NUPR1, CCDC154, NEU1, MIR424
5	RRAGD, COBLL1, PPP1R15A, GADD45B, NDRG1, DBP, WSB1, ALDOC, ENO2, RRAGC, KDM5B, P4HA1, SOX4, GDF15, BHLHE40, HRK, DUSP5, ADM, SPRY1, CREBRF, DDIT4, PFKFB3, PHLDA3, DDIT3, PTRF, JUN, IER5L
6	ZIC2, LIMCH1, RSBN1, BNIP3L, SASH1, ERRFI1, FLVCR2, PPP1R3C, DUSP1, TGFBI, RBCK1, ATG14, VLDLR, cnksr3, FAM46B, STC1, IER5, osr2, NFIL3, OTUD1, KIAA0355, EFNA1, SPSB1, AKAP17A, ENO1P1, ENSG00000257922
7	CD99, SLC7A2, CALCR, PRSS22, TNFRSF12A, ARHGAP44, MIR614, PRKCH, GRN, FUT8, GAB2, AGA, NEDD4L, LIMA1, HERPUD1, HOMER3, HEBP2, ATP9A, MCOLN3, DCBLD2, CDH3, EIF4B, CTSA, IDI1, WIPI1, st6galnac2, TESK2, RPS6KA2, ZFYVE26, NUAK1, MOCOS, NT5C2, GPR137B, AMPH, OXCT1, WDFY1, IGBP1, SLC9A1, YPEL3, GNPTG, CERS4, NRCAM, SEL1L3, MAP3K1, MZF1, MKNK2, PRODH, SEPT3, DAAM1, SIX4, DHRS2, PYGB, ZMYND8, PABPC1L, SALL4, BMP7, ASB9, TIMP1, SGCG, CTSH, CERNIP, NCALD, DNASE2, ADAP1, CAV1, HIBADH, TAX1BP1, COBL, ANKMY2, AGR2, PTGR1, PHYH, ARHGAP21, DNAJC12, VAT1, PMP22, INPP4B, TRIM2, UGDH, SC5D, folr1, PPM1H, MGP, UST, ULBP1, CAP2, PERP, FAM46A, PCDHB2, HMGCS1, MRPS30, TARS, RBP1, KAT2B, c3orf52, SLC41A3, KLHL24, SLC30A3, KYNU, EPAS1, EPHA4, DHCR24, TMEM59, RPL22, RHOU, LGALS8, RSRP1, CTSD, RAB32, PPL, KLF9, CCDC92, c1orf198, MIR4709, YPEL5, MIR1287, SOCS2, ACO1, NECAB1, OPTN, RAB9A, FAM210B, PMEPA1, BCAS4, ATXN1, AHNAK, SOX9, INSIG2, IDUA, ATF4, MYO1B, PXDN, COL5A1, SH3BGRL, RFTN1, IL13RA1, LGALS3, EFR3A, prkaa1, aldh3b2, DCLK1, CDK7, MEIS2, SPIRE1, SLC38A2, LPIN1, EMP1, YARS, FAM189A2, TRAFD1, CD63, AHI1, GNS, KIAA0513, DRAM1, FLNB, GPNMB, RAC1, SYTL2, HECW2, ITGAV, CCNG2, SHROOM3, ANXA3, WARS, MAP1LC3B, TIGD7, SLC39A6, PTPRF, CELSR2, ATP1B1, SCCPDH, PSEN2, SOX13, ABCA12, DGKQ, MARCH6, MYO10, RPL37, LHFPL2, TNFRSF21, SHROOM2, SH3KBP1, SLC16A2, MAL2, EIF3H, SH3GLB2, LCN2, PAK1, LYPD6B, rilpl2, DIP2C, TMEM45B, ACSL1, PARP8, PTPRK, ZDHHC7, CEBPG, MCOLN2, PRKCA, ENSG00000155130, DEPTOR, EEF1A1, WDR19, CLSTN2, BTG2, EFCAB14, TFF3, ZG16B, zswim5, JAK1, CAMK2N1, CAPN13, KCNF1, SLC22A15, TGFBR2, PRICKLE2, SMIM14, FAM198B, NIPBL, CMBL, CMYA5, MIOS, TNFRSF11B, TP53INP1, DYNLT3, MID1IP1, SPTSSA, GPT2, CRABP1, NAV2, STX3, SMAD3, FAM102A, PRR15L, ANKRD33, IRF2BP2, RAB31, TMEM150A, IRS1, SLC25A6, CA5B, GUSB, FAXDC2, FOS, IRX2, TANC2, PLAC1, ZNF217, CYP4F22, CEBPB, MIR5572, STOX2, TRIB1, TOMM20, FZD4, YPEL2, SCUBE2, SIX5, ULK1, SVBP, OPLAH, MTURN, SHISA2, CUEDC1, HIST3H2A, CREB3L2, ATP6AP2, SGK223, VCX, znf721, FAM46C, KCNK12, TACSTD2, SLITRK6, HIST2H2BE, SLC24A3, SMYD3, MUC1, MIR1469, GLDN, SERPINA5, SERPINA3, SPATS2L, CD55, EVL, CACNA1H, SULF2, KIAA1211L, UAP1L1, ENPP1, PARVA, PSAP, ELOVL2, TMEM116, PAPSS2, ENSG00000199004, CAPN8, MAFB, CDSN, NBPF22P, C5orf51, FAM220CP, S1PR3, ZBED1, RPL13P12, ENSG00000224628, LOC101927745, MAPKAPK5-AS1, TMSB4XP1, Snord13, ACAD11, RPL37P6, SELENOP, ENSG00000255343, ENSG00000255990, ENSG00000256121, TUBB3, ENSG00000259537, ENSG00000260822, ENSG00000261452, ENSG00000261793
8	LCP1, AGAP11, BRSK1
9	
10	FAM83D, EFHD1, ID1, ENSG00000186076
11	TSPAN6, c1orf112, SLC25A13, POLR2J, YBX2, SCIN, E2F2, UBR7, TACC3, POLA2, RPL26L1, hoxc8, SPDL1, LSG1, NOP16, RFC2, PPP1R3F, CYBA, THOC3, PKP2, POLD1, ISOC2, GSTO2, TP53BP1, COASY, PITX1, GAL, TRIP13, MCM2, CA12, WDR62, MLH1, UBE2T, HSPB11, MRPL22, GEMIN5, SLC27A5, MGST2, IPO11-LRRC70, EPDR1, MIR6875, SRRT, TPX2, RPL6, BIRC5, LAMB1, DLD, ZC3HC1, GEMIN2, TYRO3, CDC45, TMEM14A, CDC7, RANBP1, CENPM, MCM5, TSPO, FOXRED2, POLE2, CDKN3, ITPK1, VRK1, EFS, cinp, SUV39H1, PLS3, SLC25A15, ELMO3, fam173a, EARS2, FAH, OIP5, LAPTM4B, POP1, JPH1, GSDMD, RNASEH2A, ASF1B, TNNT1, ETFB, KDELR1, GRWD1, TFPT, ISYNA1, MPP6, PTCD1, TAF6, PLOD3, BCL7B, EXOSC3, CXCL12, ACTA2, KPNB1, LGALS3BP, KAT2A, NARR, FOXM1, RAD51AP1, SCNN1A, TIMELESS, CHPT1, CCND3, BYSL, KIF20A, LMNB1, PCCB, EIF4G1, RPS15, ABCB6, PASK, ODC1, SRM, TTF2, TXNIP, ARTN, DARS2, TGFB3, FAM98A, ZWINT, HJURP, PMS2P5, HMGB1P1, AARS2, c17orf53, ARMC7, SLC25A19, NKX2-2, XRCC3, PDCD2L, IFI6, FGD3, BCL11B, pkmyt1, LOC100506136, SDF2L1, KNSTRN, SGO1, GAMT, TOMM40, KIF1A, BST2, RTN4IP1, FCHO1, EXOSC2, GINS2, F12, HAUS8, TUBG1, TOP2A, SNRPA1, NUP210, RFC3, BEX1, EMC7, TMEM106C, CD36, ITM2C, TUBB2B, FGFBP2, THBS1, NUSAP1, NDUFAF1, CEP55, EFCAB11, FANCI, Uqcrc2, MYO19, P3H4, NT5C3B, PLK4, MIR3658, PIGM, ISG20L2, RGS16, ETNK2, TMEM177, POLR2D, RABL3, EIF2B5, LYAR, CCNA2, ADAMTS19, nhp2, FAM50B, CDCA5, MEPCE, NCAPG2, cxorf57, MRPS28, SIGMAR1, PDSS1, EML3, CDC42EP2, hirip3, HSPB8, gemin6, PFKM, GJA1, CARHSP1, MRPL39, CXXC1, PROM2, NUP205, FAM122B, UBE2L6, mapk13, SUSD3, CCNB2, SLC38A10, FAM213B, KRTCAP3, MRPL17, AUTS2, DUSP23, B4GALT3, MIR5187, pip, CCDC58, CBS, c21orf33, ZDHHC12, PKN3, RUSC1, PPP1R35, fgfr4, ALKBH4, MIR4467, PSMC2, AP2M1, POLR3K, c16orf59, CCNF, RPL29, IL20, ACTG2, MRPS18C, EOMES, CHCHD4, ELP6, POLR2H, RFC4, RPL39L,

	POC1A, SFXN1, PTTG1, KIAA1324L, PEX2, VCP, STOML2, MELK, DDIAS, ZNF22, MOAP1, IFI27, RPUSD2, NOLC1, C11orf74, WDR72, CENPN, CLEC3A, BEX3, FAM96A, STAT6, ACAA2, RRM1, RAB8A, GPX4, GATAD2A, GGT6, CD320, MRPL58, TK1, ABCA3, COPS6, NT5DC2, DEGS2, lcmt2, CHST14, XPO6, PRELID1, GPRIN1, NFU1, CENPX, FASN, DUS1L, DCXR, TRIM56, YWHAG, MIR4444-1, SLC16A5, GON7, CDCA4, LOC93622, LSM3, ATP6V0E2, CANT1, P2RY6, RRM2, RPS7, pop7, GNB2, COQ2, SYT12, PSMD1, ZWILCH, MRPL11, golt1a, PSMD2, FAM131A, DOLK, CCNE2, SWI5, SLC35A4, GPX2, C8orf59, RHOG, IRX3, AURKB, RRS1, MAGED1, GPC5, GEMIN4, fjx1, SLITRK4, DCTPP1, TSPYL5, S1PR5, hoxc9, D2HGDH, ANKRD34A, GINS3, MRPS11, CYB5D1, AP1S2, TEX19, FES, SLC25A10, CBX6, NPW, NIPSNAP1, HDDC3, BTBD6, SIVA1, C14orf80, PARPBP, MRPL40, C16orf53, HPDL, CMC1, ISG15, H2AFX, HBA2, C9orf152, HLA-DRB1, PLEKHG4, TUBB, RAD54B, HNRNPAB, SPANXA1, PRIM1, NUP62CL, TFDP1, HOXC4, BRINP2, PRC1, CCDC167, CENPW, MRPL38, CRHR1-IT1, FAM216A, c15orf59, POM121B, SNORD96, TRGV9, PTTG3P, ENSG00000213209, MRPL23, LINC00998, TUBBP2, CYCSP55, UBE2SP2, HSD17B8, CKS1BP2, MIR6873, TRGC2, SPANXB1, ENSG00000230195, ENSG00000230197, VARS, RPL7P21, CT45A3, KIFC1, ENSG00000233966, FABP5P7, ENSG00000235036, FABP5P1, CKMT1B, ATP5J2, PSMC1P1, ARPC1A, CT45A5, LINC00992, ENSG00000249762, I3L0E3, CHCHD10, SYS1-DBNDD2, PSMC1P9, FBXO10, ENSG00000257077, SORD2P, MRPL46, ANP32AP1, ENSG00000260164, ENSG00000261208

Chronic hypoxia rank product gene lists	
Venn Location	**Gene names**
1	CX3CL1, TRAPPC6A, MYLIP, CSDE1, SH3YL1, CAPG, HSPA5, TTC17, SLC2A3, MIR21, ZCWPW1, MFSD11, NFKBIA, MAGT1, syt17, rhov, PCOLCE, TBC1D9, HMGCR, BCL6, KDM3A, GADD45A, ESYT2, IRF2BPL, SDC4, krt17, DNAJB9, MBD4, SERGEF, DOCK6, MIR6886, KIAA1683, PNPLA7, c14orf159, VTCN1, ELF5, TSPAN31, PAN2, IER3, CBX4, RNF165, lmtk3, SELENBP1, S100A8, DEGS1, ACKR3, AMT, PLK2, TNIP1, ZNF185, AK3, UGCG, STOM, notch1, FRG1BP, TMEM219, NOCT, MAT1A, DPYSL4, NR4A2, UBALD1, TSC22D3, IER2, UBXN1, AK4, CNST, S100A9, ANKZF1, RYBP, TIPARP, MIR6732, ARHGEF3, C4orf3, DLC1, GPER1, CKB, PEX11A, SLC3A2, UPF3A, AFAP1L2, ZBTB43, THBS3, BFSP2, JUNB, ISG20, MYO1D, IRX5, cracr2b, EGR3, SSTR2, TTC3, MST1P2, RXRA, rps23, INSIG1, FNBP1, RINL, C15orf52, NRARP, ZNF358, FICD, PJA2, RN7SKP80, rn7sk, RNU4-2, NYNRIN, UCA1, LINC00243, LINC00680, EPB41L4A-AS1, C14orf132, WASH7P, DDAH2, ENSG00000230572, PTMAP4, RPS3AP25, DICER1-AS1, ENSG00000235859, RP2PLP3, FOXP1-IT1, RN7SL1, ARPC4-TTLL3, ENSG00000255730, SLC5A8, ENSG00000260043, ENSG00000260789
2	WDR54, BCAS1, P4HA2, FSCN1, DGKD, EDN1, PGM1, BAMBI, PGK1, ILVBL, GPI, CA9, EFNB3, ARHGDIB, FAM162A, PFKFB4, HES1, IGFBP5, ST3GAL5, ARID3A, CTGF, EGR1, EGR2, FOSB, ZFP36, SAT1, ZDHHC8P1, CYP1B1, CYP1A1, SIK1, TUFT1, ppfia4, CSRNP1, PAM, IGFBP3, nbl1, CIART, HK2, C19orf33, RAB26, CLIC3, TM4SF1, PTGER4, BNIP3, IRS2, ANKRD37, ZNF395, SBK1, S100A4, ENSG00000207315, PPME1, PPP1R3E, ENSG00000248721, ENSG00000256006
3	ARHGAP33, TMEM132A, ALDH3B1, ST3GAL1, SNAI2, VIM, RAI14, CDH10, CYFIP2, SPAG4, PFKP, PKM, FGFR3, MIR8085, FSTL3, TCF3, SCARB1, NOTCH3, ENO1, LXN, DNM2, PLOD1, RAD54L, Ceacam6, MIR3198-2, ITPR3, DSP, RASSF7, DDT, LGALS1, PYGL, SLCO4A1, PCSK1N, HCFC1R1, CRISPLD2, NME4, METRN, EEF2K, BCKDK, SYDE1, CNFN, ZNF175, UPK1A, LHX2, PDLIM1, KMT5B, GALNT18, UPK2, LOC100507424, GAPDH, TPI1, GHR, GBE1, ID2, qsox1, IVNS1ABP, ID3, SLC2A1, NR4A3, SORBS3, CXCR4, FMOD, DNPEP, INHA, TOX2, TRERF1, BPIFB1, MIR4329, KLF2, CHTF18, GAD1, LRRC6, EGLN3, MIR675, thoc6, DNAJB1, PPARG, ITGB4, LDHA, DTNA, NREP, GOLM1, HILPDA, TROAP, SERPINE2, TNS3, GABBR2, FLOT1, BCAR3, PHLDA1, MFGE8, NUDT7, NOL3, NARF, FBXO15, CYR61, RGL1, MALL, PLAC8, PRPS1, DOCK5, ITPRIP, TENM4, MPZL2, ALDOA, VEGFC, PRSS53, SPOCK1, NTAN1, MUM1L1, RCAN1, CLDND2, DMKN, ITGA5, DHRS3, FCRLB, ATF3, INHBB, YEATS2, F2RL1, CITED2, SLC29A4, HEY1, RNF183, E2F7, DPCD, CYB5A, WEE1, CENPV, c15orf39, vkorc1, CACNB3, KRT80, ANGPTL4, SRRM2, ATOH8, PGAM1, RND1, MYEOV, NABP1, SLCO2A1, CSRP2, DMRTA1, VPS37D, TYMS, NIM1K, HNRNPA0, ENSG00000178550, RIIAD1, SELENOW, POLR2A, TMEM45A, IDH2, BACE2, PLCXD1, PCP4, DDX41, ALDH1A3, MAP7D2, JAG2, CD24P4, FAM174B, AHNAK2, VSIG10L, MT1X, THSD4, PLSCR3, SLX4, APOD, TSC22D2, TLE1, NMB, ERO1A, S100A6, MB, hspa1b, HSPA1A, TMEM256, CCDC183, ANG, LOC107985899, PPP2R2A, TPI1P1, PGAM4, TPI1P2, C12orf75, Dgcr5, ENSG00000240289, MIF, C8orf58, PEG10, TMEM141, NEAT1, DRAIC, ENSG00000249007, H7C4C6, RNF5P1, I3L3B4, ENSG00000257540
4	RRAGD, GRN, CDH3, FAM107B, RSBN1, YPEL3, RGS17, MZF1, MKNK2, SALL4, GLTSCR2, DBP, MGP, HMGCS1, STC2, KYNU, KIAA1324, KDM5B, MYB, YPEL5, MIR1287, FAM210B, SOX4, GDF15, MACROD1, BHLHE40, SLC38A2, HOOK1, DRAM1, FLNB, DUSP5, CELSR2, ABCA12, MARCH6, VLDLR, SH3GLB2, CDK19, STC1, CAMK2N1, GBP2, CREBRF, TP53INP1, RASEF, SPTSSA, KIFC2, DDIT4, RAB31, TRIB1, PHLDA3, NUPR1, FAM46C, KCNK12, HIST2H2BE, IER5L, SERPINA3, EVL, MAFB, MIR424, Snord13, ENSG00000255343, ENSG00000255990, ENSG00000260822

5	PPP1R15A, ZMYND8, NDRG1, BNIP3L, RASD1, ALDOC, ENO2, ERRFI1, P4HA1, COL5A1, ATP1B1, ADM, TFF3, IER5, S100P, FOS, PFKFB3, MUC1
6	LIMCH1, ASB9, EPAS1, DUSP1, TGFBI, RRAS, PXDN, EMP1, TMEM45B, MARCKS, SPRY1, CA5B, PTRF, CREB3L2, CACNA1H, ENO1P1-201
7	CD99, SLC7A2, CALCR, PRSS22, TNFRSF12A, ARHGAP44, MIR614, PRKCH, SARS, FUT8, GAB2, AGA, ZIC2, NEDD4L, LIMA1, HERPUD1, HOMER3, HEBP2, PRSS8, ATP9A, MCOLN3, DCBLD2, EIF4B, CTSA, IDI1, LOC105376575, WIPI1, st6galnac2, TESK2, RPS6KA2, ZFYVE26, NUAK1, MOCOS, NT5C2, GPR137B, AMPH, COBLL1, OXCT1, WDFY1, IGBP1, SLC9A1, GNPTG, CERS4, NRCAM, SEL1L3, MAP3K1, GADD45B, PRODH, SEPT3, DAAM1, SIX4, DHRS2, PYGB, PABPC1L, BMP7, TRIB3, TBL1X, TIMP1, SGCG, CTSH, cemip, NCALD, dnase2, ADAP1, CAV1, HIBADH, TAX1BP1, COBL, ANKMY2, AGR2, PTGR1, PHYH, ARHGAP21, DNAJC12, VAT1, WSB1, PMP22, INPP4B, TRIM2, UGDH, SC5D, folr1, PPM1H, SASH1, UST, ULBP1, CAP2, PERP, FAM46A, PCDHB2, MRPS30, TARS, RBP1, KAT2B, c3orf52, SLC41A3, KLHL24, SLC30A3, FHL2, EPHA4, DHCR24, TMEM59, RPL22, RHOU, RRAGC, LGALS8, SIPA1L2, RSRP1, CTSD, RAB32, PPL, KLF9, CCDC92, c1orf198, MIR4709, FLVCR2, PPP1R3C, SOCS2, ACO1, NECAB1, OPTN, RAB9A, PMEPA1, BCAS4, ATXN1, AHNAK, SOX9, INSIG2, RBCK1, ATG14, IDUA, ATF4, MYO1B, SH3BGRL, RFTN1, IL13RA1, LGALS3, EFR3A, prkaa1, aldh3b2, DCLK1, CDK7, MEIS2, SPIRE1, LPIN1, YARS, FAM189A2, HRK, TRAFD1, CD63, AHI1, GNS, KIAA0513, FAM129A, GPNMB, RAC1, SYTL2, HECW2, ITGAV, CCNG2, SHROOM3, ANXA3, WARS, MAP1LC3B, TIGD7, SLC39A6, SAT2, PTPRF, SCCPDH, PSEN2, SOX13, DGKQ, MYO10, RPL37, LHFPL2, TNFRSF21, SHROOM2, SH3KBP1, SLC16A2, MAL2, EIF3H, LCN2, PAK1, LYPD6B, rilpl2, DIP2C, ACSL1, PARP8, PTPRK, cnksr3, ZDHHC7, CEBPG, MCOLN2, PRKCA, DEPTOR, EEF1A1, WDR19, FAM46B, CLSTN2, BTG2, EFCAB14, VPS28, SPSB3, ZG16B, zswim5, JAK1, CAPN13, KCNF1, SLC22A15, TGFBR2, PRICKLE2, SMIM14, FAM198B, NIPBL, CMBL, CMYA5, MIOS, TNFRSF11B, osr2, NFIL3, DYNLT3, MID1IP1, OTUD1, GPT2, LARP6, KIAA0355, CRABP1, NAV2, STX3, SMAD3, FAM102A, PRR15L, ANKRD33, IRF2BP2, TMEM150A, IRS1, SLC25A6, EFNA1, GUSB, ALCAM, FAXDC2, IRX2, TANC2, PLAC1, SPSB1, ZNF217, CYP4F22, CEBPB, MIR5572, STOX2, TOMM20, FZD4, YPEL2, DDIT3, SCUBE2, SIX5, ULK1, JUN, SVBP, OPLAH, MTURN, SHISA2, CUEDC1, HIST3H2A, ATP6AP2, SGK223, VCX, znf721, TACSTD2, SLITRK6, SLC24A3, SMYD3, MIR1469, GLDN, SERPINA5, SPATS2L, CD55, SULF2, KIAA1211L, UAP1L1, ENPP1, CCDC154, PARVA, PSAP, AKAP17A, ELOVL2, TMEM116, PAPSS2, ENSG00000199004, CAPN8, NEU1, CDSN, NBPF22P, C5orf51, FAM220CP, S1PR3, ZBED1, RPL13P12, ENSG00000224628, LOC101927745, MAPKAPK5-AS1, TMSB4XP1, ACAD11, RPL37P6, SELENOP, ENSG00000256121, ENSG00000257922, TUBB3, ENSG00000259537, ENSG00000261452, ENSG00000261793
8	PIP, BRSK1, HOXC9
9	AGAP11
10	SCIN, TRIP13, MCM2, HSPB11, TSPO, FAM83D, RNASEH2A, ASF1B, ETFB, ACTA2, SCNN1A, TIMELESS, EFHD1, ABCB6, PASK, TXNIP, HJURP, ID1, KIF1A, GINS2, F12, THBS1, CEP55, GJA1, CARHSP1, ACAA2, TK1, ATP6V0E2, RRM2, D2HGDH, PGAM4, TUBB, PRC1, FAM216A, CKS1BP2
11	TSPAN6, c1orf112, SLC25A13, POLR2J, YBX2, E2F2, UBR7, TACC3, POLA2, RPL26L1, hoxc8, SPDL1, LSG1, NOP16, RFC2, PPP1R3F, CYBA, THOC3, PKP2, POLD1, ISOC2, GSTO2, TP53BP1, COASY, PITX1, GAL, CA12, WDR62, MLH1, UBE2T, MRPL22, GEMIN5, SLC27A5, MGST2, IPO11-LRRC70, EPDR1, MIR6875, SRRT, TPX2, RPL6, BIRC5, LAMB1, DLD, ZC3HC1, GEMIN2, TYRO3, CDC45, TMEM14A, CDC7, RANBP1, CENPM, MCM5, FOXRED2, POLE2, CDKN3, ITPK1, VRK1, EFS, CINP, SUV39H1, PLS3, SLC25A15, ELMO3, fam173a, EARS2, FAH, OIP5, LAPTM4B, POP1, JPH1, GSDMD, TNNT1, KDELR1, GRWD1, TFPT, ISYNA1, MPP6, PTCD1, TAF6, PLOD3, BCL7B, EXOSC3, CXCL12, KPNB1, LGALS3BP, KAT2A, NARR, FOXM1, RAD51AP1, CHPT1, CCND3, BYSL, KIF20A, LMNB1, PCCB, EIF4G1, RPS15, ODC1, SRM, TTF2, ARTN, DARS2, TGFB3, FAM98A, ZWINT, PMS2P5, HMGB1P1, AARS2, c17orf53, ARMC7, SLC25A19, NKX2-2, XRCC3, PDCD2L, IFI6, FGD3, BCL11B, pkmyt1, LOC100506136, SDF2L1, KNSTRN, SGO1, GAMT, TOMM40, BST2, RTN4IP1, FCHO1, EXOSC2, HAUS8, TUBG1, TOP2A, SNRPA1, NUP210, RFC3, BEX1, EMC7, TMEM106C, CD36, ITM2C, LCP1, TUBB2B, FGFBP2, NUSAP1, NDUFAF1, EFCAB11, FANCI, Uqcrc2, MYO19, P3H4, NT5C3B, PLK4, MIR3658, PIGM, ISG20L2, RGS16, ETNK2, TMEM177, POLR2D, RABL3, EIF2B5, LYAR, CCNA2, ADAMTS19, nhp2, FAM50B, CDCA5, MEPCE, NCAPG2, cxorf57, MRPS28, SIGMAR1, PDSS1, EML3, CDC42EP2, hirip3, HSPB8, gemin6, PFKM, MRPL39, CXXC1, PROM2, NUP205, FAM122B, UBE2L6, mapk13, SUSD3, CCNB2, SLC38A10, FAM213B, KRTCAP3, MRPL17, AUTS2, DUSP23, B4GALT3, MIR5187, CCDC58, CBS, c21orf33, ZDHHC12, PKN3, RUSC1, PPP1R35, fgfr4, ALKBH4, MIR4467, PSMC2, AP2M1, POLR3K, c16orf59, CCNF, RPL29, IL20, ACTG2, MRPS18C, EOMES, CHCHD4, ELP6, POLR2H, RFC4, RPL39L, POC1A, SFXN1, PTTG1, KIAA1324L, PEX2, VCP, STOML2, MELK, DDIAS, ZNF22, MOAP1, IFI27, RPUSD2, NOLC1, C11orf74, WDR72, CENPN, CLEC3A, BEX3, FAM96A, STAT6, RRM1, RAB8A, GPX4, GATAD2A, GGT6, CD320, MRPL58, ABCA3, COPS6, NT5DC2, DEGS2, lcmt2, CHST14, XPO6, PRELID1, GPRIN1, NFU1, CENPX, FASN, DUS1L, DCXR, TRIM56, YWHAG, MIR4444-1, SLC16A5, GON7, CDCA4, LOC93622, LSM3, CANT1, P2RY6, RPS7, pop7, GNB2, COQ2, SYT12, PSMD1, ZWILCH, MRPL11, golt1a, PSMD2, FAM131A, DOLK, CCNE2, SWI5, SLC35A4, GPX2, C8orf59, RHOG, IRX3, AURKB, RRS1, MAGED1, GPC5, GEMIN4, fjx1, SLITRK4, DCTPP1, TSPYL5, S1PR5, ANKRD34A, GINS3, MRPS11, CYB5D1, AP1S2, TEX19, FES, SLC25A10, CBX6, NPW, NIPSNAP1, HDDC3, BTBD6, SIVA1, C14orf80, PARPBP, MRPL40, c16orf53, HPDL, CMC1, ISG15, H2AFX, HBA2, C9orf152, HLA-DRB1, PLEKHG4, RAD54B, HNRNPAB, SPANXA1, PRIM1, NUP62CL,

	TFDP1, HOXC4, BRINP2, CCDC167, CENPW, MRPL38, CRHR1-IT1, c15orf59, POM121B, SNORD96, TRGV9, PTTG3P, ENSG00000213209, MRPL23, LINC00998, TUBBP2, CYCSP55, UBE2SP2, HSD17B8, MIR6873, TRGC2, SPANXB1, ENSG00000230195, ENSG00000230197, VARS, RPL7P21, CT45A3, KIFC1, UBE2S, FABP5P7, LOC100421490, FABP5P1, CKMT1B, ATP5J2, PSMC1P1, ARPC1A, CT45A5, LINC00992, ENSG00000249762, I3LOE3, CHCHD10, SYS1-DBNDD2, PSMC1P9, FBXO10, ENSG00000257077, SORD2P, MRPL46, ANP32AP1, ENSG00000260164, ENSG00000261208

Appendix 2.3: HIF target gene lists

Full HIF target genes for HIF1, HIF2 and both HIF1/HIF2 are shown. These lists were compiled from ChIP-seq analysis of MCF7 cells performed in Mole et al. 2009 and Schödel et al. 2011. These genes were used in the analysis in chapter 4 where the use of HIF target genes is stated.

HIF target gene lists	
HIF1 specific	WDR54, SPAG9, ANLN, PRICKLE3, MTMR11, cyp24a1, VIM, TFB1M, CASR, FBXO42, FOXN3, ATP9A, RELT, NDC1, TBXAS1, elmo2, BCAS1, gnai3, PKM, iars2, HEATR6, ATP11A, PLA2G10, TFRC, MAP3K13, CLASP1, ENO1, C1QTNF3, CHMP2B, SMAP2, MYNN, ERGIC2, ALKBH5, TRPM7, DSP, ENSG00000100010, DAAM1, NFATC4, PFDN4, DOK5, CSTF1, BMP7, PAK5, PGK1, DGKH, PSMD7, VAC14, nomo3, ATP8B4, SQLE, FBL, PPP2R1A, TTC26, PLOD3, CA9, RAD51C, TRIM37, DHX40, TUBD1, CCDC47, SMURF2, WSB1, ALDOC, SEPSECS, STIM2, MAGOHB, LOC100507424, CDK2AP1, GAPDH, ENO2, NCOA7, HSPA9, TARS, c5orf15, FAM162A, PFKFB4, C3orf14, BBX, IQCG, GBE1, SOS1, QSOX1, RLF, KDM5B, HSDL2, MXI1, TTLL2, PAIP2, TBX4, MIR6840, MTERF4, HJURP, NCOA5, PARD6B, CDH26, BCAS4, HIST1H4B, TREM1, ATXN1, MAX, PPAT, PODXL, NDUFA5, ACKR4, PSMA1, SERGEF, BCL2L2, EAPP, HSD17B3, PNISR, BTBD3, TPT1, EDEM1, SORT1, AP4B1, LDHA, CDC73, CABLES1, ddb2, AGO4, ENSG00000135180, PNPLA8, CGA, TEX2, BRIP1, CBWD2, SMC2, FAM129B, NCBP1, MYC, SYTL2, ENSG00000138041, TMOD3, WDR89, GOLGA6D, PARN, Uqcrc2, CDR2, ZFHX3, CLEC18B, CLTC, C17orf64, BCAS3, TP53, CARD14, NARF, Tmem91, ZFP14, RIT1, RABL2A, LNPK, PTPRG, ECE2, RNF145, TNIP1, PNRC1, TBC1D32, RGS20, NDUFB9, SAP18, IPMK, PLOD2, CARHSP1, RASSF3, FEZF2, RSPH10B, MOV10, MPV17L, SMG1, KRTCAP3, HIST1H2BD, SNX29P1, PPP1R15B, EMSY, C8orf58, RAPGEF6, CIART, CCDC107, NLRP4, PEX13, RPRD2, DAPL1, HIPK1, NBPF14, SRGAP2, AZI2, ANKZF1, THOC7, PSMD6, PRICKLE2, YEATS2, STARD4, ESM1, SNAPC3, RASEF, RNF183, R3HCC1L, OPN1MW, cox11, c15orf39, DHRS13, RBPJ, HFE2, FAM84B, HSPBAP1, RAB24, FAM103A1, UGP2, foxd4, SLN, PFKFB3, MIR7706, USP32, PPM1D, SOSTDC1, PGAM1, ZNF318, LKAAEAR1, KNDC1, ZNF217, ENSG00000172886, GLRX, ZBTB21, TUBB7P, ENSG00000175483, CLK2, OR4F17, BASP1, TGIF1, MIEF2, SLC35G3, GRB2, PDE4DIP, RPL10, TMEM107, CRIPAK, C11orf71, TMEM45A, SLX1A, OR2V2, ANXA2, RPS17, ENSG00000182945, RIPK4, gpr1, DENND5A, FOXD4L1, FAM110C, TMEM121, ENSG00000177799, OR7A17, AGAP4, CFAP126, RNFT1, ZNF250, GREB1, ZNF107, GTF2IRD2, pom121, ZNF33B, CLPSL2, ENSG00000196861, METTL9, ZNF398, TRIM33, ZNF323, TUBA3D, CCT8L2, ENSG00000068990, fank1, ENSG00000112727, HIST2H2BF, PPIAL4A, HLA-G, ENSG00000112448, CBWD5, OR4A47, SERF1A, ENSG00000212867, SLX1A-SULT1A3, LAT, FOXO3, C8orf44, DNASE1, ENSG00000214272, CBWD1, CBWD1, C3orf10, ENSG00000221897, PKM
HIF1/HIF2	MIR614, CP, wisp2, MSANTD3, RSBN1, NFE2L1, DYNLL1, TF, BAMBI, CRKL, PDGFB, ZMYND8, DHX35, PLS3, BNIP3L, ILVBL, RAPGEF1, TRIM16L, TMEM97, CDKN1B, ARRDC3, STC2, UPK1B, KDM3A, ID2, DARS, IVNS1ABP, SLC2A1, PPP1R3C, TEX14, INHA, INSIG2, MIR3607, PAICS, CHD1L, SEC61G, LOXL2, DTNA, IER3, MYOF, FAM13A, HNRNPD, CCNG2, PIK3C2G, MINK1, SCYL1, NECTIN4, PLEKHA6, CSRNP1, UBC, OXSM, SLC45A3, LOC100506403, HK2, S100P, SPRY1, SAP30, CITED2, NFIL3, PCF11, TCP11L2, MS4A7, IRF2BP2, TCAF2, MAB21L3, gtf2ird2b, MIR6785, TMTC2, LINC01559, RAP2B, RAD51B, BACE2, FAM169B, CYP27C1, HIST1H1C, ASMT, S100A10, LEKR1, HILPDA, GPI
HIF2 specific	ITGA3, PFN2, CLUL1, CRYBG3, CPOX, KRT31, ASB2, MYL12A, ZNHIT1, AGR2, SFXN3, ODAM, KRT18, FAM65B, UNC93A, MFN2, KIAA1217, PDLIM2, WNT1, BMP4, MTUS1, PIK3C2B, KRT7, DRAM1, TRA2B, BLK, CTSV, IGF1R, USP3, OSBPL10, PLAC8, C4orf3, SNAPC1, UEVLD, LSS, IL6R, FSTL1, GNL3, KIAA0355, CXCL8, KRT8, CBX2, FAM174A, SLC35G5, GJC1, UPP1, S100A4, CXorf40B, ERO1A, HELZ, B3GNT6, eml6, ENSG00000215809, tff1, INHBA, PKP2, ELF3, PXDN, C8orf58, EGFR, FOS, ALDOA, DNAJB6, SCARB1, FAM65C, P2RY2, SLC2A3, KRT80, UBE2V1P2, TMEM189-UBE2V1, NDRG1, IRX1, BHLHE40, SEMA4B, DAPK2, EVL, GPR37L1, TNS1

Appendix 2.4: HER2-driven hypoxia response genes correlating with HER2 expression in cell lines

Tables for acute and chronic hypoxia showing all genes which were found to be both overexpressed in HER2 and part of the hypoxic response in MCF7 and/or MCF7-HER2 cells, and

Genes primed for acute hypoxia in MCF7-HER2 and their correlation with HER2 expression in breast cancer cell lines		
Gene name	Pearson correlation	P-value
ERBB2	1	0
PRSS8	0.615011	2.22E-19
S100P	0.501738	2.04E-12
EFNA1	0.489988	7.80E-12
NUPR1	0.443018	1.04E-09
KIAA1324	0.42151	7.68E-09
TRIB3	0.414086	1.49E-08
DBP	0.406198	2.94E-08
SPRY1	0.386189	1.54E-07
LIMCH1	0.380734	2.37E-07
KDM5B	0.369369	5.70E-07
P4HA1	0.344399	3.49E-06
WSB1	0.339203	4.99E-06
MACROD1	0.325755	1.22E-05
ALDOC	0.319791	1.80E-05
HOOK1	0.294937	8.18E-05
RBCK1	0.285681	1.39E-04
NDRG1	0.266116	4.02E-04
SASH1	0.254177	7.39E-04
SOX4	0.249483	9.32E-04
DDIT4	0.241318	1.38E-03
MYB	0.222011	3.33E-03
VPS28	0.219645	3.69E-03
AKAP17A	0.178319	1.89E-02
LOC105376575	0.172109	2.36E-02

Genes primed for chronic hypoxia in MCF7-HER2 and their correlation with HER2 expression in breast cancer cell lines		
Gene Name	Pearson correlation	P-value
ERBB2	1	0
S100P	0.501738	2.04E-12
SPTSSA	0.47189	5.61E-11
NUPR1	0.443018	1.04E-09
KIAA1324	0.42151	7.68E-09
TFF3	0.418739	9.84E-09
DBP	0.406198	2.94E-08
SPRY1	0.386189	1.54E-07
LIMCH1	0.380734	2.37E-07
KDM5B	0.369369	5.70E-07
ABCA12	0.36732	6.65E-07
CAMK2N1	0.362676	9.41E-07
P4HA1	0.344399	3.49E-06
HMGCS1	0.340146	4.68E-06
MUC1	0.339632	4.84E-06
MKNK2	0.33716	5.73E-06
MACROD1	0.325755	1.22E-05
ALDOC	0.319791	1.80E-05
ATP1B1	0.305257	4.43E-05
TRIB1	0.296971	7.26E-05
HOOK1	0.294937	8.18E-05
CACNA1H	0.274835	0.000253
HIST2H2BE	0.269225	0.000341
NDRG1	0.266116	0.000402
SOX4	0.249483	0.000932
DDIT4	0.241318	0.001382
CREB3L2	0.227049	0.002664
FAM46C	0.224653	0.002963
MYB	0.222011	0.003328
MGP	0.221995	0.003331
CA5B	0.183391	0.015728
EPAS1	0.179395	0.018193
MARCH6	0.152432	0.045273